Republic of Iraq
Ministry of Higher Education
and Scientific Research
University of Babylon
Faculty of Engineering

Electrocardiogram Based Heart Diseases Classification by Using Machine Learning Approach

A Thesis

Submitted to the Faculty of Engineering, University of Babylon in Partial Fulfillment of the Requirements for the Degree of Doctorate of Philosophy in Electronics and Communications Engineering.

By

Heyam A. Marzog

Supervised by

Prof. Dr. Haider Jabbar Abd

2023 A.D. **1444 A.H**

بسم الله الرحمن الرحيم

الله نور السموات والأرض
مثل نوره كمشكوة فيها مصباح المصباح
في زجاجة الزجاجة كأنها كوكب دري يوقد من
شجرة مباركة زيتونة لا شرقية ولا غربية يكاد زيتها
يضيء ولو لم تمسسه نار نور على نور يهدي الله لنوره
من يشاء ويضرب الله الأمثال للناس والله بكل شيء عليم

صدق الله العلي العظيم

Abstract

The heartbeat is a set of waveforms that originate from the tissues of the heart and the contraction and relaxation of the heart muscles. The difficulty in classifying the heart signal is the changes in the electrocardiogram, which are extremely important and essential in diagnosing the patient's condition. Many modern algorithms have been used in diagnosing the heart signal according to the records of the electrocardiogram. With the help of modern algorithms, a device was designed to help the doctor with prior diagnosis of the patient's condition.

The ECG signal is exposed to multiple types of noise that affect the accuracy of signal classification and correct diagnosis. These types include powerline interference noise(PL), baseline wandering(BLW), electrode motion artifact noise(EMA), and electromyography noise (EMG). The EMG noise just mentioned is the most common noise that affects electrocardiogram (ECG) signals.

Denoising the ECG signals is an essential step in obtaining pure signal features for accurate diagnosis. The study investigates multiple types of noise common to ECG signals, as well as methods for processing signals to remove noise. To remove the baseline wandering noise from the ECG signal, a Discrete Wavelet Transform) can be used. A Notch filter is capable of removing power line noise. Adaptive filter is believed to be an effective way to remove Electromyography (EMG) noise, adaptive mean-square (LMS) and frequency-least square (RLS) adaptive filters were used to reduce the noise caused by electrode movement.

As mentioned earlier, classification of the ECG signal is usually done with the aim of determining the condition of the heart, and diagnosing

cardiac diseases. The classification includes diseases such as Normal Siun Arrhythmia(NSR), Arrythmia(ARR), and Congestive Heart Failure(CHF)

When classifying the ECG signal, the ECG signals are analyzed and extract the features of the cardiac condition. Many of techniques can be used for this, including converting the signals to different frequencies using a wavelet scattering transform or separating mixed signals using blind source separation. The signal of ECG is classified using Neural networks (NN) and Support Vector Machines (SVM). These are two examples of machine learning, the data that used with these machine learning is divided in different proportions randomly 70% for training and 30% for testing. The blind source separation algorithm was applied with NN and recorded an accuracy of 99.4, while the blind source separation algorithms and SVM got a percentage of 99.38%. The wavelet scattering algorithm was used to extract the features with NN and SVM, the accuracy rates were different, as the wavelet scattering with NN got a percentage of 99.7%, while the wavelet scattering with SVM had an accuracy rate of 99.92%. Which was practically applied through a device that was designed based on a small device called a Lattepanda, which is similar to a small computer and works on Windows 10 with sensors and a sensor for the electrocardiogram signal that works as an ECG unit. GUI was used to display the results on a screen that was linked with Latttepanda when examining the patient that gives Classification results for cardiac reference for previously mentioned cases

Dedications

To my parents

to beloved family

to my dear husband Muhammad

to my children Mustafa and Razan

to all my friends and everyone who supported me in this jour

Supervisor Certification

I certify that this Thesis entitled "ECG -Based Heart Diseases Classification and Arrhythmia Detection by Using efficient Machine Learning Approach" was prepared by Heyam A. Marzog under my supervision at the Department of Electrical Engineering, College of Engineering, University of Babylon, as a partial fulfillment of the requirements for the degree of Doctorate of Philosophy in Electronics and Communications Engineering.

Signature:

Name: ***Prof. Dr. Haider Jabbar Abd***

(Supervisor)

Date: / / 2023

In view of the above recommendation, I am forward this Thesis for discussion by the Examination Committee

Examining Committee Certificate

We certify that we have read this Thesis entitled "***Electrocardiogram Based Heart Diseases Classification by Using efficient Machine Learning Approach"*** and as an examining committee, examined the student, "***Heyam A. Marzog***", in its contents and that in our opinion it meets the standard of a thesis for the degree of Doctorate of Philosophy in Electronics and Communications Engineering.

Signature:
Name: ***Prof. Dr. Kasim Karam Abdalla***
(Member)
Date: / / 2023

Signature:
Name: ***Prof. Dr. Hasan Fahad Khazaal***
(Member)
Date: / / 2023

Signature:
Name: ***Prof. Dr. Ahmad Kareem Abdalla***
(Member)
Date: / / 2023

Signature
Name: ***Asst. Prof. Dr. Hanaa Mohsin Ali***
(Member)
Date: / / 2023

Signature:
Name: ***Prof. Dr. Sameer Jasim Mohammed***
(Chairman)
Date: / / 2023

Signature:
Name: ***Prof. Dr. Haider Jabbar Abd***

(Supervisor)
Date: / / 2023

Signature:
Name: ***Prof. Dr. Qais Kareem Omran***
(Head of Electrical Engineering Dept.)
Date: / / 2023

Signature:
Name: ***Prof. Dr. Laith A. Abdul-Rahaim***
(Dean of College of Engineering)
Date: / / 2023

Acknowledgements

In the name of Allah, Most Gracious, Most Merciful

First and above all, I praise ALLAH, the almighty for providing me with this opportunity and granting me the capability to proceed with this thesis.

I would like to express my sincere thanks and gratitude to my supervisor Dr. Haider Jabbar Abd for his guidance, supervision and efforts during this work.

I would like to thank the University of Babylon/ Electrical Engineering Department, faculty members and all the Electrical Engineering Department staff for their support and assistance.

I would like to thank my colleagues and all friends who helped and encouraged me throughout this work.

Finally, I am indebted to my family for their care, patience and support during my years of study

Table of contents

List of symbols

symbol	meaning
A	Mixing Matrix
b	bais
f(net)	Activation function
f(t)	the signal under consideration
g	impulse response
g(n)	High pass filter
h(n)	Low pass filter
h*	the optimal model indexed
M	Maximum Margin
$n_1(t)$	added noise
o	neuron's output
Q	the quality factor of the filter
Q_k	octave frequency resolution
r(t)	Error Signal
S(t)	Original signal

T	specific scale
W	Separation matrix
w_i	Weight
x(t)	ECG signal
x_i	neuron inputs
y(t)	the adaptive filter output
Λk	the group of wavelet indices
ω_0	the natural frequency
ψ	stretching the wavelet
ψ_j	multiscale high-pass filter banks

List of Abbreviation

(ARR),	Arrhythmia
+P	Positive Predictivity
A	Atrial premature contraction
Acc	Accuracy
AF	Atrial Fibrillation
ANNs	Artificial Neural Networks
BLW	Baseline wander
BPM	beats per minute
BSS	Blind source separation
CART	Classification and Regression Technique
CDPW	Cardiac disease-prone weight
CHF),	Congestive Heart Failure
CNN	Convolutional Neural Networks
CPU	Central Processing Unit
CVDs	cardiovascular diseases
DAQ	Data Acquisition
D1	Training data set
D2	Training data set
DCT	Discrete Cosine Transform
DSP	Digital Signal Processing
DWT	discrete wavelet transform
ECG	Electrocardiography
ELM	Extreme Machine learning
EMA	Electrode Motion Artifacts
EMG	electromyographic
Er	Error

ESP	Electrocardiography signal processing
FIR	finite impulse response
FN	False Negative
FP	False Positive
FPGAs	Field Programmable Gate Arrays
GDB	Gradient-Boosted Trees
GND	Ground
GUI	Graphical User Interface
HRV	Heart Rate Variability
I / O ports	Input/ output port
ICA	independent component analysis
IoT	Internet of things
KNN	k-nearest neighbors
L	Left bundle branch block beat
LA	Left Atrium
LCD	Liquid Crystal Display
LMS	Least Mean Squares
LPF	Low Pass Filter
LV	Left Ventricle
MBADB	MIT-BIH Arrythmia Database
MFSS	Multi-Feature Signal Similarity
MIT-BIH	Massachusetts Institute of Technology-Boston's Beth Israel Hospital
ML	Machine Learning
MLP	Multilayer Perceptron
N	Normal beat
NN	Neural networks
NSR	Normal Sinus Rhythm

PCA	Principle component analysis
PID	Proportional–Integral–Derivative
PL	Powerline
R	Right bundle branch block beat
RA	Right Atrium
RLS	Recursive Least Squares
RNN	Recurrent neural network
RV	Right Ventricle
Se	Sensitivity
SL	Supervised Learning
SNR	Signal- Noise Ratio
SRM	structural risk minimization
SVM	Support Vector Machine
SVRF	Sampling Vector Random Forest
UL	Unsupervised Learning
USB	Universal Serial Bus
V	Premature ventricular contraction
VC	Vapnik–Chervonenkis theory
WHO	World Health Organization
WST	Wavelet Scattering Transform
WT	Wavelet Transform

list of tables

List of Figures

Chapter one

Introduction and Literature Review

1.1Overview

Electrocardiography (ECG) is a vital and effective approach for identifying cardiovascular diseases (CVDs) since it is easy to use and offers essential information about heart health. ECG is a means of evaluating the heart's electrical signal throughout time. It is a reliable noninvasive method for vast scope of biological missions, as monitoring vital signs, detecting anomalies, establishing identity, and gaining insight into movement. This signal also demonstrates the functioning of the heart, which enables the cardiologist to identify arrhythmias, which is one of the cardiovascular diseases. The area of ECG signal processing has expanded dramatically due to the significance of CVDs and the high mortality rate [1].

The electrical impulse of the heart is recorded through the electrocardiogram, often known as an ECG, employing waves such as the QRS, P, and T waves depicted in the figure (1.1). Because it shows how the ventricles are contracting, the QRS component is vital for finding and monitoring irregular heart conditions and disorders. Additionally, by analysing the amplitude, shape, timing, and interval of the heartbeat, this data offers a great understanding of how the heart functions and valuable resources for automated feature extraction [2]

Even though the QRS is the most prominent component of the ECG and is readily identified by cardiac experts, it is challenging to automate owing to its variable shape between states, noise, and interference from other waves. Therefore, it remains a topic of the current study [3] . Keeping tabs on one's health in this fast-paced, digital age has unique obstacles. This led to the widespread use of heart-rate monitors among medical professionals as the manual recording of cardiac activity was replaced by automated tracking in the late 20th century. It subsequently evolved into sophisticated technology that can track and record a person's fitness activities and monitors them regularly. As a result of this foundation, noninvasive wearable ECG sensors have been developed to notify of any observed cardiac abnormalities in real-time [4]. If these claims are true, preventing numerous cardiac disorders, arrhythmias, and coronary heart attacks may be possible. Unfortunately, people pass away due to CVDs every year [2].

Heartbeat data have been extensively studied and analyzed throughout the last two decades, as has the Pan-Tompkins method [1], widely used in cardiac detection literature. These techniques are becoming indistinguishable from our daily lives. Technological advancements have made these tools accessible even in rising countries[5] . As a result of these advancements in smart devices, the possibility of employing more efficient algorithms, such as the wavelet algorithm and the Pan-Tomkins technique, has increased [1]. Even so, using such applications in smart devices is always limited due to energy consumption in signal processing. Although the logic behind these algorithms differs and produces varying degrees of accuracy, the ancient framework of the beat detection process has remained nearly unchanged. The process can be simplified and divided into two broad parts with sub-parts. The benefit of having such stages is that each stage has a specific purpose, and it makes no difference how that purpose is solved; what matters is that at the end of that specific stage, the outcome should match the previously established results, which are universally accepted, both biologically and scientifically [6].

1.2 Heartbeat Characteristics

Many pulse characteristics are seen in the cardiac electrocardiogram, and five waves take place in one good health heartbeat: P, Q, R, S, T, and U

Arrhythmias are abnormal heartbeats with fast, slow, or irregular rhythms and are discovered and classified by ECG signals. Unfortunately, arrhythmias are the leading cause of death in CVD patients. As a result, precise arrhythmia detection and classification have been a severe worry in biomedical signal-processing research [7, 8].

Nevertheless, the detection process is important since noise impacts the ECG signal and biological fluctuation for patients; additionally, some cases of T wave with QRS-complex features. Furthermore, noise sources affecting ECG signals include muscular noise, electrode motion effects, power-line interference, and baseline wandering [9]. Several classification studies have been developed in recent decades. Arrhythmia detection and classification is an important topic in biomedical fields because it provides information about CVD. The ECG beats should be analyzed to look for any cardiac anomalies.

Predicting the possibility of developing the cardiac disease is known as disease prediction. A variety of approaches are available for disease prediction. Pattern-based approaches consider a set of patterns and perform disease prediction by measuring pattern similarity. Numerous methods simply take particular characteristics of the ECG wave into account, resulting in poor findings and a greater false ratio. In certain circumstances, ECG data were classified using algorithms based on specific properties. To tackle the ECG classification challenge, several machine learning (ML) techniques were applied. [10, 11].

The ECG can detect a variety of heart pathologies. The pathophysiology of the most prevalent heart conditions can be affected by a number of factors, such as abnormalities or obstructions in electrical impulse conduction, myocardial hypertrophy, pericardial inflammation, electrolyte imbalances, respiratory system disorders, drug interactions, a drop in body temperature, and conduction through accessory channels [10]. A normal sinus rhythm is a resting heart rate of 60 to 100 beats per minute (BPM). However, heart rate changes due to various factors such as respiration, changes in body temperature, exercise, and so on [12].

The occurrence of human error is greater when ECG is visibly monitored. Because it is a complex problem, several more efforts have been put forth to promote innovative representative and digital structures to analyse the heart signal to decrease the risk of losing important clinical information related to the patient's condition [1].

1.3 Related work

ECG growing importance and impact on human life, several methods for optimal classification of ECG signals have previously been proposed on several arrhythmia databases. To investigate the classification of ECG signals, the following previous works must be reviewed:

Bayasi, Nourhan, et al. 2015 [13]proposed a completely integrated digital ESP for predicting ventricular arrhythmia was proposed through combining a distinct collection of ECG characteristics using naive Bayes. First, real-time adaptive techniques for detecting and the fiducial endpoints were extracted after exploring and outlining P-QRS-T waves. In addition, several more features representing the intergenerational cycle of the ECG data was captured and sent into a naive Bayes classifier, which classified each pulse as normal or abnormal. As a result, a suggested ESP demonstrated an exceptional ability to predict the arrhythmia up to 3 hours before its onset. Furthermore, tenfold cross-validation with a 3-s size of the window yielded a prognosis precision of 86% on out-of-sample validation data.

Serkan Kiranyaz, Turker Ince, Ridha Hamila and Moncef Gabbouj 2015 [14] used adaptive 1D CNNs to extract features from raw ECG data from each patient in the database and classify them. To maximize the CNN analogy and maybe have a "CNN-only" architecture without the MLP single layer, the neurons of the buried CNN layers were modified to accommodate both convolution and subsampling operations. The benchmark MIT/BIH arrhythmia database was used in classification studies, which showed that the suggested technique had the highest classification accuracy of 97.6.

Kasar, Smita L., and Madhuri S. Joshi (2016) [15] distinguished between healthy and myocardial infarction signals. First, a notch to remove the components of noise. After that, principal component analysis was utilized to refine a signal further. The signal's P, Q, R, S, T, and Q amplitudes as well as its Q time were all retrieved. The Q and R amplitudes ratio was one of the characteristics that was calculated using these characteristics. The preprocessed feature vector data were sent to the classifier training module. Two algorithms were compared: J48 and the Classification and Regression Technique (CART). A straightforward, simple-to-use approach that can handle high-dimensional data is the J48 decision tree. A few more characteristics, including the ratio, were computed using these characteristics. CART's classification accuracy was 92.5%, but when the J48 algorithm was used, it increased to 98.5%.

Elhaj et al. (2016) [16] offered the idea that cardiac arrhythmias may be categorized by using morphological and statistical features taken from various heartbeats. Principal component analysis (PCA) of discrete wavelet transform coefficients combines linear features with nonlinear features like exact mathematical statistics and supposed to reflect and nonlinear feature extraction techniques. In particular, the support vector machine and neural network approaches with tenfold cross-validation were used to test the characteristics' capacity to discriminate between various types of information. With a high degree of accuracy 98.91%, they could categorize the N, S, V, F, and U arrhythmia classes using a combination of support vector machines and the radial basis function approach.

S. Sultan Qurraie and R. Ghorbani Afkhami (2017) [17] proposed median filter to remove baseline wander as preprocessing of the ECG signal. They categorized cardiac arrhythmias using three different characteristics derived at different time frequencies. The frequency was separated into 9 windows, and the ECG segment and peaks were retrieved from each window. Classification is based on extracted features. The utilization of time-frequency windowing to the extraction of pseudo-energy features, followed by classification using a collection of decision trees [17]. The classification accuracy of proposed methods for the percentage of "N", "S", and "V" classes derived by tree decision technology was 99%.

U. Rajendra Acharya et al. (2017) [18] proposed a novel approach for automatically identifying ECG heartbeats' N, S, V, F, and Q categories. After training with set A, a CNN was trained using set B to undertake performance analysis. The baseline was cleared of all ECG signals using filters from Wavelet 6 by Daubechies. Pan-Tompkins was used to carry out R-peak detection. All ECG signals were segmented, and Z-score normalization was used to normalize each segment for feature extraction. The CNN network then received the features for testing and training. In authentic and noise-free ECGs, the CNN, which was trained using the enhanced data, had a diagnostic classification accuracy of 94.03%.

Shraddha Singh et al. (2018) [19] utilized Recurrent Neural Networks (RNN) to categories normal and abnormal ECG beats. They could instantly tell the difference between regular and erratic beats. The MIT-BIH Arrhythmia database was used to determine the beat accuracy of classification. A substantial amount of standard ECG time-series data was used as inputs to a Long Short Term Memory Network. They separated the dataset into subgroups for training and testing. They provided examples of the efficacy, accuracy, and detection capacities of their methods for ECG arrhythmias. The total number of beats properly categorized as normal or arrhythmic was known as the classification accuracy, and it was 85.4% for the RNN classifier.

S Celin and K. Vasanth (2018) [20] categorized the ECG signal, the submitted an technique for classification. First, high-frequency noise from the input signal was pre-processed by applying filtering techniques as low-pass, high-pass, and Butterworth filters. After preprocessing, high points were identified using a peak detection technique, and features for the signal were retrieved using statistical parameters. In the end, SVM, Adaboost, ANN, and Nave Bayes classifiers were used to distinguish between normal and pathological ECG signals using the retrieved features. According to the experimental testing, the accuracy of the SVM, Adaboost, ANN, and Nave Bayes classifiers was 87.5%, 93%, 94%, and 99.7%, respectively. When compared to the accuracy of other classifiers, the accuracy of the naive Bayes classifier is quite high.

Pooja M Kagalkar and **et al. (2019) [21]** preprocessed the ECG signal with the Wavelet toolbox and improved the SNR by removing high-frequency, low-frequency, and baseline wandering noise from the signal. The R-peak and other peaks in the ECG signal were located using the Min-Max technique. To extract features from an ECG signal, the MATLAB Wavelet toolbox was also used. An ECG signal's normal or abnormal status was assessed using a Bayesian classifier. Instead, different Arrhythmia classes were separated from the ECG signal.

Syama S. et al. (2019)[22] reduced signal power line interference using Butterworth and Notch filters. The signal was slowed down using the wavelet algorithm. They anticipated employing Haar and Daubechies wavelet techniques to handle the ECG signal's split into 8 levels. As a consequence, accurate feature extraction was achieved by a comparative analysis of both wavelet transformations. For ECG classification, they utilised MLPNN and SVM classifiers, with MLPNN classifier having an accuracy of 94% and SVM classifier having an accuracy of 85%.

R. Karthik et al. (2019) [23] shown an effective process to distinction ECG signals depending on each other disorders utilizing the Pan Tompkins method and neural networks. The Pan Tompkins method took features from electrocardiography (ECG) signals. Neural networks (NN) was used to recognize and classify signals into four cardiac diseases: sleep apnea, arrhythmia, supraventricular arrhythmia, long-term atrial fibrillation (AF), and a normal heartbeat. Additionally, it proposed a brand-new method for categorizing signals that uses already-in-use NN classification models.

Fajr Ibrahem Alarsan and Mamoon Younes (2019) [24] proposed the discrete wavelet transformer for extracting features from ECG data that could be used as input for classification algorithms. They offered a practical approach for correctly categorising ECG signals. To simplify numerous techniques, including machine learning, they employed Spark-Scala tools (ML). Consequently, Spark-Scala is preferable to other technologies when processing too huge data. Using Spark-machine Scala's learning libraries, various classification methods, including Decision Tree, Random Forests, and Gradient-Boosted Trees, are simple to build (GDB). The findings show that their approach produced overall accuracy for binary classification of 96.75% and 97.98% for the Gradient Boosting tree technique and random forest, respectively. It used Random Forest to obtain 98.03% accuracy for multi-class classification.

Yang, Hui, Zhiqiang Wei (**2020**) [25] Yang, Hui, and Zhiqiang Wei (2020) [28] proposed a novel technique connected with a novel morphological feature via reliable detection and classification of arrhythmias. The ECG signals' activities were first discovered. Then, parametric features of the ECG morphology, such as amplitude, interval, and duration, were retrieved from the selected ECG areas. Then, a novel feature for visual pattern analysis of QRS complex morphological changes and a new clustering-based feature extraction technique were suggested. Eventually, the feature vectors were input into three well-known classifiers for an automated diagnostic test (neural network, SVM, and KNN). As advised by the Association for Progression of Medical Equipment, the suggested approach was tested using a variety of heartbeats from the MIT-

BIH arrhythmia database, and it obtained the highest overall accuracy of 97.70%, depending on KNN.

Sudestna Nahak and Goutam Saha (2020) [26] classified arrhythmia (ARR), congestive heart failure (CHF), and normal sinus rhythm (NSR). For each lesson, they utilized 30 ECG records. features may not be sufficient to identify the classes independently. They considered wavelet-based features, auto-regressive parameters, and feature representations derived from the heart rate variability (HRV) of the ECG signal. They developed feature-level fusion to use complimentary information from several feature kinds. After feature fusion using Support Vector Machine, the maximum accuracy for three- categories classification was obtained (93.33%). (SVM).

Kumari, Ch Usha, et al. (2021) [27] used a machine learning technique referred to as SVM classifier with discrete wavelet transform (DWT). This study included ECG samples from the MIT-BIH and BIDMC databanks for Normal Sinus Rhythm, Congestive Heart Failure, and Cardiac Arrhythmia. The preprocessed data were given a Discrete Wavelet Transform to have 190 features extracted from them. DWT was chosen because it lets window sizes change based on how often something happens. The SVM classifier, which is the best for classification, was given the retrieved features. The data were analyzed using the testing set, and a confusion matrix was employed to organize the results. The accuracy of the model's performance is 95.92 %.

S. T. Aarthy and J. L. Mazher Iqbal (2021) [10] improved the disease classification or prediction ability using a real-time time series. This work offered a fuzzy rule-based Naive Bayes ECG classification and illness prediction technique. The method first redacts noise from the ECG signals that are currently accessible. After the pre-processing and feature extraction were finished, the features were extracted. The technique developed fuzzy rules based on the features discovered for various illness classifications. The proposed technique calculates posterior probability based on mapping various fuzzy rule features. To achieve classification or illness prediction, multi-feature signal similarity (MFSS) was measured. The Cardiac disease-prone weight (CDPW) for different categories was determined using a predicted MFFS value.

XU, Yuefan, et al. (2021) [28] divided the heartbeat approach into two stages: offline training and online classification. Three stages pre-processing, segmentation of the heartbeat, and hybrid feature extraction were used to combine these steps. In the processing stage, median filters eliminated baseline wander from the ECG signals. Next, the continuous pulse signal was divided into distinct heartbeat segments. The RR interval characteristics and wavelet coefficient features of heartbeat signals are extracted. Finally, the trained Extreme Machine learning (ELM) model classifies the online heartbeat signals using the offline training data. The ELM accuracy score is 98.61%.

Reddy, S. Dhanunjay et al. (2022) [29] employed three workflow phases: preprocessing, feature extraction, and classification. A Low Pass Filter (LPF) and a 2-phase median filter were suggested for removing any signaling artefacts for effective feature extraction. Therefore, a preprocessed data was fed into the dynamic ECG feature extraction. Then, with all conceivable kinds of arrhythmia from the MIT-BIH arrhythmia database, the chosen Sampling Vector Random Forest Classifier (SVRF) suggested technique was tested. The suggested SVRF outperforms other known approaches in accuracy, achieving 98.22%.

As shown in Table 1.2, many studies implemented classification systems for ECG signals in various ways under various conditions. This study designed a classification system based on feature extraction and processing for classifying normal and abnormal signals. ECG data used for this work was found in the PhysioNet library to design a device utilized in real data to classify ECG signals. This work is typically similar to the reference [29]. Furthermore, the reference [30] is similar to the current work.

Table (1.2) related work

authors	Published year	Feature extraction methods	Classification Technologies	Accuracy ratio
Bayasi, Nourhan, et al	2015	ESP uses an original collection of ECG characteristics in conjunction with naive Bayes.	Naive Bayes.	86%
Serkan Kiranyaz, Turker Ince, Ridha Hamila and Moncef Gabbouj	2015	1D CNN	1D CNN	97.6%
Kasar, Smita L., and Madhuri S. Joshi	2016	Principal component analysis (PCA)	CART J48 decision tree	92.5% 98.5%
Elhaj et al.	2016	principal component analysis(PCA)	mixed support vector machine and radial basis function	98.91%
S. Sultan Qurraie and R. Ghorbani Afkhami	2017	RR interval	Tree decision	99%
Rajendra Acharya et al	2017	R-peak detection by Pan-Tompkins	CNN	94.03%

Shraddha Singh et al.	2018	Long Short-Term Memory	RNN	85.4%
S Celin and K. Vasanth	2018	Point peak utilizing statistical parameters	SVM, daboost ANN, and Naive Bayes	87.5%, 93%, 94, and 99.7%,
Pooja M Kagalkar and Chaitanya K Jambotkar(	2019	R-peak using Min-Max algorithm	Bayesian	
Syama, S., et al	2019	ECG signal into 8 levels using Haar and Daubechies wavelet methods	MLPNN and SVM	94% 85%
Fajr Ibrahem Alarsan and Mamoon Younes	2019	Discrete wavelet transform	Gradient Boosting tree algorithm random Forest	96.75% 97.98%
Yang, Hui, and Zhiqiang Wei	2020	QRS analysis	neural network, SVM, and KNN	97.70% KNN
Sudestna Nahak, and Goutam Saha	2020	(HRV) and wavelet	SVM	93.33%
Kumari, Ch Usha, et al.	2021	DWT	SVM	95.92%
S. T. Aarthy, J. L. Mazher Iqbal	2021	fuzzy	Naïve Bays	
XU, Yuefan, et al	2021	RR interval and wavelet coefficients	Extreme Machine learning	98.1%
Reddy, S. Dhanunjay, et al.	2022	Sampling Vector Random Forest Classifier (SVRF)	Sampling Vector Random Forest Classifier (SVRF)	

Wang, Tao, et al	2022	RR-intervals, higher-order-statistic, discrete wavelet transform	AdaBoost	

1.4 Motivation

1- According to WHO reports, the world's leading cause of death is heart disease, accounting about 30% of deaths worldwide.

1. Researchers are interested in studying these topics because the success of the research will lead to the development of diagnoses of heart-related diseases and treatment for them, thus saving human life.
2. The trend is designing rapid technologies that save more time and effort to speed up diagnosis with the possibility of applying them in smart devices.

1.5 Research Problems Statement

Through the literature reviews of the ECG signal classification and the methods used for this, some of the problems that have been addressed in this research are indicated

1- The ECG signal is exposed to types of noise that may cause problems in the accuracy of diagnosis. Counting accuracy in the diagnosis may lead to the loss of the patient's life sometimes

2- Classifying ECG signals manually requires a lot of time and effort. The researchers aim to develop automatic classification systems capable of improving efficiency and classification accuracy

3- There are many databases used in the classification of ECG signals. This diversity must be addressed and models and techniques developed that are generalizable to a wide range of databases.

4- Classification of ECG signals requires high accuracy to identify important events such as peaks, maximum values, and cardiac pathologies. Researchers need to improve existing techniques and use artificial intelligence and machine learning to achieve better classification accuracy.

1.6 **Aim and Objectives**

1- Remove the noise from the input signal to increase resolution of training and testing dataset

2- Proposed feature extraction is matching with machine learning algorithms to obtain high-accuracy classification as Wavelet Scattering Transform(WST) and Blind Source Separation(BSS) to get separate of feature embedded three signal(NSR, ARR, CHF) for Neural Network(NN) and Support Vector Machine(SVM)

3- Design two structure of machine learning(Neural Network and Supported Vector Machine) to test performance in classification input signal

4- Design and implement device to classify the signal of ECG and diagnostic some diseases of heart as Arrthmyia(ARR) and Congestive Fauilar Heart(CHF) compare with normal state (NSR)

5- Applied this model to increase framework efficiency in the shortest period of time.

1.7 contribution of this work

1- An ECG biometric system identifies people based on their recorded ECG signal, whereas an ECG classification system differentiates normal (healthy) and abnormal (unhealthy) signals of ECG.

2- Applied wavelet scattering and BSS models are used to extract features for the proposed ECG auto-classification system architecture.

3- Applied One of the previous algorithms on manufactured device by lattePanda

1.8 Outline of Thesis Chapters

Chapter One: overview of ECG signal and related work

Chapter Two: It gives a general background about ECG, Machine Learning, wavelet scattering transform and Blind Sources Separation, also some devices which used to design device for diagnostic diseases of heart.

Chapter Three: Design the Proposed System to diagnostic some diseases of heart and Its Implementation," presents the proposed feature extraction and classification methods with the proposed diagnostic system based on these methods.

Chapter Four: The simulation and implementation results of the designed algorithms

Chapter Five: The conclusions of this thesis and present some suggestions and future works

Chapter two

Theory aspects to classification of ECG signal and analysis methods

2.1 Introduction

The heart is considered among the most important organs in the human body. Therefore, developing a system to monitor its features and functions is critical. Electrocardiography (ECG) is widely regarded as the most powerful medical diagnostic equipment and is regularly used to evaluate the heart's capabilities. The electrocardiogram (ECG) is the standard non-invasive technique for interpreting the heart's electrical activity in real-time. An external device records the electrical cardiac signals by attaching sensors to the external skin surface of the patient's thorax. These streams stimulate the cardiac muscle, causing the heart to contract and relax [1] .

Cardiology has made huge progress in using computers to diagnose physiological data to date clinically. There are many causes for this. For starters, ECG potentials are easy to estimate; second, the ECG is a highly good predictor for both screening and diagnosis. Furthermore, certain ECG abnormalities are well-described and easily identifiable [2].

The majority of ECG analysis applications need precise ECG classification. Software ECG classification has been a focus of study for more than 30 years, and advancements in the computer sciences have shaped algorithmic progress [3]. Designing with FPGAs is hot right now. Microprocessor-based systems constantly improve their memory and computational capabilities while reducing their size, price, and power consumption [4]. In order to construct high-performance digital systems, FPGA-based designing platforms have become essential components. The challenge for monitoring technology is designing an implementable and usable system with low computational, cost, and reliability.

The monitoring system for real data consists of several main parts: input of signal, processing these signals for features extraction and classification as a result of the monitoring operation. Finally, the results are displayed to the patient, the doctor, or/and the family [2] Also, technologies is improved by using the new processor to get the best signals of ECG to give high accuracy diagnosis as LattePanda [1]. LattePanda is represented as mini computer. This project involves an Lattepanda evaluation board for digital monitoring and processing. The board will be connected to a LCD screen as a host to display and monitor the ECG signals via a graphical user interface (GUI). ECG signals are continuously sampled, evaluated, and displayed in real-time on the monitor. This work aims to improve people's lives by saving time, reduce costs, and improving the quality of medical services.

The heart and cardiac electrical system are described in this chapter. In addition, as is the concept for some techniques of machine learning and features extraction methods utilized in this work.

2.2 Real-Time ECG Classification System Using DSP Technology

The digital signal processing (DSP) approach has been used to monitor real-time ECG signals. A DSP processor captures the ECG signal from the patient in real time and transfers it to a computer or LCD screen. Skin electrodes placed at specific locations on the body collect ECG measurement data. ECG signals are typically small and susceptible to the noise of various types, including power line interference, electrode contact noise, and motion artifacts. As a result, measuring the ECG signal is a difficult task [1]. A signal amplifier is used to amplify the ECG signals captured by the electrodes. However, noise may still affect ECG signals after the signal amplifier. As a result, the next step is eliminating different types of noise.

2.3 Electrocardiogram (ECG)

The electrocardiogram (ECG) is a method of capturing heart activity. It is a heart electrogram, which is a visual representation of the signals produced by the heart's electrical activity using surface electrodes [5]. These electrodes pick up on the minute electrical alterations brought on by the heartbeat and cardiac muscle depolarization and repolarization [1]. The normal ECG pattern may be altered by several cardiac disorders, including irregular heartbeat (such as ventricular tachycardia [7] and atrial fibrillation [9]), insufficient coronary artery blood flow (such as myocardial ischemia and myocardial infarction), and electrolyte imbalances (such as hypokalemia and hyperkalemia). The normal cardiac cycle duration is between 0.6 and 1.0 seconds, representing the heart rate or the number of heartbeats per minute (BPM). As a result, the normal heart rate ranges from 60 to 100 BPM. The amplitude is normally in the 1 to 5 mV range [1].

2.4 Formulation of the Electrocardiograph:

An electrocardiograph measures the electrical activity of the heart. To guarantee that it is the heart, it is important to consider the anomalies that vary from a normal abnormality to a fine heartbeat function. The electrical conduction through the heart is understood to follow a fixed pathway in natural conditions. The Electrocardiogram signal seen in Fig.(2.1) below explains the pattern that should be specific for a normal working heart. Even with a minor interruption, the threshold values evaluated by the beat detection system are accurate. The following main formulas should be taken explicitly into account about the intervals and durations [8].

As mentioned earlier, the ECG signal symbolizes the function of the human heart and is made up of a sequence of waveforms, six of which are distinguishable as P, Q, R, S, T, and U waves. A fixed model of waveforms emerges in the case of a subject with a normal heart. A typical ECG waveform, as well as the time intervals, were chosen to take by each waveform from beginning to end [30].

The first wave is a P-wave, which is small and slightly curved. The QRS complex is a sharp mixture wave that consists of a sharp descending Q-wave, followed by the upward R-wave, and finally, a downward S-wave. The final waves, the T-wave and the U-wave are rolled, and a U-wave can be seen on the ECG. The length of the waves on an ECG tracing, the range of allowable amplitudes (voltages), and the topology of the gaps between the waves are all predictable. Any variation from the norm results in the possibility of pathology and has clinical importance. We can explain those details in table (2.1).

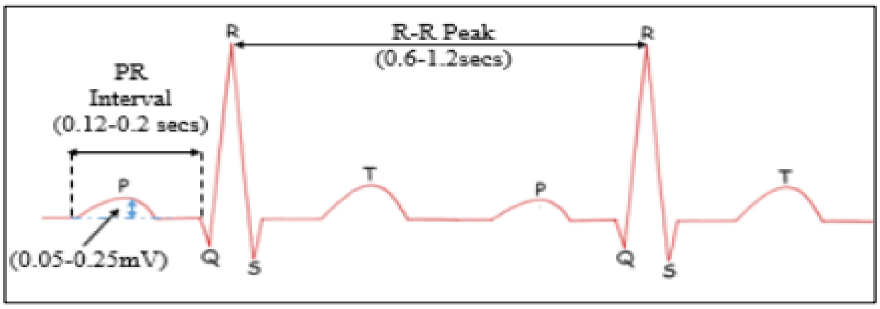

Figure 2.1 Schematic diagram of the ECG signals.

- PR Interval: The PR duration is scaling from the start of the QRS complex to the start of the P wave. Start of the QRS complex.

- QRS Length – The duration of the QRS reflects the time required by the VentricularIt's depolarization. Since the ventriculum has more muscle mass than the atriums, the electrical pulse has a large conduction speed, producing maximum R peaks.
- ST part – While the QRS complex indicates the beginning of ventricular depolarization, the ST segment following the QRS complex is the time while both ventricles are entirely depolarized.
- QT Interval – QT Interval represents the cumulative length and duration of depolarization. Repolarization, which means that it denotes the time the heart needs to contract and then fill up with blood before the next contraction begins.
- T-wave – Ventricular repolarization, commonly called ventricular regeneration, is reflected by the T-wave. The form of the T-wave is rounded sharply or bluntly with an amplitude of less than 5mm.
- R-R Interval-This is the time between QRS complexes. This period plays an important role in assessing the instantaneous heart rate of advanced wearable ECG sensors.

Each wave in a typical electrocardiogram signal has a fairly broad range of values in terms of time and amplitude. Any significant change from these norms may be indicative of a particular arrhythmia. In most cases, arrhythmia results in ineffective blood pumping through the body. Most cardiac arrhythmias are short-term and don't hurt, but some can be life-threatening and must be treated immediately. Sustained Ventricular Arrhythmia is usually caused by a damaged heart muscle and is one of the most serious arrhythmias [9].

The achievement of ECG model classification is robustly based on the properties power of the features that are taken from the signal of ECG and the designing of the classifier (classification pattern) [10]. The method of

ECG classification by R-R interval depends on discrete cosine transform (DCT) conversion [8]. The random tree classifies the beats through applied DCT conversion of RR interval. In some works, two types of arrhythmia are dependent on ECG classification, namely LBB and RBB [11]. Cardiac arrhythmia is classified into 5 kinds,

1- Atrial premature contraction (A)
2- Normal beat (N)
3- Right bundle branch block beat (R)
4- Left bundle branch block beat (L)
5- Premature ventricular contraction (V).

It is important to understand how the heart works. There are four chambers in the human heart: the left atrium (LA), the right atrium (RA), the left ventricle (LV), and the right ventricle (RV). RA and RV have tricuspid valves, whereas LA and LV have mitral valves. These valves impede atrium-to-ventricle blood flow. Also, ventricle valves keep blood from flowing backwards into the veins. Figure (2.2) shows the right ventricle's pulmonary valve and the left's aortic valve.

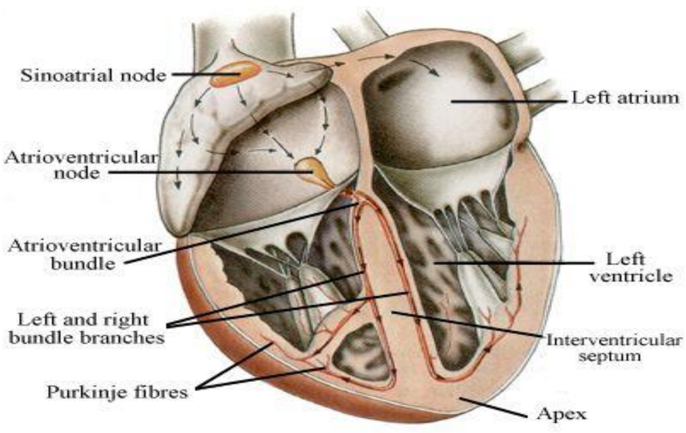

Figure 2.2 Conducting System of Heart

Table(2.1) a waveforms sequence of ECG signal

Feature	Description	Pathology	Duration
P wave	The P wave indicates the atria's depolarization. Depolarization of the atrial extends from the SA node in the heart to the AV node along with the right atrium to the left atrium. .	Unless for a VR, the P wave is usually upright; an atypical P wave axis (inverted in other leads) might suggest an ectopic atrial pacemaker. If a P wave is exceptionally lengthy in interval, it might indicate atrial hypertrophy. A big right atrium often produces a tall, peaked P wave, whereas a large left atrium produces a 2-humped bifid P wave..	<80 ms
PR interval	The period of the P-R is the distance from the start of the P wave to the start of the QRS complex. The period represents the duration it takes for an electrical signal to pass from the sinus node to the AV node.	A P-R duration of less than 120 ms indicates that the electrical signal skips the AV node, as in Wolf-Parkinson-White syndrome. APR durations which are regularly greater than 200 ms are indicative of first-degree atrioventricular insufficiency. In pericarditis, the P-R slice (the tracing section following a P wave and before the QRS complex) may be depressed.	120 to 200 ms
QRS complex	The QRS complex is caused by fast depolarization of the right and left ventricles. Because the ventricles contain more muscle mass than the atria, the QRS complex is a significantly greater	When QRS complex has too lengthy (more than 120 ms), it indicates a problem with the heart's propagation system, as in LBBB, RBBB, or ventricular arrhythmias such ventricular tachycardia. The QRS complex can also be widened by metabolic disorders such as acute hyperkalemia or tricyclic	80 to 100 ms

	amplitude than the P wave.	antidepressant abuse. A very low-amplitude QRS complex might indicate pericardial effusion or infiltrative myocardial disease, while an excessively long QRS complex could indicate left ventricular hypertrophy.	
J-point	The J-point marks the end of the QRS complex and the start of the ST segment.	As a normal version, the J-point may be raised. The presence of a distinct J wave or Osborn wave at the J-point indicates hypothermia or hypercalcemia.	
ST segment	The ST segment links the QRS complex and the T wave; it symbolizes the depolarization of the ventricles. .	It is generally isoelectric, however with myocardial infarction or ischemia, it might be depressed or raised. LVH or digoxin can also produce ST depression. Pericarditis, Brugada syndrome, or a normal variation (J-point elevation) can also induce ST altitude .	
T wave	The T wave reflects the ventricle's repolarization. Except for aVR and leads V1, it is normally straight in all lead	Reverse T waves can be caused by cardiac ischemia, left ventricular hypertrophy, excessive intracranial pressure, or metabolic issues. T waves that have peaked can suggest hyperkalemia or a very early myocardial infarction.	160 ms
Corrected QT interval (QTc)	A QT period represents the time between the start of the QRS complex and the finish of the T wave. However, because permissible ranges	A lengthy QTc period increases the possibility of ventricular tachyarrhythmias and unexpected death. Long QT syndrome can develop as a result of a hereditary disorder or as a side effect of certain drugs. Severe	<440 ms

	change with the heart's rhythm, it has to be adjusted to QTc using dividing by the square root of the R-R duration.	hypercalcemia can cause an abnormally short QTc.	
U wave	The U wave is thought to be induced by interventricular septal repolarization. It has a modest amplitude and, more frequently than not, is totally missing.	A strong U wave might indicate hypokalemia.	

2.5 Noise Types of ECG

Noise greatly influences ECG readings, making automated evaluation challenging. The error is essentially defined by the imperfect signal strength and, as a result, misclassifying the heartbeat, resulting in a misdiagnosis [12]. The signal enhancement is done by filtering process to reduce the noise as suggested by the expert and intended to be investigated in further depth. All of this contributes to an improvement in the signal type and filtering process, both of which are essential components of the analysis of the signals of ECG. Baseline wander, electrode motion artefacts, power line interference, and electromyographic (EMG) noise generated by thoracic muscle activity is the primary noise contributors to ECG signals [1, 13].

These noises make it hard to determine a disease-specific morphological eccentricities of ECG signals [14]. Some common ways of processing heart signals are summed up through rigorous research into the most recent technologies for processing the heart's electrical signal. Using these techniques may lead to inaccurate diagnosis [15] since they involve processing the signal to eliminate any noise that otherwise interferes with it. This section summarizes most noise issues, the most prominent one that can have an impact on the ECG signal and lead to an incorrect diagnosis. Furthermore, it also discusses some of the processing methods used to treat ECG signal noise. There are many different kinds of arrhythmia, and each one has its own set of health problems. Arrhythmias can be found by watching the heart's electrical activity and looking for changes in the shape of the ECG waves [16]

2.5.1 Baseline wander

Baseline wander results from the basis axis (x-axis) of a signal 'wandering' or shifting up and down rather than being straight. The whole signal is therefore diverted from its usual basis. Baseline wander in an ECG signal is caused by bad electrodes (electrode-skin impedance), movement of the patient, and breathing (respiration) [20]. Figure (2.3) shows an perfect ECG signal that is affected by baseline drift. The baseline wander's frequency ranges from 0.5 Hz to 1 Hz. Conversely, with the more vigorous movement of the body or standardized testing, the frequency data of baseline wander increases [21]. To put it another way, breathing and changes to the electrode contact are the two main causes of baseline wander [14, 18].

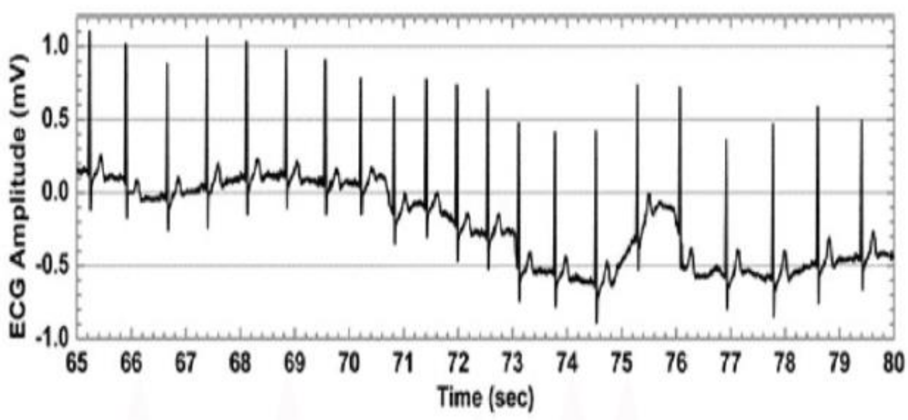

Figure 2.3 An ECG Signal with baseline wander[17]

2.5.2 Powerline Interference (PLI)

Bioelectrical signals and powerline-induced electromagnetic fields contribute to ECG noise. This kind of noise can be described by interference with 50 or 60 Hz sinusoids, which several harmonics may accompany. Narrowband noise complicates ECG interpretation and analysis by leading to misinterpreting low-capacity waveforms and generating spurious waveforms. Additionally, powerline interference entirely superimposes low-frequency ECG waves (P and T); hence these must be eliminated from ECG signals [19, 20]. Figure (2.4) shows how a powerline interfacial changes an ECG signal.

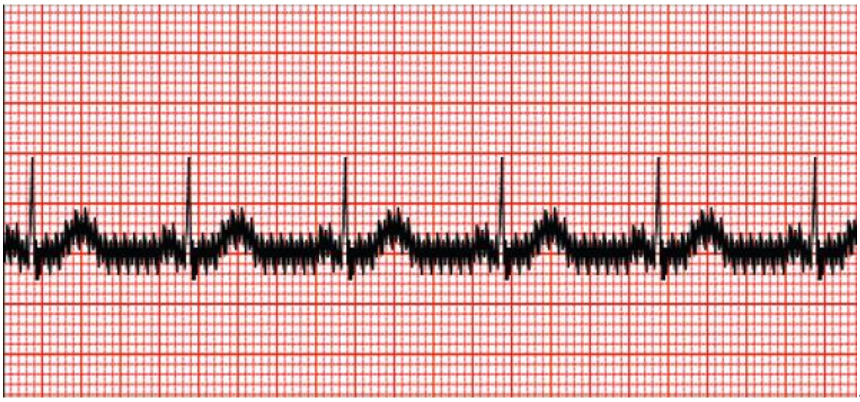

Figure 2.4 ECG affected by powerline (50/ 60 Hz) interference [17]

2.5.3 Artifacts of Electrode Motion

The most frequent reason for electrode interference is for an electrode to be stretched off the skin, which alters the skin's resistance surrounding the electrode. Motion artefacts have comparable signal properties to BLW but are more challenging to overcome because of their high spectrum overlap with the PQRST complex [21]. They occur most often between 1 and 10 Hz. The ECG may display these distortions as large-capacity waveforms inappropriate for QRS complexes [17, 22]. The figure (2.5) explain the noise of artifacts of electrode motion

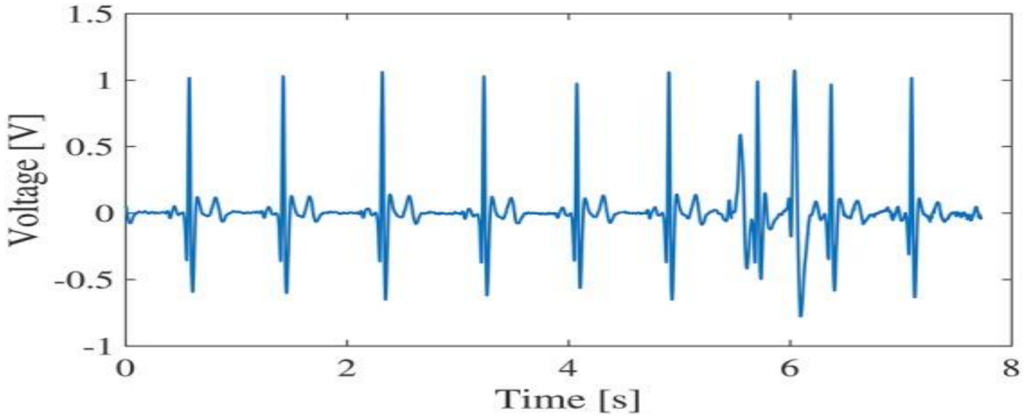

Figure 2.5 Artefacts of Electrode Motion of ECG

2.5.4 EMG Noise

As illustrated in figure(2.6), muscle noise may completely disorganize ECG waveforms, especially during exercise [23]. Narrowband filtering removes baseline wander and 50/60 Hz interference but not muscle noise. Furthermore, muscle function spectrum information considerably overlaps any PQRST complexes, making filtering more difficult [24]. Muscular noise may be decreased utilizing evoked potential processing technology since the ECG is repeated. On the other hand, noise may be reduced by averaging all of the QRS morphologies together; however, this approach is restricted to only one [25, 26] .

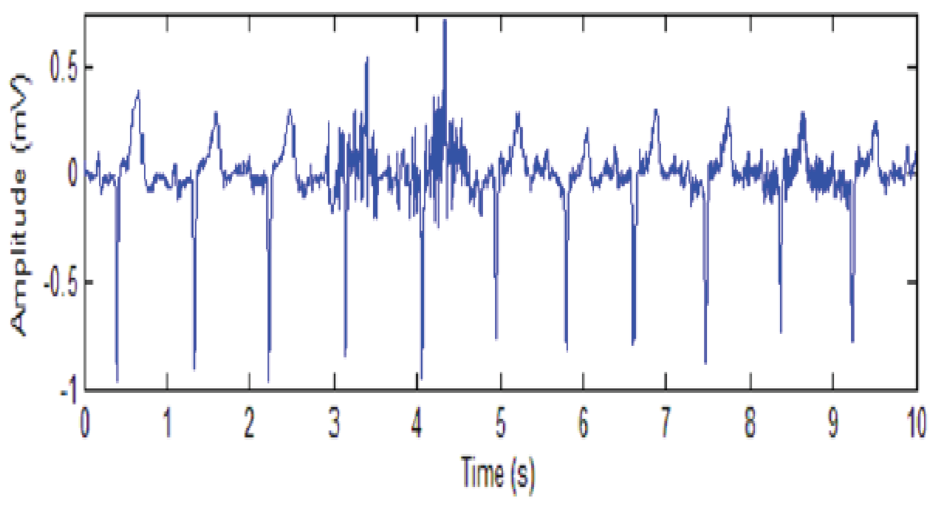

Figure 2.6 ECG signal with electromyographic (EMG) noise

2.6 Database

Databases are used in the model's creation or design. As shown in Figure 2.3, the database has two sections: training sets (D1) and testing sets (D2). For each information set, the dataset is partitioned to balance the number of individuals and the number of heartbeat types [16]. The divide among patients must be considered when dividing the database into training and testing sets. Specifically, to design or create the classifier (D1), choose topics which are not the same as the ones which have been utilized to improve the classifier (D2).

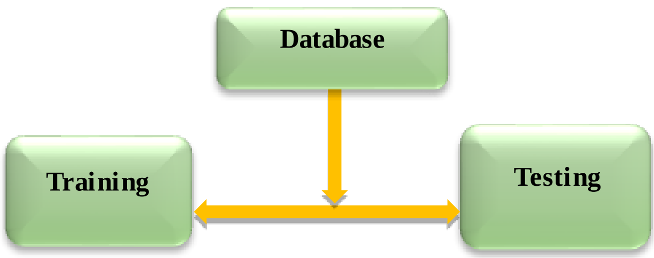

Figure 2.7 database

There are several Physionet databases containing the necessary datasets to create an algorithm. Some of these are a BIDMC Congestive Heart Failure Database, a MIT-BIH Normal Sinus Rhythm Dataset, and the MIT-BIH Arrhythmia Dataset.[31] ARR, CHF, and NSR categories each need around 8 minutes of data from 30 recordings. In addition, a Physionet library's MIT-BIH and BIDMC databases' ECG data have been utilized for the algorithm's verification and validation. For use by biomedical researchers, PhysioBank is a large and growing collection of well--characterized digital recordings of biological signals.

2.7 Signal Preprocessing

Signal processing has been around for a long time, with its technology spanning disciplines such as entertainment, communications, space exploration, biomedical, archaeology, and industrial process analysis and control, to name a few. The study of signals in digital representation and their processing methods are known as digital signal processing. Signal processing is subdivided into digital signal processing and analog signal processing. Signal processing is typically studied in one of the following domains: time domain (one dimension), spatial domain (multidimensional domain), frequency domain, autocorrelation domain, and wavelet domain. The domain will be chosen based on the best representation of the signal's characteristics [1].

Different types of noise pollute the ECG signal, which may be classified as [13]

• Grid of power interruption at 50 Hz (or 60 Hz).

• Noise resulting from a lack of skin-to-electrode interaction.

• Problems resulting from patient motion and electrodes

• Electromyography noise created through electrical reactions in a muscles.

• The more prevalent reason for baseline deviation is breathing.

• Noise from the ECG recording device.

• Noise is produced by other electrical devices.

• Noise in sampling and quantization

Signal processing disturbances

The clinical personnel can handle noise-presenting signals, but automated classification systems are badly impacted, necessitating the need to reduce or remove them by filtering or eliminating signals. As a result, many methods, including low-pass, high-pass and linear-phase filters, have been used to deal with noise. The average median has instead been given a baseline correction using medium-sized and high-pass linear phase filters[14]. Recursive digital filters of the finite impulse response (FIR) attenuate known frequencies, such as the mains' frequency, according to literature study[15]. The signal, however, becomes worthless for detecting the cardiac disease when numerous filters are used. Adaptive neural network filters have been built for the latter scenario, with promising results [16]. The findings are excellent, and the methods based on wavelet transformations are easy to use. Among them, the multi-adaptive bionic wavelet transform has shown even better outcomes.

Nonlinear Bayesian filters and extended Kalman filters are other helpful techniques (they are the ones that have the best effect so far). Finally, the signal-to-noise ratio is a typical metric used to describe the findings.[17], enough research has been done to determine how the preprocessing of the ECG signal affects the output of the classifiers employed after it.

2.8 Machine Learning

Machine Learning (ML) algorithm deals with big data within artificial intelligence in many applications. Data science includes artificial intelligence and statistics [18]. Machine learning algorithms are part of artificial intelligence the figure (2.8). The essential of machine learning is to train the data and give it to a learning algorithm. The learning algorithm is building rules set which depends on the data's conclusion. This is the basic set of a new algorithm. The learning algorithm can be used to create various models using different training data. Machine learning is used to educate machines how to better cope with data. [19, 32, 33].

Sometimes, looking at the data, it cannot expound the pattern or extract information from the data, so we use machine learning. For example, teach the computer to translate languages or predict the stock market using a learning algorithm.

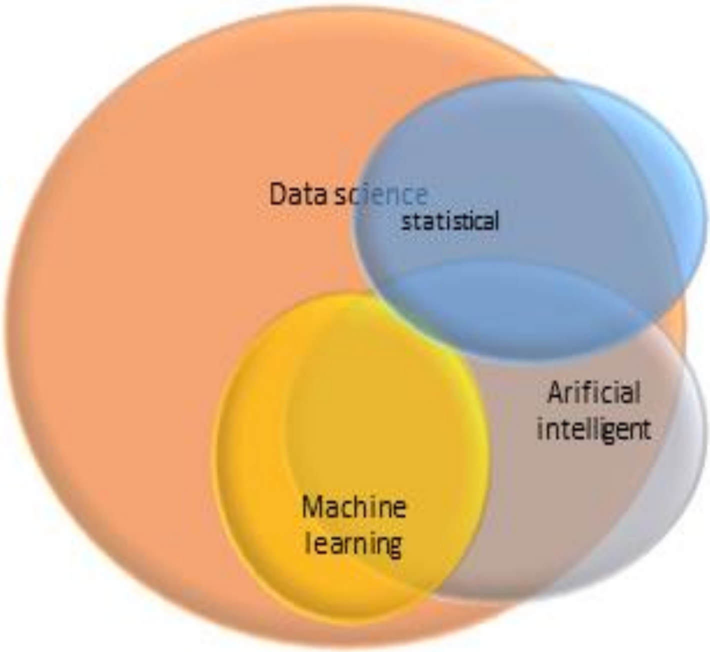

Figure 2.8 the different among science of data, artificially intelligent, statistics and machine learning

Machine Learning is becoming a cornerstone of information technology and, as a result, a rather central, albeit often hidden, part of our lives. With ever-increasing volumes of information available, there is cause to suppose that smart data analysis will become much more prevalent as a necessary component of new technologies[21].

Machine learning strategies are classified into three kinds. supervised, unsupervised, and reinforcement, as shown in figure (2.9)

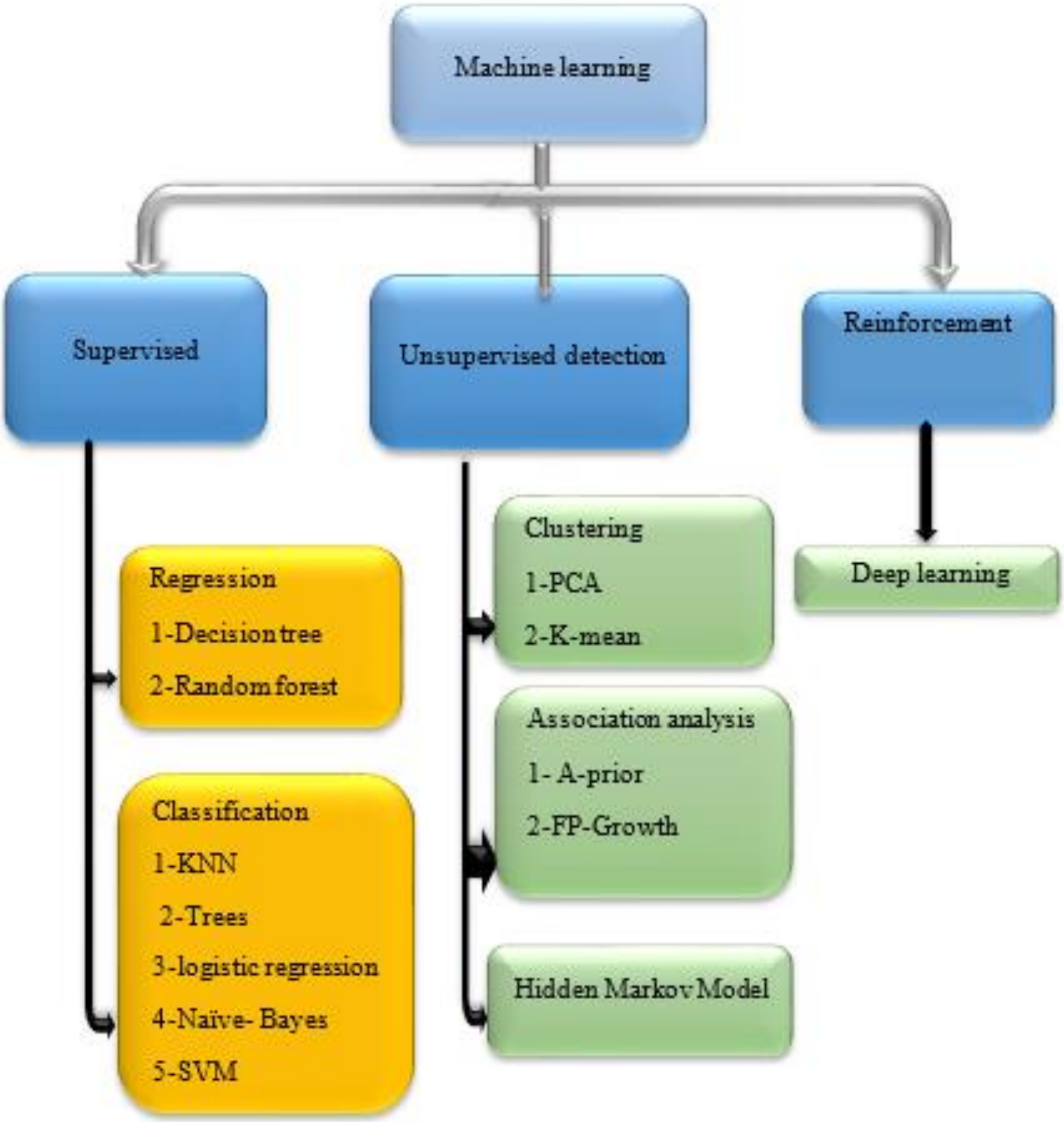

Figure 2.9 Family of Machine learning[12]

Machine learning is used to teach machines more efficient data management. Sometimes after examining the data, we cannot understand the information collected[34]. When that occurs, machine learning is used. The need for machine learning is growing due to the abundance of datasets. Machine learning is used in many fields to pull out useful information. The purpose of machine learning is to learn from data.[35] Numerous research has examined ways to teach machines to learn autonomously without pattern recognition. Many mathematicians and computer programmers use different methods to solve this problem, which involves many data [36].

ML incorporates a range of techniques to solve data challenges. However, scientists who work with data quickly point out that not every issue can be solved with the same method. Instead, the technique depends on the issue's nature, the quantity of variables, optimal model, etc. As a result, ML comes in a variety of forms[37].

2.8.1 Supervised Learning

Supervised learning is the process of using machine learning to create a function that, given instances of input and output combinations, converts an input to an output [38]. It generates a function from labelled training data, that is made up of a collection of training samples. Algorithms for supervised machine learning are those that need outside help. Train and test portions of the input dataset are separated. In other words, Supervised Learning generates a function that converts inputs into the outcomes you want. The training dataset comprises an output variable that must be predicted or categorized [39, 40]

Supervised Learning (SL) aims to learn how to predict the best output vector given a set of input vectors. Classification tasks are applications in which the target labels contain a bounded number of discrete classes. Regression tasks are used when the target labels comprise one or more continuous variables [41] When it comes to data mining, supervised Learning can be split into two kinds of problems: classification and regression:

Classification issues use a technique to precisely categorize test data, while regression employs an algorithm to determine the relationship between dependent and independent variables[42]. Regression analysis is useful for numerical forecasting values utilizing a variety of data points. The supervised Learning can be displayed in Figure 2.10 below

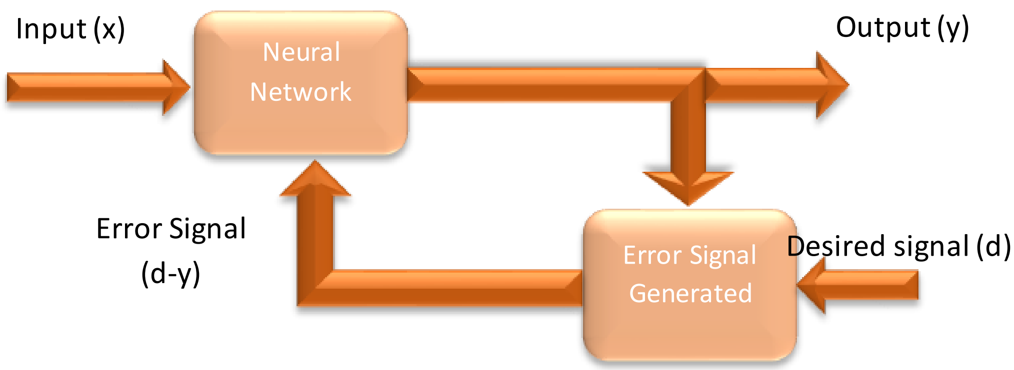

Figure 2.10 Supervised Learning

An ANN's supervised learning paradigm is proficient and finds solutions to various linear and non-linear problems, including classification, plant control, forecasting, prediction, robotics, and so on.

2.8.2 Unsupervised Learning

The capability to absorb and process the information without supplying an error signal to assess the potential solvent is called Unsupervised Learning (UL)[43]. In unsupervised Learning, the absence of guidance for the learning algorithm can sometimes be beneficial because it allows the algorithm to look back for patterns that were not initially thought[44].It is difficult to define the goal of unsupervised Learning. One of the primary aims is to find reasonable clusters of identical samples inside the data of input, a process recognized as clustering[45]. Furthermore, by pre-processing the initial input parameter, the objective might be to discover a suitable internal representation of the input data. and transferring it is now in a new parameter space. [46]. The pre-processing phase, known as feature extraction, can remarkably promote the outcome of the subsequent ML algorithm. The unsupervised Learning can represent by the figure (2.11)[41]

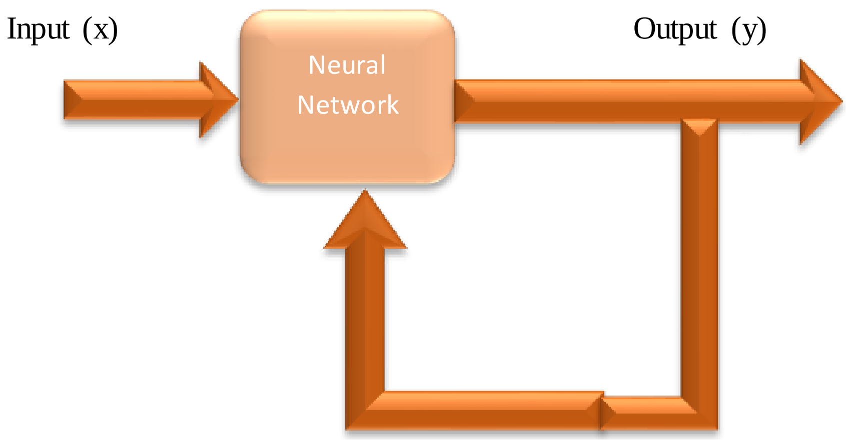

Figure 2.11 Unsupervised learning

UL is so named since, unlike supervised Learning, there are no right answers and no teacher[47]. Techniques are left to explore and reveal a fascinating structure within the data. UL algorithms use the data to learn just a few features. Once new data is introduced, it uses prior knowledge features to identify the data's class. Its primary applications are clustering and extraction of features [48].

2.8.3 Reinforcement Learning

Reinforcement learning is a subfield of machine learning that investigates how software elements should act in certain circumstances in order to improve some concept[49]. One of the three essential machine learning principles is reinforcement learning, which includes both supervised and unsupervised learning. [48].

2.9 Artificial Neural Network

Artificial Neural Networks (ANNs), frequently referred to as neural networks, are innovative systems and computing methodologies for machine learning, understanding demonstration [50], and, lastly, using gained information to improve the final outcomes of complex systems[51]. An Artificial Neural Network (ANN) is a statistical paradigm that depends on how nervous systems that are biological, such as the brain, analyze data. Several artificial intelligence specialists believe that artificial neural networks are the greatest, if not the only, way to develop intelligent machines[52].

The structure of ANN is identical to that of the human brain, with neuron nodes connected in a web-like arrangement. There are billions of neurons in the human brain. Each neuron thus has a cell body that processes data by sending inputs and outputs to and from the brain[53].The fundamental concept behind such networks is (in part) inspired by how the biological neural system processes data and information to acquire knowledge[54]. Creating new frameworks for the information processing system is the main idea behind this notion. Figure 2.12 shows the basic structure of an artificial neural network.

A neuron is the basic processing unit of a neural network. A biological neuron, in essence, receives input from many other sources, integrates it in some way[55], needs to perform a generally nonlinear operation on the outcome, and then outputs the final result.

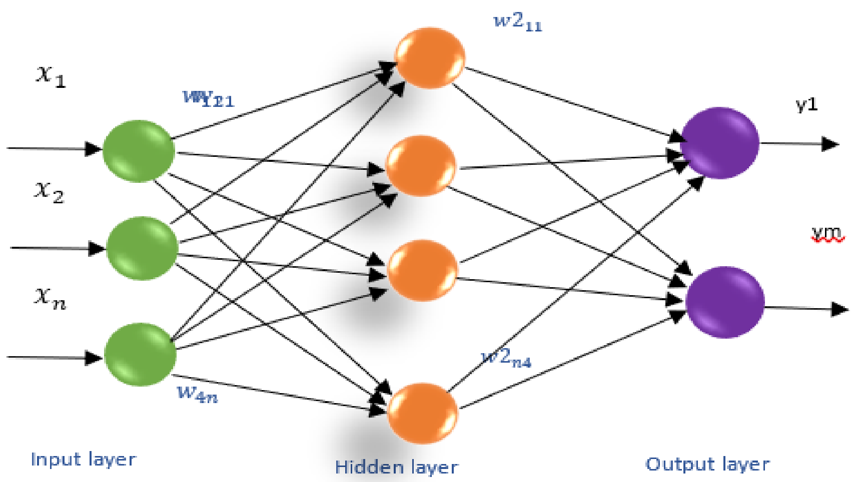

Figure 2.12 Architecture of neural network [33]

The biological names for the four main sections of natural neurons are dendrites, soma, axons, and synapses. Dendrites are growths that look like soma hairs and work as input channels. Synapses connect these input channels to other neurons. The soma then takes the time to process the signals as they come in. The soma then turns the processed value into an output sent to other neurons through the axon and synapses. Each neuron has an activation function and a threshold value, and each connection has a weight[56]. It is determined if each input has a positive or negative weight according to the sign of its weight.

The signal intensity at an interaction is affected by the weight [56]. Neurons have an upper limit beyond that no data is sent until the whole signal surpasses it. The weighted total of the summing units is the Activation amount, and the signal from this activation value is used to generate the output[57]. Figure(2.13) depicts the basis for designing a large neural networks' family

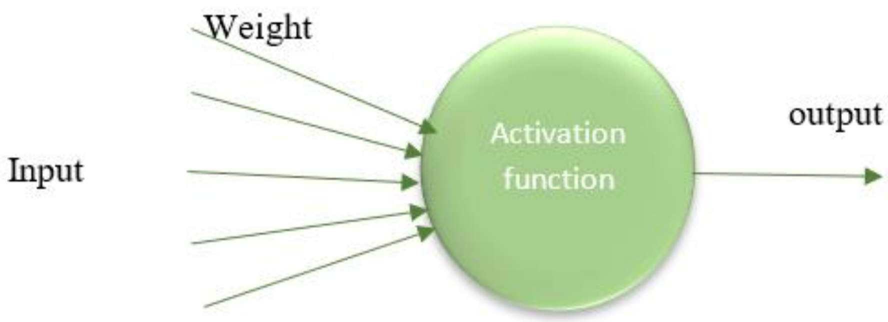

Figure 2.13 ANN system (Input, Output and weight of each element)[58]

As mentioned previously, each neuron model comprises a processing portion with synaptic input contacts and a single output. The signal movement of neuron inputs(x_i) is regarded as unidirectional, as specified by arrows, like is the signal movement of a neuron's output (o)[59]. This graphical representation depicts a set of weights(w) as well as the neuron's processing unit, or node. The following relationship describes the neuron output signal[60]

$$o = f\left(\sum_{i=1}^{n} w_i\, x_i\right) \qquad 2.1$$

where

$$net = \sum_{i=1}^{n} w_i\, x_i) \qquad 2.2$$

$$o = f(net) \qquad 2.3$$

Activation function The activation function (s) expresses neuron output in the form of the activated local field [61].

Three types of activation functions are described below:

- ***The Threshold Function***

a- In this type of activation function ***(Unipolar)***

$$\boldsymbol{f(net)}=\begin{cases} \mathbf{1} & \boldsymbol{x > 0} \\ \mathbf{0} & \boldsymbol{x \leq 0} \end{cases} \qquad \mathbf{2.4}$$

b- The activation function ***(Bipolar)***

$$\boldsymbol{f(net)}=\begin{cases} \mathbf{1} & \boldsymbol{x > 0} \\ \mathbf{-1} & \boldsymbol{x \leq 0} \end{cases} \qquad \mathbf{2.5}$$

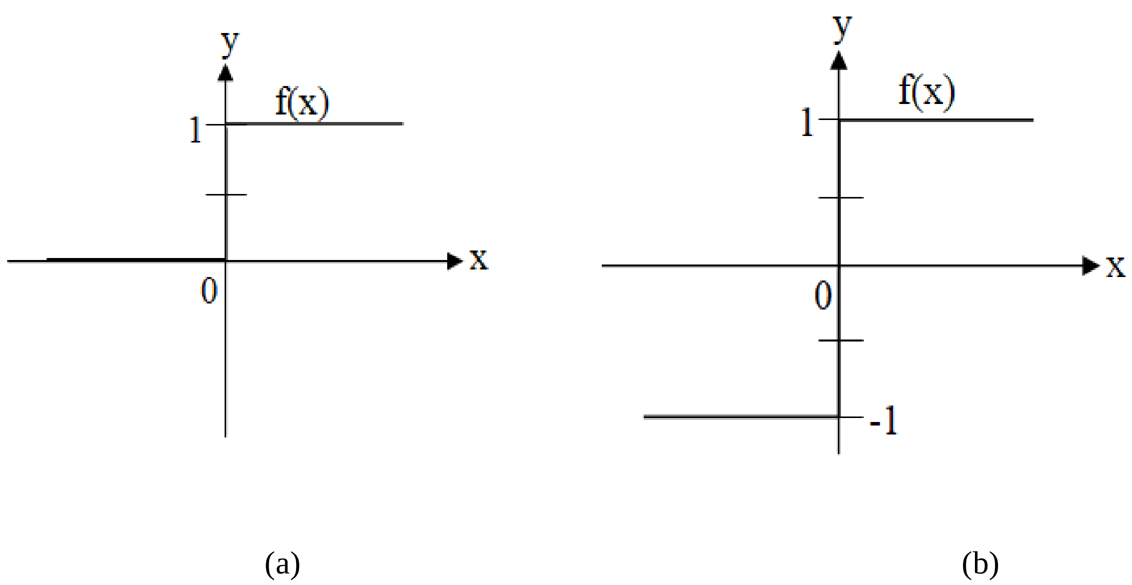

Figure 2.14 Activation functions of a neuron: (a) bipolar continuous and (b) unipolar continuous

❖ **Sigmoidal function**

a- unipolar continuous activation function

$$\boldsymbol{f(net)} = \frac{\mathbf{1}}{\mathbf{1+e^{-\alpha net}}} \qquad \mathbf{2.6}$$

b- bipolar continuous activation function

$$\boldsymbol{f(net)} = \frac{\mathbf{2}}{\mathbf{1+e^{-\alpha net}}} - \mathbf{1} \qquad \mathbf{2.7}$$

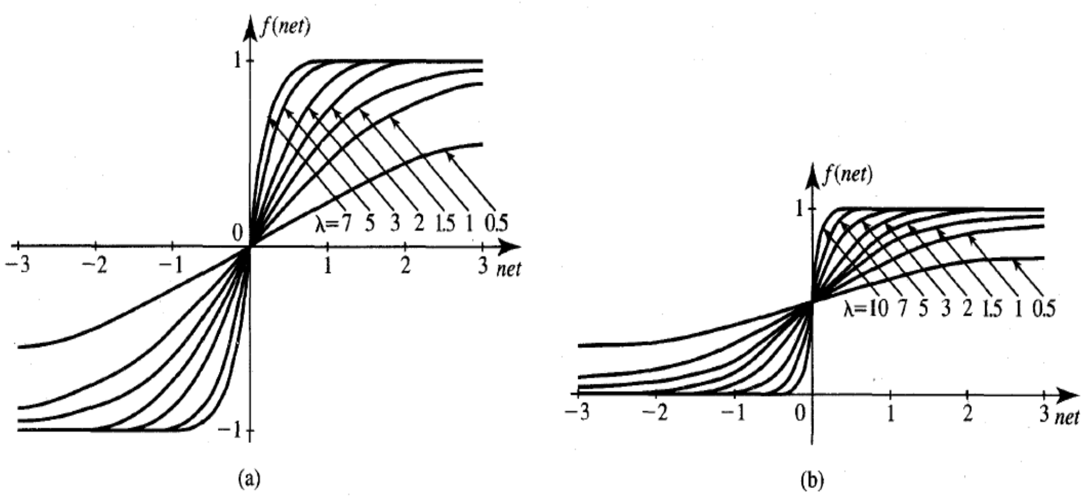

Figure 2.15 Sigmoidal functions of a neuron: (a) bipolar continuous and (b) unipolar continuous

❖ **Hyperbolic tangent function**

$$\boldsymbol{f(net) = tanh(net)} \qquad \mathbf{2.8}$$

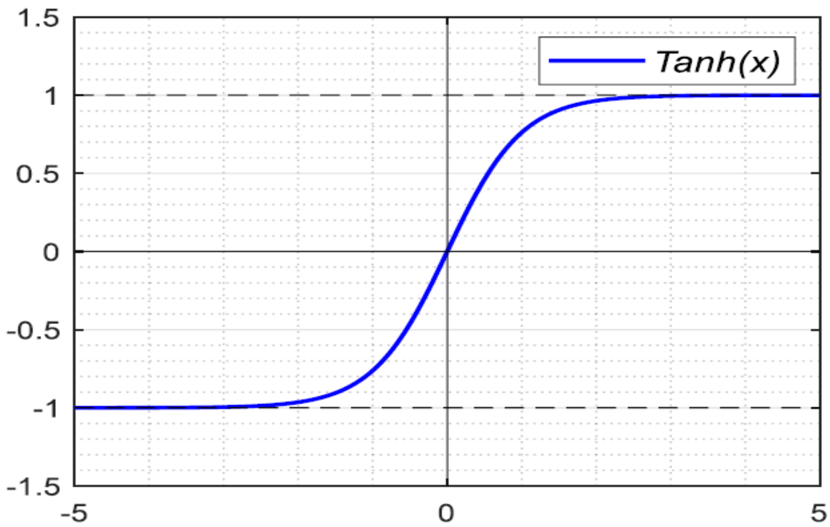

Figure 2.16 Hyperbolic Tangent (Tanh) activation function

2.10 Support Vector Machine (SVM)

The SVM algorithm is widely used in biological as well as other sciences. Support Vector Machine is another popular cutting-edge machine learning technique (SVM)[62]. Support-vector machines are supervised methods of learning through the use of linked learning algorithms that examine data utilized by machine learning for classification and regression analysis. In moreover to linear classification, SVMs can perform non-linear classification efficiently by employing the kernel trick, which involves implicitly mapping their inputs into high-dimensional feature spaces[63]. It essentially draws margins among the categories. The margins are derived wherefore the distance between the footnote and the classes is as small as possible, reducing classification error[42]

SVMs are extremely effective at solving problems of regression and classification. An SVM training algorithm creates a pattern which categorizes new examples into one of two groups, resulting in a non-probabilistic binary linear classifier[64]. The goal of using SVMs is to find the best line in two dimensions or the best hyperplane in more than two dimensions to assist us in classifying our space. Many people prefer support vector machines because they produce significant precision while using less computation power[65].

SVM employs structural risk minimization (SRM) with meets requirements for duplication and convexity. SRM is an inductive concept that chooses a learning pattern from a limited training database [66]. SRM suggests a trade-off between the VC dimensions, which it, the hypothesis of optimization problem and the empirical error, as a criterion of capacity control. SRM's formulation is a convex optimization problem with n variables in the cost function to optimize and m constraints that can be solved in polynomial time. SRM employs a group of patterns that are ordered in increasing complexity [67].

Non-complex models have a large error because a simple model is unable to represent all of the complexity of the signal, resulting in an underestimating condition. As the complexity index rises, the mistake for the optimum pattern (h*) falls before rising again.[68]. For high pattern indices, the framework begins adjusting its learning approach to the training data, resulting in the classifier, which decreases the training error value and tends to increase the model VC at the expense of a worsening test error [67]

The Vapnik Chervonenkis (VC) theory establishes the existence of a VC bound on risk. VC measures the complexity of the hypothesis space. The VC axis represents the greatest number of points that hypothesis H can shatter [69]. H shatters N points if he successfully differentiates all good examples from the negative ones. In other words, the VC capacity equals the number of training points N which the pattren can divide into 2N distinct labels [67]. The value of the training data available determines this capacity. The generalization error is affected by the VC dimension h, circumscribed by /w/where w is the splitting hyperplane's weight component and R is the radius of the lowest sphere including all of the training points. The following properties describe what makes SVM an appealing machine learning structure[70]:

- SVM is a sparse method. SVM, as parametric models, requires which all training data be available, that is, in the memory during the training phase when the SVM model's parameters are learned. However[71], once the pattern variables have been established, SVM utilizes just a portion of all of these training examples., or support vectors, to predict future outcomes[72]. SVM is a sparse algorithm. SVM, as parametric models, require which all training data be accessible, that is, in memory during the training stage while the coefficients of the SVM pattern are learned. meanwhile the pattern variables have been determined[71], SVM just utilizes a portion of these training instances, or support vectors, to predict future outcomes[72]. Support vectors determine the borders of the hyper planes. Support vectors are discovered via Lagrange relaxation after an optimizing phase that includes a target function normalized by an error component and a limitation[73]. The number of support vectors retained from the original dataset is data-dependent and varies according to data complexity (a type separability and data dimensionality)[74]. The maximum value for the total amount of support vectors is 50% of the size of the training dataset, yet in execution, this is frequently achieved[75]. A mathematical description of the SVM model in this section is written as a weighted average of the support vectors, that gives an SVM framework with the exact identical benefits as parametric methods in conditions of decreased computational duration for testing and demands of storage. [76].

- SVM is a kernel method. SVM, like other machine learning techniques, utilizes the kernel function to map the data into a space with more dimensions before resolving the task of machine learning as a convex optimization trouble with analytical instead of heuristic optimization. In the main input space, real-world data can sometimes be separated by linearity. In this case, because cases with multiple labels overlap the input space [78], a linear hyperplane cannot distinguish between all of the categories involved in the classification task. Since the split surface will at least be of the second order[79], Trying to learn a nonlinear separation limit in the input space raises the computational requirements within the optimization phase [80]. SVM, on the other hand, transfers the input into a new but higher-dimensional space in which a linear separator may differentiate between the various categories using predetermined kernel functions.. As a result, the SVM optimization phase will only involve learning a linear discriminant surface in the mapped space. Of course, the kernel function's selection and settings are critical for SVM performance [81].

- The maximum margin separator is SVM. SVM enforces an extra limitations on the optimal control trouble:[82] the hyperplane must be defined as close to the various categories as possible. Therefore lowering the error or implementing a cost function depending on the training databases (like with other discriminant machine learning algorithms) [83]. Since it is at an equal and highest separation from the categories, it compels the optimum control step to discover the hyperplane that will ultimately general well.[84]. It is critical because a selected portion of the population is trained., whereas prediction is made on yet-to-be-seen instances with a distribution that may differ slightly from the subset trained on[85].

Large Margin Intuition

In SVM, we take the output of the linear function and identify it with one class if it is greater than 1, and another class if it is less than 1. Because the threshold values in SVM are changed to 1 and -1, we get this reinforcement range of values ([-1,1]) that acts as a margin[86].

To segregate the data, several linear classifiers (hyperplanes) are employed. However, just one of these accomplishes maximal isolation. We need it since using a hyperplane to classify[87] may result in it being closest to a specific set of datasets than others, which we don't want to happen, as seen in figure (2.17). As a result, we regard a maximum margin classifier or hyperplane as an apparent solution[88]. The figure below depicts an optimal margin classifier instance that addresses the recently discussed problem[89].

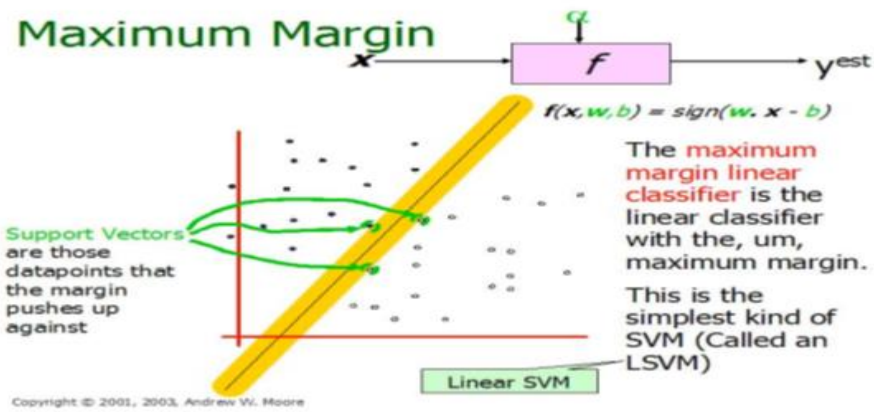

Figure 2.17 Linear SVM illustration [2]

Because they are utilizing example plotting to assist students comprehend the ideas involved in it, the narrative is not explained.The SVM method is a classifier that tries to find a hyperplane or function that perfectly distinguishes two classes with the greatest margin of error[90].

$$\boldsymbol{f(x) = x.w + b} \qquad \textbf{2.9}$$

Where

x: Input, w: weight b: bais

The goal of calculating the SVM is to classify all of the data accurately. We have mathematical formulas

a) $\boldsymbol{wx_i + b \geq 1 \quad when\ Y_i = +1}$
b) $\boldsymbol{wx_i + b \leq 1 \quad when\ Y_i = -1}$
c) $\boldsymbol{y_i(w_i + b) \geq 1 \qquad for\ all\ i}$

By maximizing the x, we can find the distance between the closest point on the hyperplane and the origin. Similarly, we have a similar incident for the other side points.[91] Solving and subtracting the two distances yields the summation distance between the separating hyperplane and the nearest points. Maximum Margin (M) is

$$\boldsymbol{M = \frac{2}{\|w\|}} \qquad \textbf{2.10}$$

Where

w: weight

2.11 Wavelet Scattering Transform

The Wavelet Transform (WT) is a popular tool for analyzing transient and non-stationary signals as well as image texture. It can categorize signals in both the scopes of time and frequency at the same duration, though a few restrictions have been identified[92].

A wavelet scattering transform produces translation-invariant, stable, and informative signal representations. It is resistive to deflections and maintains its capacity to discriminate across categories[93], which makes it particularly valuable for categorization. We identify with it because of its outstanding job success in categorization. We could certainly follow the annotation in [1]. Let f(t) denote the signal in question.. The low-pass filter and wavelet function is intended to create filters encompassing the entire frequency local and produce translation invariant explanations of (*f*) at a specific scale T.[94] Λk denotes the set of wavelet indices with an octave frequency resolution Q_k. Multiscale high-pass filter banks (ψ_j) can be formed by extending the wavelet. S0 f(t) = f ⋆ϕ(t) provides a regional generate translation invariant characteristic of *(f)* and results in a lack of high-frequency signals information[95]. Those lost high frequencies can be recovered using a wavelet flexible modulus transform.

$$|\boldsymbol{W_1}|\boldsymbol{f} = \left\{\boldsymbol{S_0 f}(\boldsymbol{t}), \left|\boldsymbol{f} * \psi_{\boldsymbol{j1}}(\boldsymbol{t})\right| \right\}_{\boldsymbol{j1}\in\boldsymbol{\Lambda 1}} \qquad \textbf{2.11}$$

The first-order scattering coefficients are obtained by average the wavelet operand parameters with ϕj

$$\boldsymbol{S_1\, f(t)} = \{|\boldsymbol{f} * \psi_{\boldsymbol{j1}}| * \boldsymbol{\phi J}\ (\boldsymbol{t})\}_{\boldsymbol{j1}\in\boldsymbol{\Lambda 1}} \qquad \textbf{2.12}$$

We may obtain complementary high-frequency values of coefficients to recover the information lost owing to averaging by taking $S_1\ f(t)$as the low-frequency component of $|f * \psi_{j1}|$ |, as illustrated below.

$$|\boldsymbol{W_2}||\boldsymbol{f} * \psi_{\boldsymbol{j1}}| = \left\{\boldsymbol{S_1 f}(\boldsymbol{t}), \left||\boldsymbol{f} * \psi_{\boldsymbol{j1}}| * \psi_{\boldsymbol{j2}}(\boldsymbol{t})\right|\right\}_{\boldsymbol{j1 \in \Lambda 2}} \qquad \textbf{2.13}$$

In second -order of scattering coefficients

$$\boldsymbol{S_2\ f}(\boldsymbol{t}) = \{|\boldsymbol{f} * \psi_{\boldsymbol{j1}}| * \psi_{\boldsymbol{j2}} * \boldsymbol{\phi J}\ (\boldsymbol{t})\}_{\boldsymbol{j1 \in \Lambda i}} \quad i = 1,2, \dots \dots \qquad \textbf{2.14}$$

The above approach is iterated to produce wavelet integrand convolutions.

$$\boldsymbol{U_m\ f}(\boldsymbol{t}) = \{\ \left||\boldsymbol{f} * \psi_{\boldsymbol{j1}}| * \dots |* \psi_{\boldsymbol{jm}}|\right|\}_{\boldsymbol{j1 \in \Lambda i}} \qquad \boldsymbol{i} = \textbf{1,2,...,m} \qquad \textbf{2.15}$$

Scattering coefficients at m-th order

$$\boldsymbol{S_m\ f}(\boldsymbol{t}) = \{|\boldsymbol{f} * \psi_{\boldsymbol{j1}}| * \dots . |* \psi_{\boldsymbol{jm}}| * \boldsymbol{\phi J}\ (\boldsymbol{t})\}_{\boldsymbol{j1 \in \Lambda i}}\ \boldsymbol{i} = \textbf{1,2,...,m} \qquad \textbf{2.16}$$

The final matrix of scattering is

$$\boldsymbol{S_m\ f}(\boldsymbol{t}) = \{\ \boldsymbol{S_m\ f}(\boldsymbol{t})\}_{\boldsymbol{0 \leqslant m \leqslant l}} \qquad \textbf{2.17}$$

In brief, Wavelet scattering (or scatter transform) produces a representation that is fixed to data rotation/translation and steady to data deformations[96]. Non-informative variations in your data, such as a timeshifted audio sample, are discarded. Information for subsequent tasks, such as classification, is saved[97]. Wavelet scattering requires no training and works well with small amounts of data. Figure (2.18) depicts the scattering process. The scatter representation comprises averaging/low pass filter coefficients, order 1 wavelets, and order 2 wavelets. Correct (x) is directly impacted after implementing a displacement field that has mostly covered up the original structure of the signal with a sine wave[98].

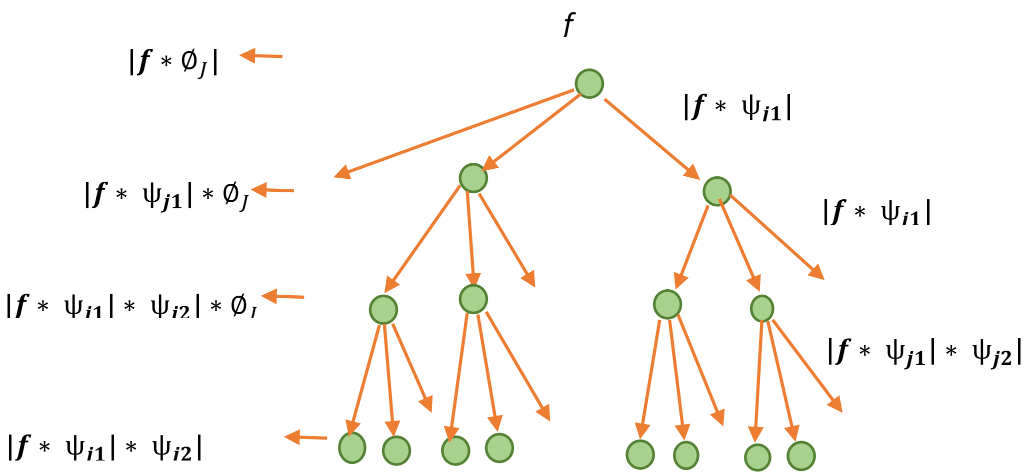

Figure 2.18 the tree network of wavelet scattering

2.12 Blind Source Separation

blind source separation is also known as blind signal separation. In a nutshell, it is a separate set of signals that come from a mix of sets of sources without any assistance or with very basic information about the input signals. Previously[99], researchers concentrated solely on how to separate space-time signals such as audio. In today's world, BSS is used in many fields, such as images and tensors, which are multidimensional data with no time dimension[100].

Blind source separation (BSS) has been investigated for decades, and the research is still ongoing. The expression "blind" indicate to a scenario in which the source operations and information about the mixing scheme are unidentified[101]. For example, for BSS, Consider a room with a number of people revealed and many microphones for recording. When one or more people speak simultaneously, each microphone records a unique mixture of audio signals from each speaker[102]. BSS's job is to separate these mixtures into their sources, the audio signals from individual speakers. This is a tough problem in general due to several complex factors. Even if audio signals are concentrated on, a variety of diverse objectives for creating this technology, For example, extracting the desired language in a noisy setting to improve recognition of speech outcomes. [103] .

Multiple observations are performed by an array of sensors to recover the initial mixing of the source signals in blind source separation (BSS)[104]. The concept "blind" describes that no specific information about the concrete mixture or the existing source signals is available. The BSS technique is depicted schematically in Figure (2.19)[105]

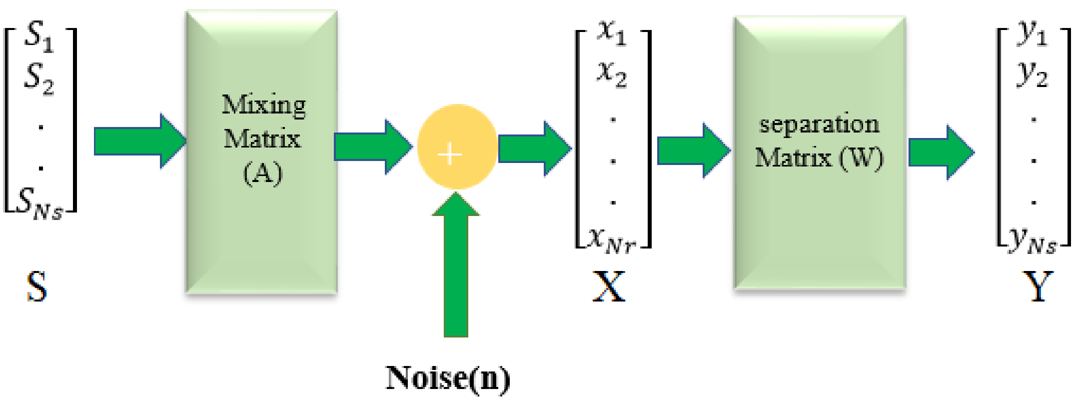

Figure 2.19 Blind source separation scheme [106]

$$\boldsymbol{S(t) = [S_1(t), S_2(t), S_3(t), \ldots\ldots, S_{Ns}(t)]^T} \qquad \textbf{2.18}$$

S(t) is represented the original signal; following that, matrix A will completely at random mix all resources to produce the mixture matrix[107]

$$\boldsymbol{X(t) = [X_1(t), X_2(t), X_3(t), \ldots\ldots, X_{Ns}(t)]^T} \quad \textbf{2.19}$$

$$\begin{bmatrix} X_1(t) \\ X_1(t) \\ . \\ . \\ X_{Ns}(t) \end{bmatrix} = \begin{bmatrix} a_{11} & a_{12} & \ldots . a_{1N} \\ a_{21} & a_{22} & \ldots . a_{2N} \\ . & & . \\ . & & . \\ a_{N1} & a_{N2} & \ldots . \; a_{NNs} \end{bmatrix} \begin{bmatrix} S_1(t) \\ S_1(t) \\ . \\ . \\ S_{Ns}(t) \end{bmatrix} \Rightarrow X(t) = AS(t) \quad \textbf{2.20}$$

The equation above depicts the particular computational formula of blind source separation. There is no noise in the model.

The primary goal of BSS is to obtain the source signal. It is accomplished by combining A or the inverse of A. The un-mixing matrix W is the inverse of matrix A[108]

2.13 Discrete Wavelet Transform (DWT)

A signal is decomposed into a set of reciprocal orthogonal wavelet basis functions by the Discrete Wavelet Transform (DWT). These functions differ from sinusoidal fundamental functions as they can be spatial restricted, that is, they are nonzero only for a fraction of the whole signal duration. Wavelet functions are also dilated, translated, and scaled versions of the mother wavelet expression. The DWT, like Fourier analysis, is injective, which means that the original signal can be recovered completely from its DWT representation [109] The capability to extract local spectral and temporal information is the primary advantage of the Wavelet Transform over the Fourier Transform. The Wavelet Transform can be used to analyze ECG signals that comprise periodic transient signals of importance.

The DWT refers to a group of transforms with wavelet basis functions. The Haar wavelets and the Daubechies wavelets are two of the most common as explain in figure (2.20).

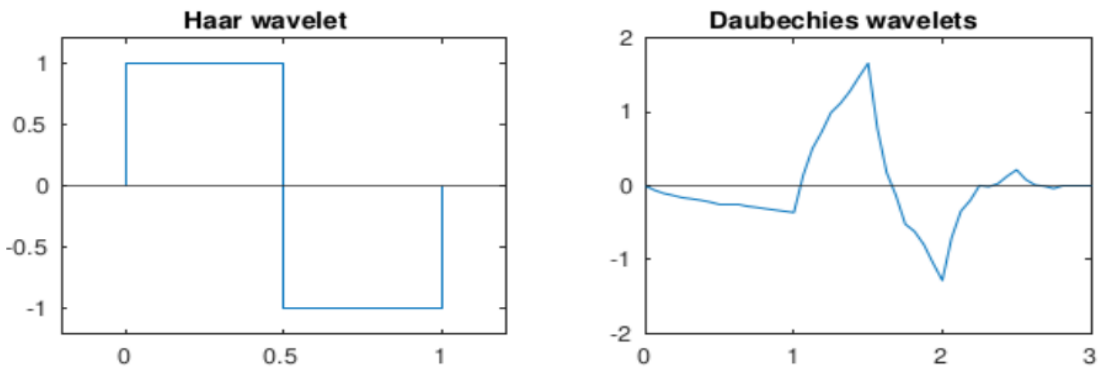

(a) (b)

Figure 2.20 Discrete Wavelet Transform (a) Haar Wavelet (b) Daubechies Wavelet

In DWT, the most significant data displays at high amplitudes, whereas the least important information shows at extremely low amplitudes. By discarding these low amplitudes, data compression can be accomplished. The wavelet transforms allow high compression ratios with good reconstruction quality[110]. The discrete wavelet transform employs low-pass and high-pass filters, h(n) and g(n), to extend a digital signal. They are known as analysis filters. A decimator is now used to perform the dilation for each scale. The coefficients are obtained by converging the digital signal with each filter and decimating the output.

The coefficients are called coarse coefficients because they are produced by the low-pass filter, h(n). The high-pass filter generates the coefficients known as detail coefficients. Detail coefficients provide information about high frequencies, whereas coarse coefficients provide information about low frequencies[111]. Coarse and detail coefficients are produced at multiple scales by iterating the process on the coarse coefficients of each scale. A tree-structured filter bank is used to compute the entire process.

A signal x's DWT is determined by exceed it during a series of filters. The samples are first run through a low-pass filter with impulse response g, which results in a convolution of the two:

$$\boldsymbol{y}[\boldsymbol{n}](\boldsymbol{x} * \boldsymbol{g})[\boldsymbol{n}] = \sum_{\boldsymbol{k}=-\infty}^{\infty} \boldsymbol{x}[\boldsymbol{k}]\boldsymbol{g}[\boldsymbol{n}-\boldsymbol{k}] \qquad \textbf{2.21}$$

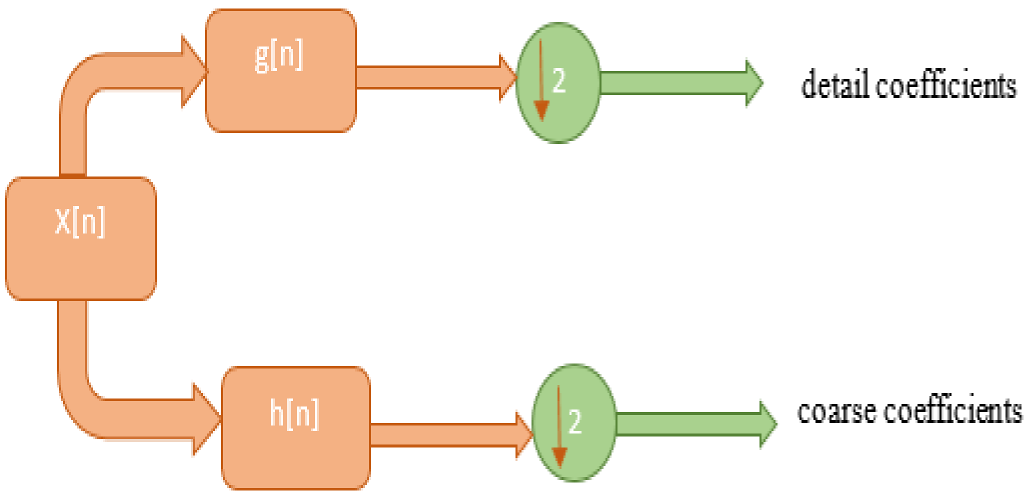

Figure 2.21 Discrete Wavelet Transform(DWT) system

Furthermore, since 50% of the frequencies in the signal were recently removed, a half of the samples may now be disposed of depend on Nyquist's rule. The filter result of the low-pass filter g in figure (2.21) is then subsampled by 2 and further handled by running it across another low-pass filter g and a high-pass filter h with a frequency cut-off that is half that of the previous one[112].

$$y_{low}[n] = \sum_{k=-\infty}^{\infty} x[k]g[2n-k] \qquad \mathbf{2.22}$$

$$y_{high}[n] = \sum_{k=-\infty}^{\infty} x[k]h[2n-k] \qquad \mathbf{2.23}$$

The discrete wavelet transform has several uses in science, engineering, mathematics, and computer science. It is typically utilized for signal coding, which is intended to demonstrate a discrete signal in an increased repeated form, frequently as conditioning for data reduction. Real-world applications include signal excitation analysis for gait evaluation, image processing, digital communications, and a range of other domains.

The discrete wavelet transform [113] (discrete in scaling and shift but continuous in time) is effectively applied as an analog filter branch in biomedical signal processing for the creation of low-power pacemakers and ultra-wideband (UWB) wireless communications.

2.14 Notch filter

Notch filters are band-reject or stop-band filters constructed to provide the highest attenuation or rejection to a specific frequency range. A notch filter is a band-reject filter with a restricted stop band. Notch filters are utilized in various tasks, such as signal processing, detection, and filtering [114]. This can be used to reduce noise in a signal or to decrease the bandwidth of a signal without altering the frequency. Notch filters are also important in removing unwanted radio frequency signals in various applications, including radar systems, Broadband wireless networks and satellite communications are two examples. Furthermore, in order to account for resonant styles, servo motor control mechanisms typically need a notch filter in addition to the normal PID regulator. There are two regions for the notch filter, as shown in figure (2.22).

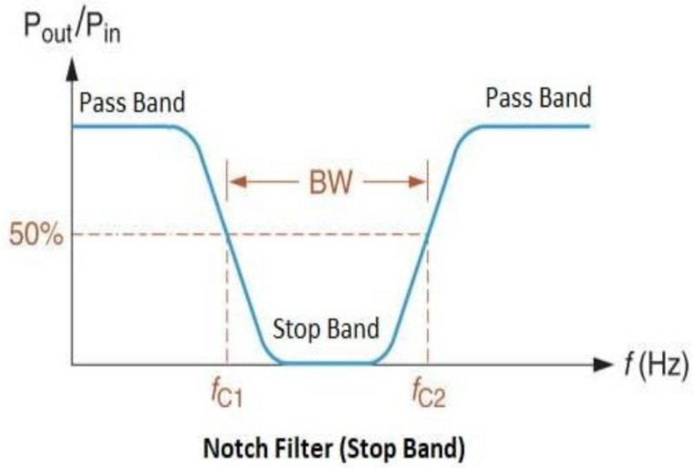

Figure 2.22 Notch filter regions

Most of the time, it is best to limit application to transfer ratios with only two complex conjugate poles. A cascade of simplified circuits of the type and one or more passive RC networks can achieve any given transfer function[115]. A second-order notch filter's classic transfer function is

$$\boldsymbol{H(s) = \frac{s^2+\omega_0^2}{s^2+\frac{\omega_0}{Q}s+\omega_0^2}} \qquad \textbf{2.24}$$

where: ω_0 is the natural frequency and Q is the quality factor of the filter (tied to the filter bandwidth after $Q = \frac{f_0}{\Delta f}$). The inherent frequencies of the zero and pole pair must match to achieve symmetrical gains in the passband and strong reduction at the target frequency.

2.15 Adaptive Filter

Adaptive filters, on the other hand, have coefficients that can change over time. They are utilized when the best filter response for a specific task is unknown a priori or if the nature of the operating conditions is expected to shift over time[116]. For example, a normal system goal would be for a filter to repress unwanted noise as much as possible while leaving the target signal alone. This filter has the following advantages:

• quick response time when filtering data.

• lower error rates.

• filter works effectively in a variety of situations.

2.16 confusion matrix

A confusion matrix is a standard way for displaying the classification effectiveness of any classifier. A confusion matrix displays different actual/wanted categories, whereas columns represent anticipated categorization. Every diagonal cell in such a matrix represents the total amount of samples successfully categorized for the relevant class label, as represented by the related row/column label[117]. Any cell which is not on a diagonal indicates a category that was erroneously categorized.

Metrics of Performance. Class sensitivity (Se), class positive predictivity (Pp), and overall accuracy are used to assess classification performance. The percentage of samples with positive model predictions in those with positive labelled data is reflected in category sensitivity. The percentage of samples with true positive labels in all samples with positive model predictions is denoted by e-class positive predictivity[118].

Metrics of performance Previous studies employed a variety of metrics. To validate our method, we use four generally utilized metrics (precision, recall, f1, and accuracy) that are formally defined:

- $ACC = \frac{Tp+TN}{TP+TN+FP+FN}\%$ **(2.25)**
- $+P = \frac{Tp}{Tp+Fp}\%$ **(2.26)**
- $Se = \frac{Tp}{Tp+FN}\%$ **(2.27)**
- $Er = \frac{FN+FP}{TP}\%$ **(2.28)**

Where Se: sensitivity, +P: positive predictive, FN: False Negative, FP: False Positive, Acc: accuracy and Er: Error

2.17 LattePanda

LattePanda is a single-board computer (SBC) that first appeared in 2016. Its small size and the fact that it runs a full version of Windows 10 make it a popular choice among developers, hobbyists, and enthusiasts looking for a compact and versatile computing platform[119]. It is powered by an Intel Quad Core processor with 3-ports of USB, integrated WiFi, and Bluetooth 4.0. It as well comprise an Arduino co-processor, which allows you to control Interacting equipment utilizing thousands of plug-and-play peripherals to master the physical world. Instead of a laptop, we will utilize this processor, which can perform comparable functions to a computer by being pre-programmed[120]. It has everything a standard PC has and can do everything a standard PC can do. It works with almost every device you own, including printers, joysticks, cameras, and more. Any peripheral that works on a PC will also work on a LattePanda. A LattePanda also has an integrated Arduino-compatible co-processor, allowing it to control and sense the physical world[121]. A LattePanda single board computer can help your creative process whether you are a Windows provider, IoT developer, DIY enthusiast, interactive designer, robotics whiz, or maker!

Since LattePanda V1.0, we have modified the processor. As a result, all LattePanda models now include an upgraded CPU (Intel Z8350 - up to 1.92GHz), the figure (2.23) explain the general of lattepanda

Figure 2.23 Lattepanda

2.18 Health Sensors

The sensor is an electronic apparatus that converts physical parameters into electrical signals [122]. For various applications, different sensors are used. Sensors with low power, fast response time, and low cost are commonly used.

Biomedical sensors are sensors that are linked to the human body and are used in health care applications. Biomedical sensors convert signals representing biomedical variables into electrical or optical signals. As a result, the biomedical sensor functions as a link between a biological and an electronic system[123]. Biomedical sensors are divided into two categories based on their interaction with the patient's body. The invasive sensor, which is positioned inside the body, is the first of a kind (or some types of surgically). The second type is the non-invasive sensors located on the body's surface or does not even need to encounter the authority to perform their measurements[122].

The advancement of biomedical sensing technologies results in the modernization of medicine, which includes micro, smart, non-invasive, and remote control [124]. Biomedical signs have irregular and vulnerable characteristics, as well as interference and sharp noise, and they allow for dynamic change. As a result, biomedical calculation techniques are more complex and dependable than standard automated detection technology. It includes biological, physical, and chemical signal detection. For instance, consider the following:

- EMG, ECG, and EEG are electrophysiological signals.
- Physiological signals that are not electrical, such as body temperature, blood pressure, breathing, pulse, and blood flow.
- Urine and blood are biological or chemical signals.
- Proteins, enzymes, antigens, and antibodies are examples of biological signals.

Physical and biomedical sensors are classified into four groups based on their signs (Figure 2.24). Group 1 addresses X-ray sensors as radiation sensors and gamma-ray-based sensors. In addition, ultrasound and class 2 mechanical sensors, such as pressure, are included.

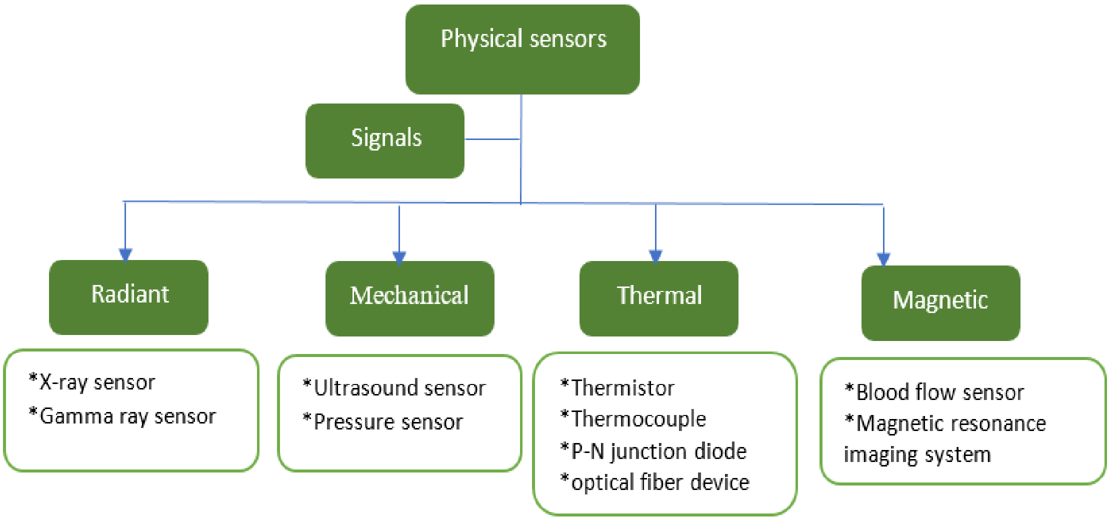

Figure 2.24 Classification of physical sensor concepts in biomedical applications

The advancement in medical sensor technology has significantly changed the traditional situation, influencing the orientation of smart improvement, small, multi-parameter, remote, and quasi-control, as well as making some major technological advances[125]. The medical sensor technology revolution assists in creating sensors in medical technology.

ECG Sensor

The AD8232 ECG sensor is on special offer. The board is used to calculate the electrical activity of the human heart. This action can be graphed like an electrocardiogram, with the output being an analog reading[126]. As illustrated in Figure (2.25), the AD8232 ECG sensor was chosen for our system because it is appropriate for laboratory tests, is small, and inexpensive. We will use it to obtain a person's heart rate and then send it to the suggested method via Arduino. Ad8232 has multiple probes on the human body for sensing purposes.

Figure 2.25 The AD8232 ECG sensor

Chapter Three

Design and Implementation the Proposed ECG Classification System

3.1 Introduction

The main objective of this research is to find reliable methods to classify the ECG signal and to obtain an accurate diagnosis of heart diseases through the correct extraction of features of ECG signals of people whether they suffer from a heart disease or not, as well as the design of many practical applications such as ECG monitor devices or classify it. This work is divided into two parts: theoretical and practical parts, theoretical is doing by simulation using MATLAB 2019b with many algorithms. Practical part, one of the algorithms used during the theoretical part has been verified experimentally using LattePanda hardware .

The theoretical and simulation part is consisting of three major stages: pre-processing, feature extraction, and classification as illustrate in figure (3.1) below. All of the mentioned theoretical stages are preceded by the entry of data from the MIT-BIH and BIDMC databanks. Whist the experimental and validation part is that one of feature extraction with classification algorithms will be used on panda device which the processor analyzes recorded heart signals from several people then classify it.

Various techniques were employed to analyze the ECG signal in order to achieve the best performance for determining the condition of the person being tested. The experts were given the most credit for the modern medical techniques used to treat heart disease

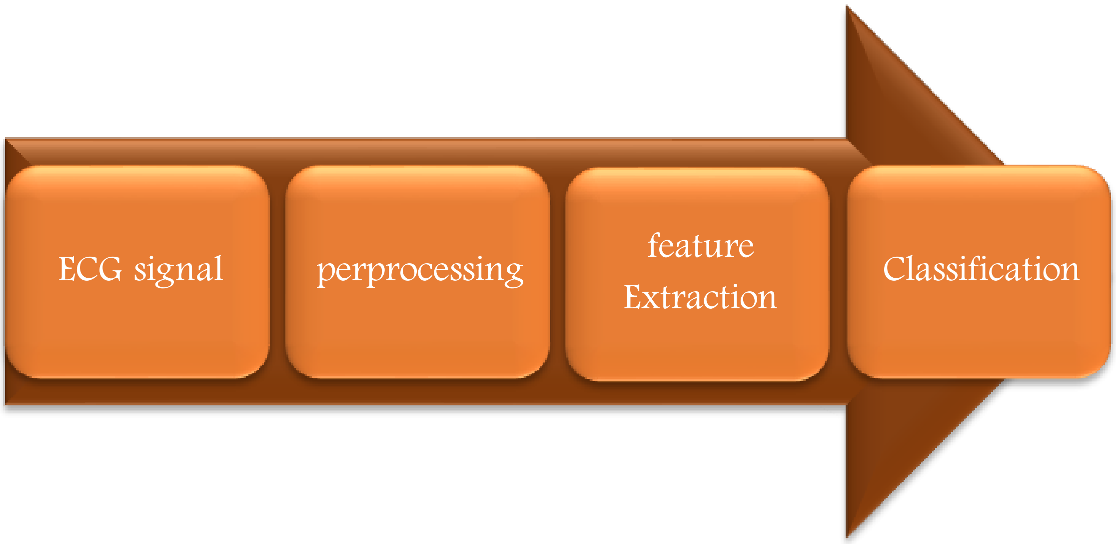

Figure 3.1 ECG classification stages for theoretical part (simulation part)

The studies ranged from the development of methods for analyzing ECG signals to the application of modern methods and the testing of their results. In below, we will illustrate crucial algorithms used in each stage of theoretical part.

3.2 Dataset

In our current work, the existing databases were adopted from various Physionet databases. The data came from the MIT-BIH Arrhythmia Database, the MIT-BIH Normal Sinus Rhythm Database, and the BIDMC Congestive Heart Failure Database. Approximately 10-minute data for different recordings are utilized for every of the ARR, CHF, and NSR categories. ECG data is called and arranged in the form of a matrix sorted by 162 by 65536, where each row represents the number of samples and the columns represent the time period of the sample series, and the data is randomly divided into two sets, a set of training and a set of the testing each of the databases mentioned above as described briefly below.

1) Database of MIT-BIH arrhythmia: it is constituting the ARR data utilized in our work. It includes 96 ECG tracks sampled at 360 Hz for male and female groups ranging in age from 23 to 89 years [20], but in this case, we utilized 10-minute data from just 30 recordings
2) Database of BIDMC congestive heart failure: it includes 36 ECG tracks sampled at 250 Hz for male and female groups ranging in age from 22 to 71 years. The CHF database utilized for this research consisted of 30 recordings of each matter.
3) Database of MIT-BIH normal sinus rhythm: we utilized 30 recordings of NSR data in this search for groups of males and females which aged 20 to 50 with samples of 128 Hz. It should be indicated that they did not have any significant cardiac abnormalities.

The ECG data utilized in the algorithm's verification and validation came from the PhysioNet library, specifically the MIT-BIH and BIDMC databases. PhysioBank is a huge and increasing archive of well-characterized digital recordings of biomedical signals for biomedical researchers to use. It is freely available online via the link PhysioBank ATM (physionet.org).

3.3 Preprocessing

The electrocardiogram (ECG) signals include many various kinds of noises that must be eliminated because it is not possible to obtain a correct reading of the ECG signal, which leads to a wrong diagnosis as baseline wander, powerline interference, electromyographic (EMG) noise, and electrode motion artifact noise. The process of pre-processing and removing noise from the ECG signal is one of the most important stages that we undertake to prepare the data for the feature extraction process and then classify the ECG signal.

To choose the most effective methods for minimizing noise from signals of ECG. The different signal processing approaches for reducing noise types of ECG signal have been depicted in this section. These techniques are straightforward and effective, which explain each one according to type of noise. The data for the cases taken in this work will be in the form of a matrix (162 * 65535), it will be 96 for ARR, 36 for CHF, while the NSR will be 30 records. The data is processed in several ways, as we mentioned earlier. Techniques used to remove noise

3.3.1 Discrete Wavelet Transform (DWT) to remove baseline wander

As mention previously, the effect of a signal's base axis (x-axis) 'wandering' or shifting up and down rather than being straight is known as baseline wander. As a result, the signal as a whole is deflected away from its normal base. The baseline wander has low frequency in the 0.5 Hz range.

The wavelet transform (WT) is one of the most widely used methods in signal evaluation with multiple resolutions due to its ability to decompose a signal at different resolutions. This enables the observation of high-frequency, short-period states in stochastic signals. The wavelet transform is utilized to cancel baseline wander which found in an ECG signal. The initial signal is divided using (LPF) and (HPF) according to the discrete wavelet transform (DWT). The LPF and HPF cut-off frequencies which be 50% of the sampling frequency. The data for the cases taken in this work will be in the form of a matrix (162 * 65535), it will be 96 for ARR, 36 for CHF, while the NSR will be 30 records. The data is processed in several ways, as we mentioned earlier.

Since the frequency of the ECG signal ranges from 0.05 Hz - 150 Hz and the noise of baseline has frequency usually between 0.05 Hz - 0.5 Hz, it is easy to affect the ECG signal, so the DWT method is effective to remove this type of noise

Where the data set that was entered is dealt with using Daubechies DWT, where the data that is entered is a separate time signal. The signal is represented as a series of samples, and DWT works on that sequence to decompose it into different frequency sub-bands. It analyzes the signals at multiple levels in the form of approximate and detailed coefficients, then passes them with low-pass and high-pass filters, which reduces the size of the signal due to the disposal of some samples. The signal is reconstructed based on the detailed parameters that preserve the properties of the original signal

3.3.2 Notch filter to remove Powerline Interference.

The power line noise is a kind of sinusoidal interference with a frequency ranging from 50 - 60 Hz, which is accompanied by a lot of harmonics and its interference with the ECG signal, which has few frequencies, makes the accurate diagnosis in the ECG signal wrong. So it is possible to use the notch filter, which is one of the simplest techniques used can be utilized to get rid of this kind of noise.

The notch filter, which is a very simple method to minimize powerline interference described by a couple of complex conjugated zeros on the circle at the interfere frequency. Because it has a notch with a reasonable bandwidth, this filter will help reduce ECG waves with frequencies close to zero, as well as the frequency of the power line. As a result, the filter must be tweaked to make the adding two poles of complex-conjugated pointing in the same direction corresponding to a zero to make it even more much selective. The notch bandwidth, which decreases as pole radius r methods the circle of one unit. The bandwidth is clearly reduced with a expense of the transient reaction time of the filter.

A powerline noise is removed from the ECG signal using a notch filter. When the input signal enters the filter, it generates a signal opposite to the signal it removes, represented by the noise signal, with the phase difference between the two signals. The two signals were mixed using the Infinite impulse response (IIR) filter technique and the signals that form the output of the bandwidth were eliminated, and the peak in the signal was weakened by the presence of the reversed signal.

3.3.3 Adaptive filter to remove Electromyographic Noise

Adaptive filtering is a noise-reduction technical that iteratively attempts to model the two signals in order to produce noise-free signals. In any way, the adaptive algorithm is responsible for the majority of the output signal's quality and functionality. With system components, the correlating weight is updated. If the error norm is statistically reduced. The parameter is changed when the system is time-varying, that is, when it changes depending on the time. There is only one adjustable parameter in the adaptive algorithm that affects the convergence rate.

Choosing the appropriate filter type for the adaptive filter, which is the filter of infinite response. When entering the input signal that contains muscle noise, a reference signal is generated that is similar to the noise signal to be removed. The frequency of muscle noise may vary from person to person and from case to case. It can range between 25 Hz and 150 Hz. The input signal containing the noise is mixed with the reference signal and the weights are continuously updated to obtain the optimal signal and remove the noise according to the action of the adaptive filter. A large number of weights was not chosen, because this requires large mathematical transactions, which makes it difficult to implement in real time, so the statics was used. The size of the data was determined so that it was not too long, because there would be a delay in implementation

3.3.4 Electrode Motion Artifacts Removal Techniques

Adaptive filters are one of the most prevalent utilized technical for minimizing electrode motion artifacts. The original and reference signals are required by the basic architecture of the adaptive noise cancellation filter utilized in this work the formula is

$$k(t) = x(t) + n_1(t) \qquad \textbf{3.1}$$

x(t) represents the signal of ECG and $n_1(t)$ represents added noise. A signal with noise are supposed to be not related. The other input noise is *u (t),* which is related with $n_1(t)$ however comes from a different source. New samples are also obtained from the input signals, the adaptive filter parameters W_k are modified. The principle of learning for modifying coefficients is depended on Mean Square Minimization to the error signal.

$$r(t) = k(t) - y(t) \qquad \textbf{3.2}$$

y(t) has a adaptive filter result. LMS and RLS are adaptive algorithms that are used in Electrode Motion Artifacts noise cancellation in an ECG signal. The LMS, RLS algorithm in this suggested approach modified its weights to reduce an adequate error signal norm. The corresponding weight is modified with system coefficients if the error norm is statistically reduced. The parameter is changed when the system is time-varying, that is, when it changes based on the time. There is only one adjustable parameter in the optimization technique that affects the convergence rate.

Figure (3.2) depicts a schematic diagram of the basic configuration of noise having to cancel adaptive filtering. Electrode Motion Artifacts noise removing by adaptive filters depended on LMS and RLS algorithms are important steps in the preprocessing of the ECG signal. Whereas, RLS reduces the error function by selecting appropriately parameters for the filter and updating the weights when new data arrives. Where the LMS updates the weights until it approaches the optimal weight for the filter, because when using the same weight for more iterations, the error will continue to increase, so the weights of the filter are constantly updated to reduce the error rate, and as a result we get rid of the noise

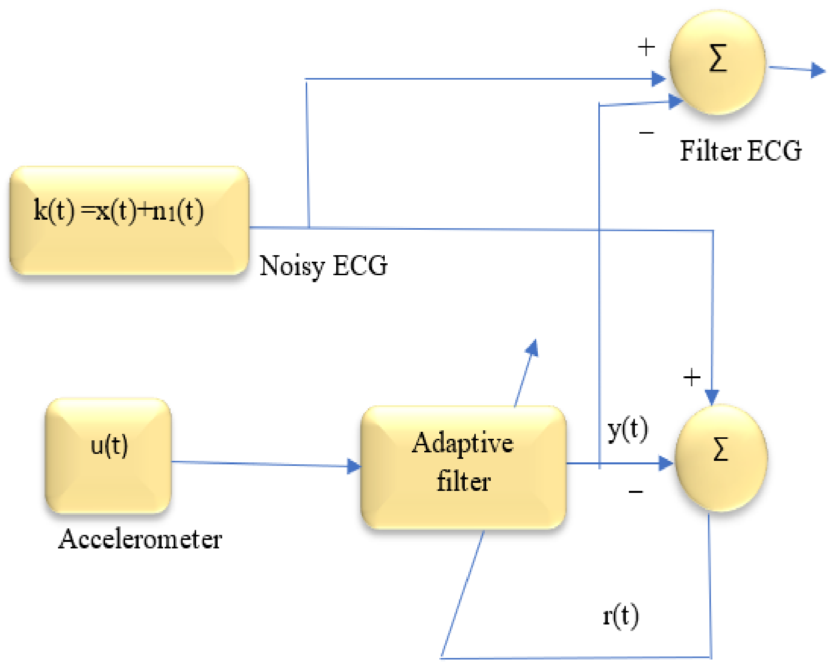

Figure 3.2 system of Adaptive filtering

We removed the baseline noise and the types of noise that were previously mentioned that interfere with the motion noise, as the motion noise deals with high frequencies, unlike the frequency of the baseline noise. The reference signal is identified and is identical to the motion artifact noise and then algorithms apply (LMS or RLS) to the input signal and reference signal in the adaptive filter and iteratively update the weights and adjust the step size applied to the ECG signal in real time

We can summarize the process of reprocessing that uses four different techniques to get rid of the different types of noise that the ECG signal is exposed through the simple diagram shown in Figure (3.3).

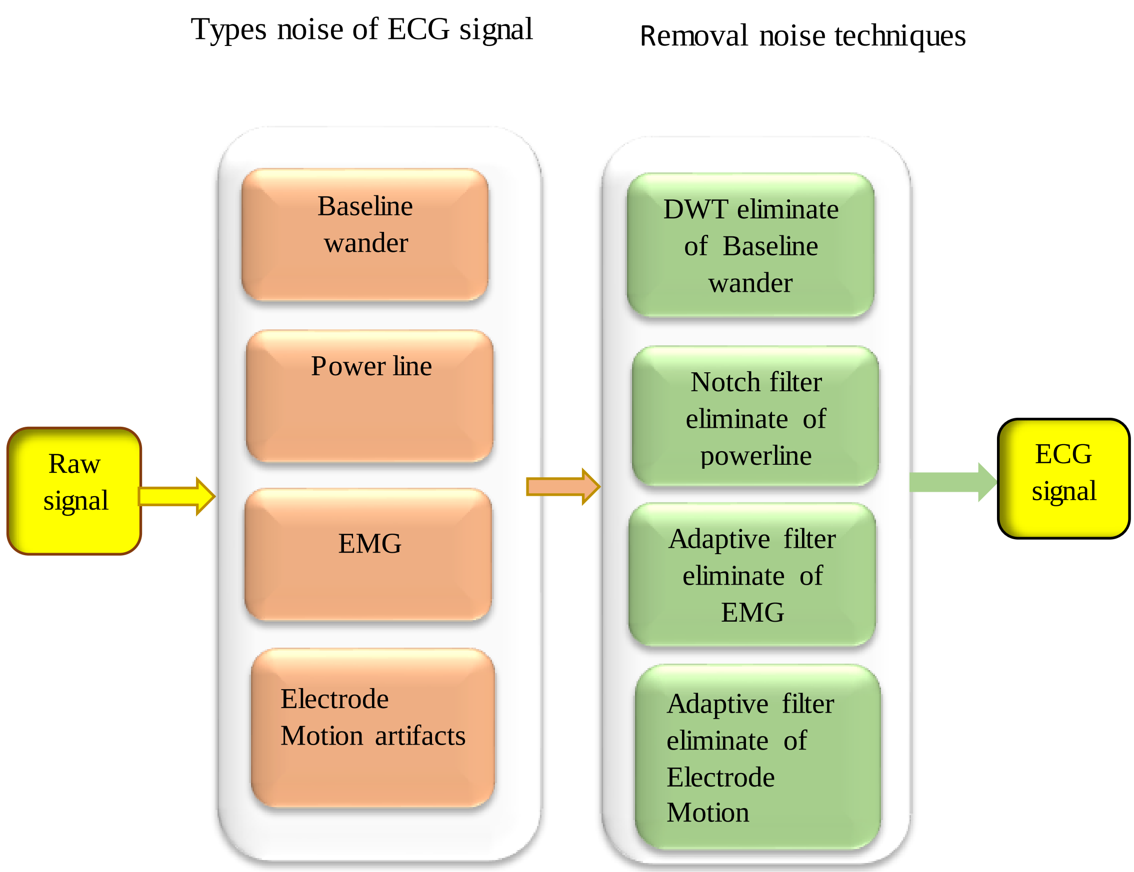

Figure 3.3 block diagram of preprocessing of ECG signal

3.4 Feature Extraction of ECG signal

The feature extraction process is important to the achievement of arrhythmia heartbeat classification utilizing the ECG signal. Any information extracted from a heartbeat that is utilized to differentiate its category may be taken into account as a feature. A set of methods for mapping input features to new output features is defined as feature extraction. The extraction of features in the time and frequency domains may not be adequate to describe the detail and fluctuation which was revealed in the ECG signal during the changes to which the signal is exposed thus, we used wavelet scattering transform-based analytical models to extract more advanced structures in addition to Blind Source separation (BSS) which used to feature extraction to ECG signal

The wavelet scattering method first performs the re-processing process on all inputs through high-pass and low-pass filters to get rid of any noise that may be present. A temporal representation of the ECG signal of the frequency range was prepared by means of wavelet scattering to analyze the signal into different levels. We apply the wavelet transform to a series of wavelets in order to get the invariant- translation representations and it captures the low and high frequency information until the signal is represented stably. After that the features that are different are extracted. A set of features such as (amplitude, phase, variance and mean) are extracted. These features will be applied in methods of classification

The most important variables to define in a wavelet time scattering decomposed are the scale of the time invariant, the total amount of wavelet transformations, and the amount of wavelets per octave in every one of the wavelet filter banks. A cascade involving two filter banks is often sufficient to obtain decent performance. In the present study, we use the default filter banks to produce a wavelet time scattering decomposition: 8 wavelets per octave in the first and 1 wavelet per octave in the second. The invariance time scale is set to 150 seconds.

The wavelet scattering algorithm divides each signal into a predefined set of scattering windows and uses wavelet transformations to extract features from them. After which, each scattered window is classified totally independent, and the initial segment is assessed depending on unified weighting (voting) of the classification of each scattered window. The wavelet scattering method involves a three-stage iterative signal transformation as follows: wavelet convolution, modulation, and filtering.

This approach is related to a convolutional neural network (CNN), except that the convolution filters are not discovered but rather are predetermined wavelet functions. The scattering coefficients are designed to also have a low variance within a category and a high variance between categories. Furthermore, they are unresponsive to input transcriptions on an invariance scale and get some useful characteristics such as multiscale contractions, linearization of hierarchical symmetries, and the generation of scattered data models.

The scattering dissolution can detect slight differences in the amplitude and duration of ECG signals, that are difficult to assess but indicate the heart's condition. As a result, we employ the wavelet scattering network to generate robust depictions of ECG heartbeats which reduce variations within one arrhythmia classification while ensuring adequate discriminability between them.

Individual signals can be extracted from superpositions, a process known as blind source separation. In the processing and extraction of ECG, BSS techniques have been given the most attention. The appeal of BSS stems from its adaptability, as the separation of blind sources requires no prior knowledge for any component of the processed signal. We used blind source separation method to extract the features in the heart stitching signal such as amplitude, space and frequency. The blind source separation mixes the signals from multiple sources, which were represented by the cases that were used from different diseases in addition to the normal state of the heart signal. The mixed source matrix is formed, the high-frequency components and the low-frequency components are determined, and we take the inverse of the matrix to obtain the original signal, which is considered as an input to the classifier that is used to classify the heart signal

The methods that were used to extract the features such as wavelet scattering and blind signal separation are good methods that can get rid of any noise that the signal may be exposed to during the classification process, and thus the use of these features may lead to enhanced classification accuracy. compared to the methods that were used by some researchers, which will be clarified through the results

3.5 Classification of ECG signal

In this section, we will introduce our algorithms for classification of ECG**.** In this work, it is explained briefly utilized approaches of classifiers that combine features to the predict of category for ECG signal. To choose the convenient classifier must be depended on specific criteria as, the classifier must be utilized in previously works to compare with them and, it must have been able to handle high dimension and huge size training data efficiently. As the selected classifier is of the supervised category, classification entails two stages: learning the data and thereafter testing it. All ECG segments of the very same heartbeat type are saved in a single feature vector, and the process is repeated for one of the other kinds of

ECG segments. All of these heartbeats are mapped using feature extraction methods from our research methods.

The machine learning power is in its ability to generalize by correctly classifying invisible data depending on pattern construction by training data. Herein anyone can utilize a Support vector machine to construct a module of machine learning for the dataset of ECG, utilizing a part of the data (70%) for training and (30%) of the remaining for testing the module. Also, anyone can use Neural Network (NN) in the same manner to classify the ECG signals through divide the data 80% for training and (20%) for testing.

3.5.1 Classifier of Neural Network

The neural networks are used for classification in the current work. The neural networks' power stems from their parallel processing structure and capability to learn from perception. They can be employed to pretty accurately classify input data into classes if they have previously been trained to do so. The classification accuracy is determined by the training efficiency. The learning experience's knowledge is saved in the form of connection weights, that are utilized to make a decision on new input.

3.5.1.1Neural Network with wavelet scattering

A well-established physiologically concept, NNs, is a favorable machine learning technique to identify nonlinear ECG signals for biometric recognition. The network model is supported by some input nodes that receive input data or features, a hidden layer made up of nodes with activation functions that accomplish some procedure on the data of input and a node of the output that provides the foretell class of test data.

The weights of the network were determined using the training dataset. Furthermore, during the training stage, the network was investigated on the validation dataset to accomplish slightly earlier shutdown for overloading reduction objectives. The last network was investigated on a test dataset using the last stored weights that produces great results on the validation dataset.

After the signal processing process to get rid of the types of noise that the ECG signal is exposed to, we perform the feature extraction process, which is to extract the useful and required features from the data, which facilitates the classification process and improves its performance, as using a lot of data by entering it into the classification algorithms takes time, so we use feature extraction, which is this idea is to reduce the dimensions and build a set of variables while maintaining the accuracy of the information.

When using wavelet scattering with the neural network, the scattering coefficients are calculated only for paths with low frequencies, because the use of all data that are of a large size requires continuous training of the wavelet scattering, which takes time and complexity of calculations. Wavelet-scattering transform constructs a stable and consistent signal that contains all the information and is distributed over multiple paths with a series of wavelet coefficients.

First, the heart signal that was filtered from noise and extracted features was segmented into time windows, which would be input to the neural network. As for the data segmentation, it was divided as follows: 20% test and 80% training. The set of training will be utilized for training of the neural network, whilst the set of testing will be utilized to valuation its achievement. Each ECG sample is represented as a feature vector. This vector contains the extracted features as the input to the neural network.

The training process involves repeated passes back and forth across the network using the training data. As for the neural network that has been configured to classify the signal, it is the feedforward neural network, which consists of 20 hidden layers. The data is trained with the appropriate weights that are adjusted by calculating the difference between the real and expected outputs through the backpropagation algorithm, and the network adjusts its weights based on the calculated gradients to reduce the specific loss function.

The feature extraction process improves the ECG signal classification performance, as mentioned earlier. The NN model used in this work has one input layer, twenty hidden layers, and one/three output layers for binary/multiclass classification. The network is tested with various internal process activation functions, and it is discovered that the sigmoid function provides the highest precision. The network’s weights were saved every time it achieved a good outcome on the validation dataset.

3.5.1.2 Neural Network with Blind Source Separation

In the processing and extraction of ECG, BSS techniques have been given the most attention. The appeal of BSS stems from its adaptability, as the separation of blind sources requires no prior knowledge for any component of the processed signal as mention previously. The network pattern is supplemented by input terminal that obtain incoming data or features, a hidden layer factitious of nodes with activation functions that perform several steps on the data of input and terminal of an output which supplies the foretell category of testing data. The network's weights are specified utilizing dataset of training. Apply blind source separation algorithms to the preprocessed ECG signals. BSS method such as Independent Component Analysis (ICA) has been used to separate the underlying independent components to extract relevant features from the separated source signals. These features have been captured important characteristics of the ECG signals, such as statistical measures. Common feature extraction techniques include time-domain analysis, frequency-domain analysis (as using Fourier Transform or wavelet analysis).

Moreover, through the training step, the network was evaluated on the validation data to achieve relatively early closing to reduce overloading purposes. The ultimate network was tested on a test data with the most recently saved weights, and it performed admirably on the validation dataset.

Weights were saved whenever the network performed well on the validation data. The NN paradigm utilized in this work for binary multi-class classification has single input layer, twenty-layers of hidden, and multi-layers of the output. The network is assessed using a variety of internal process activation functions, with the sigmoid function providing the highest precision. The weight updating process begins with the output layer, with the objective of increasing the rate of error prevention. Figure(3.5) illustrate the proposed system of NN classifier

3.5.2 Classifier of Supported Vector Machine

It is a learning algorithm with several beneficial properties. It identifies information trends and is attributed to data analysis. It uses a linear discriminate function for classification. Nonlinear classification, on the other hand, is possible with the use of a nonlinear kernel. SVM works well in real time, is reliable, and easy to recognize. When compared to other classifiers, it appears to have a coherent approach.

3.5.2.1 Supported Vector Machine with Wavelet Scattering

As mentioned earlier regarding the support vector machine, it is a learning algorithm with a number of advantageous properties. It identifies trends in information and is attributed to data analysis. For classification, it employs a linear discriminate function. Nonlinear classification, on the other hand, is possible if a nonlinear kernel is used. SVM works well in real time, is robust, and is simple to recognize. It seems to have a comprehensive solution when especially in comparison to other classifiers. A classification task usually necessitates knowledge of the data to be classified.

The initial stage was to obtain the data, the ECG data is a structured matrix with two fields: data and labels. Data includes an ECG recording at 128 Hz while labels include ARR, CHF and NSR diagnoses. We have reorganized the multi-signal scattering transform into a material to produce a matrix suitable for the SVM classifier. The framework produced a matrix with the dimensions 416-by-16-by-113 for the provided signal length and quality attributes. There were 416 scattering paths, with 16 representing a scattering time window.

Wavelet scattering is applied to preprocessed data and wavelet scattering contains a series of wavelet transform and modulus operations to extract features. It is suitable for cardiac signal analysis by equipping it with translation-invariance representations. Each data point represents a feature vector and each feature represents a particular characteristic or measure of an input, these features are including statistical measures. The vector support network divided the data obtained from feature extraction into training and testing at a ratio of 80:20% to be trained by the network. Where the network finds the best hyperplan to separate the classes by the largest margin between them. SVM separates the different classes better by mapping the input data to a higher dimensionality of the feature space because a hyperplane is defined that gives the decision boundary to increase the margin and distance between the nearest data points for each class.

3.5.2.2 Supported Vector Machine with Blind source separation

The VSM algorithm is used to take advantage of its multiple advantages. It identifies information patterns and is refer to analysis of the data. It utilizes a function of linear discriminate for classification. Non-linear classification, in contrast, hand, is feasible with the use of a non-linear kernel. SVM performs well in real-time, is reliable, and is easy to realize. When compared with other classifiers, it appears to have a comprehensive solution. Knowing of the data to be classified is usually required for a classification task.

We have reorganized the multi-signal Blind Source Separation (BSS) to a material in order to generate a matrix adequate for the classifier of SVM. For the supplied signal length and quality aspects, the framework generated a matrix with the components 416-by-16-by-113. The SVM is a classifier that adjusts an optimum model to provide the greatest margin of separation between categories.

The SVM approach has two stages: training and testing. In the first stage, we must "teach" the method which a specific set of data belongs to a particular category. The collected data from the BSS technique and the shape/statistical feature extraction are utilized as the input of the SVM in the second step, and the results are obtained. It is important to note that the data set used in training is dependent on the classifier input because we evaluate the results utilizing BSS data after the BSS technique and generated by the system.

The classifier utilizes the information obtained from the separation methods and shapes statistical feature extraction in this step to determine which patterns are involved in the process. SVM has been utilized the extracted features from the BSS step as input and the corresponding class labels as the target output. SVM has been utilized to separate the various classes depend on extracted features by find optimal hyperplane. In finally, we can explain the general system of classification in figure(3.4).

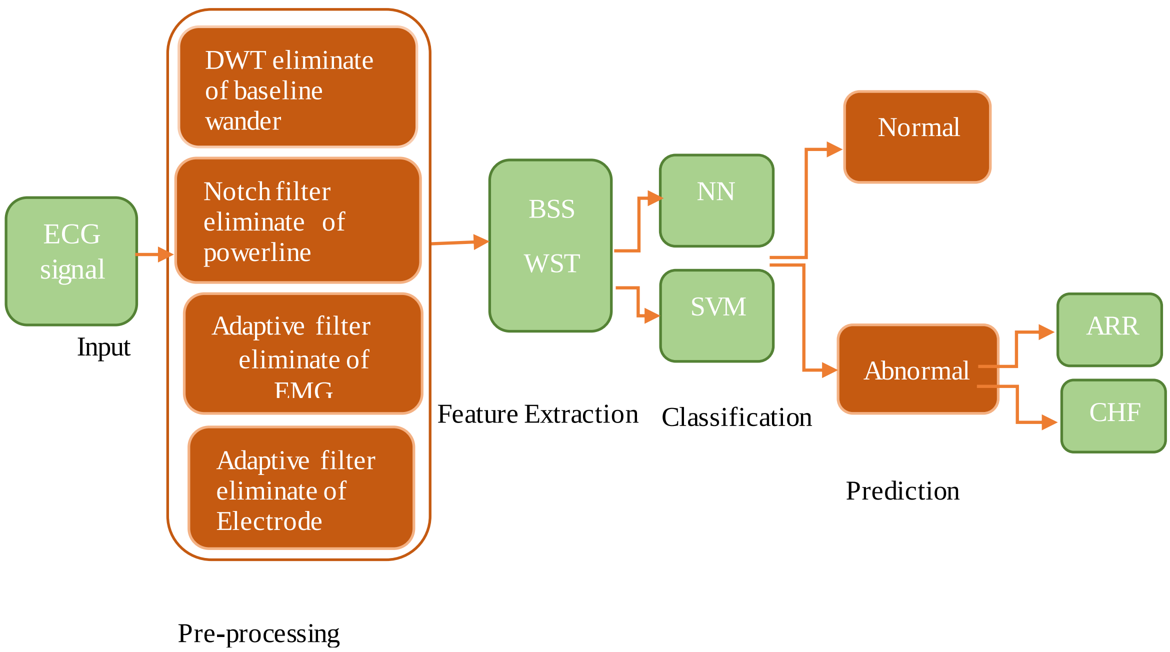

Figure 3.4 the proposed system of the classifier

The schematic diagram (3.5) shows the flow of steps that were performed by signal bisection using machine learning with feature extraction by wavelet scattering while the steps of the ECG signal classification process by machine learning, feature extraction using blind source separation, are illustrated by diagram (3.6).

After applying the aforementioned algorithms for machine learning from the neural network and the support vector machine with the methods of extracting the features represented by separating the blind sources and scattering the wavelets and comparing the results obtained through the accuracy and the time spent in training, we found that the algorithm of the support vector machine with the scattering of the wavelets is the one that got the highest Therefore, it was practically applied to the device that was designed using LattePanda with some heart signal sensors, an LCD screen, and supporting accessories, and the figure below is an illustration of the workflow

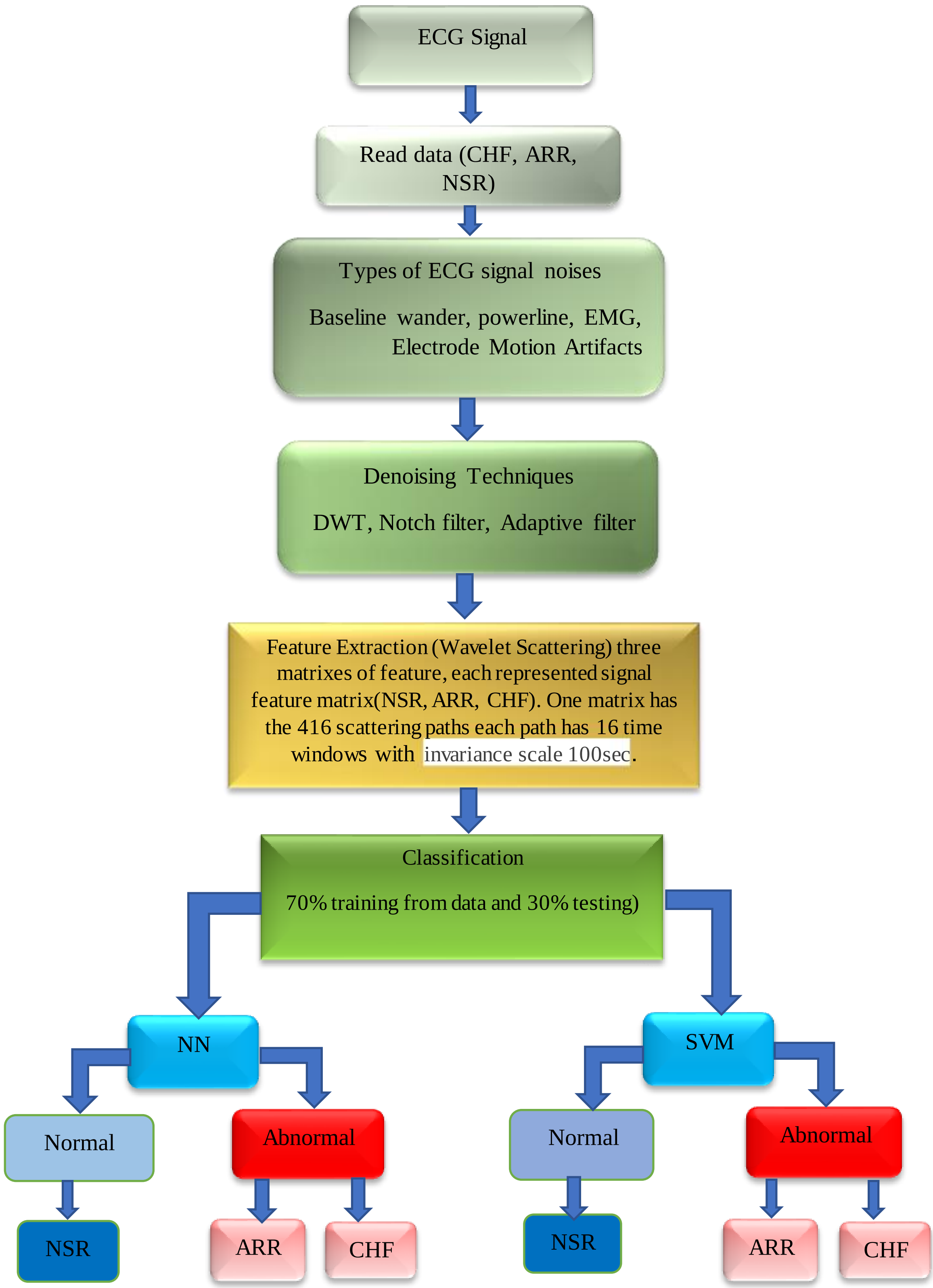

Figure 3.5 Flowchart of Proposed system (wavelet scattering with NN and SVM

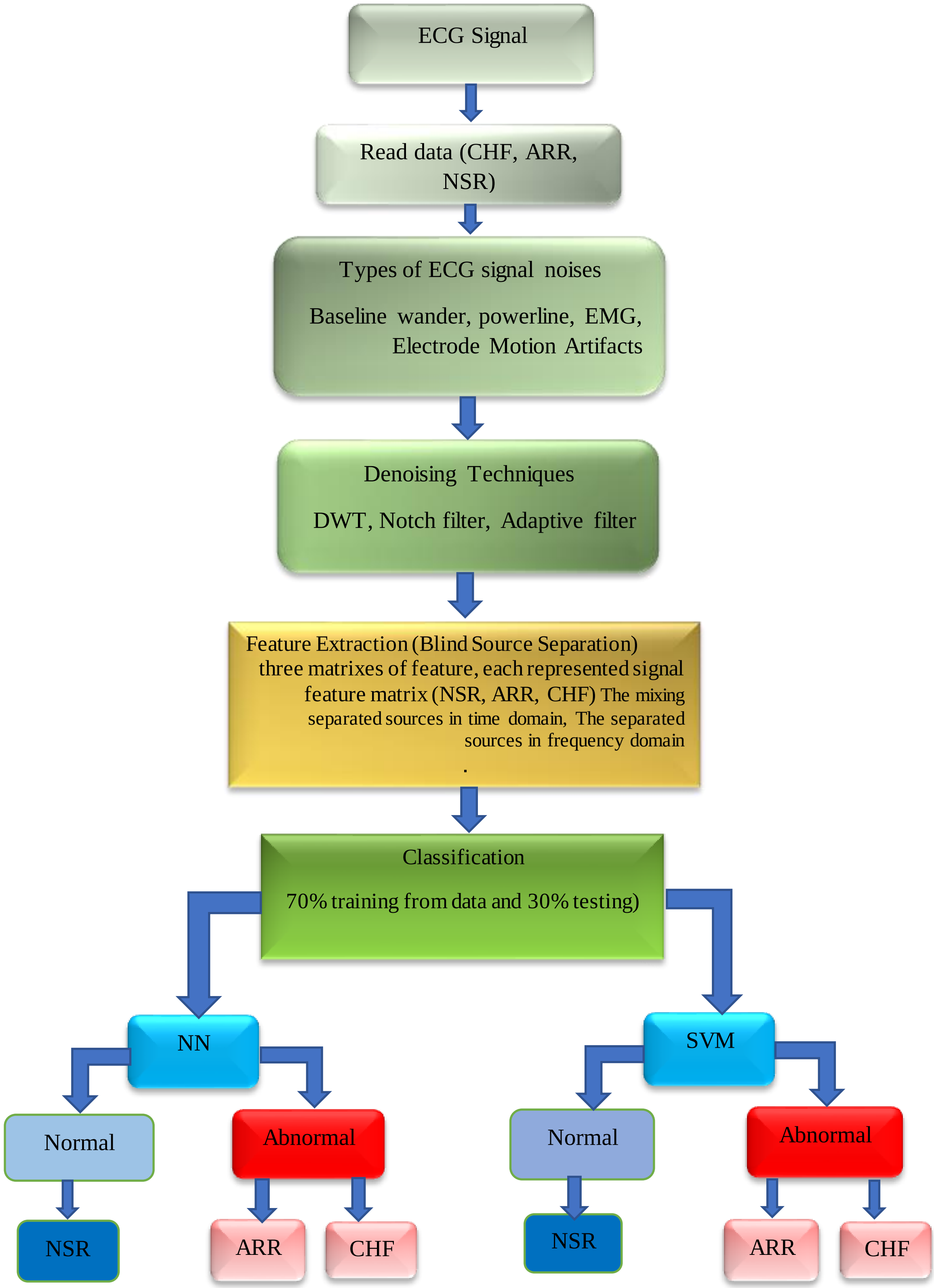

Figure 3.6 Flowchart of Proposed system (BSS with NN and SVM)

3.6 Proposed system of ECG signal classified practically

The designed system can classify the ECG signs of the patient. The proposed system comprises many parts; sensors, Lattepanda as an embedded system, ECG unit and monitor to exhibit the output.

3.6.1 Lattepanda

The Lattepanda structure is merely one board computer (mini personal computer), depicted in the Figure below. It can run many applications like a typical computer and is compatible with the (Windows 10) operating system. Furthermore, because it is incorporated with Arduino, Lattepanda is regarded as a controller. We will use the Lattepanda processor because it can do similar work for the computer. Figure (3.7) illustrates the small size of lattepanda by comparing it to the size of an iPhone 6. Lattepanda has main several features as:

1. small size (dimensions:2.76" × 3.46")
2. consumes less power during both work or shutdown,
3. supports various types of I / O ports
4. working on MS-Windows 10, with integrated Arduino Co-ATmega32u4 processor (Arduino Leonardo)
5. requires less time to work
6. Processor: LattePanda boards usually have an Intel processor, with models offering everything from Intel Atom to Intel Core m3 or m7 processors to recent model core i5.
7. RAM and storage: RAM capacities range from 2GB to 8GB, and aboard memory sizes range from 32GB eMMC to 64GB or more.
8. Connectivity: It has a variety of connectivity options, involving USB ports, Ethernet, Wi-Fi, Bluetooth, and HDMI for video output. Additional interfaces, such as GPIO headers and aboard sensors, may be included in some models.

9. Display: LattePanda supports a variety of exhibit resolutions, involving HD and 4K, and can be connected to a monitor or TV.
10. LattePanda operates a full version of Windows 10, making it compatible with an extensive variety of software applications and drivers.

It can not only be utilized as a normal low cost Windows PC. The LattePanda is also equipped with an Arduino compatible processor, allowing it to assist you control and sense the physical world, so it used in many applications. Overall, the LattePanda adheres to general data processing principles on a Windows-based computer. It combines the Intel processor's processing power, RAM memory management, storage capabilities, and the flexibility of the Windows operating system to handle and process data based on the applications and software running on the board.

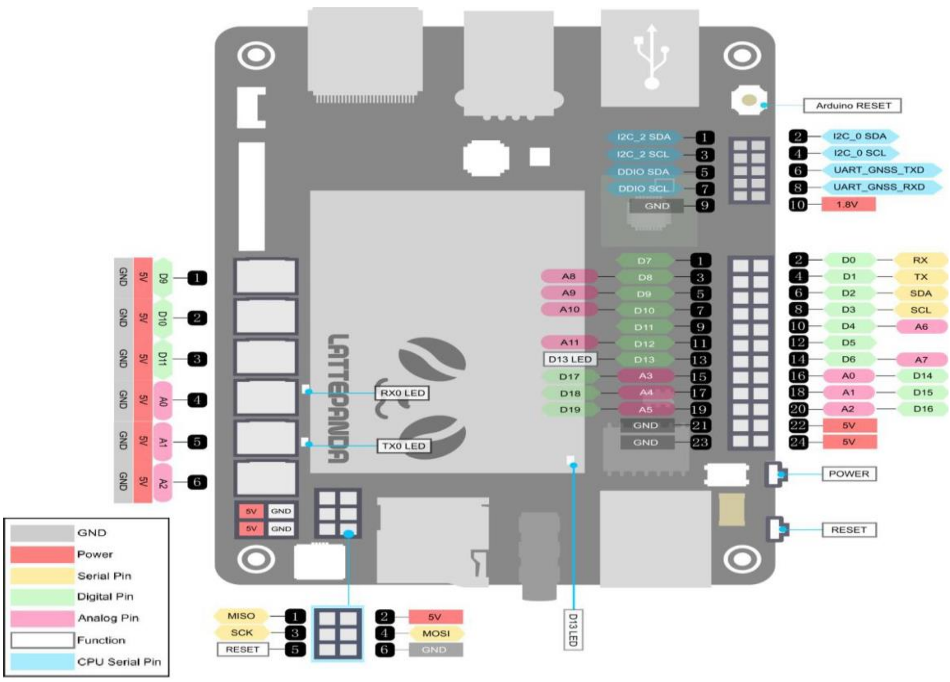

Figure 3.7 Internal design of LattePanda

In figure 3.8 explain power up of LattePanda

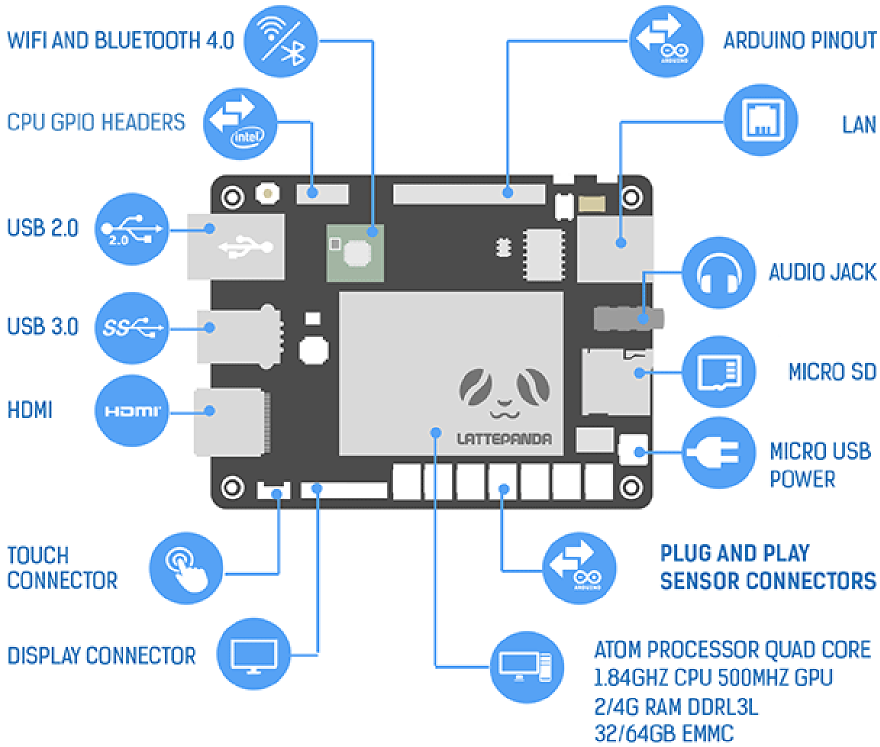

Figure 3.8 structure of LattePanda

3.6.2 ECG Sensors

The sensor of AD8232 ECG as board of the electronic utilized for determining the heart signal and can eliminate the noise that the ECG signal is exposed. Its working principle is similar to that of an operational amplifier to obtain clear signals. In another word, AD8232 sensor used for enlarge, excerption and filter vital signals which have low in noisy status like those created using distal electrode substitution in addition movement. For sensing, AD8232 has three probes located on the patient's body.

The AD8232 monitoring the heart rate sensor has the following pins: pin of LO+, pin of LO-, pin of output, pin of voltage is 3.3V, and pin of ground (GND). Therefore, we as designers could be attached pins to the integrate circuit (IC) and link it to developmental platforms as an arduino.

The table 3.1 in below despite the connect between LattePanda and ECG sensor

Table 3.1 connecting between ECG sensor and LattePanda

NO.	LattePanda	ECG sensor
1.	VCC:5V - pin 22	3.3V
2.	D5 -pin 12	LO +
3.	D6-Pin 14	LO -
4.	Analogue -A2-pin20	OUTPUT
5.	GROUND – pin 23	GND

Furthermore, the board has connectors for specialized sensors like the (RAM), (LAM), and (RLM). The board includes an indicator of LED that displays the rhythm of human heartbeat.

Specifications and Features

The following are the main characteristics of this sensor.

- one equipped operation scope from 2V to 3.5V.
- The main side has been completely integrated and just uses lead ECG.
- Using integrated reference data, the simulated ground may be constructed..
- Internally, a filter of RFI is utilized.
- The supplied current has weak, about 170 A.

3.6.3 Screen of LED

A 24" LED screen was used to display the results, and it was connected to Lattepanda via HDMI cable. The reason for using this type of screen is that there is no need to program it, and it is input dc power, so it has less influence on the measurement period as shown in figure (3.10).

Figure 3.9 LED Screen

3.7 Implementation of proposed system design of ECG classification

It Get Started guide demonstrated how to turn on the LattePanda for the first moment while setting up a physical computing software platform with Visual Studio and Arduino Firmata. Using Panda to work with the window system makes it simple to use any application.

Our device of LattePanda arrives with 2GB RAM, 32GB eMMC flash memory, and Windows 10 previously installed and activated, making it a breeze to get initiated. Simply connect your peripheral devices and turn on:

- Connect the HDMI cable to the monitor.
- Connect a 5V - min 2.0A power supply of good quality to the micro USB power socket (we used a 5.1V / 2.5A supply).
- Start Windows by turning on the power supply. The red LED on the board's underside will illuminate for 30 seconds.

The figure (3.10) (a, b, c) depict connection of the designed ECG classification device

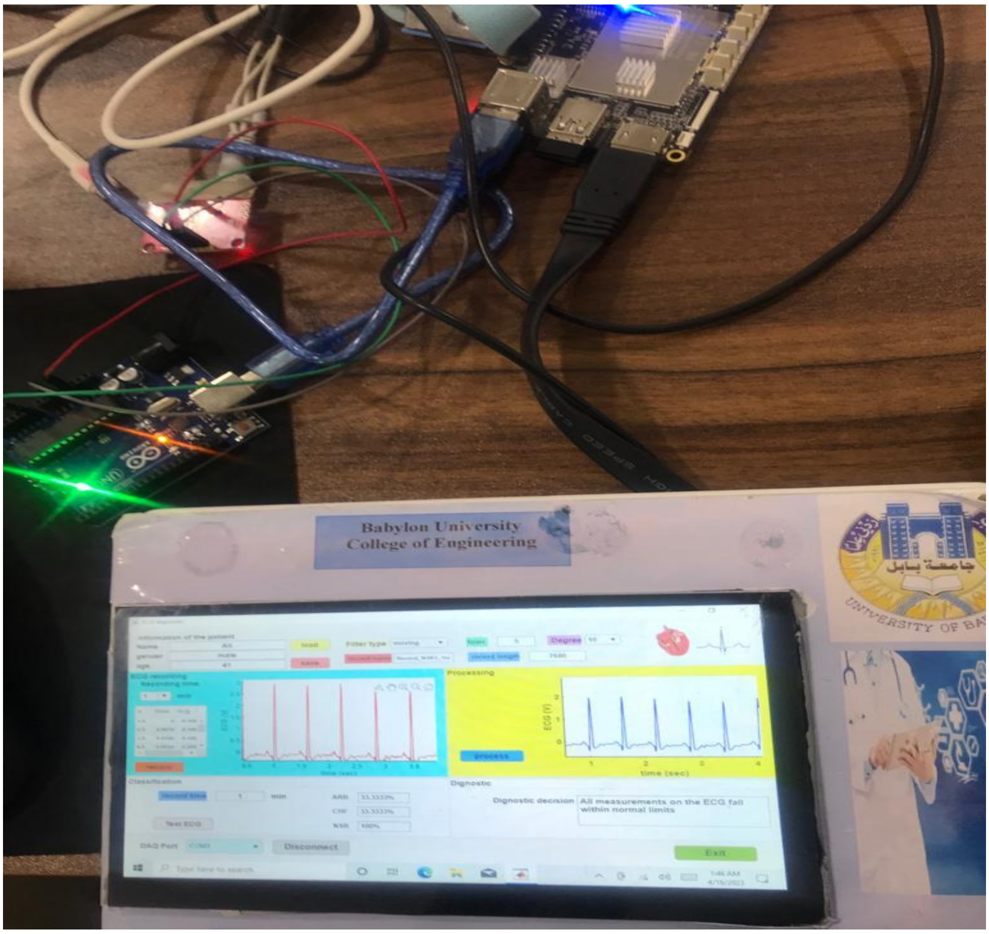

(a)

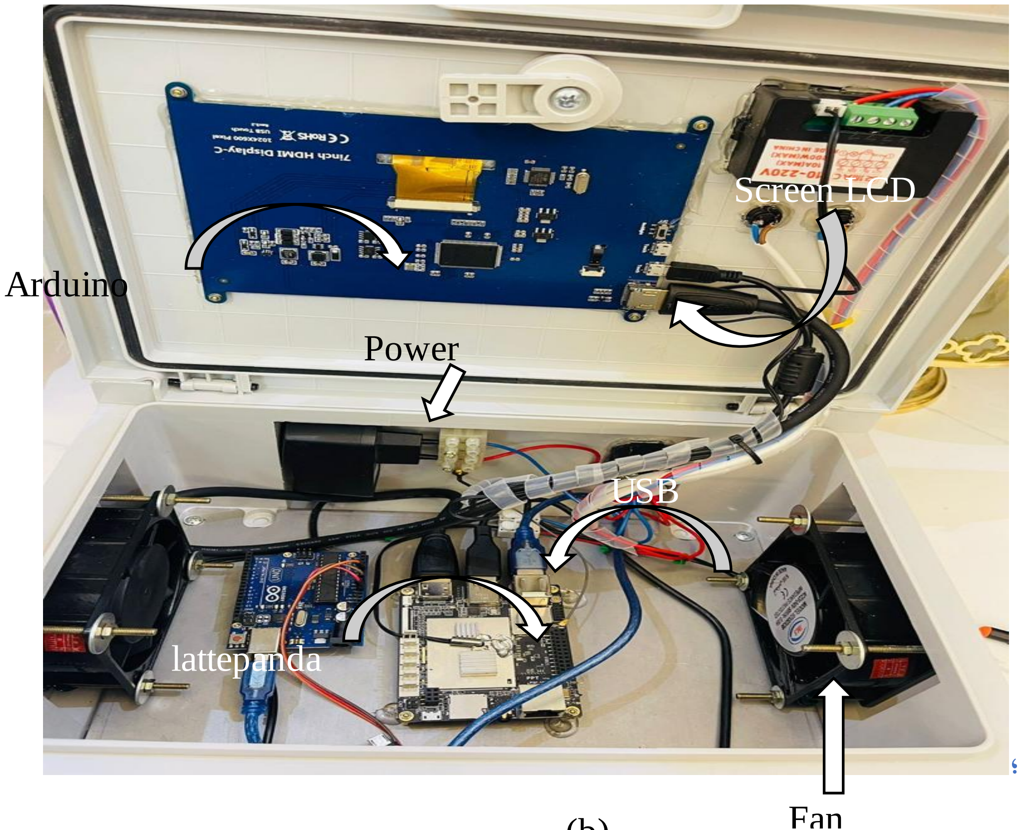

(b)

(c)

The figure 3.10 (a, b, c) the designed ECG classification device

As we mentioned earlier, Panda represents the main part of the implementation system, which is similar to a small computer with an ECG unit and sensors. The sensors collect data and send it to the electrocardiogram unit, which reads it and sends it to the panda device, which processes the data using one of the filters as a Notch filter or moving filter to get rid of the noise that the signal is exposed to after the signal processing process and obtain a pure signal because the presence of noise may lead to an error in diagnostics one of the previous algorithms used in feature extraction is used with machine learning.

We applied wavelet scattering with SVM because it gave better results than the algorithms that were used

3.8 Interface devices of ECG classification

An interface for a device that is used to process and classify the ECG signal was designed in Visual Studio, which is one of the languages that are applied on the Lattepanda, which represents one of the languages that are chosen to make simple an application that is implemented on a Lattepanda device to make it easier to use. T he interface of device include important special information of patient as (name, gander, old) which it implement by GUI

Addition the interface of device is consist on multi-windows as ECG recording, processing, recording time and diagnostic decision. There are also some fields that comprise save, testing, DAQ Port, and others windows. The save field used to save the patient's data so that it can be retrieved at any time we need as shown in figure(3.11).

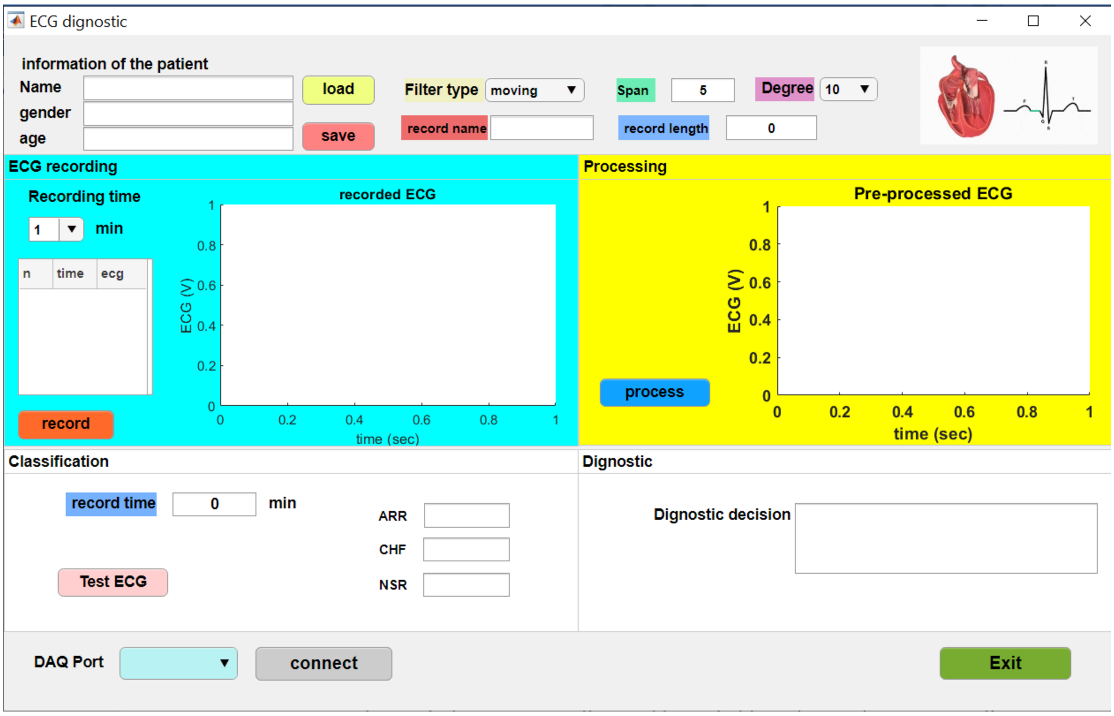

Figure 3.11 the interface of device

There are also three options present within the classification window, in which there are the types of diseases that have been approved in our work in addition to the healthy condition, and they are classified after pressing the ECG test key.

The result of the diagnosis appears depending on the highest percentage after testing the data that was fully read and processed by one of the algorithms that were previously used as shown in figures (3.12) and (3.13). The method wavelet scattering with neural network was chosen, which is considered the best, because it showed better results in terms of accuracy

The operation of reading the data begins when the sensors are attached to the patient in three parts of his body, on his left and right wrists, and on his feet. The ECG unit begins to read this data and transfer it to the ECG unit, which in turn transmits it to the filters to get rid of all kinds of noise that were mentioned previously. Moving filter was used to obtain a pure signal through which it is classified and diagnosed types of diseases.

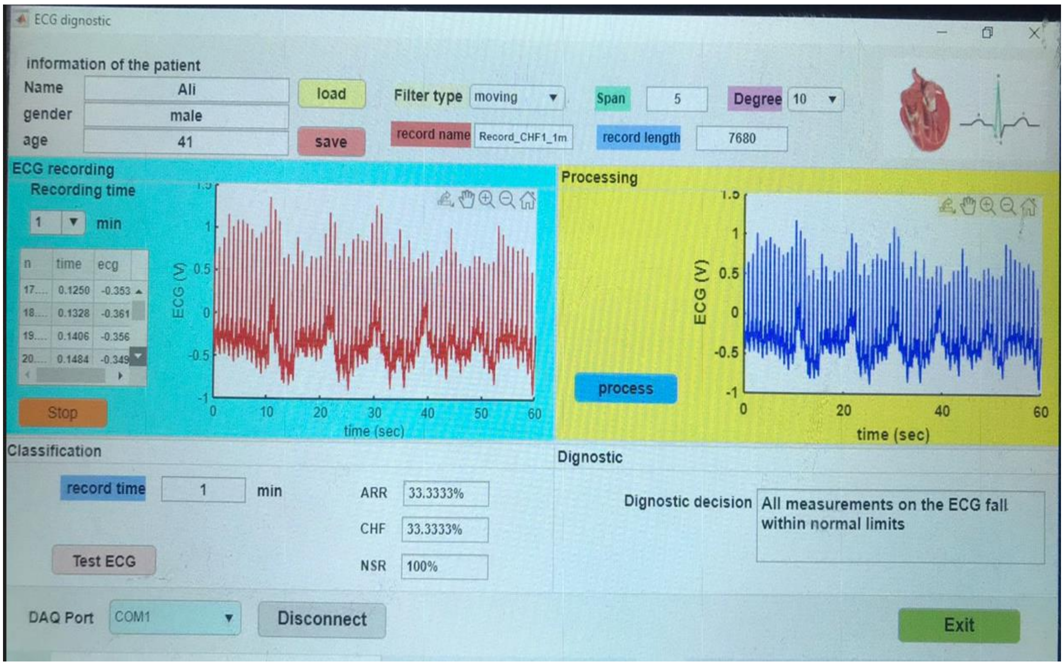

Figure 3.12 example of normal state of ECG

After the process of processing and getting rid of the noise, the pure heart signal is classified by one of the machine learning methods, which was previously discussed as the automatic vector support method. The length of the signal is 8 milliseconds used to deal with it, and here to diagnose the patient’s condition, either it is normal or abnormal, and in the abnormal case, the type of disease is diagnosed according to the species that were previously identified in our study, and this is done by means of the threshold value of 85%. The case that constitutes a percentage more than the percentage of the threshold value is placed under the diagnosis of the case as shown in the figure(3.14) below. Whilst figure (3.15) explain flowchart of the practical part algorithm

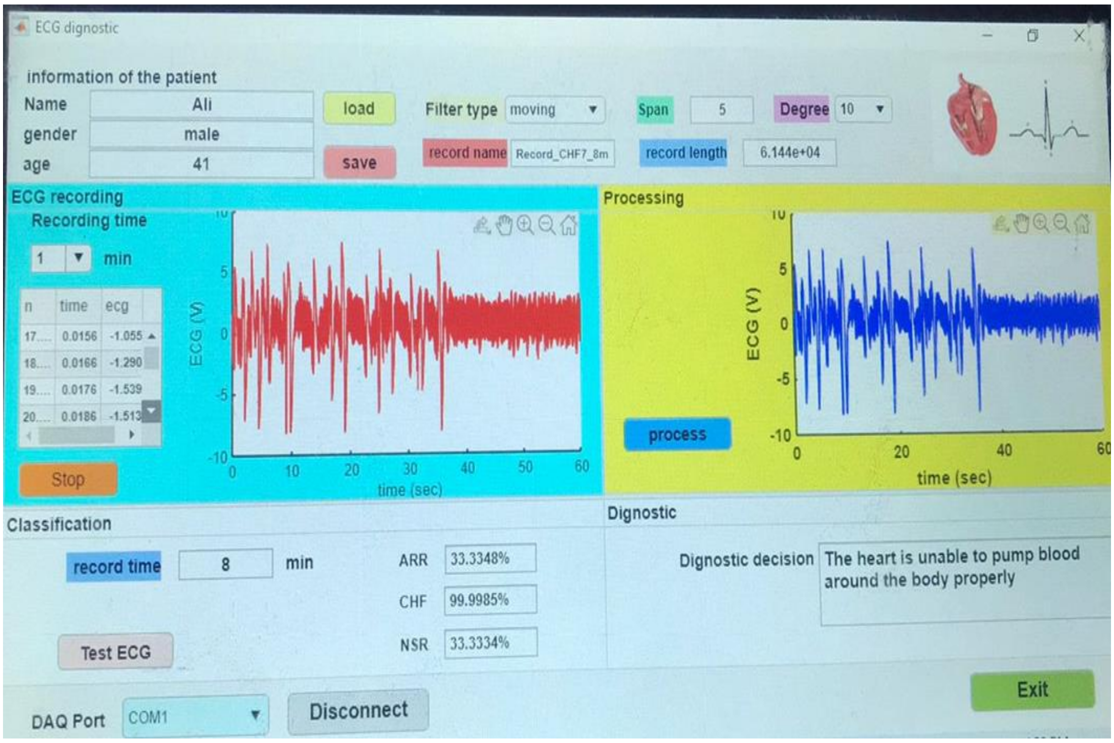

Figure 3.13 example of ubnormal state(CHF) of ECG

Chapter Four

The results and discussion of the Proposed ECG Classification System

4.1 Introduction

This chapter presents the results and discussions for the thesis objectives. The outcomes for each objective are presented in the same order as in the previous chapter. As a result, the subsection presents findings and discussions for a specific goal. The results are linked to achieve high accuracy for the system in real-time to use to provide an initial diagnosis of the patient's condition.

The heartbeat monitoring system was put to the test. The test results will be presented in this chapter, along with a discussion of these results from various perspectives to demonstrate the system's accomplishments. As previously stated, the system is divided into two parts: theoretical (which includes simulation using MatLab2019b to execute machine learning algorithms such as NN and SVM) and practical (which uses the LattePanda device). The two parts discuss how to diagnose specific cases that have been identified (ARR, CHF, NSR) which illustrated in figure (4.1).

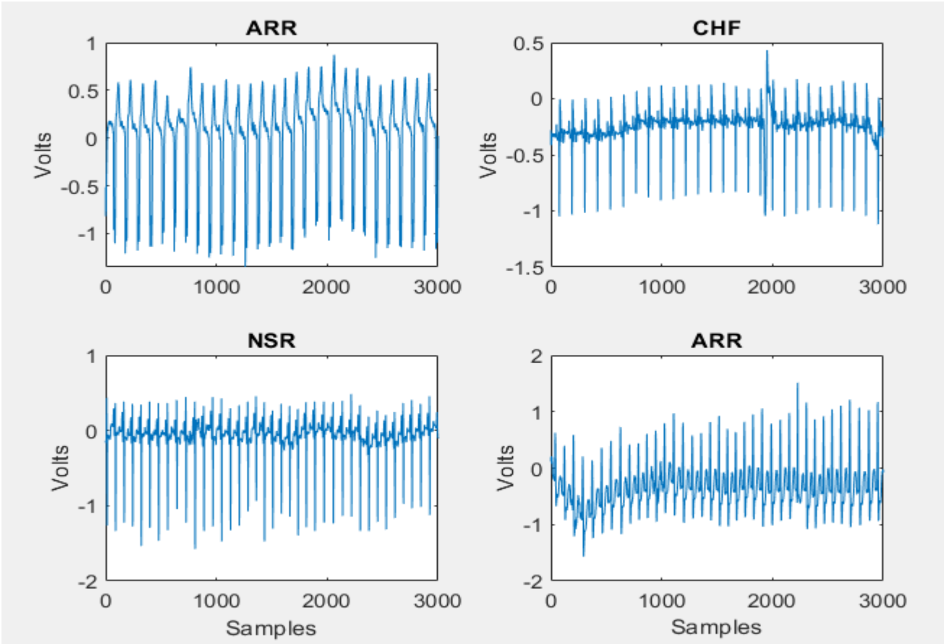

Figure 4.1Three classes of ECG signal

All ECG signal classification simulation results have been explored. This chapter is a record of the results obtained from the theoretical section. The obtained and recorded results are divided into three sections. The first section discusses the results of the remove noise technique, the second section discusses the results of the developed feature extraction technique using one of two methods (BSS and Wavelet scattering), and the final section illustrates the results of classification.

Results of classification. The effectiveness of the proposed methods was determined by comparing the results. The suggested technique uses an ECG signal from the database of MIT-BIH to classify the output as normal or abnormal. To pre-process the signal of input, filter techniques such as DWT, Notch filter, and others are utilized.

4.2 The results of ECG pre-processing

A wide variety of noise sources greatly impact electrocardiogram (ECG) results. Denoising the signal involves eliminating unnecessary elements from the presentation. We introduce the new approach, show how it works with signals, and explain its characteristics. The most typically impacted noise on ECG readings includes power line interference (PLW), noise of a baseline, noise of the electrode motion artifact, also noise of an electromyography (EMG). Denoising ECG data is an important step in acquiring pure signal characteristics for reliable diagnosis. This study looks at the numerous causes of noise in ECG data as well as strategies of the processing of the signal to reduce a noise.

To reduce baseline noise from an ECG signal, the Discrete Wavelet Transform (DWT) can be utilized. The Notch filter may reduce noise of powerline. Adaptive filtering is regarded to be a useful technique to remove EMG noise. Electrode Motion artifact noise is removed using adaptive filters with (LMS)and (RLS) algorithms.

Preprocessing is the important point in processing of the signal of ECG, and it includes removing noise from the input signals. Noise eradication includes various approaches for different noise sources when pre-processing the ECG signal.

Removing the noise of the ECG signal as baseline wander elimination utilizing multi resolution wavelet transform, powerline using notch filter, EMG and Electrode Motion Artifacts noise removing by adaptive filters depended on LMS and RLS algorithms are important steps in the preprocessing of the ECG signal. We used the entire MIT-BIH database signal for this study. The ECG signal was cleaned up by removing different kinds of noise. The baseline wander in an ECG signal can also be removed using the wavelet transform. Baseline wander occurs at a rate of about 0.5 Hz. We use DWT to remove the baseline wander, before that we must remove any other noise at high frequencies so that we can remove the line noise at low frequencies.

The initial signal is divided using (LPF) and (HPF) and per a discrete wavelet transform (DWT). The LPF and HPF cut-off frequencies will be half of the sampling frequency. To the DWT coefficients of the frequency's low sub-bands, use an appropriate thresholding approach. Thresholding is the process of reducing coefficients that are less than a specific threshold to zero while keeping important coefficients. This phase aids in the suppression of baseline drift elements. We can show the result of noise removal of baseline wander from ECG signal of NSR in figure (4.2).

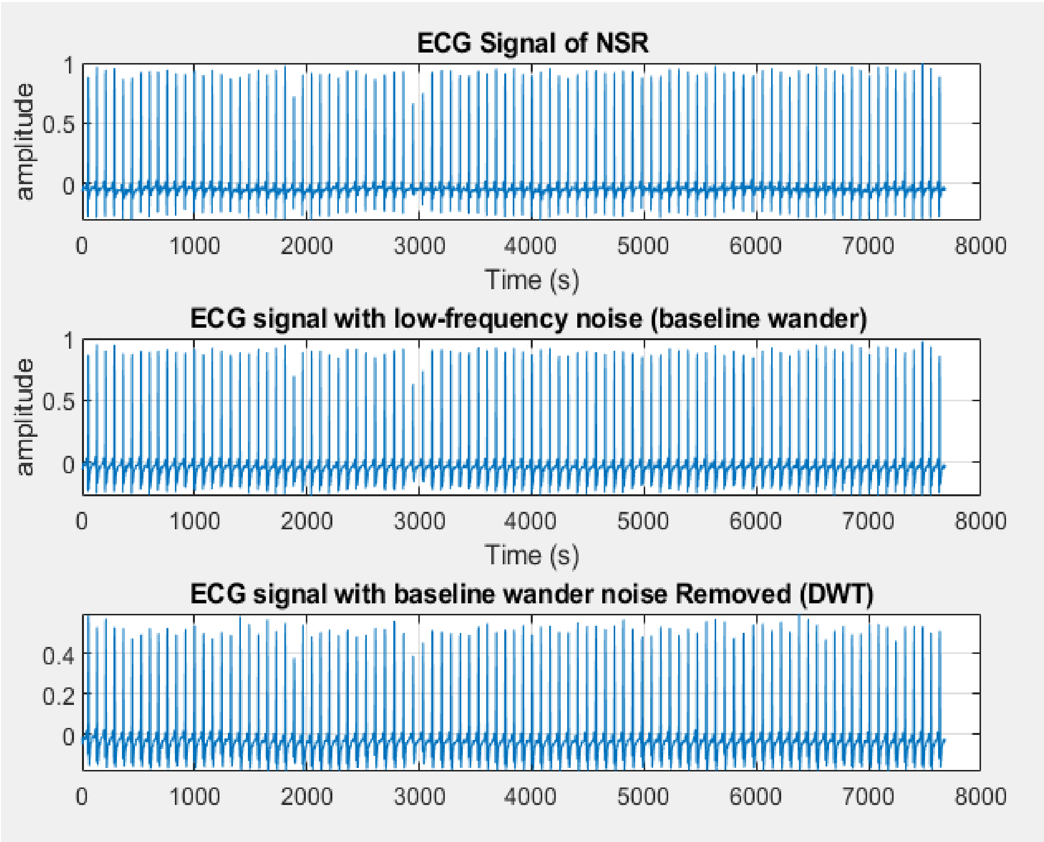

Figure 4.2 NSR of ECG signal, NSR with baseline wander ,remove the noise using DWT

As a very simple method to reducing powerline interference, consider the filter specified by the conjugated complex couple of zeros which keep lying on the circle at the interfering frequency. Not the powerline frequency only, but also waveforms of ECG with frequencies near to zero will be diminished by this filter because It has a grade with a significant bandwidth. As a result, the filter design must be altered so that the notch is becoming pickier. The pole radius r gets to determine the notch bandwidth, which decreases as r approaches the unit circle. The figure (4.3) despite the powerline noise removed by notch filter. To remove the power line noise using the notch filter, we must take into account its affecting frequencies ranging from 0-50/60Hz. When designing the filter, we need to calculate the cut-off frequency, which should be chosen slightly above and below the power line frequency, because the severity of the frequency response may cause the filter to Higher to steeper inclines which may cause a lot of distortion, it was selected for 62 Hz

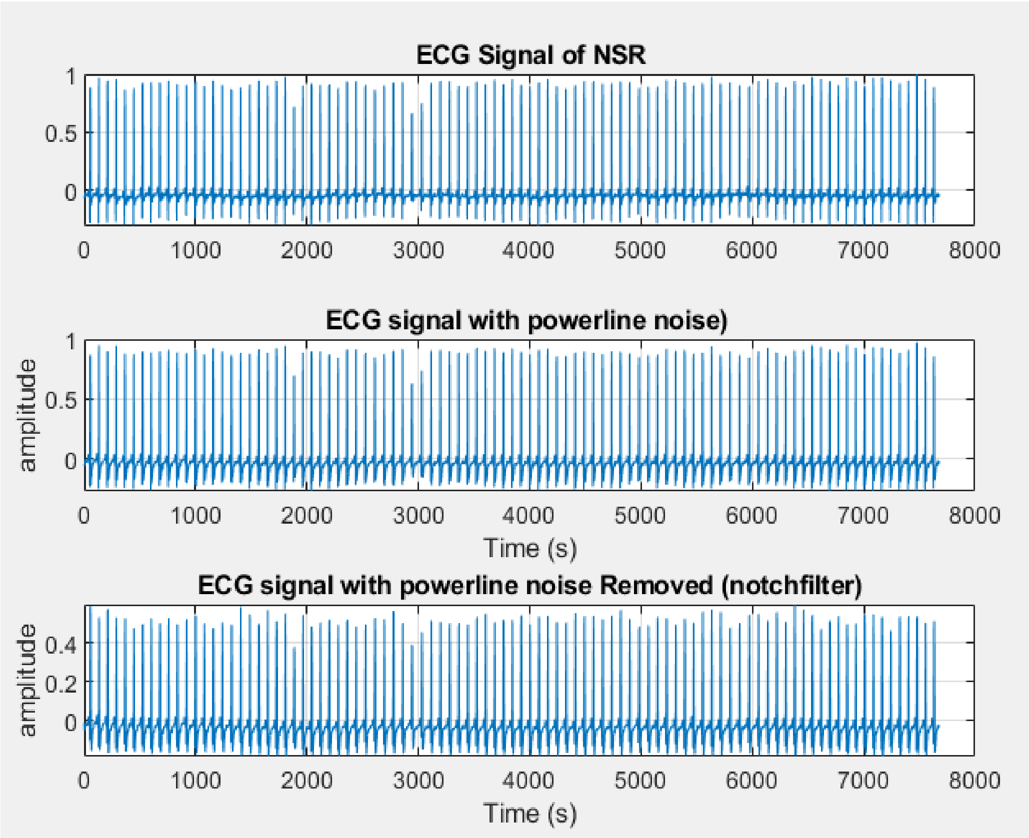

Figure 4.3 ECG signal of NSR, NSR with powerline noise, remove powerline noise using (Notch filter)

As powerline noise, in a representation of power line noise, the amplitude and frequency components of the signal could require to be adjusted. These features will not alter considerably throughout an ECG signal detecting assessment or signal measurement investigation since they are typically consistent for a specific testing condition.

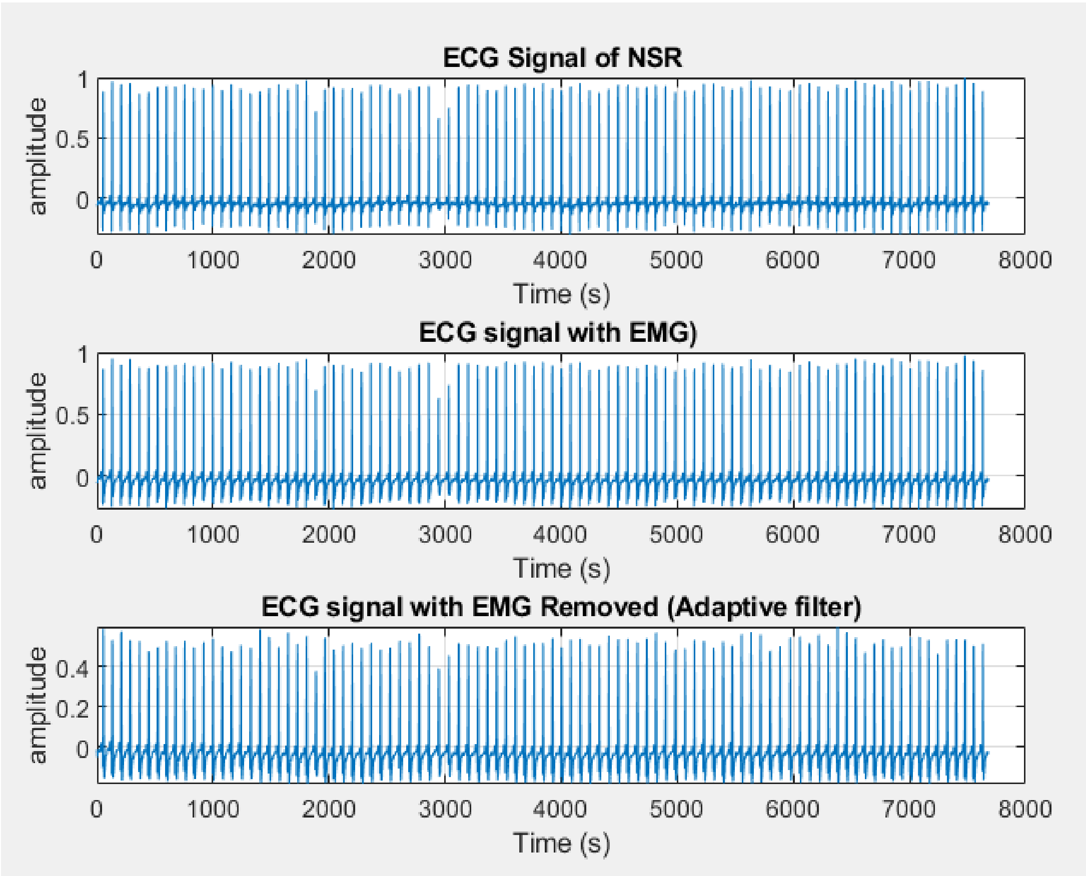

Figure 4.4 ECG of NSR, NSR with EMG noise, remove EMG noise using (Adaptive filter)

Adaptive filter algorithm LMS is used to filter the Electrode Motion Artifacts noise of the ECG signal that is used as input. The algorithms of LMS adaptive process the original ECG signal. Adaptive filters are the most overused technologies to remove electrode motion traces and EMG noise. The basic and reference signals are needed by Adaptive noise filter structure cancellation used through this work. New samples of the input signals are attained, the adaptive filter parameters W_k are updated. The learning base for modifying parameters is depended on reductions in the error signal's mean squared. The most extensively utilized adaptive filtering techniques are (LMS) and (RLS). The figure (4.4) explain remove EMG noise from ECG signal of NSR by adaptive filter while figures (4.5) and (4.6) despite remove motion artifact of NSR using adaptive filter with RLS and LMS algorithms.

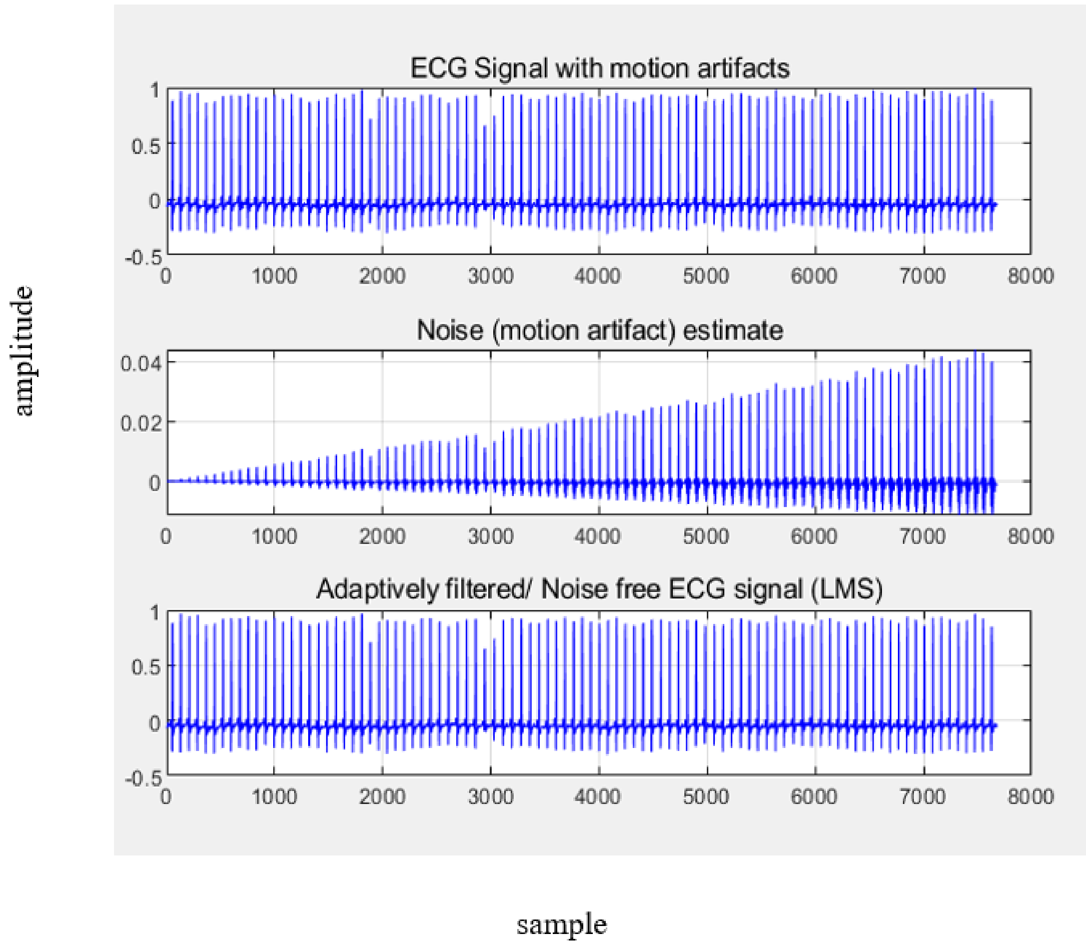

Figure 4.5 ECG of NSR, NSR with motion artifact noise, remove motion artifact using adaptive filter with LMS algorithm

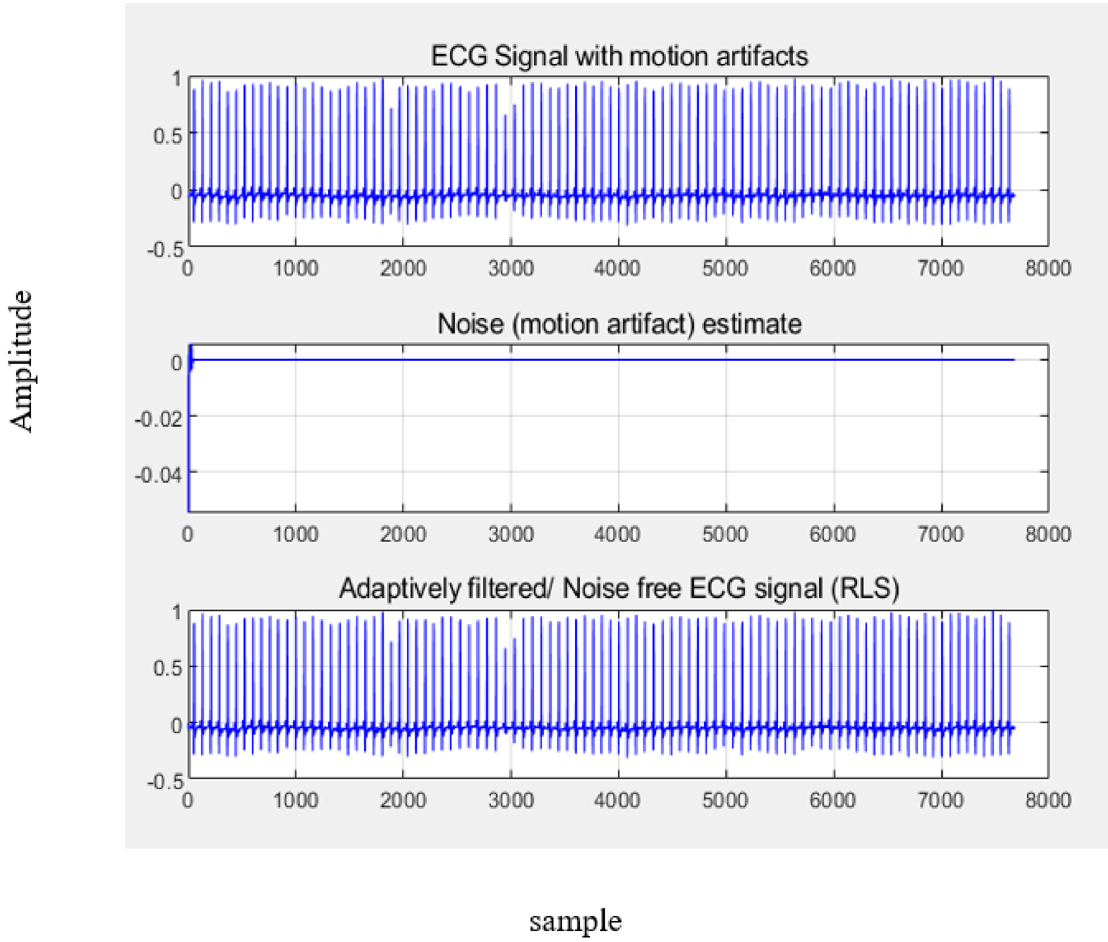

Figure 4.6 ECG of NSR, NSR with motion artifact noise, remove motion artifact using adaptive filter with RLS algorithm

In ARR which is considered as one of the abnormalities in ECG classification, also, it is exposed to different types of noise which were mentioned in the previous section. In which various techniques have been used to remove noise from NSR, they will be applied to remove noise from the signal such as DWT techniques, Notch filter and Adaptive Filter. The figure (4.7) illustrate remove noise of baseline wander

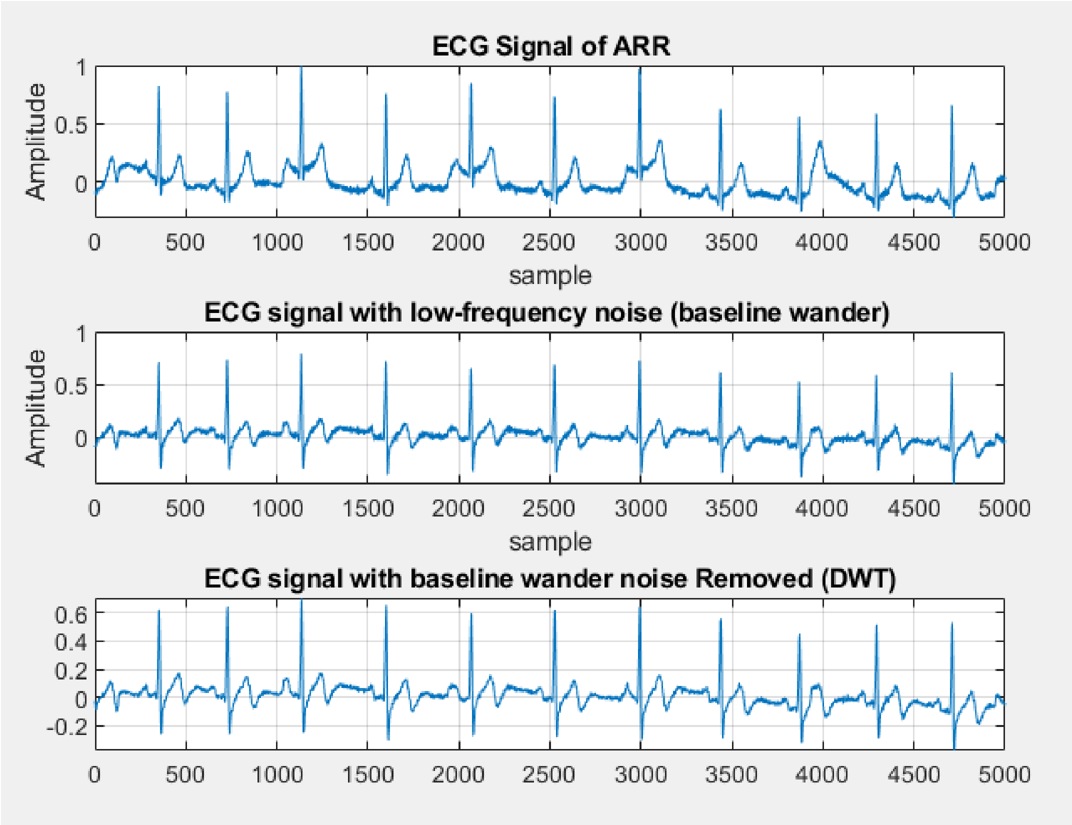

Figure 4.7 ARR of ECG signal, ARR with baseline wander ,remove the noise using DWT

As for, the figure (4.8) explain remove noise of powerline from ARR signal by Notch filter which utilized Infinite impulse response (IIR). Both signals were combined using the infinite impulse response (IIR) filter method, and the signals that comprised the bandwidth response were deleted, as well as the signal maximum, which was dampened owing to the existence of the inverse signal.

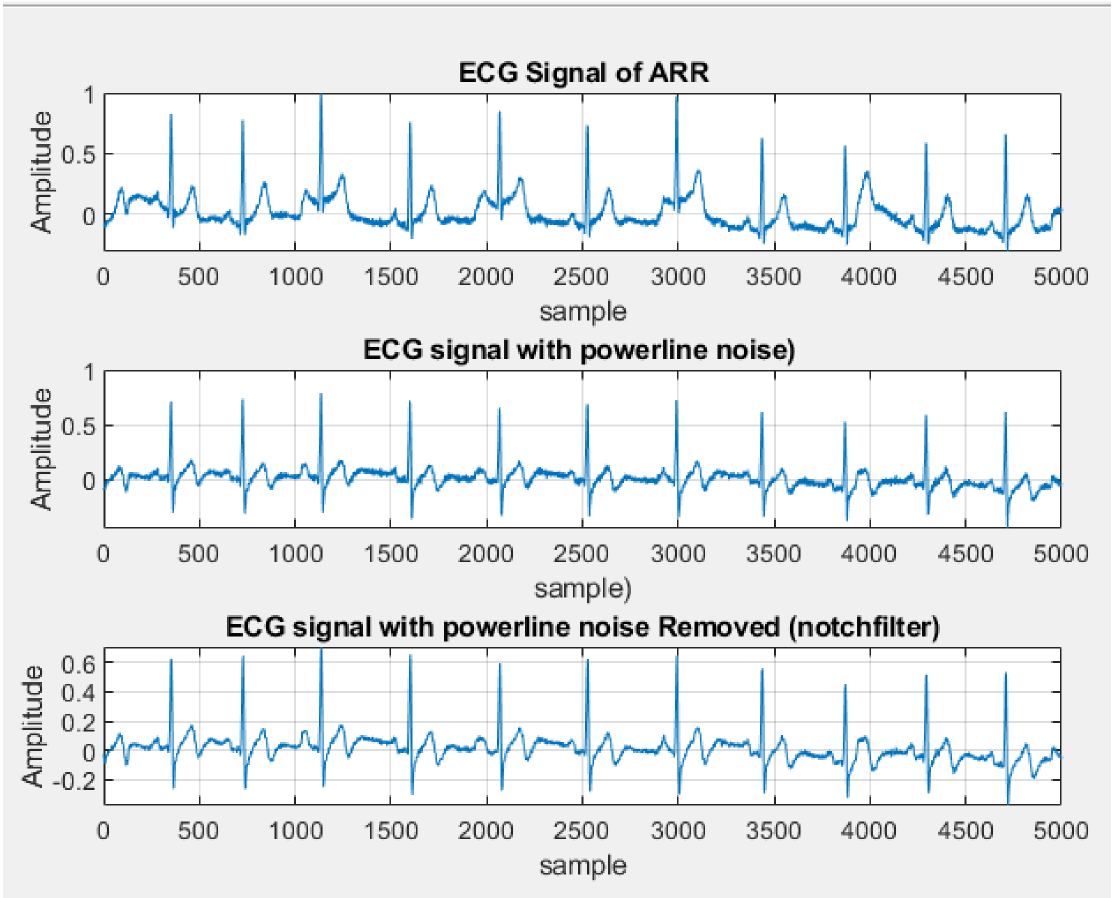

Figure 4.8 ECG signal of ARR, ARR with powerline noise, remove powerline noise using (Notch filter)

Selecting a suitable remove kind for the adaptive filter, that is an endless response filter. Whenever a muscular noise-containing input signal is entered, a reference signal which is identical to the noise signal to be eliminated is created. Muscle noise frequency varies from person to person and case to case. It has a frequency range of 25 to 150 Hz. The noise-input signal is mixed with the reference signal, and the weights are continually updated to achieve the ideal signal and eliminate the noise based on the adaptive filter's action. The figure (4.9) illustrate the output of adaptive filter at applied it on ARR signal which has Electromyography (EMG) noise nd remove it.

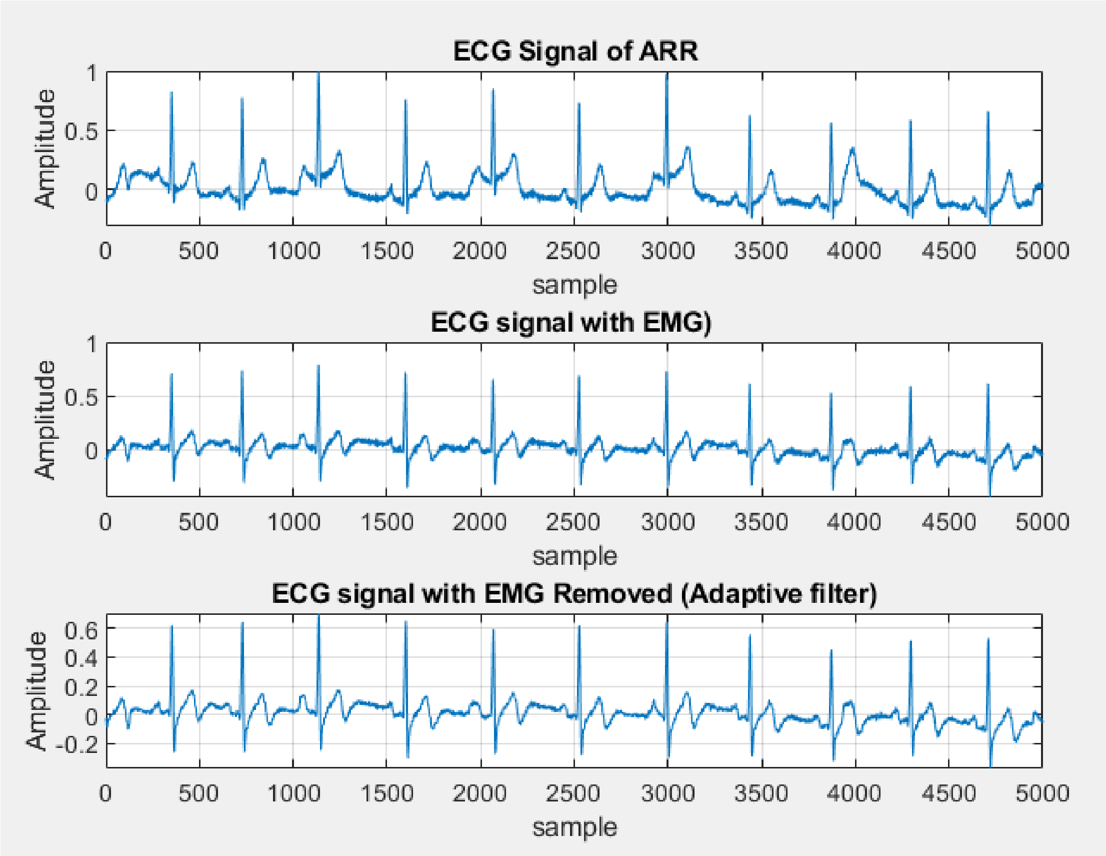

Figure 4.9 ECG of ARR, ARR with EMG noise, remove EMG noise using (Adaptive filter)

When using adaptive filter based on Algorithm(LMS), we start by selecting filter(w) parameters whose values are very small. At each step, we calculate the output of the adaptive filter taken from multiplying the weight by the input signal, as well as estimating the error by subtracting the output signal and the desired signal. The filter parameters are updated frequently according to the step size, which is either of a large size, which makes the convergence fast, but affects the stability, unlike when it is small, the convergence is slow, but the stability is high, and it was chosen with a value of (0.007) to obtain a pure signal from Noise is used to classify the ECG signal as explain in figure below (4.10)

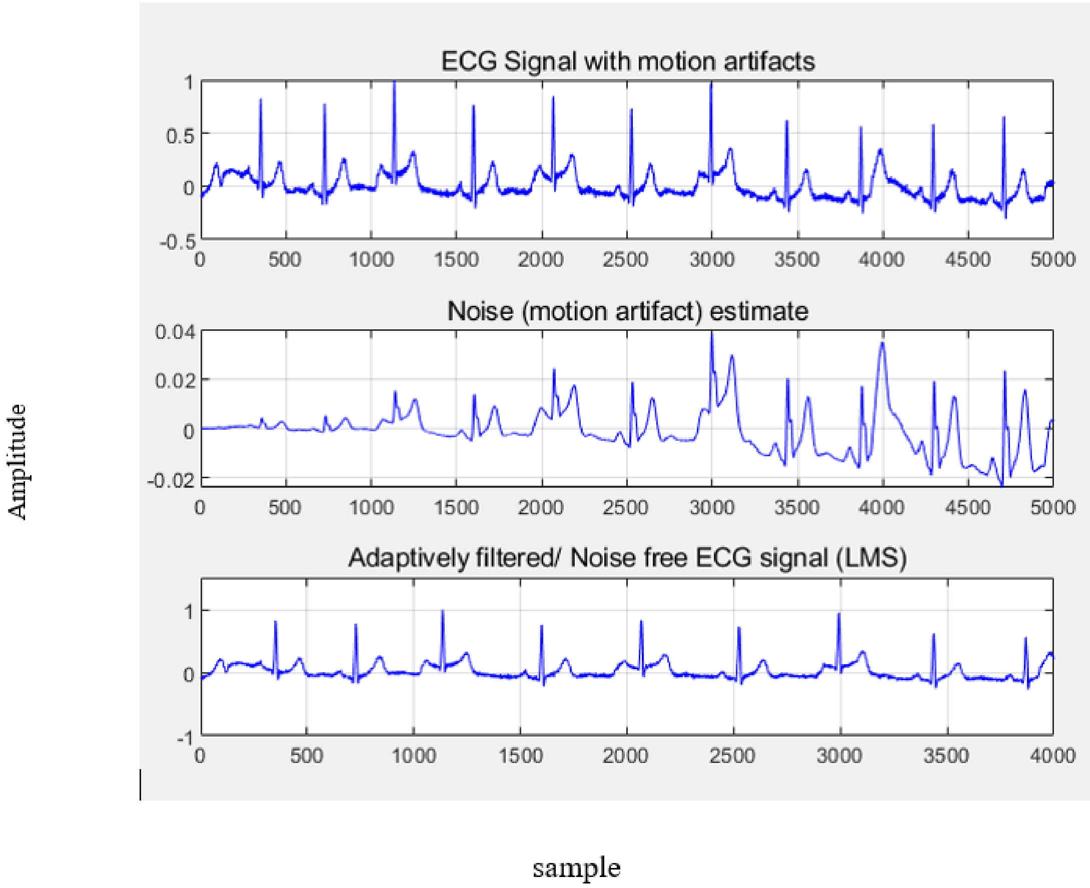

Figure 4.10 ECG of ARR, ARR with motion artifact noise, remove motion artifact using adaptive filter with LMS algorithm

We applied the adaptive filter with two algorithms (LMS and RLS) to remove electrode motion artifact noise which effect on ECG signal also accuracy of diagnostic like other noise which expose to ECG signal. To estimated the RLS is working a recursive and adaptive technique. It repeatedly adjusts the filter coefficients depending on the current input signal which represented (ARR) and the desired signal. For each time, filter output is calculating by produce between input signal and weight of filter. Then estimate the error through subtract desired signal from the output. We can see the output of adaptive filter to remove motion artifact noise from ARR signal which in figure (4.11)

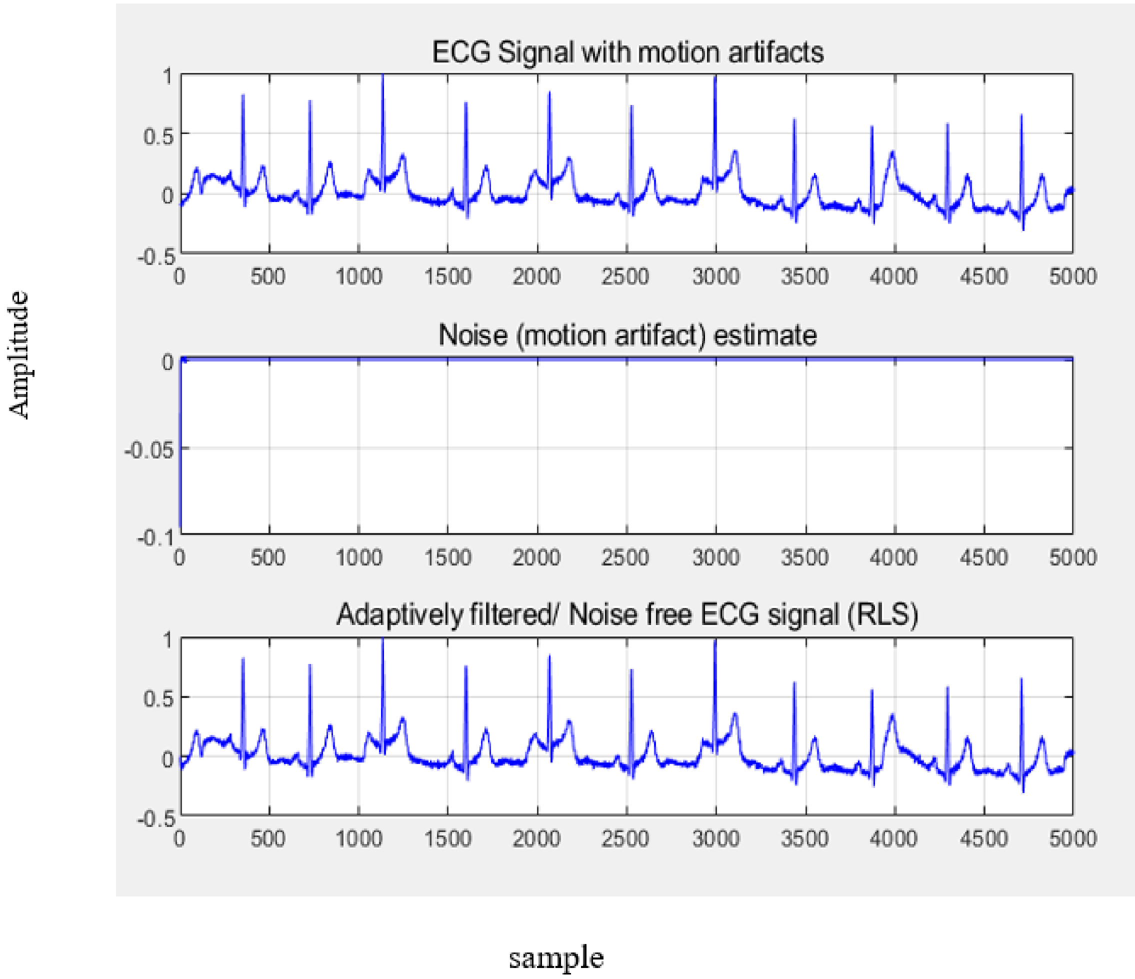

Figure 4.11 ECG of ARR, NSR with motion artifact noise, remove motion artifact using adaptive filter with RLS algorithm

The CHF signal is filtered from the baseline noise using DWT, where we choose the threshold value to reduce the filter coefficients after dividing the signal levels into secondary levels within a high and low pass filter, and DWT takes into consideration the low frequencies that are commensurate with the baseline wander frequencies as shown in figure (4.12)

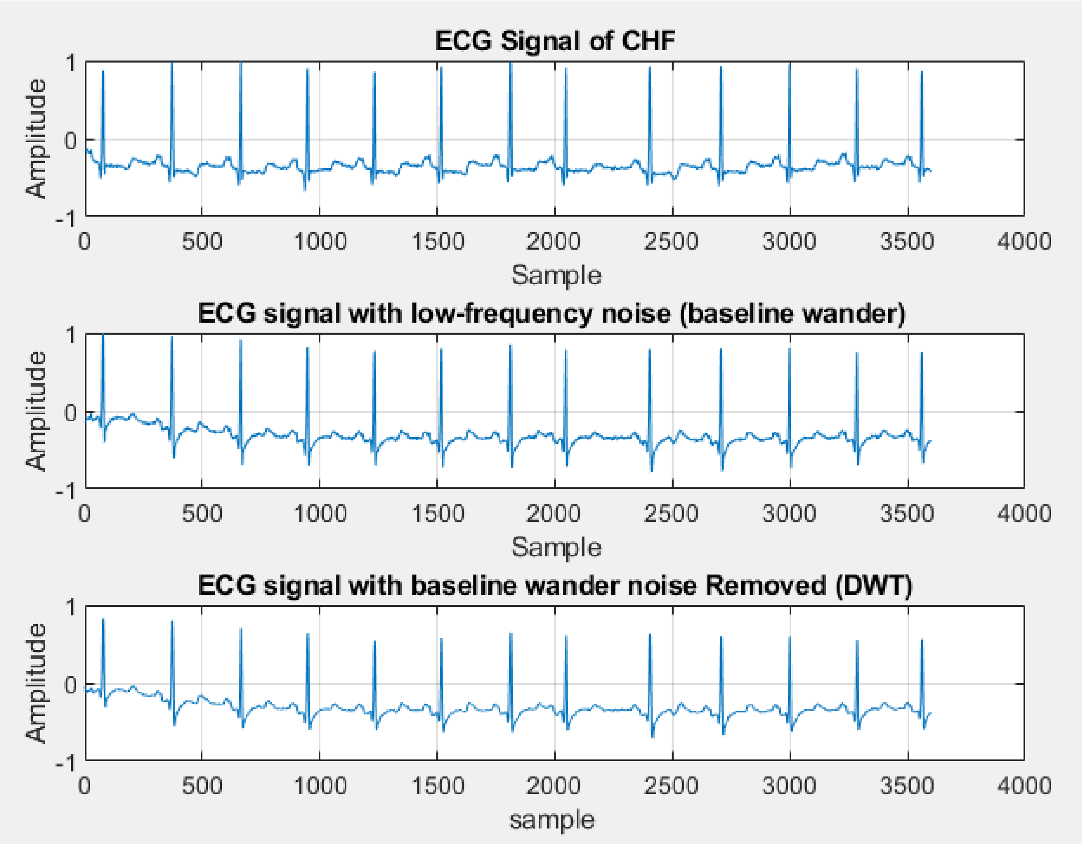

Figure 4.12 CHF of ECG signal, CHF with baseline wander ,remove the noise using DWT

When the notch filter is used to remove power line noise from CHF, an opposite signal is generated similar to the noise signal to be removed with the phase difference between the two signals, then the signals are mixed. The signals that make up the bandwidth output are discarded, we can see the output filter in figure (4.13)

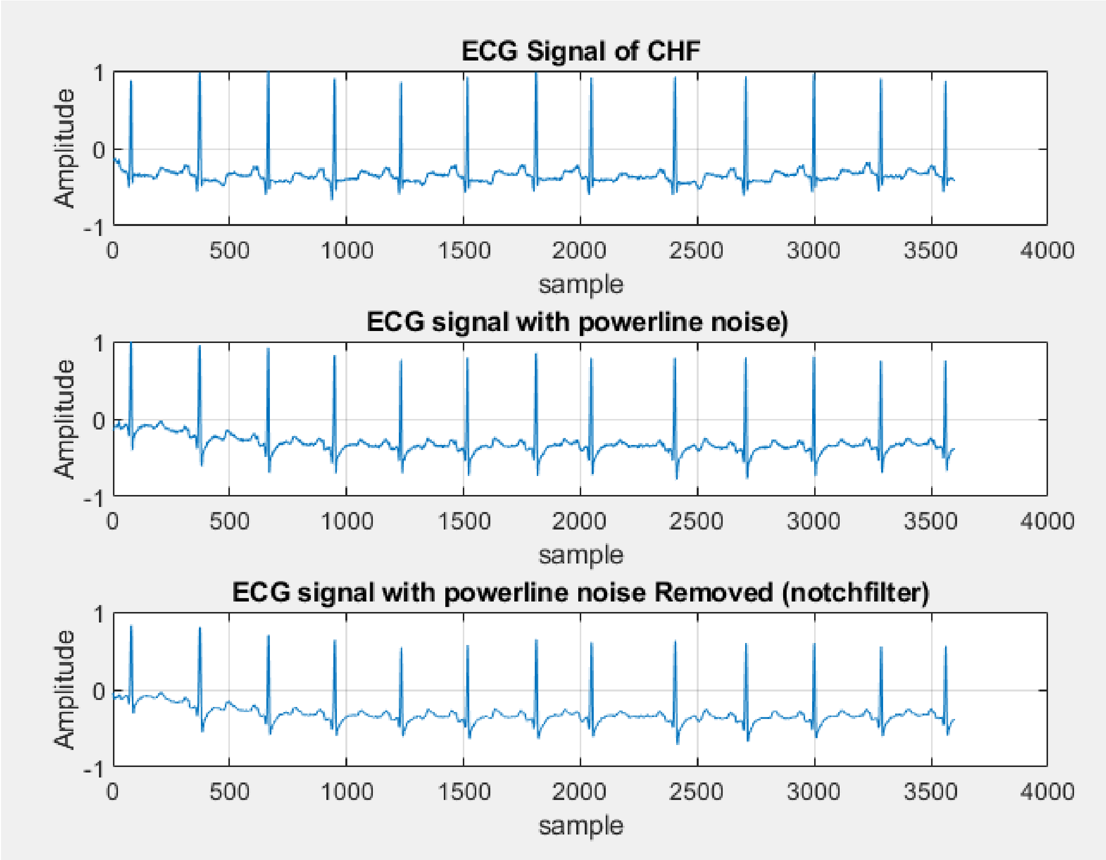

Figure 4.13 ECG signal of CHF, CHF with powerline noise, remove powerline noise using (Notch filter)

The figure (4.14) which exhibit the output of adaptive filter to remove the EMG noise from CHF signal. Choosing an appropriate removal type for the adaptive filter, which is an endless response filter. When a muscle noise-containing input signal is entered, a reference signal is generated that is equal to the noise signal to be deleted. The frequency of muscle noise varies from person to person and case to case. It operates at a frequency of 25 to 150 Hz. Depending on the adaptive filter's action, the noise-input signal is mixed with the reference signal, and the weights are constantly updated to reach the ideal signal and eliminate the noise.

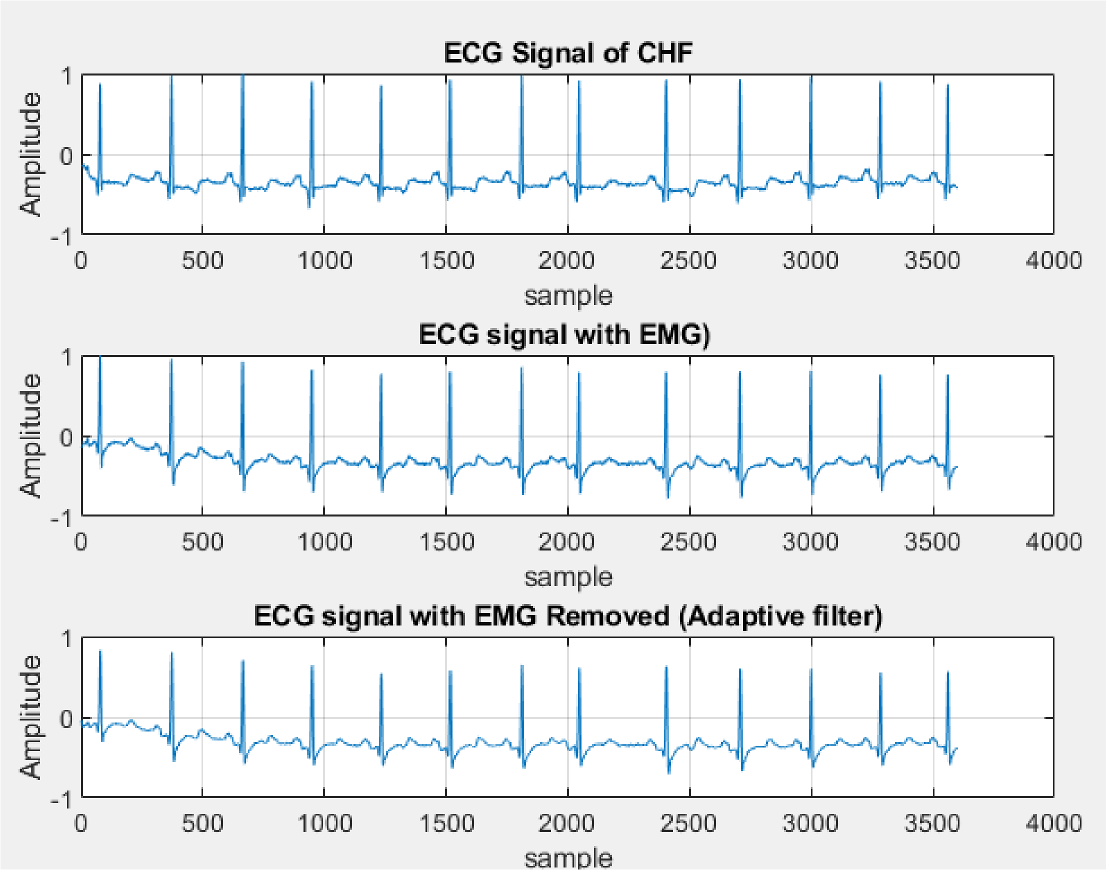

Figure 4.14 ECG of CHF, CHF with EMG noise, remove EMG noise using (Adaptive filter)

Algorithms for adaptive filtering LMS and RLS are used to filter the ECG signal's Electrode Motion Artifacts noise. The LMS and RLS adaptive algorithms process the initial ECG signal. The most often utilized technology for removing electrode motion traces and EMG noise is adaptive filtering. Adaptive noise filter structure cancellation, which is employed in this study, requires the basic and reference signals. When additional input signal samples are obtained, the adaptive filter parameters W_k are modified. The filter settings are continuously modified based on the step size. The figures (4.15) and (4.16) are illustrate the output of adaptive filter to remove noise of electrode motion artifact with algorithms (LMS and RLS)

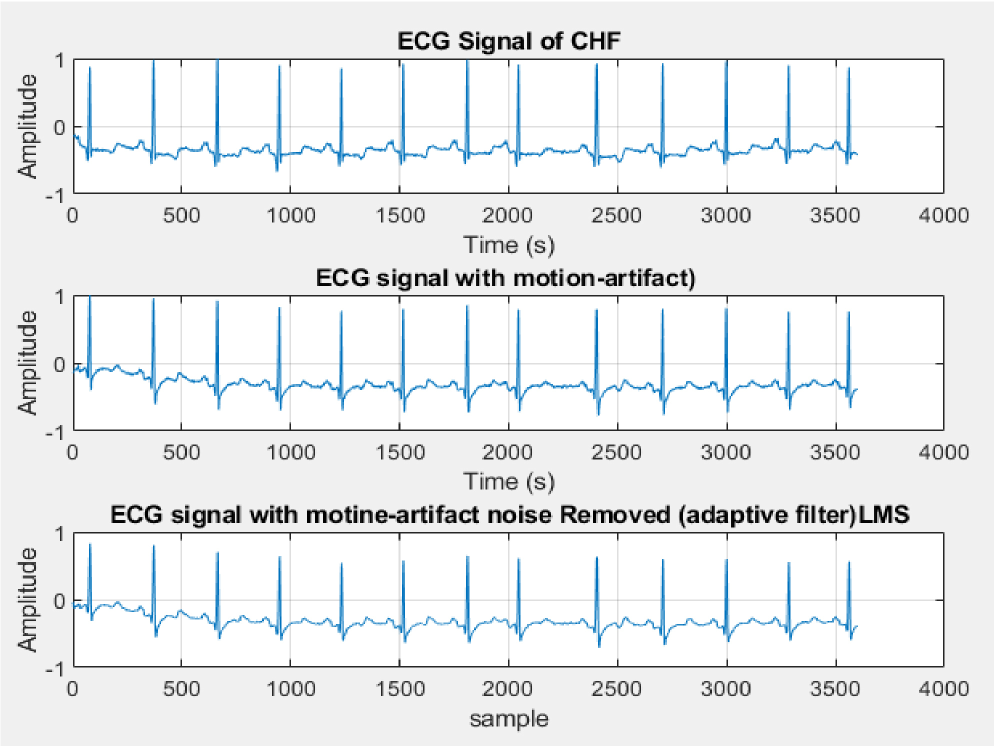

Figure 4.15 ECG of CHF, CHF with motion artifact noise, remove motion artifact using adaptive filter with LMS algorithm

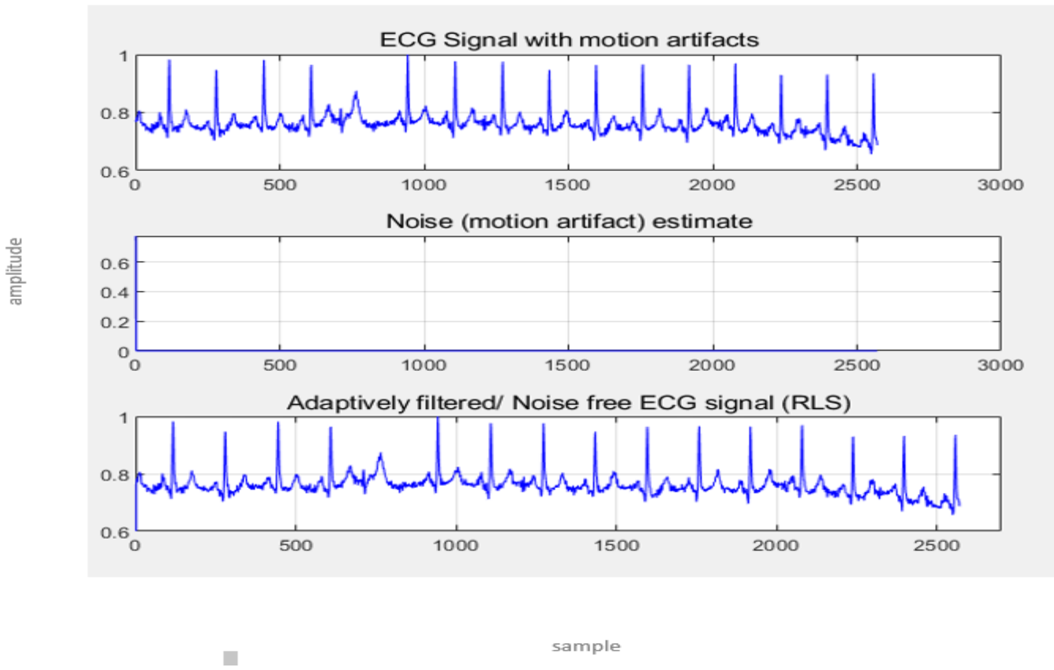

Figure 4.16 ECG of CHF, CHF with motion artifact noise, remove motion artifact using adaptive filter with RLS algorithm

Table 4.1 SNR of procced signals

case	BLW	PLI	EMG	Electrode motion
CHF	23.0464	22.9772	23.8330	**23.0972**
ARR	22.5556	22.8466	22.5042	**23.0122**
NSR	29.5811	27.67445	27.6751	**28.0459**

4.3 Feature extraction by BSS with Machine Learning

Because poor feature selection can degrade classification performance, feature extraction is the most important aspect of biomedical signal classification. Dimension reduction/feature selection selects the smallest subset of features from the original set of features to achieve the greatest degree of generalization. The figures (4.17-4.20) illustrate feature extraction by BSS with neural network as separation the mixing source in time and frequency domains

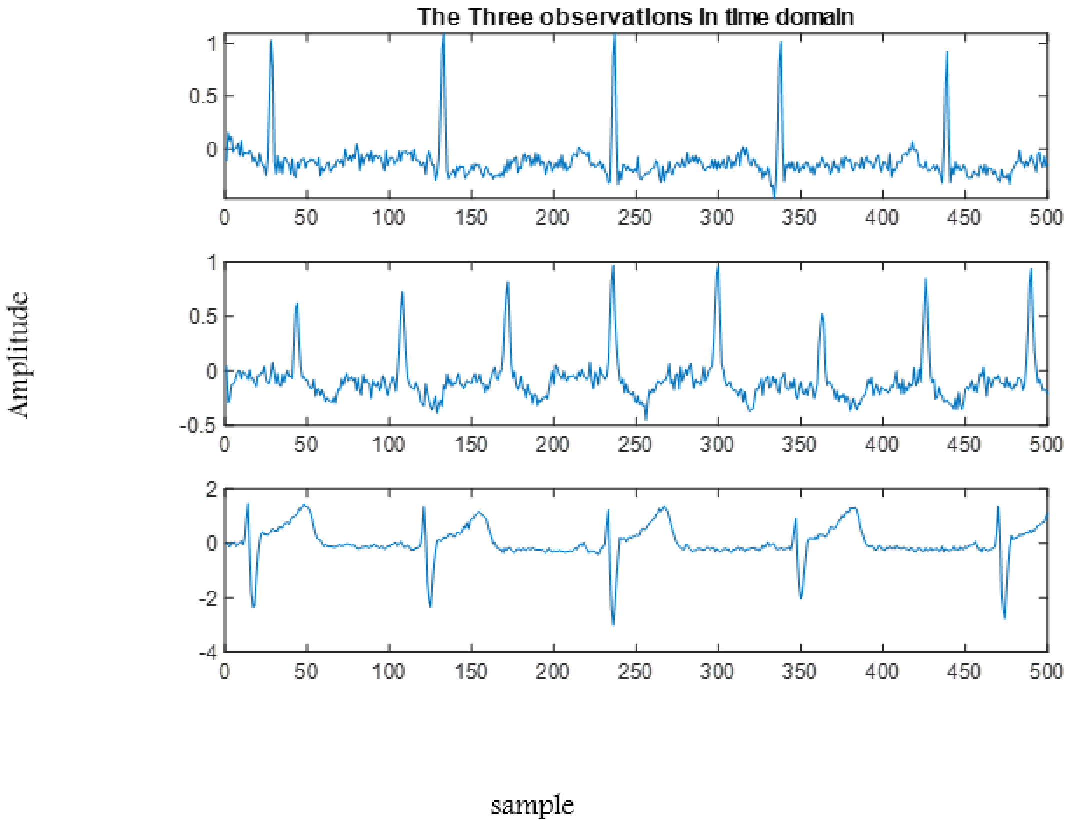

Figure 4.17 mixing signals before process(BSS+NN)

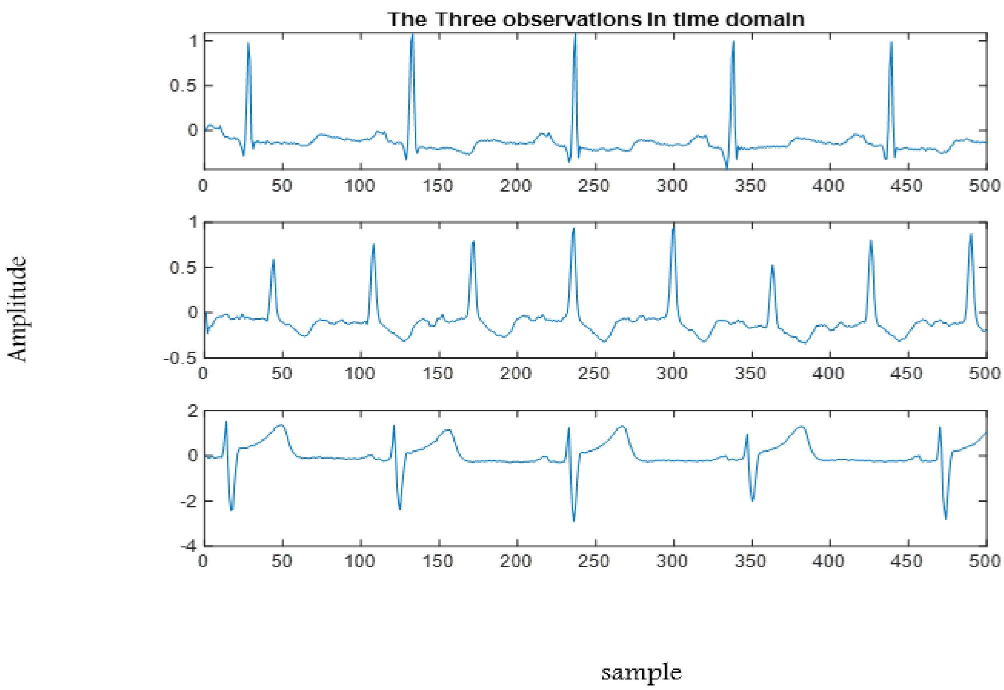

Figure 4.18 mixing of signal after process(BSS+NN)

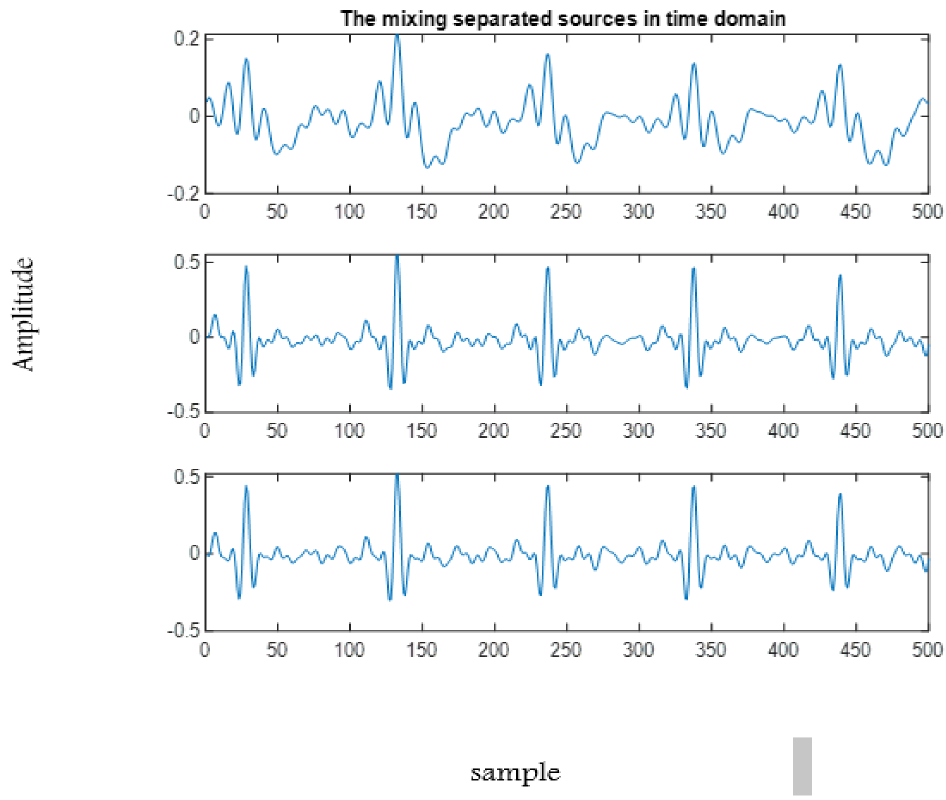

Figure 4.19 separated source in time domain (BSS+NN)

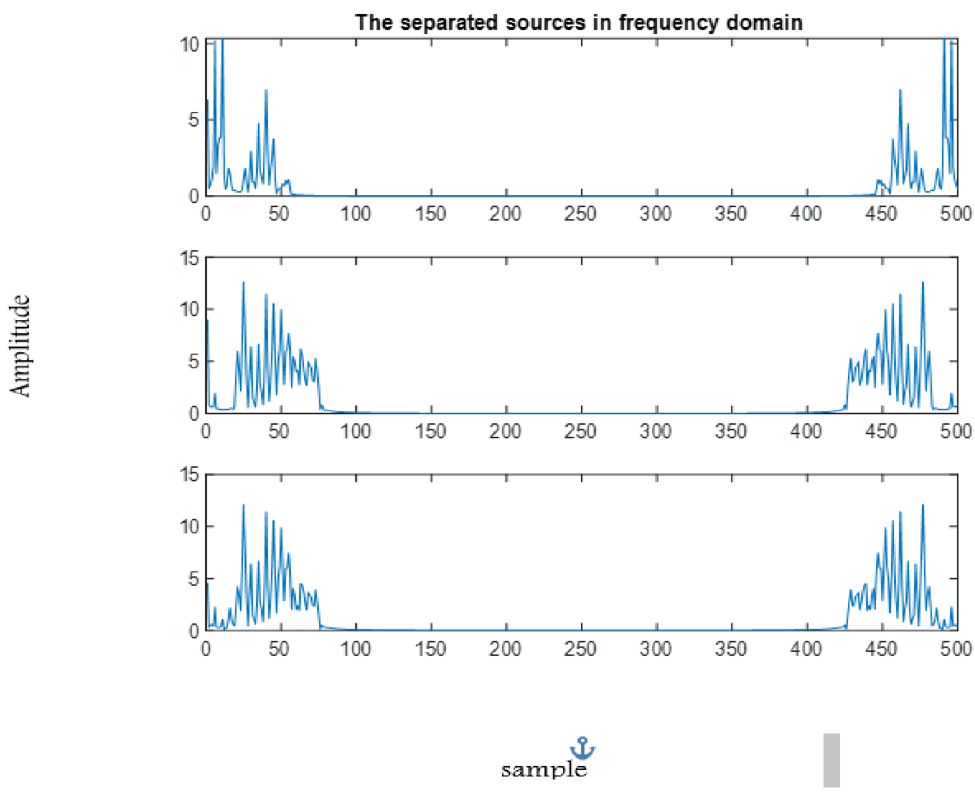

Figure (4.20) separated source in frequency domain(BSS+NN)

As mention previously, BSS (Blind Source Separation) is a technique of the signal processing whose goals to separate individual signals from a mixture of signals without having to know the specific properties of each signal. BSS may be utilized to extract features in a variety of applications, including speech recognition, image processing, and bioinformatics. The made by mixing signals are first disintegrated into independent sources utilizing BSS techniques in BSS-based feature extraction. The extracted sources may be utilized as features for classification. The data of the signals(ARR, CHF, NSR) are mixing by BSS technology as single signal as shown in figure below(4.21)

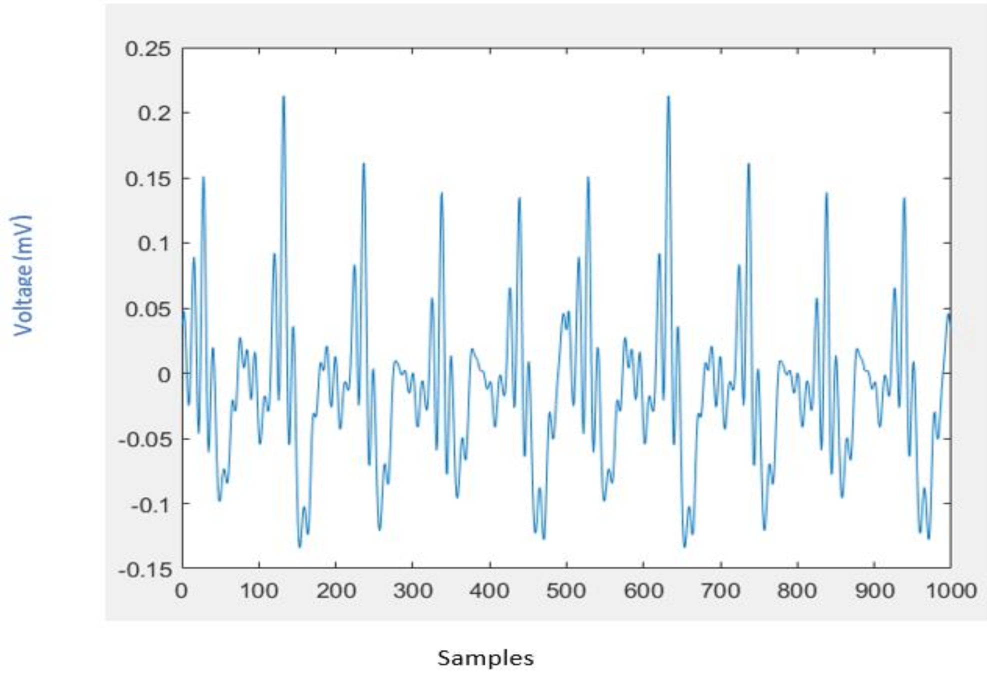

Figure 4.21 mixed signal for three signals

After extract features which are utilizing to classifier by NN or SVM will be compute the accurcy of algorithms performance and know the best validation performance at epoch after training of the data as shown figure(4.22) below which appear best validation performance at epoch 38 with value is 0.0087425 when is classifier NN and BSS as feature extraction

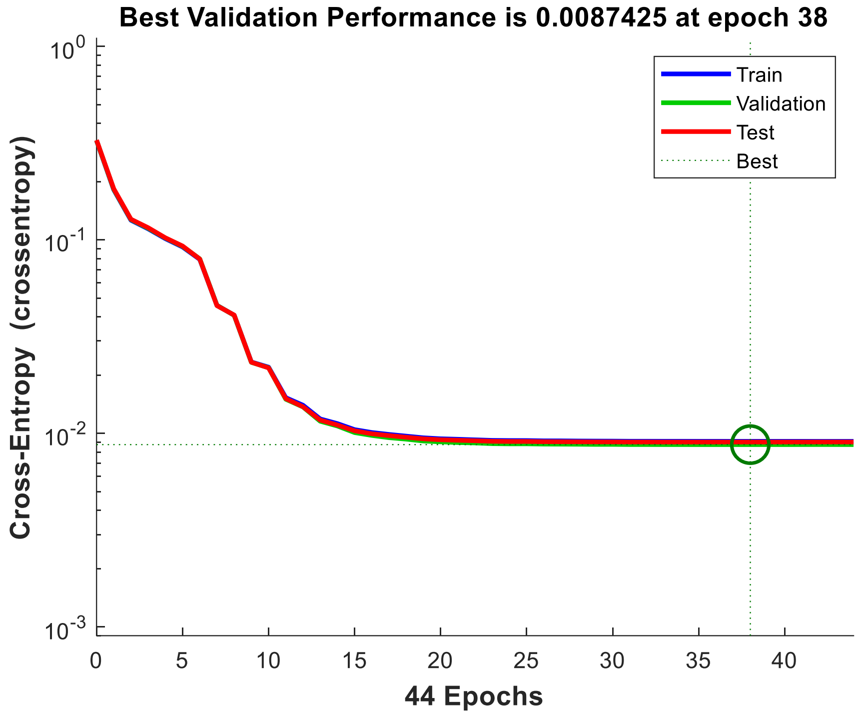

Figure 4.22 best validation performance at epoch 38

In figure (4.23) below is represent error histogram, A histogram of errors is a diagrammatic display of the statistical method of errors in a dataset. It is a histogram script that displays the number of errors in each dataset bin or interval. The histogram's x-axis denotes the dataset's intervals or bins, and the y-axis denotes the recurrence of errors in each bin. Through the error histogram, it is possible to know the location of the error and analyze it in the data set. It was found here that the error is with 20 bins as explain in figure below

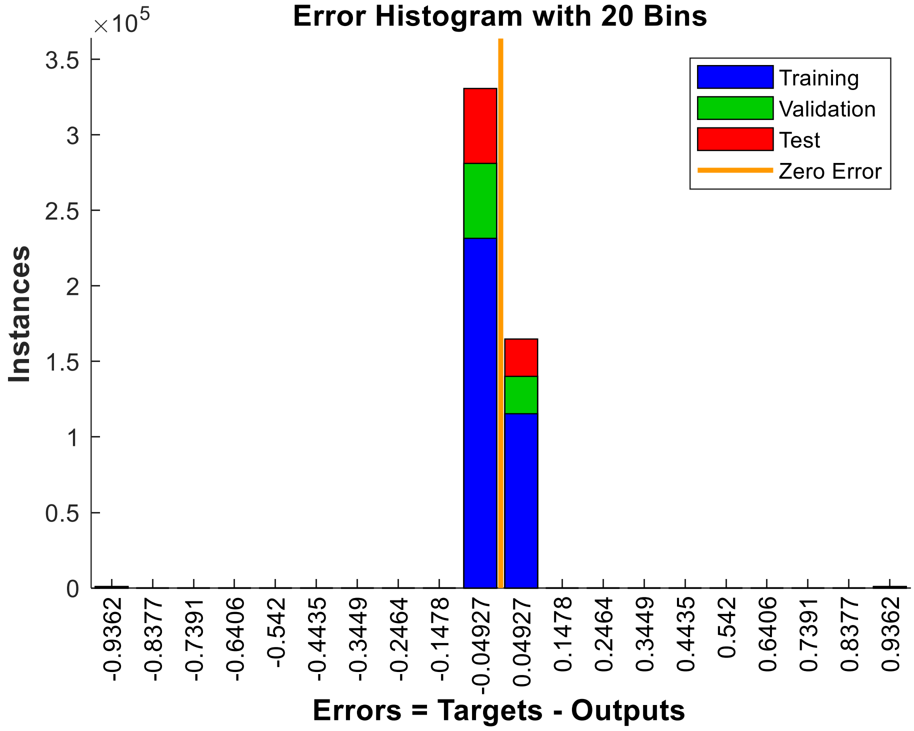

Figure 4.23 the error histogram

A confusion matrix is a popular way of representing any classifier's accuracy. It has rows that indicate the current category labels and columns that indicate the predicted target category. Each diagonal cell in such a matrix shows the amount of samples properly identified for a variety of distinct categories, is stated through the row/column description. Each cell which does not on a line indicates a category that was erroneously categorized. Time of training is equal 6.8906 in neural network with BSS with accuracy of classification is 99.4 as shown in figure (4.24)

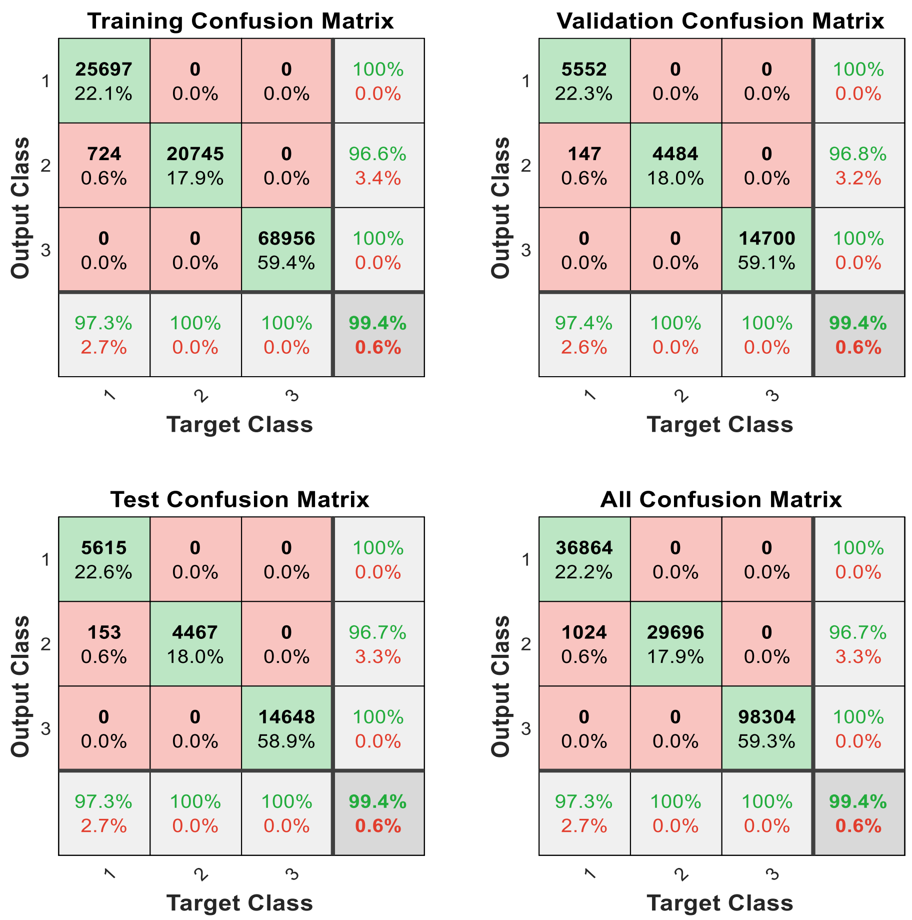

Figure 4.24 confusion matrix of BSS with NN

The table 4.1 exhibit the result of confusion matrix of BSS with NN algorithms to classification (ARR, CHF, NSR) according to the equation (2.26- 2.27) to performance measure of system

Table (4.2) the result of confusion matrix BSS-NN

BSS_NN					
case	TP	FP	FN	Se%	Pp%
ARR	36864	0	0	100	100
CHF	29686	1024	0	96.7	100
NSR	98304	0	0	100	100

The data extracted using the BSS method as feature extraction is fed into the SVM, and the results are produced. Figure (4.25) depicts the confusion matrix BSS of feature extraction and SVM, which has a provided accuracy of 99.38%, However, because each time window is classified separately here, the actual performance is improved. So every signal is classified into 16 distinct classes. For each window representation, a one class prediction must be obtained.

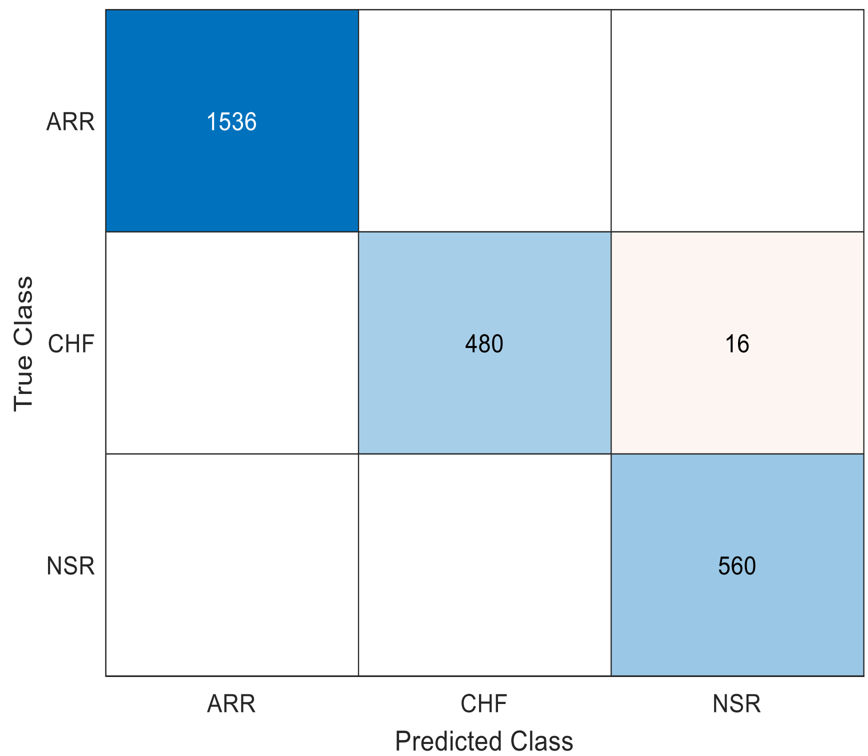

Figure 4.25 Confusion matrix of SVM+BSS.

The performance of system can be seen by the results of confusion matrix that shown in table (4.2) BSS feature extraction with classify by SVM

Table (4.3) the result of Confusion matrix of SVM+BSS.

BSS_SVM					
case	TP	FP	FN	Se%	Pp%
ARR	1536	0	0	100	100
CHF	480	16	0	96.8	100
NSR	560	0	0	100	100

4.4 Feature extraction by WST with Machine Learning

As previously stated, the experimental data was gathered from the PhysioNet 2016 heart database. ECG data were obtained from both healthy people and heart disease patients, and these data are in various recordings; the length of heartbeat recording varies. Classification is based on three classes that depict (ARR), (CHF), and (NSR) during 162 recordings. While the machine learning algorithms were running, the data was randomly divided into 70% for training and 30% for testing.

Scattering coefficients in particular time windows contain far more delegate information than scattering coefficients in other time windows. The reduction in time window dimensionality eliminates feature redundant information, which not only improves classification performance but also reduces computation complexity. The results of this study show that the scattering coefficients of the time window contain enough information to classify arrhythmias. The output of the feature matrix in this case is 416-16-by-113. The main parameters to define in a wavelet time scattering decomposition are the size of the time unaltered, the wavelet numeral transformations, and the wavelets number every interval in each of the banks of the wavelet filtering. A sequence of two filter banks is often sufficient to obtain acceptable efficiency. In the work, Using banks of the standard filter, we generate a wavelet time scattering decomposition: 8 wavelets every interval in the initial stage and 1 wavelet every interval in the second one. The constant time scale has been adjusted to a duration of (150 sec). Figure(4.26) explaine the Scaling function which appeare scattering coefficients of the time window

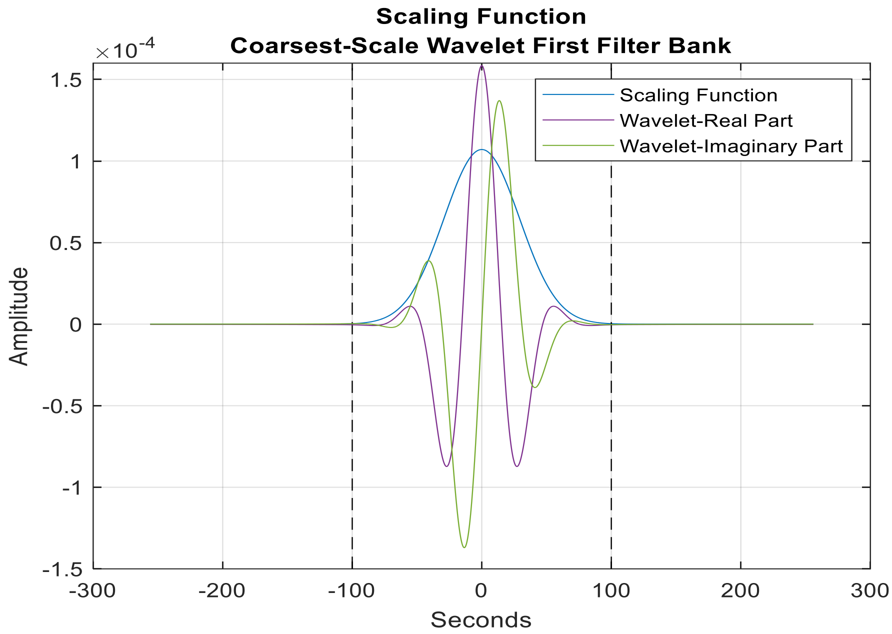

Figure 4.26 Scaling Function

After developing the scattering disintegration framework, we created a matrix of the scattering parameters for the training data. When using multiple signals in feature matrix, each of the columns is regarded as a separate signal.

After extracting features for use in a classifier by NN and SVM. In NN classifier, the accuracy of the algorithms' performance will be computed, and the best validation performance at epoch 117 will be known as shown in figure (4.27), which appears best validation performance at epoch 117 with value 0.015495 when classifier NN and WST as feature extraction.

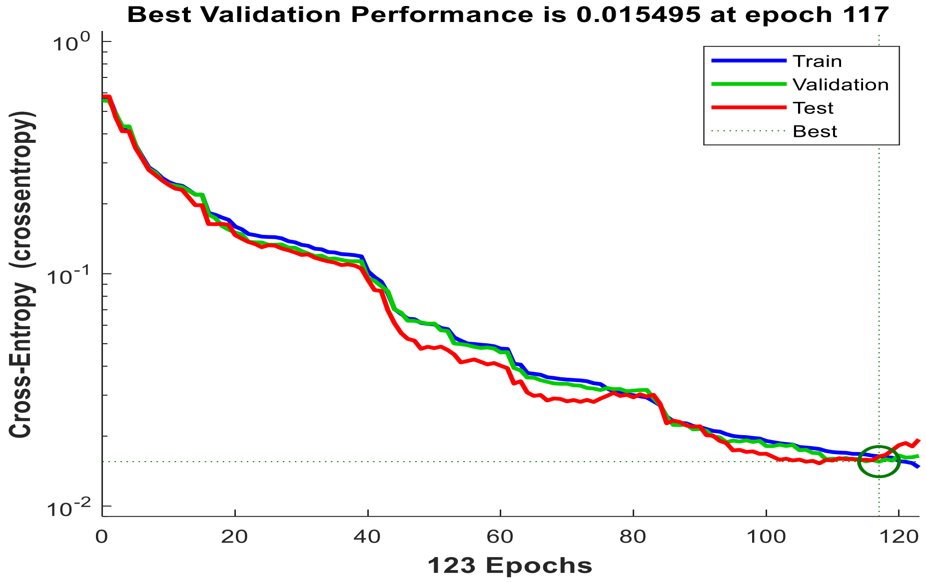

Figure 4.27 best validation performance at epoch 117

As we explained earlier, the error histogram is depicted in figure (4.28). A histogram of errors is a graphical representation of the statistical method of errors in a dataset. It's a histogram script that shows how many errors are in each dataset bin or interval. The error histogram can be used to pinpoint the location of the error and analyze it in the data set. It was discovered here that the error is with 20 bins, as illustrated in the figure below.

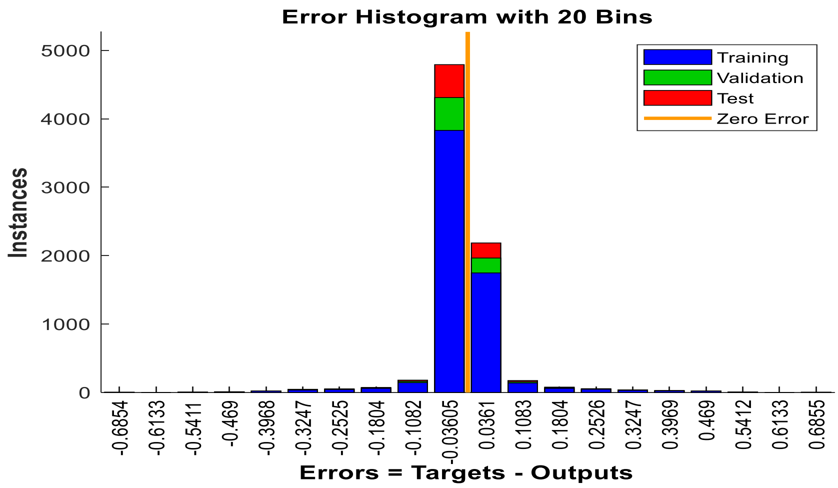

Figure 4.28 the error histogram at WST feature extraction

The scaling function's bandwidth is utilized to severely downsample the wavelet scattering transform in time. As a result, each of the 416 scattering paths has 16 time windows. A matrix of the confusion is the common method of representing the efficiency of classification of every classifier. A confusion matrix's rows contain the current labels of categories, whilst the columns of the matrix indicate the expected target category. In this kind of matrix, each diagonal cell reflects the number of correctly identified samples for each category label, as indicated by the associated row/column labeling. Each cell that does not lie on a diagonal indicate the category that was erroneously categorized. Time of training is equal 5.4375 in neural network with WST at accuracy classification is 99.7 as shown in figure (4.29)

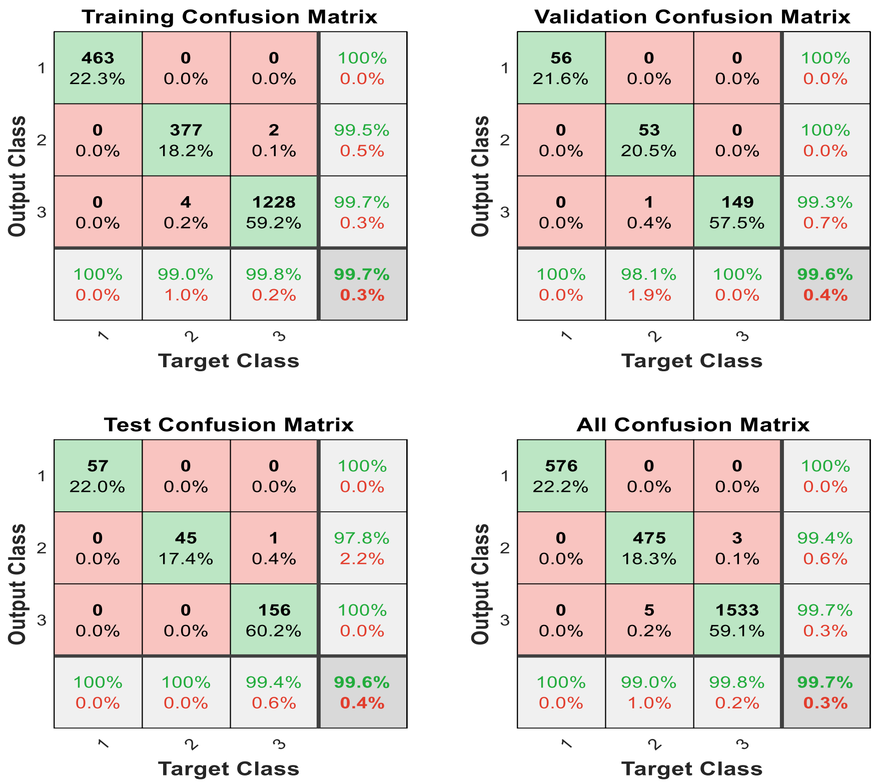

Figure 4.29 confusion matrix of WST with NN

Table (4.4) the result of Confusion matrix of WST+NN.

WST+NN					
case	TP	FP	FN	Se%	Pp%
ARR	576	0	0	100	100
CHF	475	3	0	99.4	99.0
NSR	1533	5	0	99.8	99.7

While WST with SVM, After 117 subsequent increases in validation error structure, the training is terminated, and the best probable performance is reached from the epoch with the lowest validation error. Figure (4.30) depicts the confusion matrix with wavelet scattering of feature extraction and SVM, a method with a given accuracy of 99.92%, which is very good, and the actual performance is better because each time window is classified separately here. Each signal is divided into 16 distinct categories. With each representation of scattering, utilize a easy majority to derive an only category estimate. The table (4.4) explain the sensitivity and prediction for system that utilized WST with SVM to classify the data

Table (4.5) the result of Confusion matrix of WST+SVM.

WST_SVM					
case	TP	FP	FN	Se%	Pp%
ARR	576	0	0	100	100
CHF	475	3	0	99.4	99.0
NSR	1533	5	0	99.8	99.7

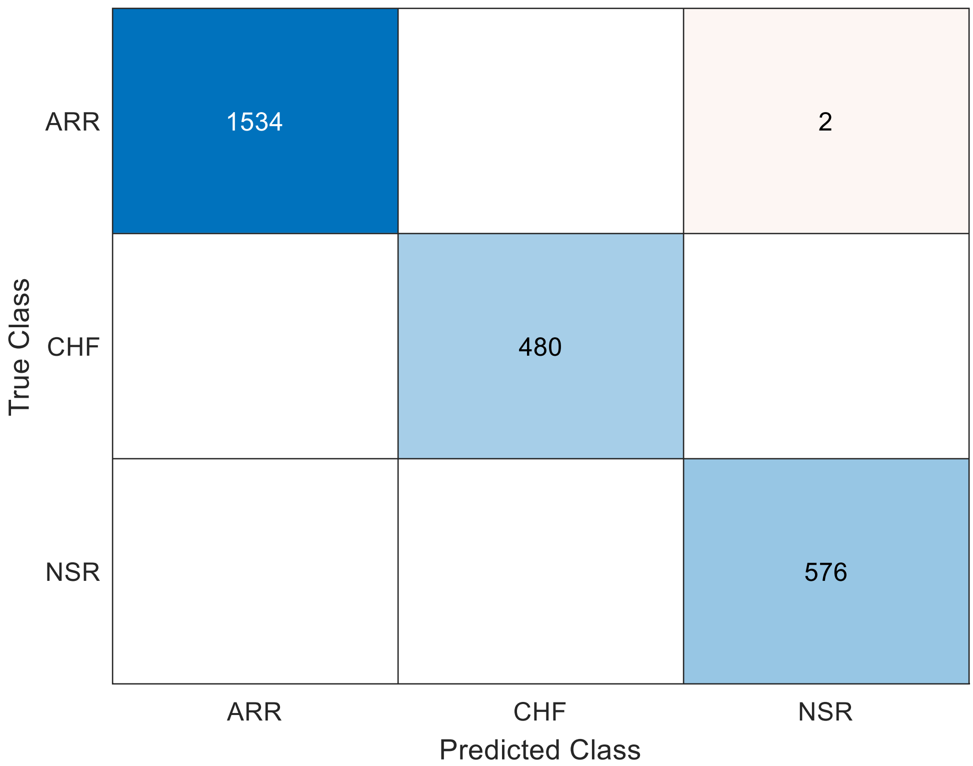

Figure 4.30 Confusion matrix of SVM+WST

After applying a number of algorithms in extracting features as in (separation of blind sources and transforming wavelet scattering) and algorithms of machine learning in classification as in (neural network and support vector learning) and obtaining the results in each case as mentioned above and comparing we proved that the best case is using Wavelet scattering transform with support vector machine which gave accurcy 99.92

Compare between wavelet scattering and blind source seperation

Wavelet scattering and blind source separation are among the algorithms used to extract features in ECG signal classification. After applying them in this work and obtaining the results that were previously mentioned above, they are compared as follows.

1- Wavelet scattering transform is a signal processing technique that aims to provide a stable representation of signals. It achieves this by applying a series of wavelet transforms and nonlinear modulus operations. The resulting scattering coefficients capture low-frequency and high-frequency information, making them well suited for the analysis of complex and non-static signals. Dispersion coefficients show stability for small distortions or variations in the input signal, which can be useful for tasks such as classification or pattern recognition. Blind signal separation is used to separate multiple signals from a group of mixed signals without the need for prior knowledge of the original signals. Capable of handling severe interference between signals and providing accurate separation between different components.
2- The wavelet scattering conversion is designed to be robust and stable under the presence of small distortions or changes in the input signal. This invariance can be useful for capturing invariant task features of

such differences, making them suitable for tasks such as signal classification. While blind source separation is commonly used for sound processing.

4.5 The results of ECG diagnostic system

The system is excuited on mini- computer which called LattePanda with some supported components to get on

A variety of methods has been established for pre-processing ECG signals in terms of frequency content and signal morphology. The various methods for forecasting the signals all produced favorable outcomes. High accuracy and low computational algorithm to classify the normal and abnormal heartbeats are designed and evaluated. The wavelet scattering algorithm and the developed SVM classification method are used in three cases (NSR, ARR, CHF) classification method. The overall algorithm features for heartbeat and classification to the three categories are highly efficient and low computational. As an outcome, the ECG monitoring and diagnostic system employs a three-class heartbeat classification method that employs the wavelet scattering algorithm to extract features using the SVM method.

The algorithm was programmed into the microcontroller that is inside the mini-computer (Lattepanda), Lenardo Arduino is the processing inside device and is based on C and C++ programming to create the programming codes and provide these codes to any compatible boards after they have been verified and compiled.

Two procedures have been implemented to assess the performance of the system for monitoring and diagnosing ECG signals. First, the system was tested and assessed using the same data records that were utilized in the previous section to assess the diseases classification approach.

Second, the ECG sensors read the actual ECG signal from a human body. The system is analyzed the ECG samples by executing the feature extraction and classification programming algorithm. Windows are typically used as the main way of exhibiting information and handling applications in GUIs. Each window indicates a distinct task or application and can be resized, relocated, reduced, or closed. The Lattepanda device connected to the LCD screen through the HD connection which displayed the running progress and the algorithm outputs. The interface of system utilize many menus, these menus are frequently used in GUIs to provide a hierarchical list of options and commands. Menus can be accessed via the top-of-the-window menu bar or a right-click context menu. They enable users to perform various actions and access various application functions as shown in figure 4.31. The outputs can appear the following:

- Information of the patient(name, gender, age)
- Filter type
- Recorder name
- Recorder length
- Load (load the recorder of patient)
- Save (save the information and state of patient)
- ECG recording(No of samples, ECG shape of patient)
- Processing (pre-processing of ECG)
- Classification
  - Record time
  - Test ECG
  - Three cases (ARR, CHF, NSR)
- Diagnostic decision

- DAQ port (chose com3)
- Connect
- Exit

The system saves the ECG samples and the patient report in the memory of device for recall the data when needed . The folder contant the information and report of the patient, it will saved the folder in name of patient to upload from device memory in any time.

Actual ECG signal reads from a human body were used to test the system. At the same sampling frequency, the sensors read the ECG signal from the body. The system then analyzes the ECG samples by running the feature extraction and classification programming algorithm. The system's results are promising for high accuracy and Arrthymia detection to disease diagnostics.

After the data processing process to eliminate noise and the data extraction process, it is classified into normal, abnormal, and normal conditions, and then the abnormal condition is diagnosed in the two cases (arrhythmia, congestive heart failure). The diagnosis is made for the pathological condition for each case according to the percentage of the threshold value of accuracy 85%. The case that forms a percentage more than this value indicates the concerned condition of the patient.

This section provides an analysis of the results with specific examples from some patients. Manual inspection revealed that feature selection was utilizing all of the required features for each case.The classification of all cases appears to have a high degree of accuracy.

The amount of beat type and number in the patient is undoubtedly the main reason for differences in diagnostic results of patients' conditions. For example, if the patient has 465 premature ventricular contractions and

1522 regular beats, the network will see both possible combinations for a sufficient number of times. Despite its widespread use, ECG analysis is an intricate process that necessitates the expertise of a specialist with broad specific knowledge.

Not only the patient's health, but also his or her life, is frequently dependent on the timely decoding of all data. This is complicated further by the complexity of manual ECG analysis, which increases the possibility of errors or incomplete diagnosis in interpretation. As a result, many studies aim to detect abnormalities using automated methods, such as DNNs in ECG analysis. The system effectiveness has been tested on 17 patients in different cases as explain in table 4.5 and figure 4.32

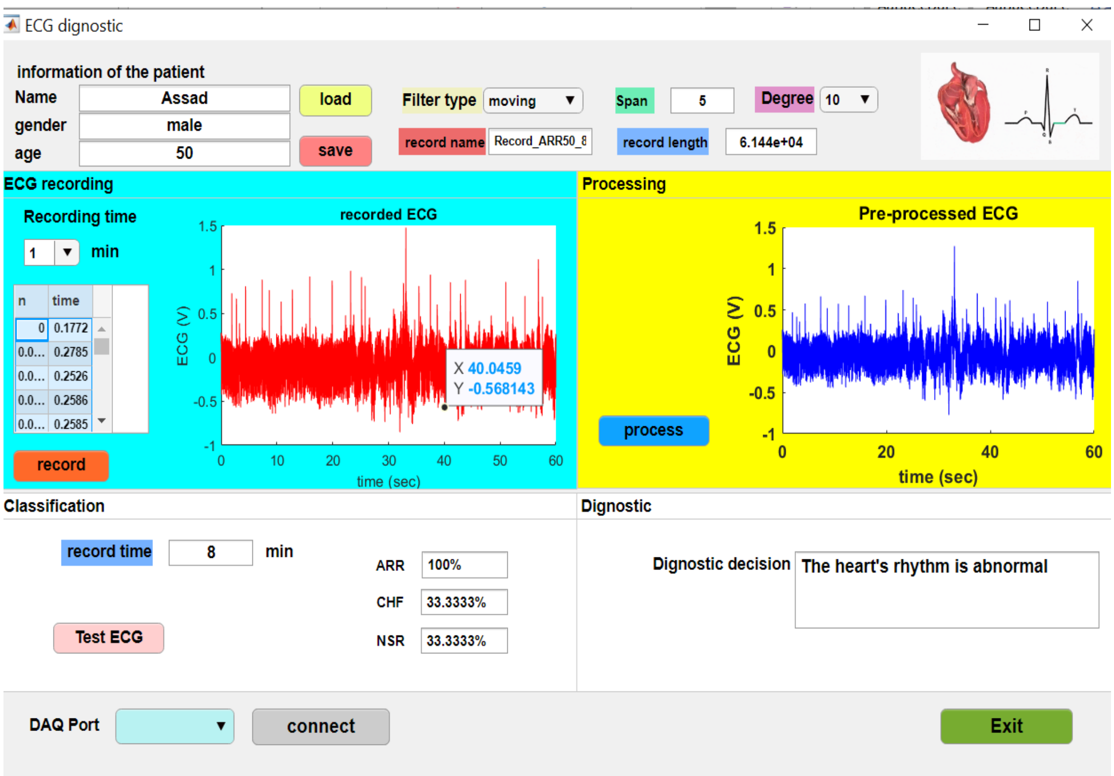

Figure 4.31 example to appear the output of system

Table 4.6 recorders of Patients

No. of case	Details of case	No. of samples	Ratio of diagnostic	Diagnostic
Case 1-	Ali-42- male	7680	99.832	ARR
Case 2-	Assad-51-male	61440	100	NSR
Case-3-	Adyan-19-famale	61440	99.8	NSR
Case4	Ahlam-60-famale	30720	99.9996%	ARR
Case-5-	Haider-46-male	30720	99.97	ARR
Case-6	Mena-46-famale	61440	99.9	CHF
Case-7	Marwa-37-famale		99.8322	ARR
Case-8	Obaid- 73-male	30720	99.83	ARR
Case-9	Mohmmed-44-male	30720	99.97	ARR
Case-10	Rabab-33-famal	61440	100	ARR
Case-11	Qussy-42-male	7680	100	NSR
Case-12	Huda-35-famal	61440	99.99	CHF
Case-13	Bushra-62-famale	30720	99.88	CHF
Case-14	Sana-51-famale	7680	99.99	ARR
Case-15	Mustafa-17-male	30720	99.99	NSR
Case - 16	Rewyda-34-famale	30720	99.99	NSR
Case - 17	Zahra-68-famale	61440	99.89	CHF

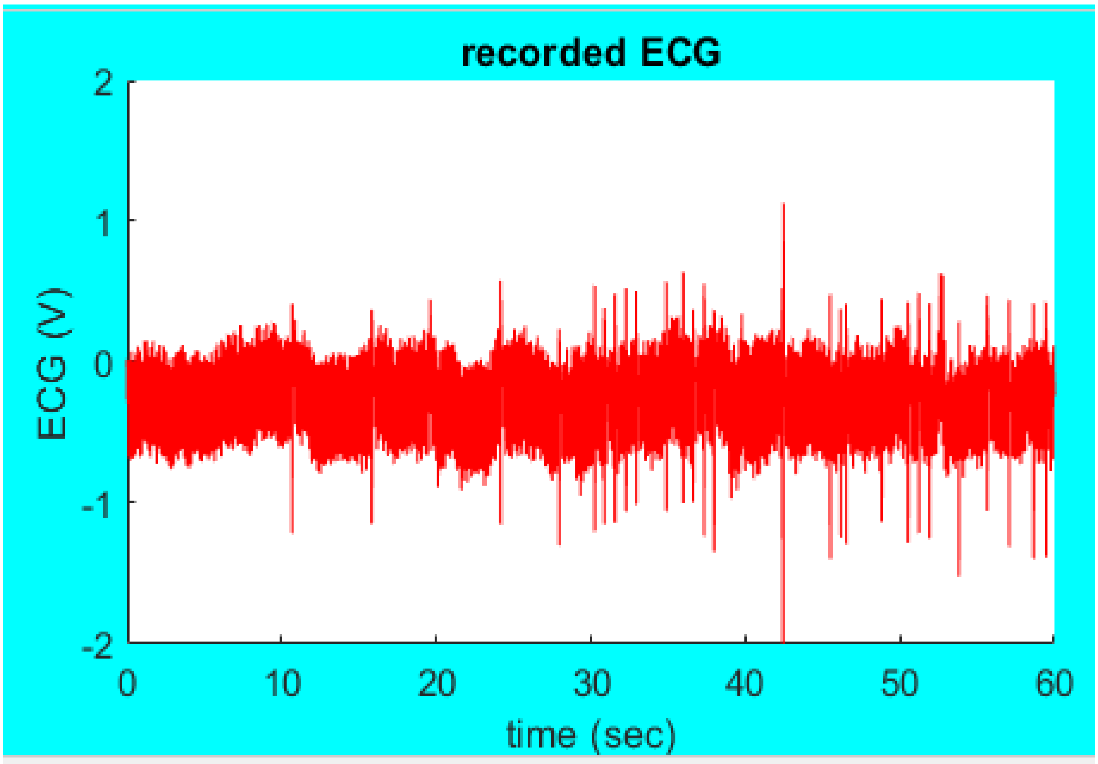

Case-1-ARR-before Pre-processing

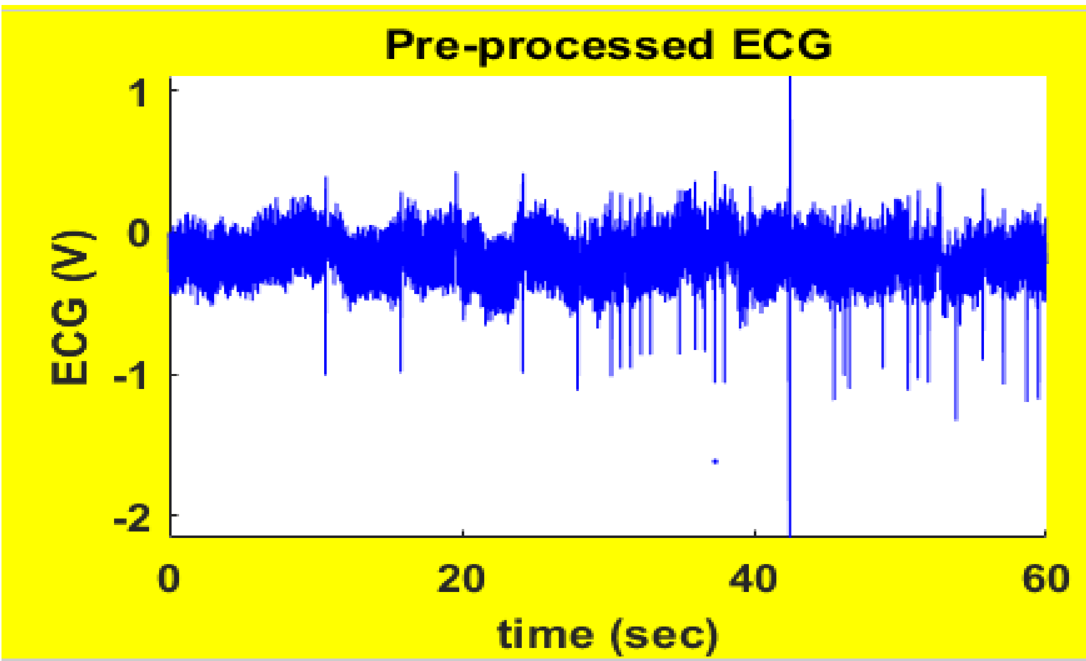

Case-1-ARR-after Pre-processing

(a)

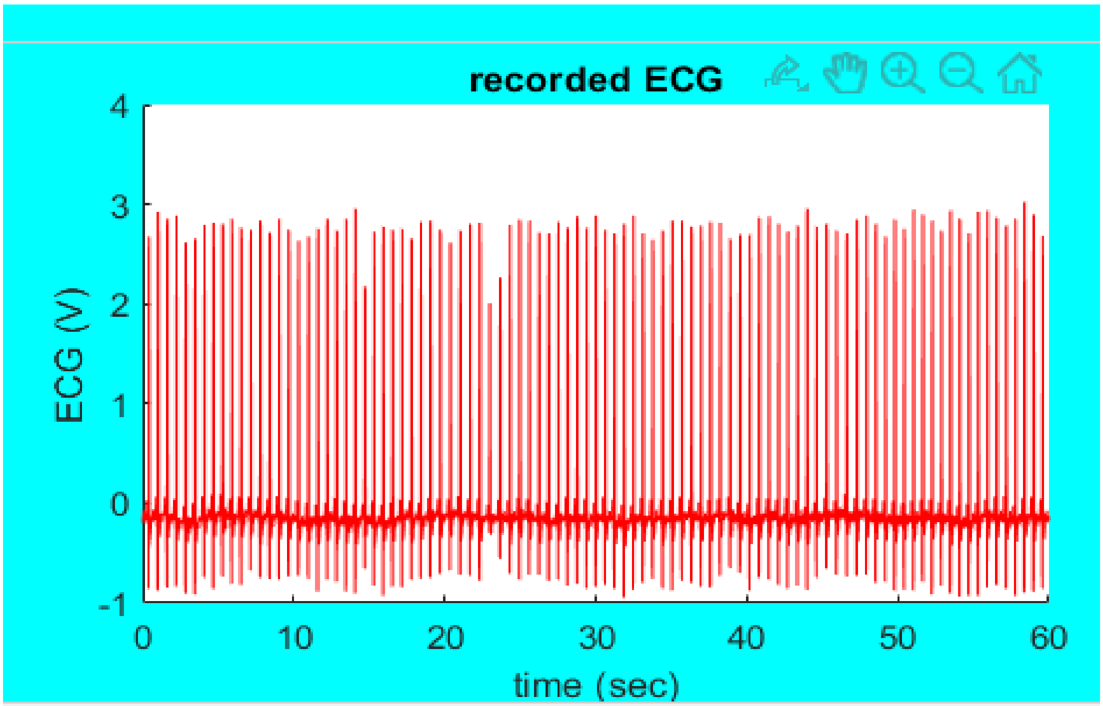

Case-2-NSR-before Pre-processing

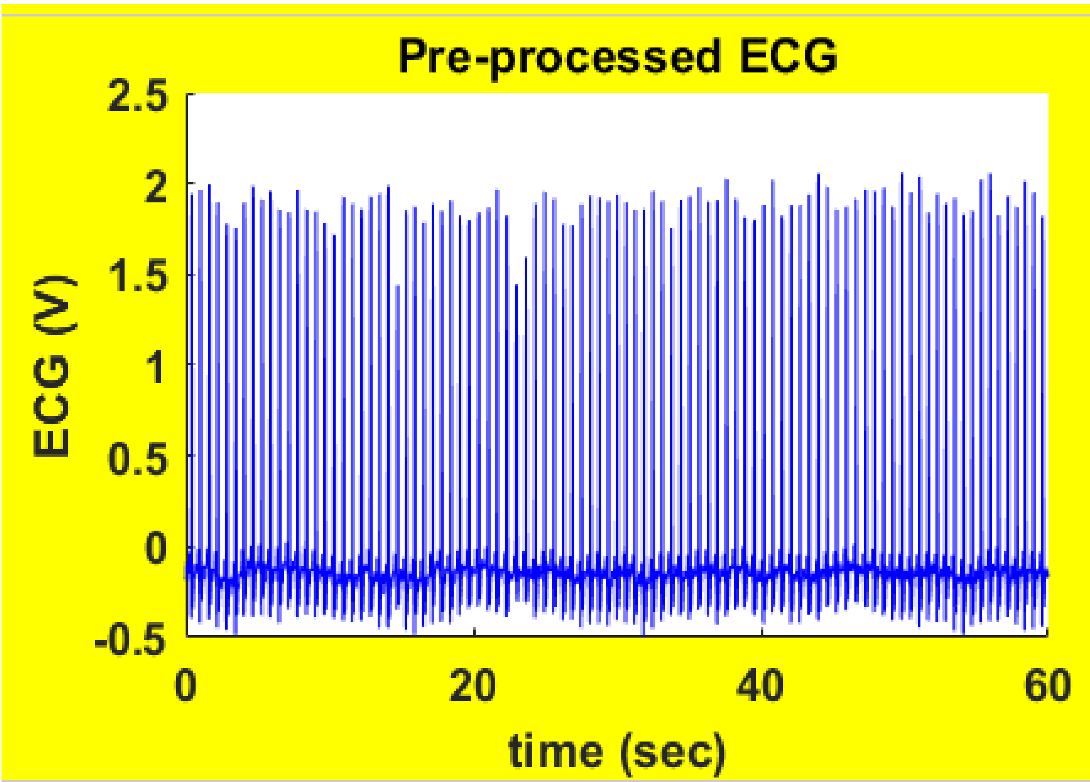

Case-2- NSR-after Pre-processing

(b)

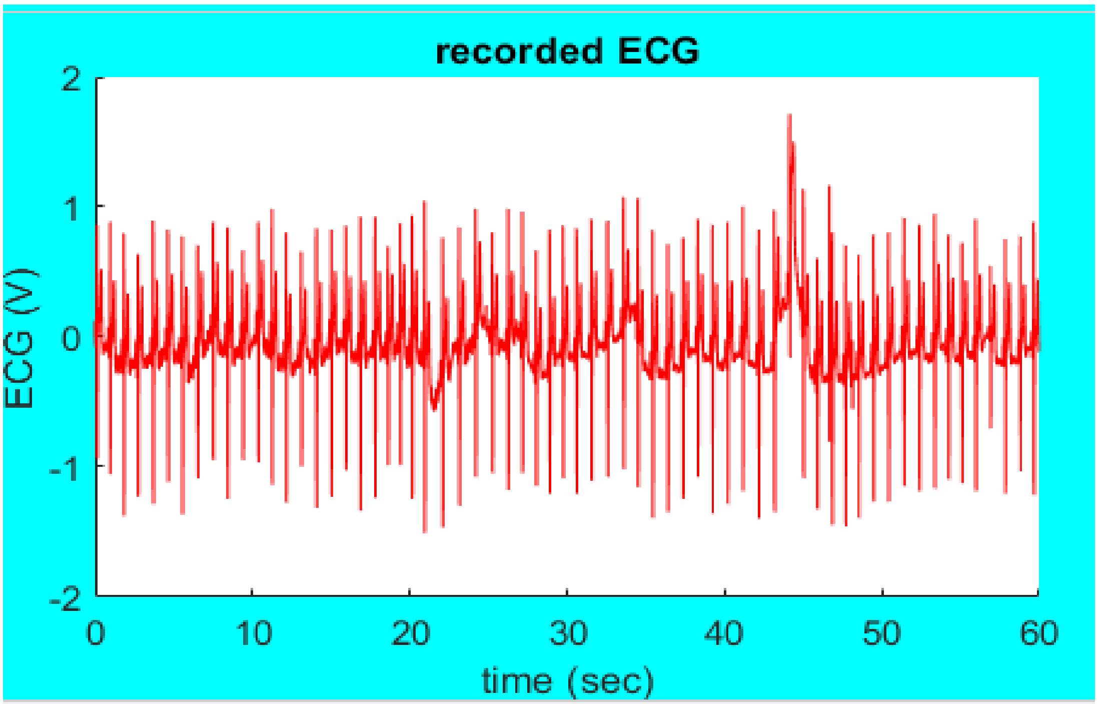

Case-3-NSR-before Pre-processing

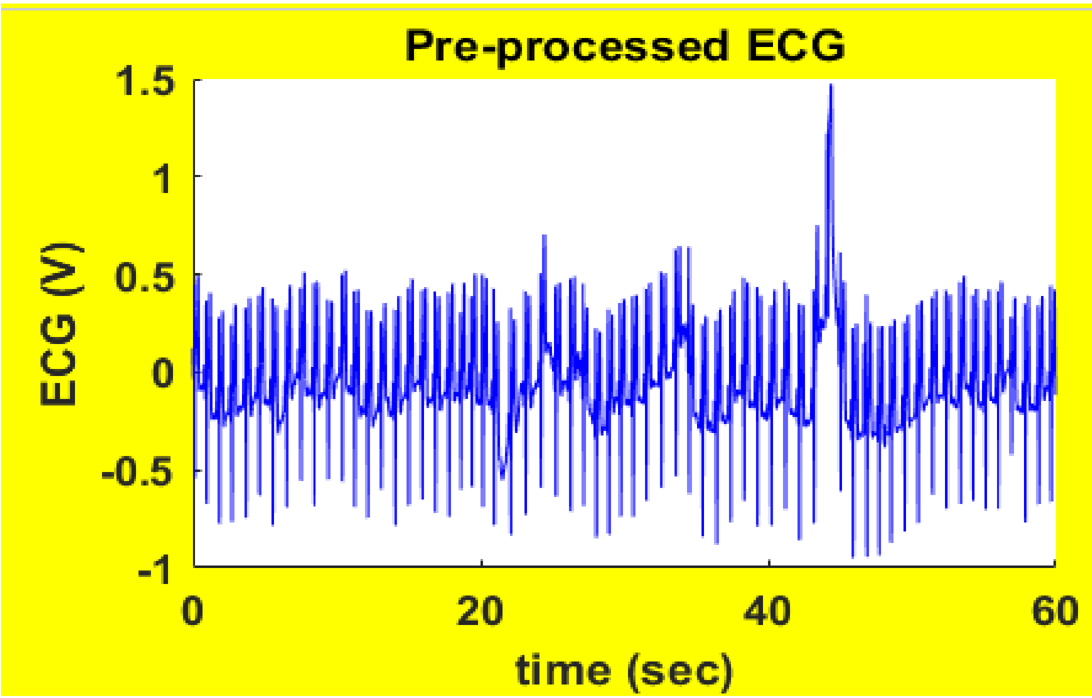

Case-3- NSR-after Pre-processing

(c)

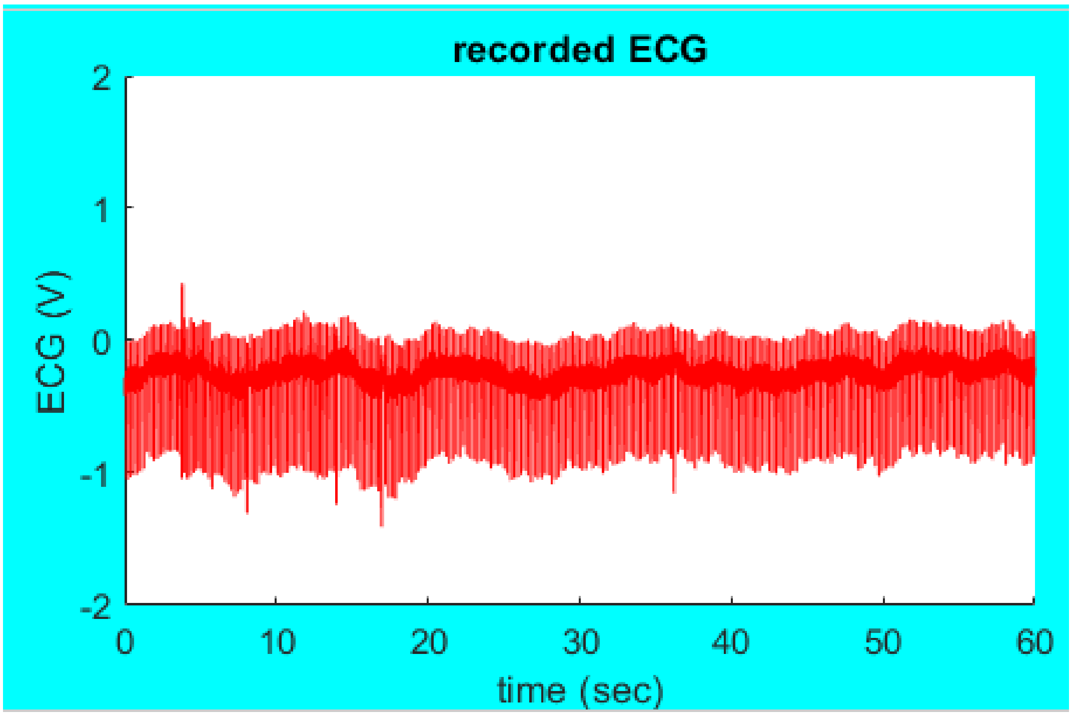

Case-4-ARR before Pre-processing

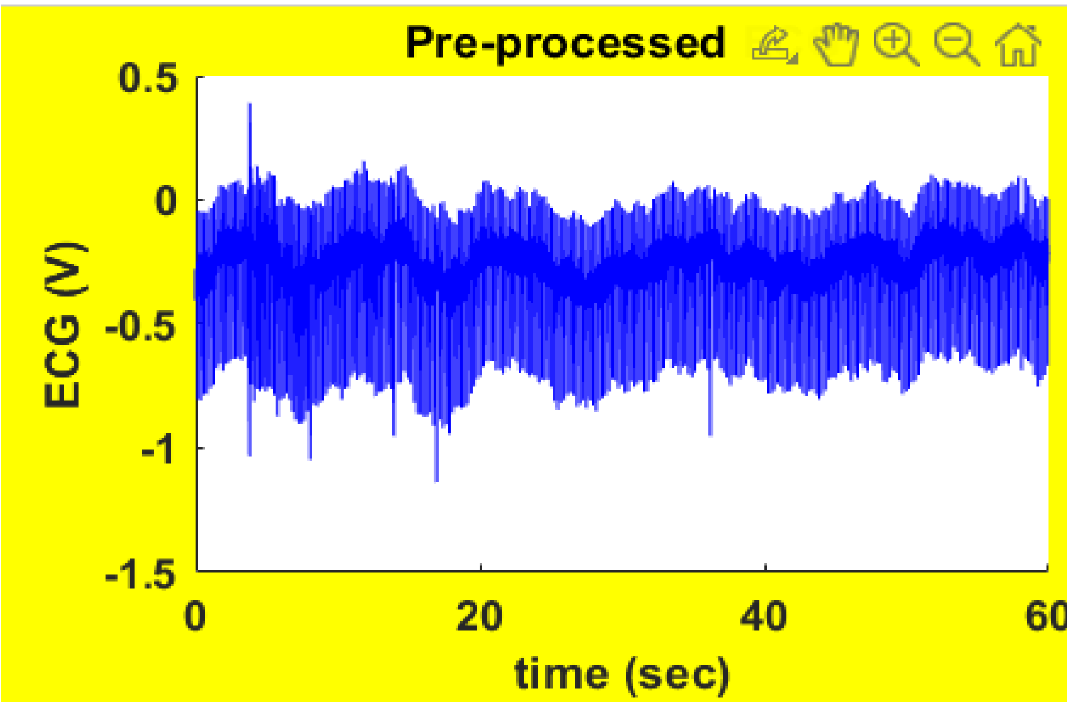

Case-4-ARR-after Pre-processing

(d)

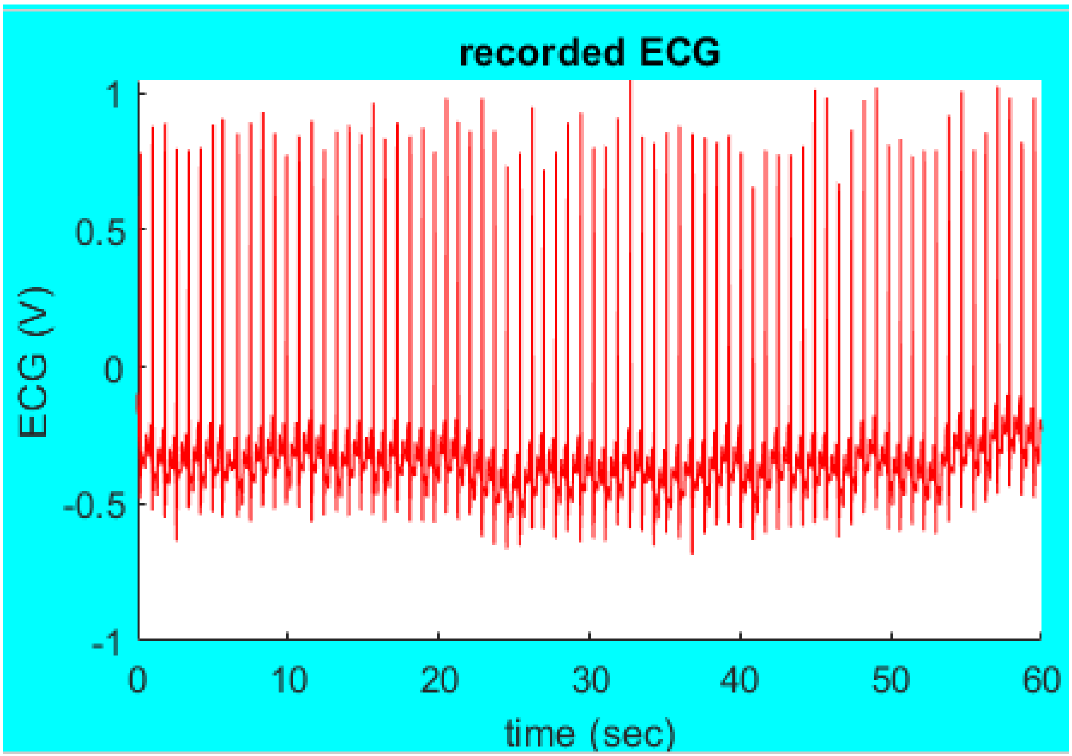

Case-5-ARR before Pre-processing

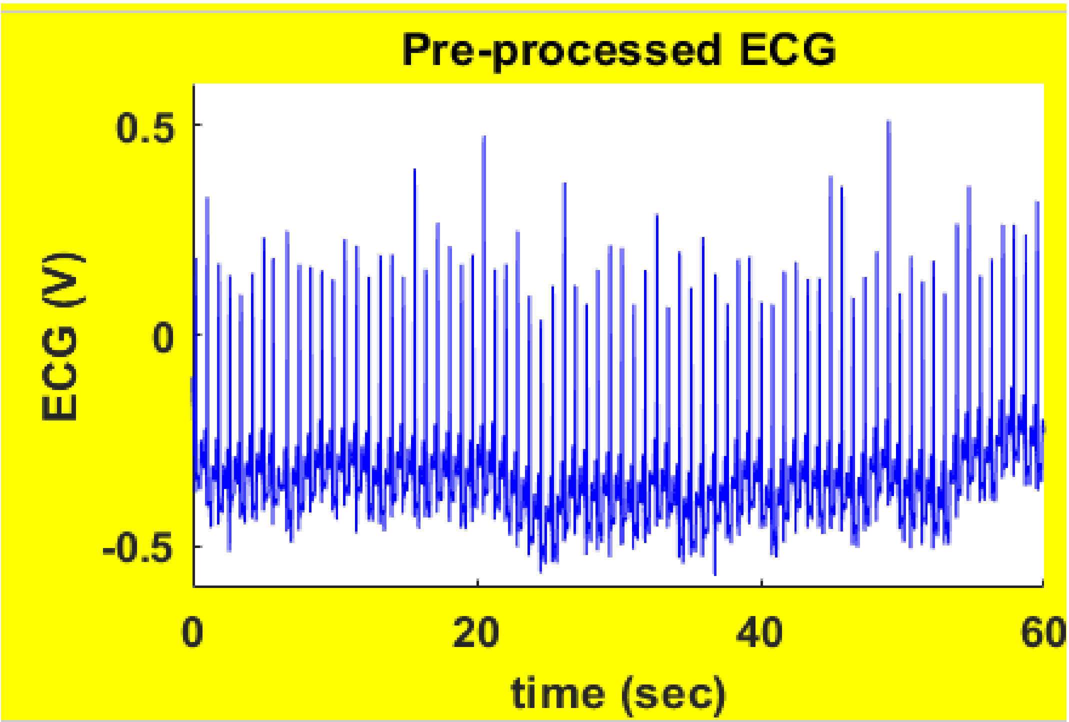

Case-5-ARR-after Pre-processing

(e)

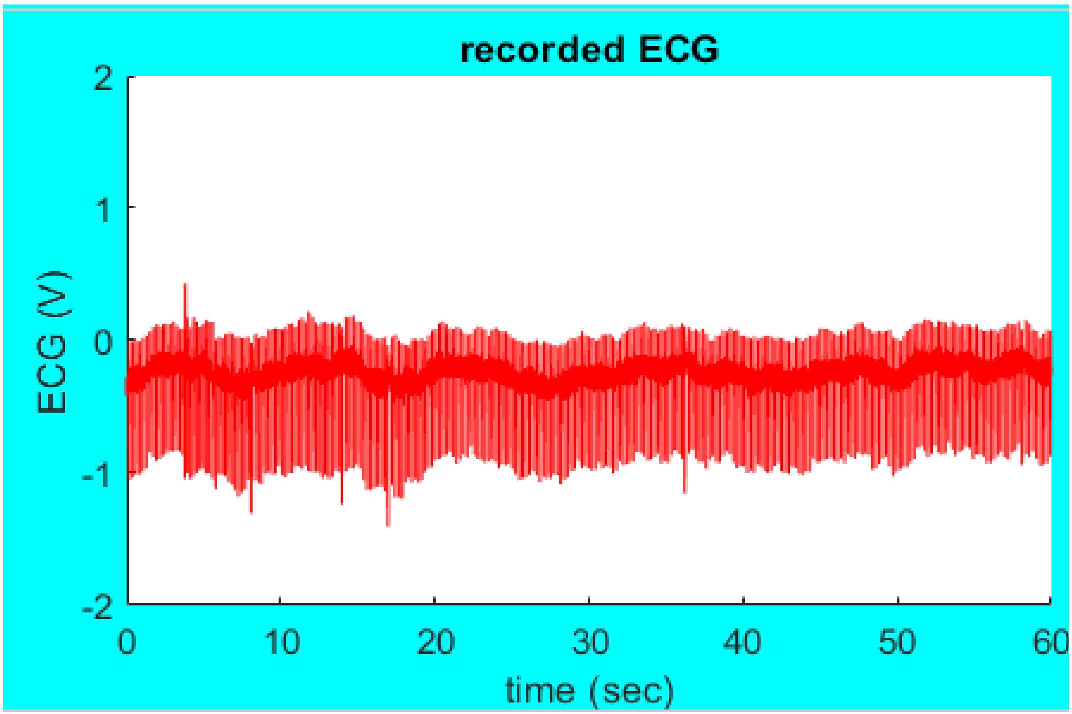

Case-6-CHF before Pre-processing

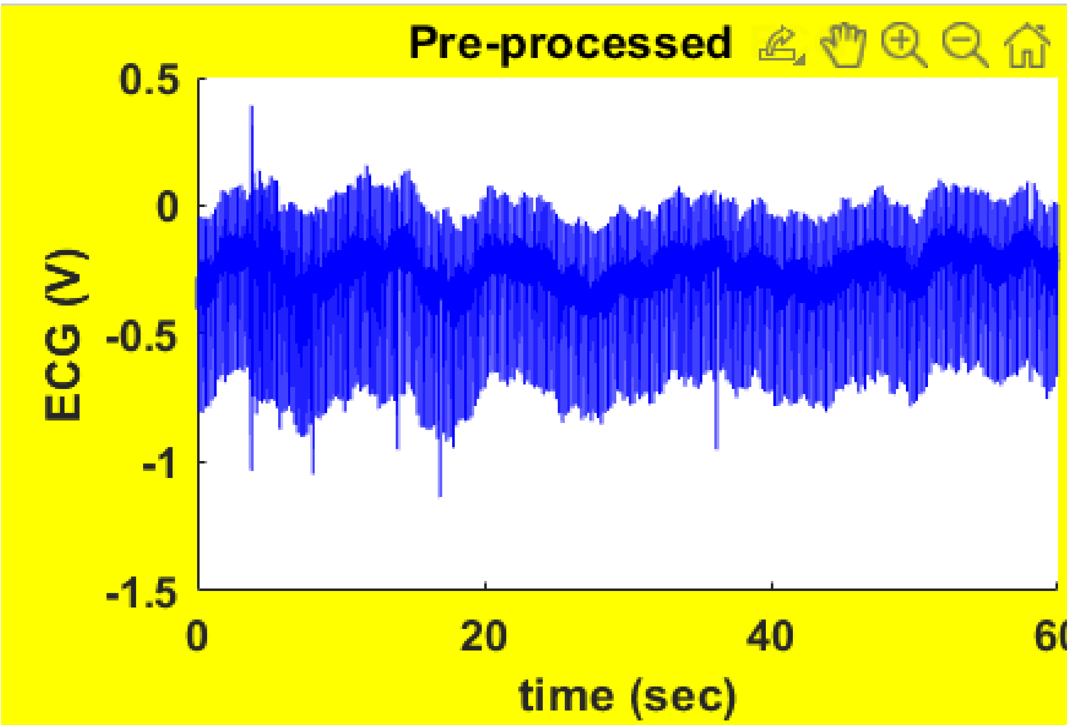

Case-6- CHF-after Pre-processing

(f)

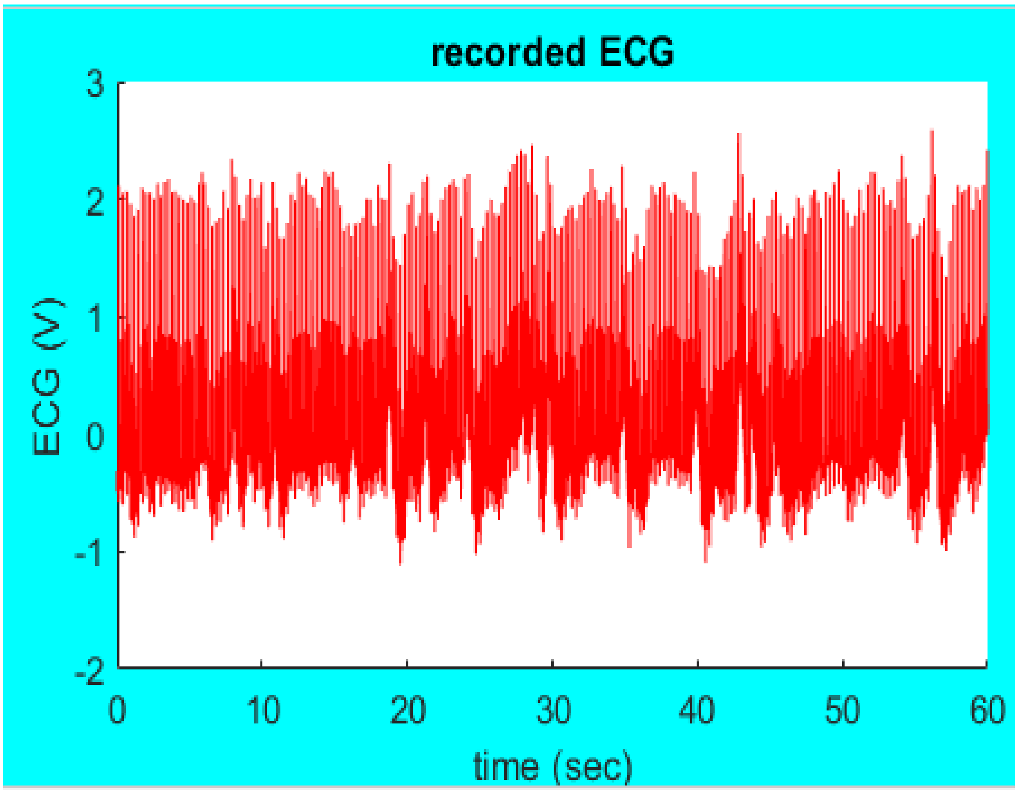

Case-7-ARR before Pre-processing

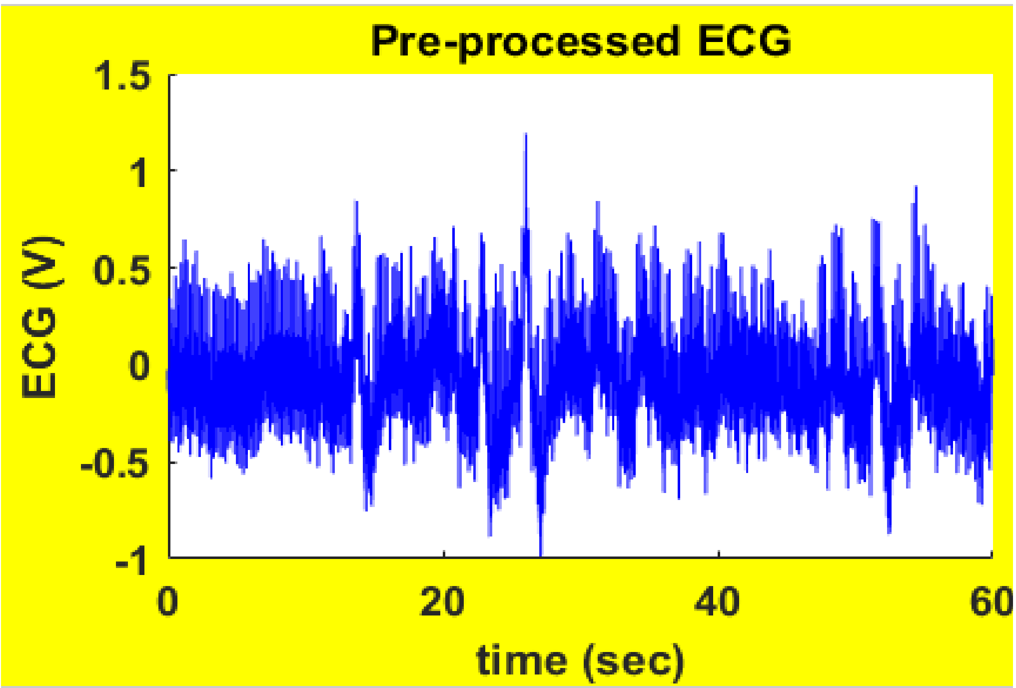

Case-7- ARR-after Pre-processing

(g)

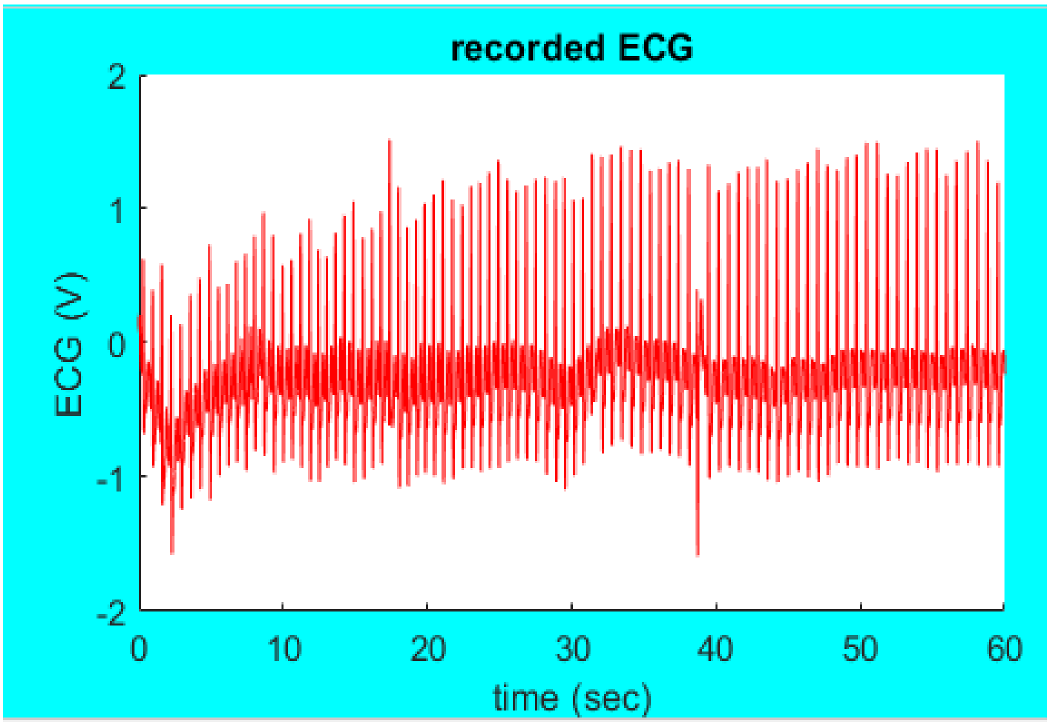

Case-8-ARR before Pre-processing

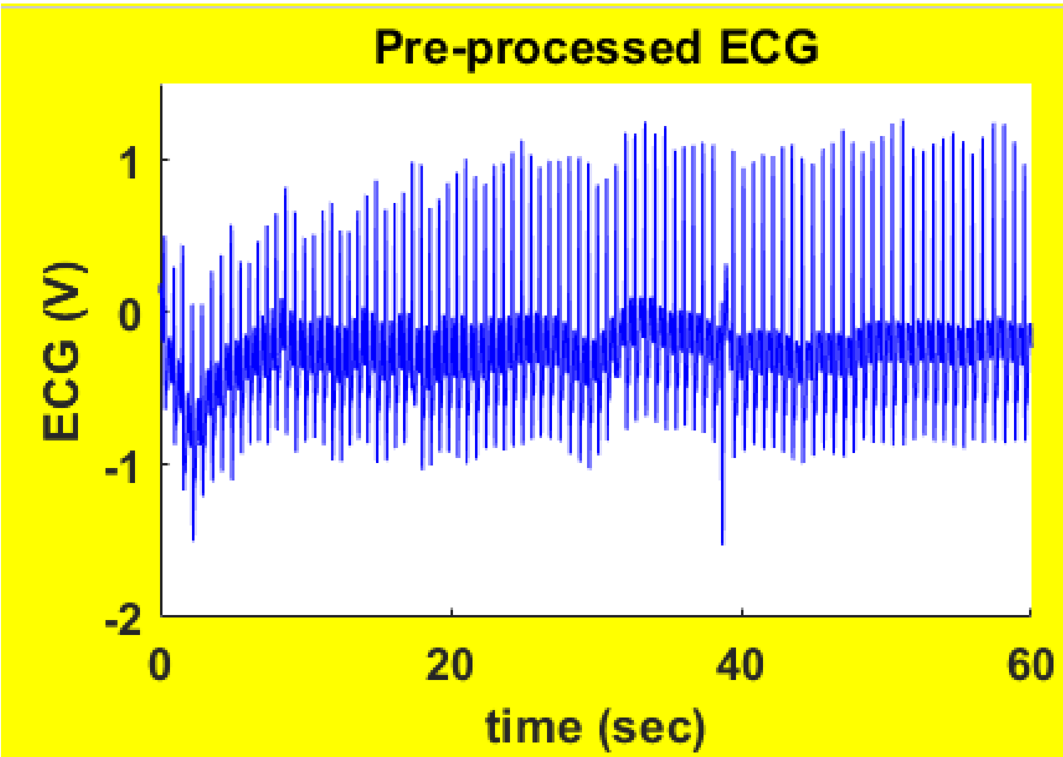

Case-8- ARR-after Pre-processing

(h)

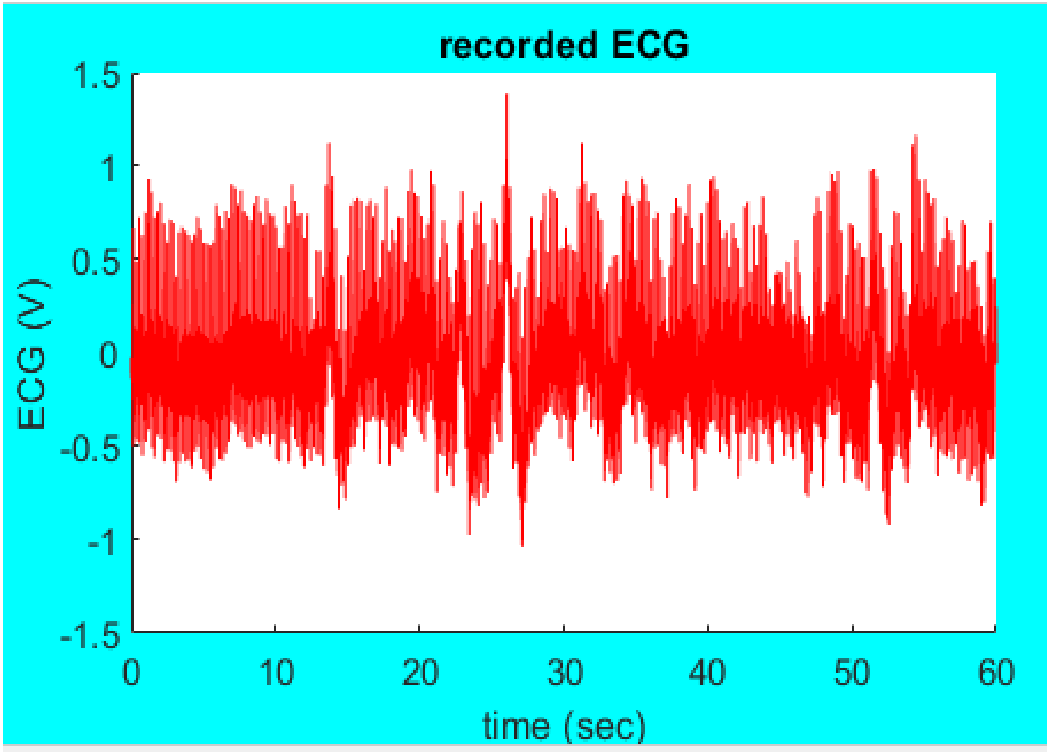

Case-9-ARR before Pre-processing

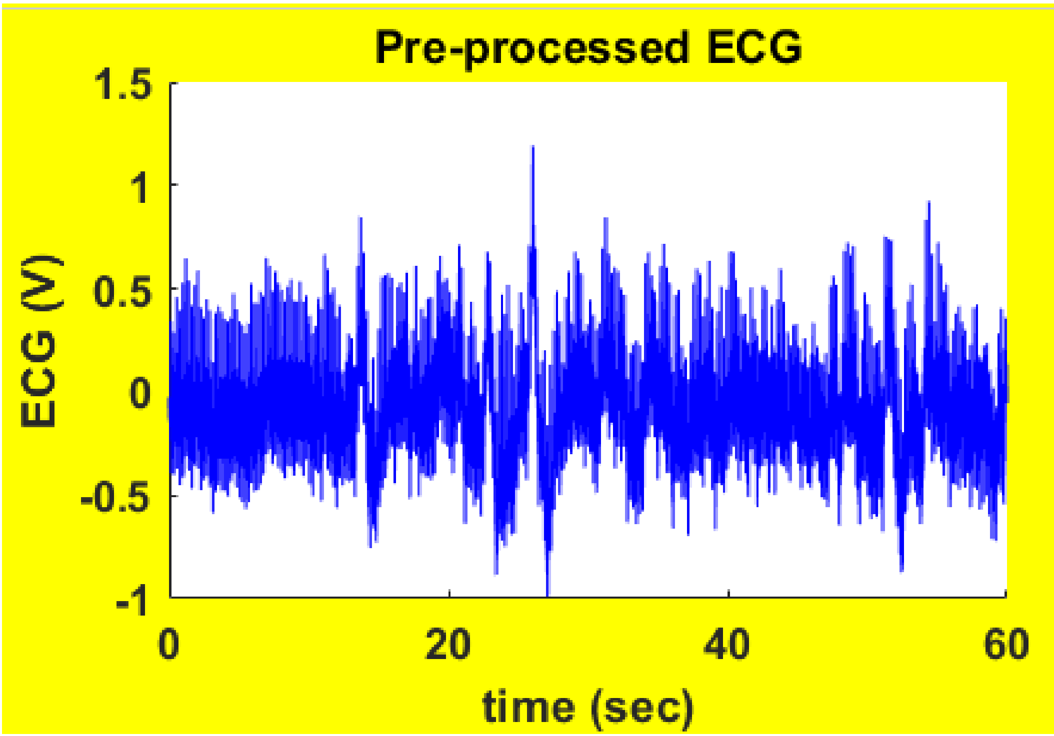

Case-9- ARR-after Pre-processing

(i)

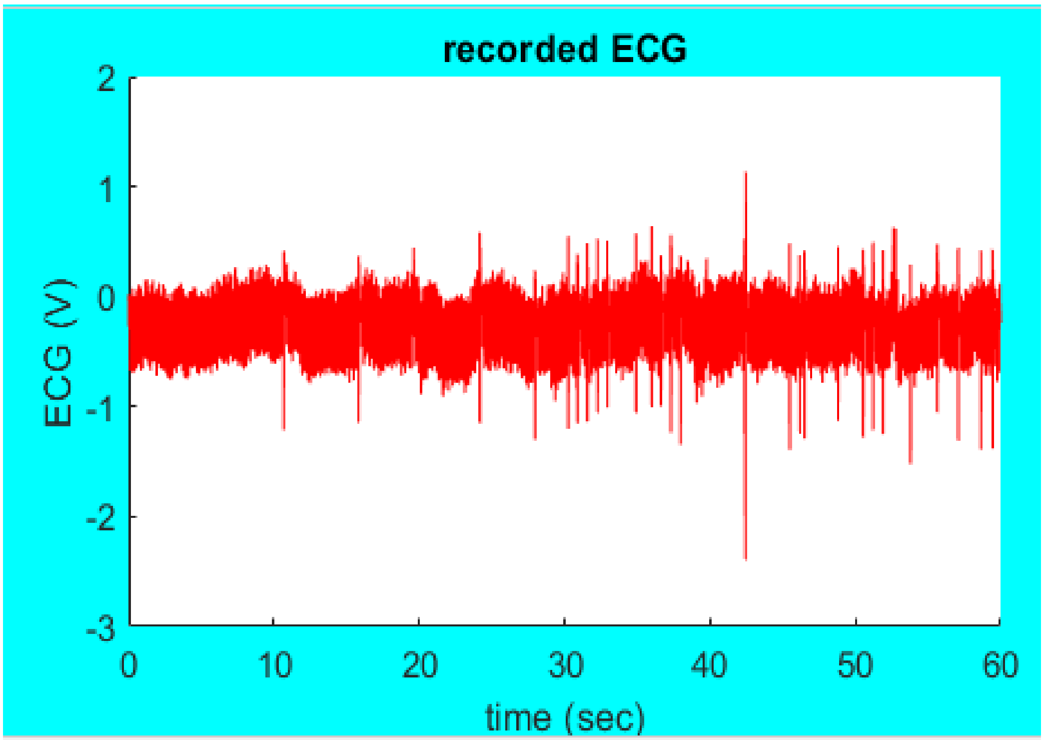

Case-10-ARR before Pre-processing

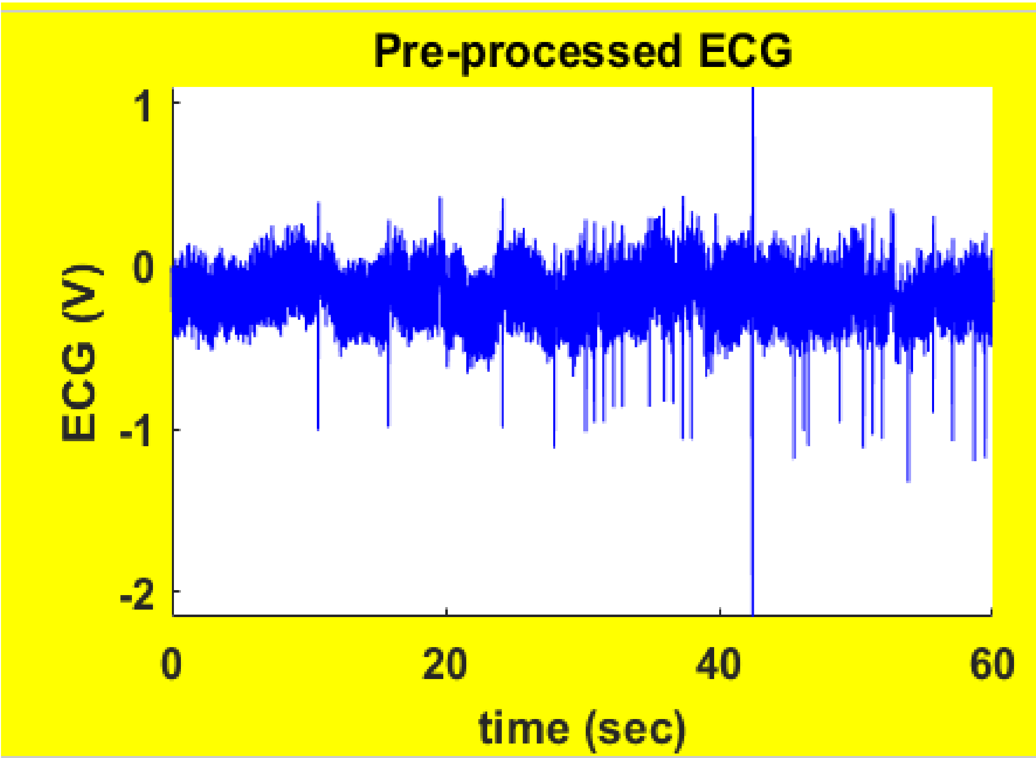

Case-10- ARR-after Pre-processing

(j)

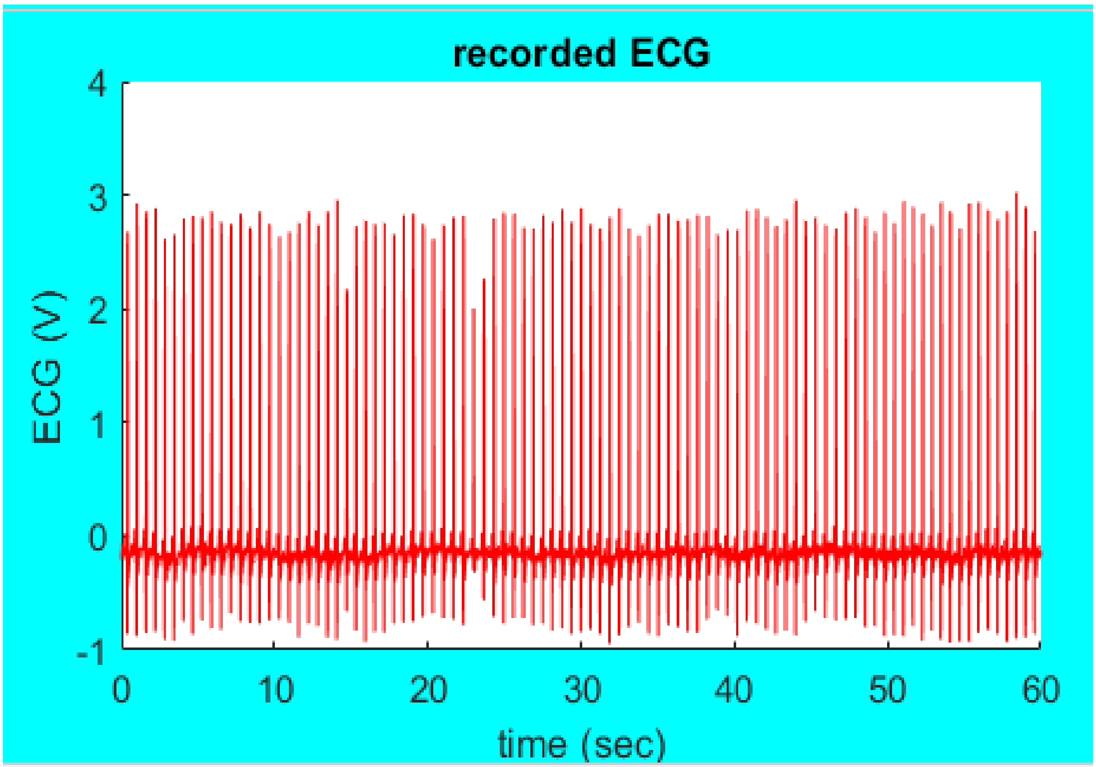

Case-11-NSR before Pre-processing

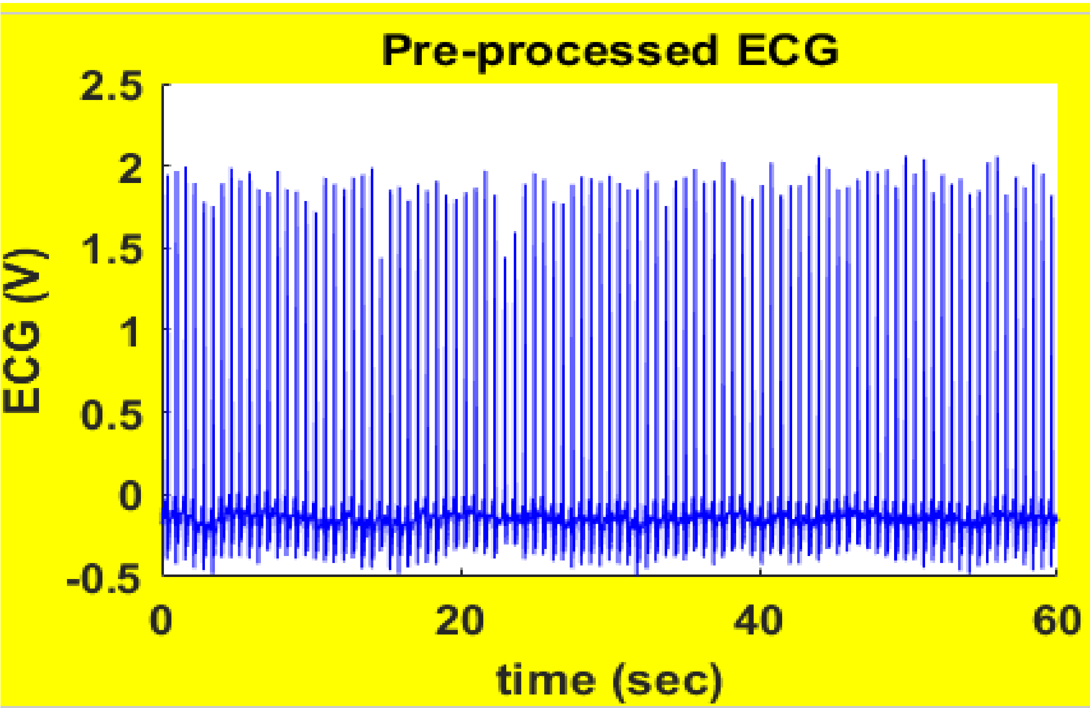

Case-11-NSR-after Pre-processing

(k)

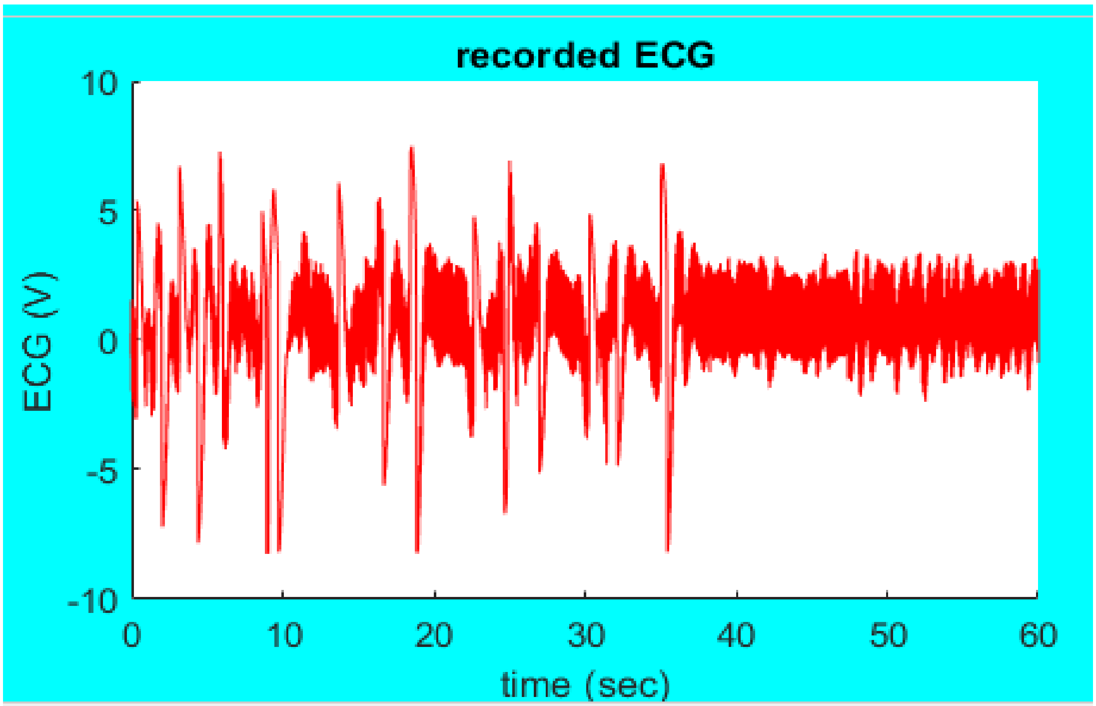

Case-12-CHF before Pre-processing

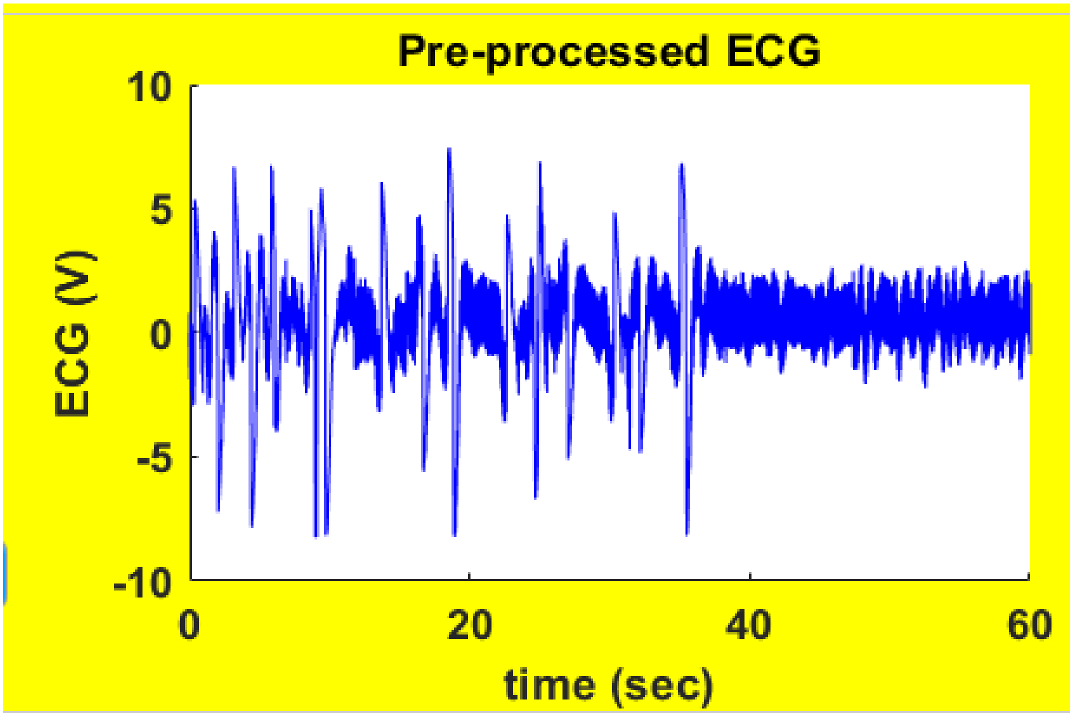

Case-12-CHF-after Pre-processing

(l)

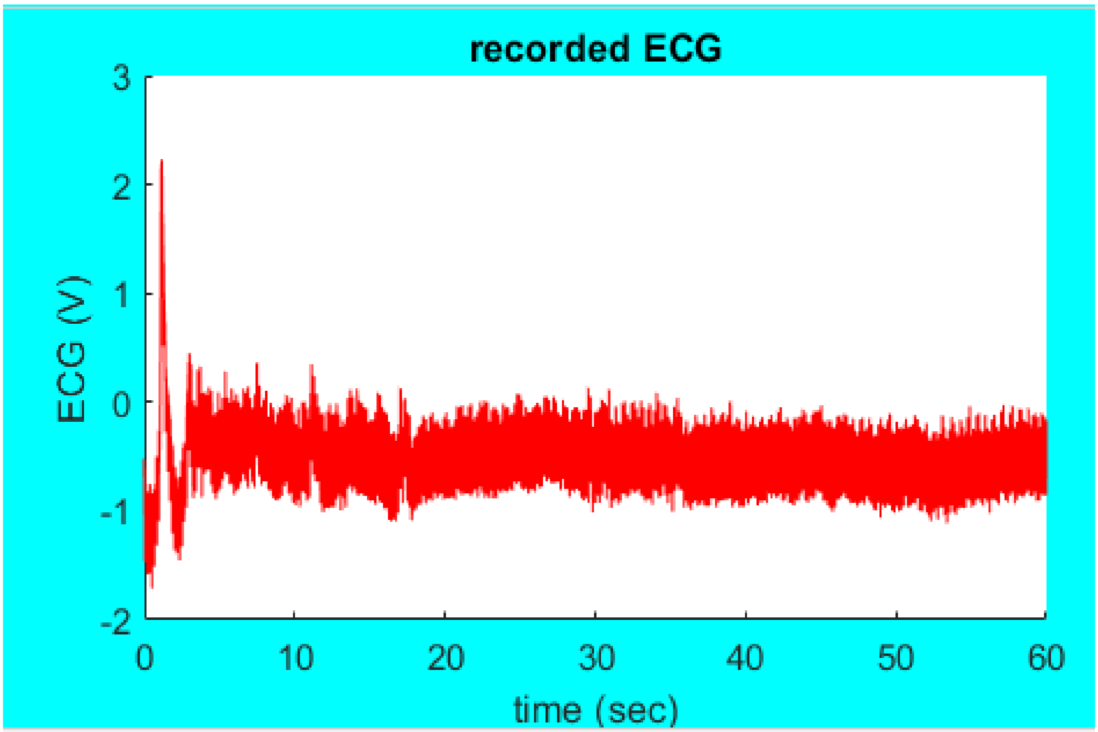

Case-13-CHF before Pre-processing

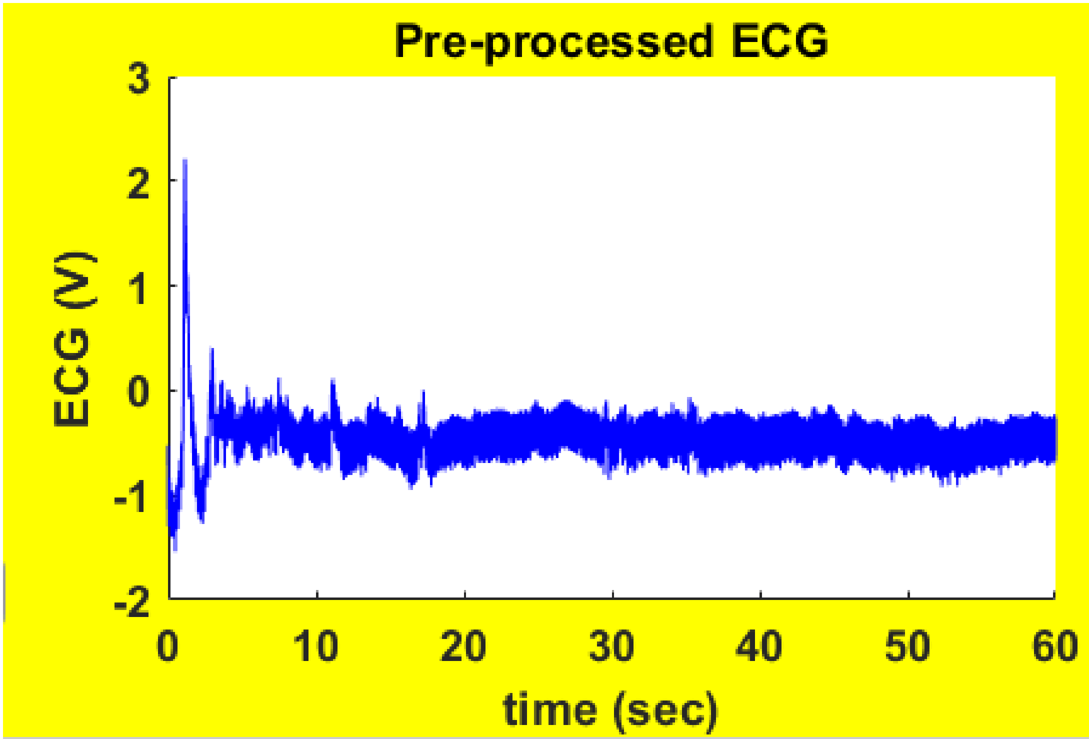

Case-13-CHF-after Pre-processing

(m)

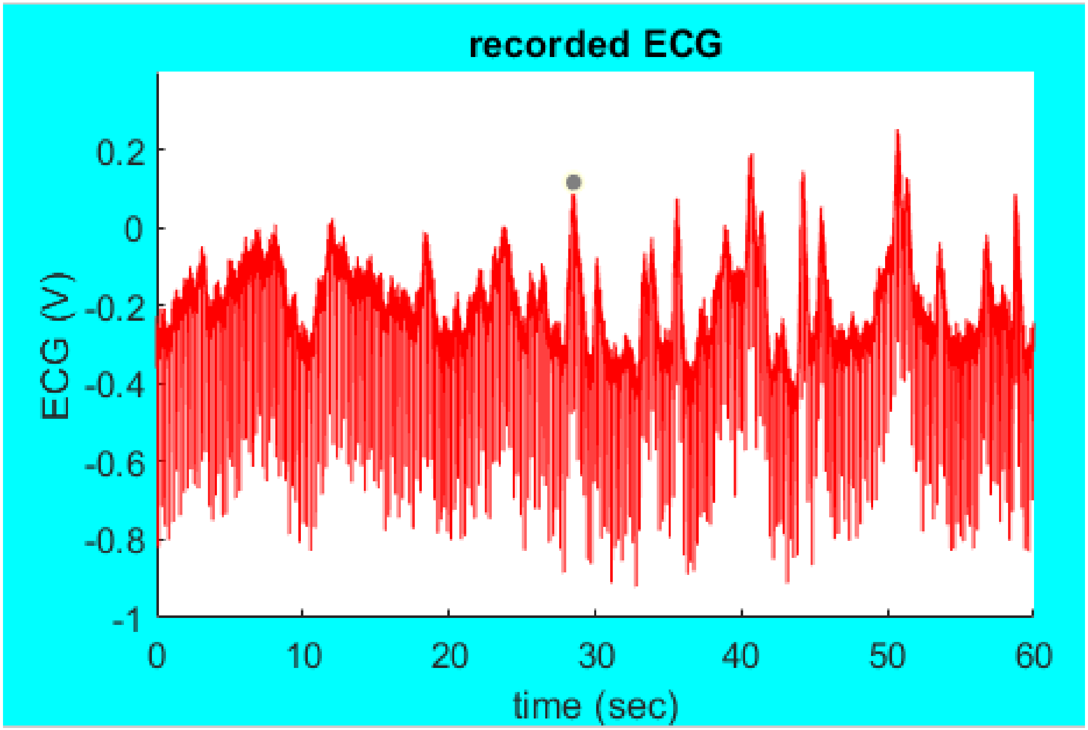

Case-14-ARR before Pre-processing

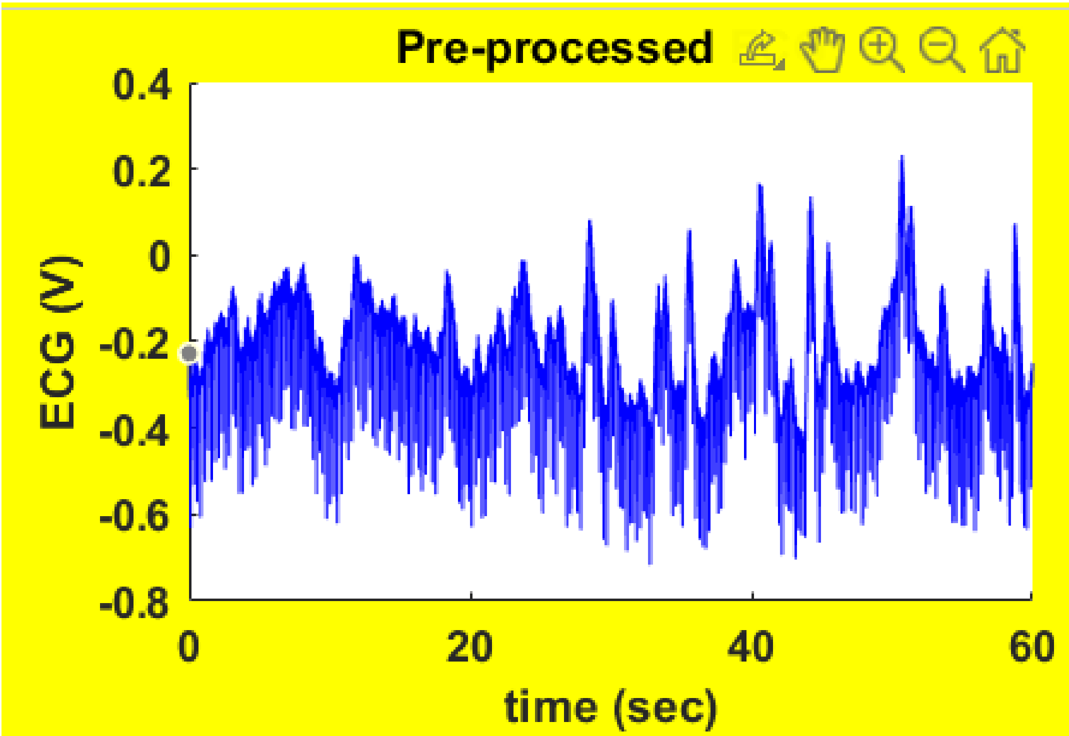

Case-14- ARR -after Pre-processing

(n)

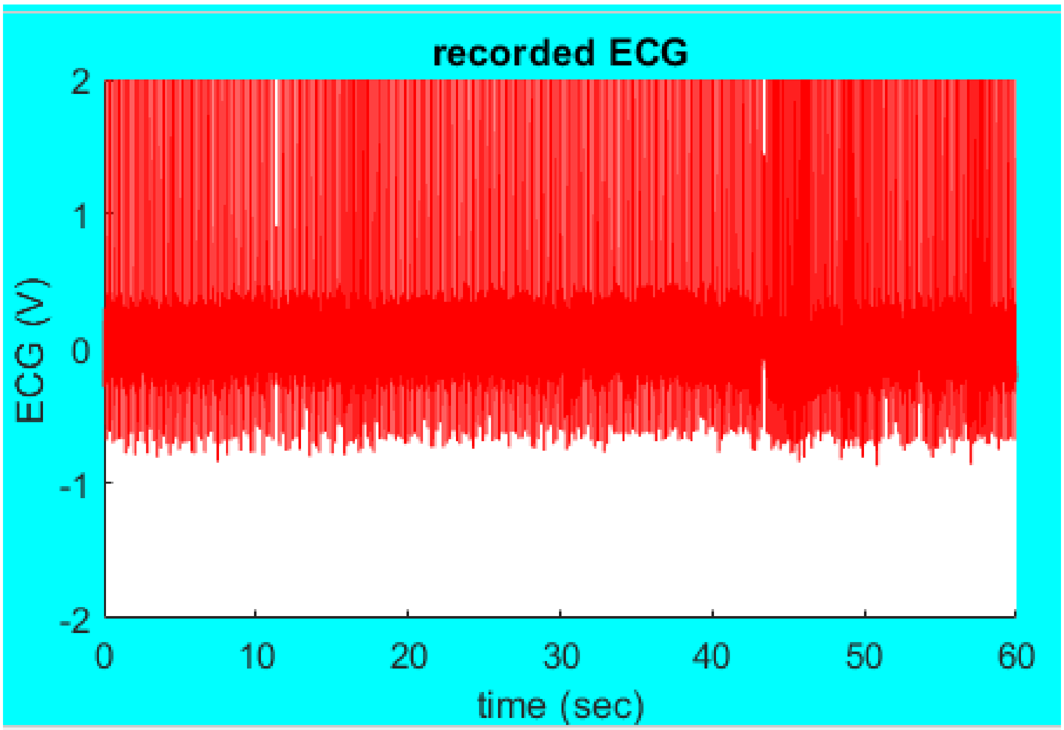

Case-15-NSR before Pre-processing

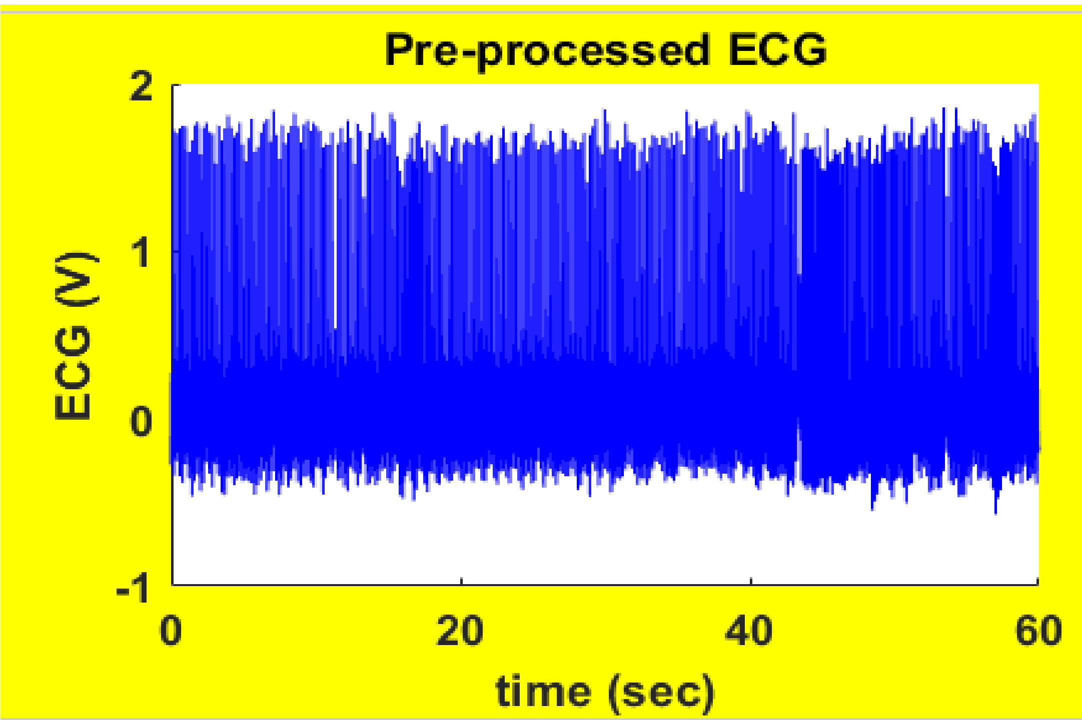

Case-15-NSR -after Pre-processing

(o)

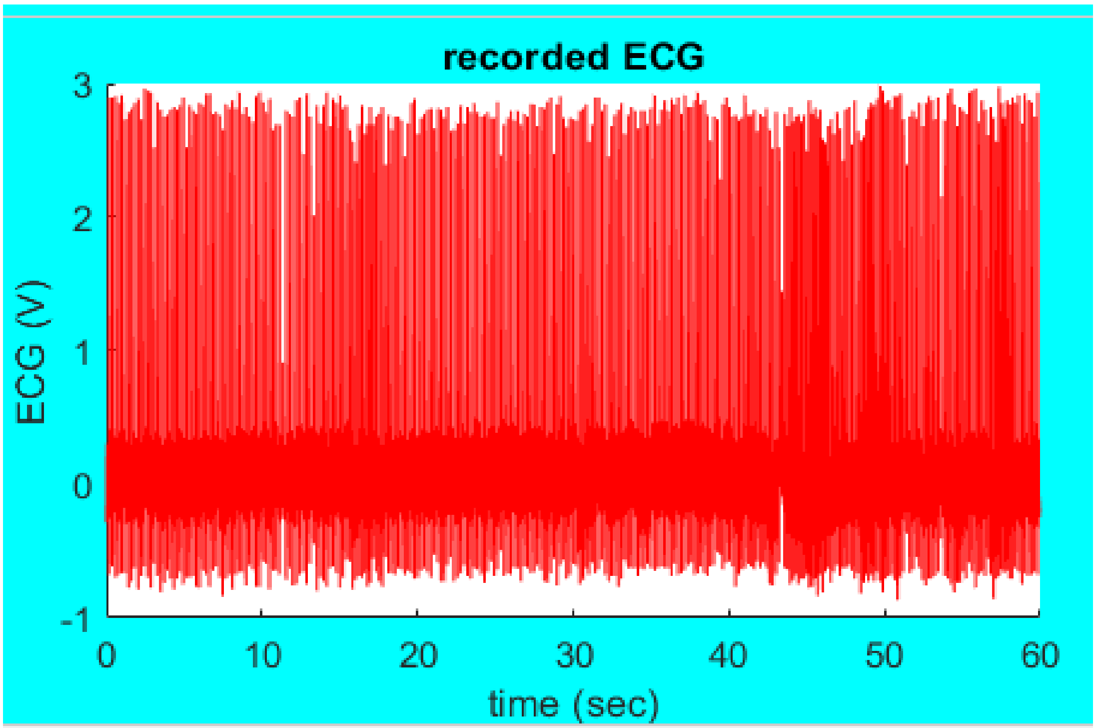

Case-16-NSR before Pre-processing

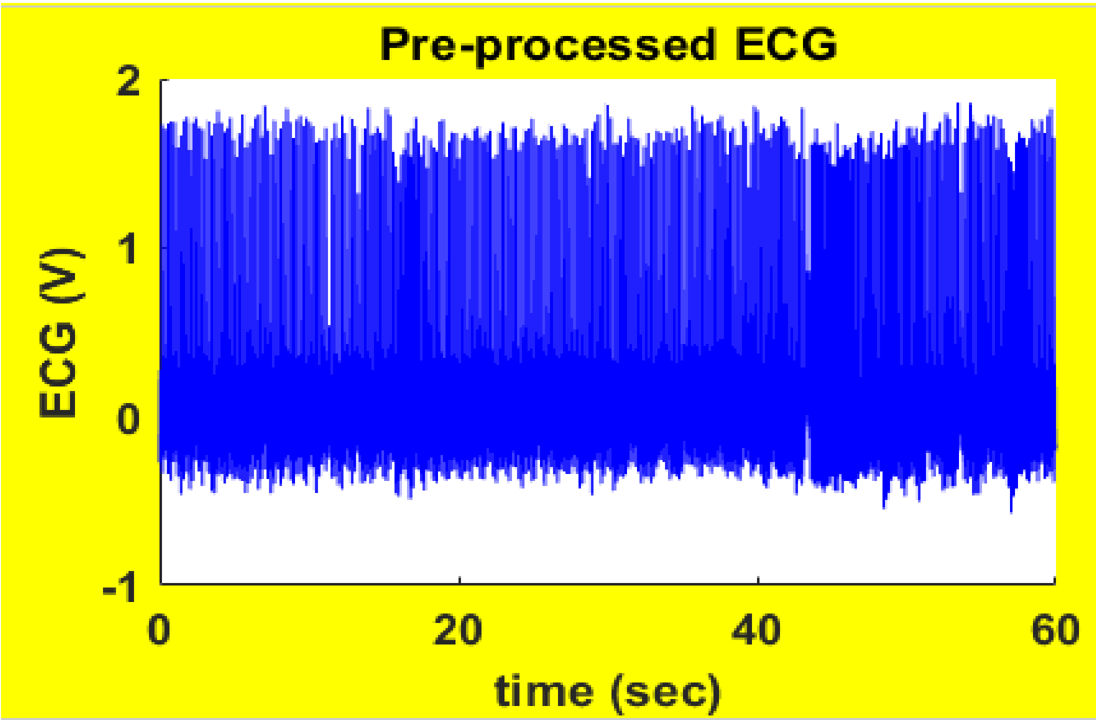

Case-16-NSR -after Pre-processing

(p)

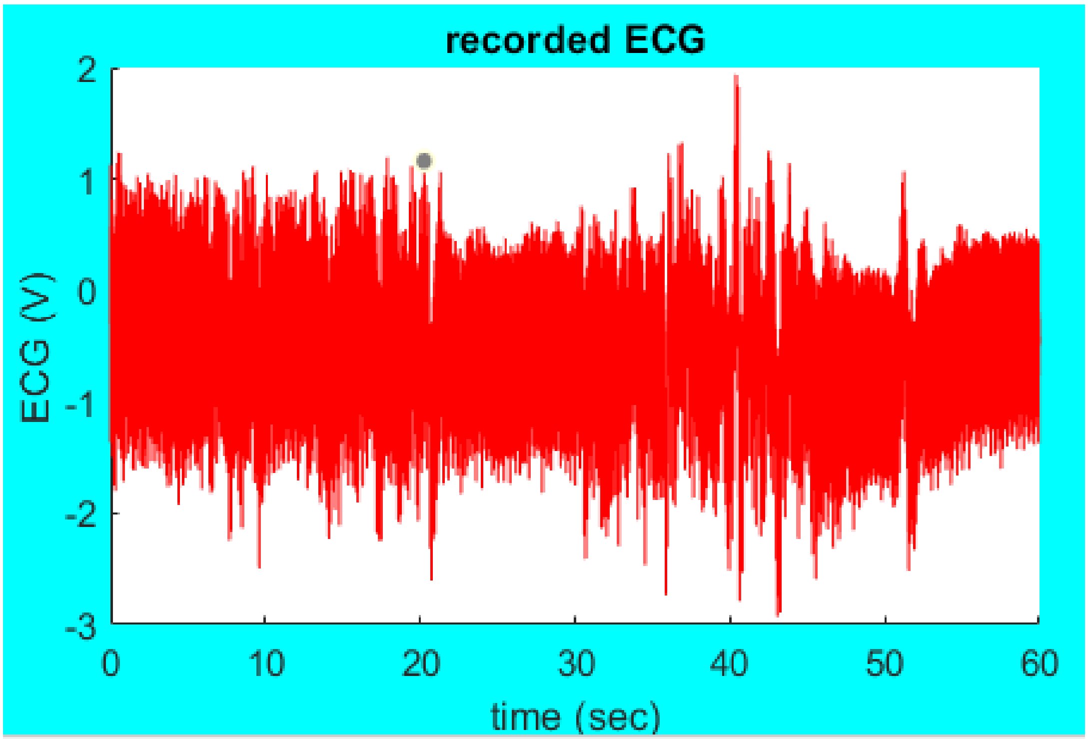

Case-17-CHF before Pre-processing

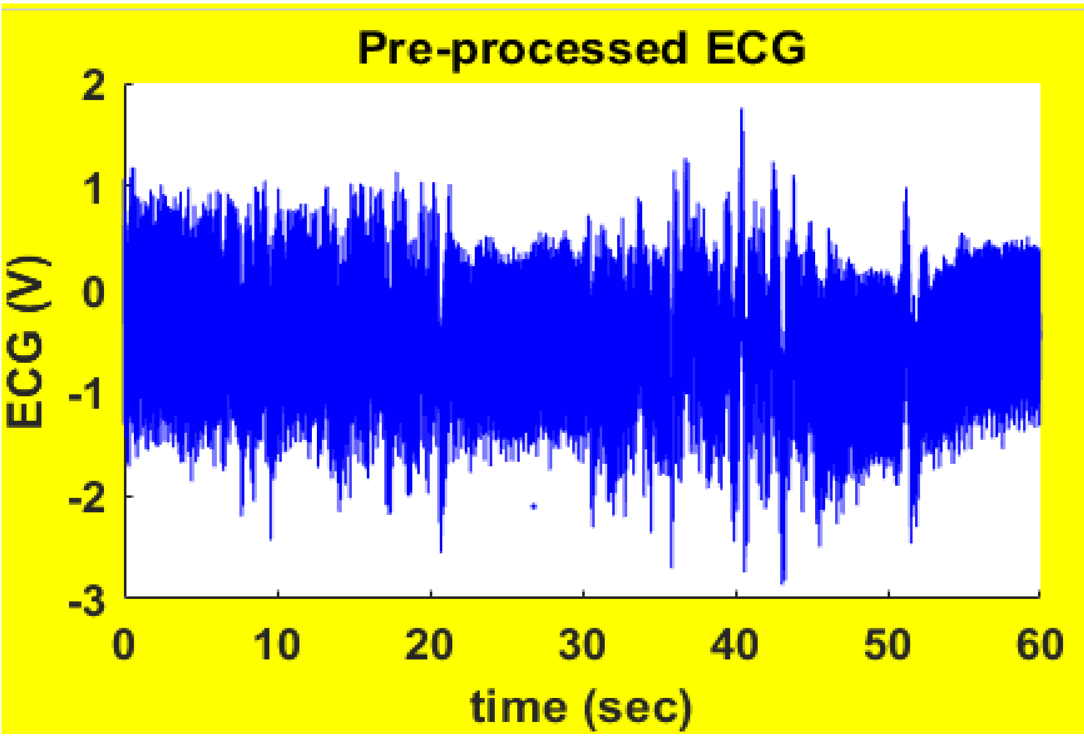

Case-17-CHF-after Pre-processing

(q)

Figures 4.32, a-q the patients cases of the implementation system

Table (4.7) Comparison of the methods performance

No. of ref	Feature extraction and classification	Se%	Pp%	Acc%
[4]	QRS detection - ANN	99.88	99.89	99.7
[26]	RR, WT with AR-SVM	-	-	93.33
[27]	DWT+SVM	96.11	92.59	95.92
[34]	RR-interval-Extreme Machine learning	-	-	98.1
[36]	tunable-Q wavelet transform	99.833	99.881	-
Our work	BSS +NN BSS+SVM WST+NN WST+SVM	100 98.9 99.7 99.8	97.3 100 99.5 100	99.4 99.38 99.7 99.92

In this work, the model have been proposed to classify the ECG signal with high accuracy for different algorithms as (BSS+NN, BSS+ SVM, WLS+ NN and WL+SVM) that given accuracy rate (99.4%, 99.38, 99.7 and 99.92) respectively. For comparable purpose, the other methods illustrate in Table (4.7) have been examined and contrasted with our work to comprehend our methods overperformance. The detection of QRS with ANN to classify the signal of ECG might not perform as well as other method although the accuracy is (99.7) in [4]. Employing the support vector method is considered one of the widely used methods that show good results in machine learning. While using R-R as feature extraction, it may not analyze the signal and rely only on R-R as in [26], which gave an accuracy rate for classifying the signal of (93.3). Signal analysis and feature extraction based on discrete wavelet transform, which deals with high and low levels of signal frequencies. It helps in analyzing the signal at all frequency levels. The lack of directional selectivity in DWT has been reduce important feature in[27] that given accuracy (95.92). Wavelet scattering and Blind Source Separation as feature extraction with NN and SVM for classification of ECG signal have been given good rate of accuracy compare with other methods which used by many researchers.

Chapter five

Conclusion and Future Work

5.1 Introduction

The thesis describes the proposed work in analyzing and processing the ECG signal and how to divide the signal from normal for healthy people and abnormal for people with heart diseases that have been studied and classified.

5.2 conclusion

In this research, several techniques were used to analyze the signal and purify it from the types of noise that the ECG signal is exposed to. After obtaining a pure signal, different algorithms are used to extract the features that are then used to classify the signal by one of the machine learning methods**.** These algorithms' performance was evaluated by running them through the MIT/BIH Arrhythmia dataset. The conclusions are divided into the following categories:

- The noise removal of ECG signal is based on multi-techniques:
  - Discrete Wavelet Transform(DWT) to remove baseline wander.
  - Powerline Interference removal using Notch filter
  - Noise Removal of Electromyographic (EMG) by Adaptive filter
  - Electrode Motion Artifacts Removal using Adaptive filter with LMS and RLS
- The feature extraction algorithms is based on multi- techniques:
  - The wavelet scattering algorithm is a mathematical framework that is utilized to analyze signals and extract features. The algorithm begins by transforming the input signal using a wavelet transform. A wavelet transform divides a signal into

frequency bands and time scales. It records both the signal's local time and frequency.

   - Blind Source Separation (BSS) is a technique for separating mixed signals into their primary source components without previous knowledge of the sources or the mixing process.

- The algorithms are utilized in classification using machine learning as SVM and NN, the dataset divide to 70% for learning and 30% for testing which recording different percentage for each algorithm, SVM with wavelet scattering is recording high rate of accuracy with 99.7%.
- Design and implement device by LattePand to classify ECG signal for normal or abnormal then diagnostic abnormal for ARR or CHF. SVM with wavelet scattering is selected among algorithms which used because high accuracy ratio

5.3 Future Work

A device for measuring the ECG signal and classified can be developed as follows

1- Adding a small printer that prints the signal on a graphic sheet to be attached with the report to the doctor

2- The device can be linked to the central computer used in the hospital or clinic to save data in the patient record so that the doctor and patient can retrieve it when needed

3 - The device can be linked to the computer cloud, where data can be sent to the doctor from anywhere, which gives the doctor the opportunity to view the patients' condition via a smartphone or any computer.

4- Temperature, accelerometer, and pressure sensors can be added to the classification system. Improving diagnostics by incorporating new sensor readings for data analysis.

6- Improving algorithms so that the device can be used to classify all heart diseases

References:

1. Kumar, Ashish, Deepak Berwal, and Yogendera Kumar. "Design of high-performance ECG detector for implantable cardiac pacemaker systems using biorthogonal wavelet transform." *Circuits, Systems, and Signal Processing* 37.9 (2018): 3995-4014.
2. Safari, A., et al. *A novel method for R-peak detection in noisy ECG signals using EEMD and ICA*. in *2016 23rd Iranian Conference on Biomedical Engineering and 2016 1st International Iranian Conference on Biomedical Engineering (ICBME)*. 2016. IEEE.
3. Steinhubl, Steven R., and Eric J. Topol. "Moving from digitalization to digitization in cardiovascular care: why is it important, and what could it mean for patients and providers?." *Journal of the American College of Cardiology* 66.13 (2015): 1489-1496.
4. Khalaf, Akram Jaddoa, and Samir Jasim Mohammed. "A QRS-Detection Algorithm for Real-Time Applications." *International Journal of Intelligent Engineering & Systems* 14.1 (2021)..
5. Kalidas, V. and L. Tamil. *Real-time QRS detector using stationary wavelet transform for automated ECG analysis*. in *2017 IEEE 17th international conference on Bioinformatics and Bioengineering (BIBE)*. 2017. IEEE.
6. Berkaya, Selcan Kaplan, et al. "A survey on ECG analysis." *Biomedical Signal Processing and Control* 43 (2018): 216-235..
7. Afkhami, R.G., G. Azarnia, and M.A.J.P.R.L. Tinati, *Cardiac arrhythmia classification using statistical and mixture modeling features of ECG signals*. 2016. **70**: p. 45-51.
8. Romdhane, T.F., M.A.J.C.i.B. Pr, and Medicine, *Electrocardiogram heartbeat classification based on a deep convolutional neural network and focal loss*. 2020. **123**: p. 103866.
9. Castells-Rufas, D., J.J.B.S.P. Carrabina, and Control, *Simple real-time QRS detector with the MaMeMi filter*. 2015. **21**: p. 137-145.
10. Aarthy, S., J.M.J.J.o.A.I. Iqbal, and H. Computing, *RETRACTED ARTICLE: Time series real time naive bayes electrocardiogram signal classification for efficient disease prediction using fuzzy rules*. 2021. **12**(5): p. 5257-5267.
11. Masetic, Z., A.J.C.m. Subasi, and p.i. biomedicine, *Congestive heart failure detection using random forest classifier*. 2016. **130**: p. 54-64.
12. Velayudhan, A. and S.J.I.J.E.C.E. Peter, *Noise analysis and different denoising techniques of ECG signal-a survey*. 2016. **1**(1): p. 40-44.

13. Bayasi, Nourhan, et al. "Low-power ECG-based processor for predicting ventricular arrhythmia." *IEEE Transactions on Very Large Scale Integration (VLSI) Systems* 24.5 (2015): 1962-1974..
14. Kiranyaz, S., et al. *Convolutional neural networks for patient-specific ECG classification*. in *2015 37th Annual International Conference of the IEEE Engineering in Medicine and Biology Society (EMBC)*. 2015. IEEE.
15. Kasar, S.L. and M.S.J.I.J.o.C.A. Joshi, *Analysis of multi-lead ECG signals using decision tree algorithms*. 2016. **134**(16).
16. Elhaj, Fatin A., et al. "Arrhythmia recognition and classification using combined linear and nonlinear features of ECG signals." *Computer methods and programs in biomedicine* 127 (2016): 52-63.
17. Sultan Qurraie, S. and R.J.B.e.l. Ghorbani Afkhami, *ECG arrhythmia classification using time frequency distribution techniques*. 2017. **7**: p. 325-332.
18. Acharya, U. Rajendra, et al. "A deep convolutional neural network model to classify heartbeats." *Computers in biology and medicine* 89 (2017): 389-396..
19. Singh, Shraddha, et al. "Classification of ECG arrhythmia using recurrent neural networks." *Procedia computer science* 132 (2018): 1290-1297..
20. Srikanth, G. and B.M. Bhaskara. *Design and analysis of low power architecture for electrocardiogram abnormalities detection using artificial neural network classifiers*. in *AIP Conference Proceedings*. 2023. AIP Publishing.
21. Kagalkar, P.M. and C.K. Jambotkar, *CLASSIFICATION OF ECG ARRHYTHMIAS USING BAYESIAN CLASSIFIER*.
22. Syama, S., et al. *Classification of ECG signal using machine learning techniques*. in *2019 2nd International Conference on Power and Embedded Drive Control (ICPEDC)*. 2019. IEEE.
23. Karthik, R., et al. *Implementation of neural network and feature extraction to classify ECG signals*. in *Microelectronics, Electromagnetics and Telecommunications: Proceedings of the Fourth ICMEET 2018*. 2019. Springer.
24. Alarsan, F.I. and M.J.J.o.b.d. Younes, *Analysis and classification of heart diseases using heartbeat features and machine learning algorithms*. 2019. **6**(1): p. 1-15.
25. Yang, H. and Z.J.I.A. Wei, *Arrhythmia recognition and classification using combined parametric and visual pattern features of ECG morphology*. 2020. **8**: p. 47103-47117.

26. Nahak, S. and G. Saha. *A fusion based classification of normal, arrhythmia and congestive heart failure in ECG*. in *2020 National Conference on Communications (NCC)*. 2020. IEEE.
27. Kumari, C.U., et al., *An automated detection of heart arrhythmias using machine learning technique: SVM*. 2021. **45**: p. 1393-1398.
28. Xu, Yuefan, et al. "Extreme learning machine for heartbeat classification with hybrid time-domain and wavelet time-frequency features." *Journal of Healthcare Engineering* 2021 (2021).
29. Reddy, S.D., et al., *Classification of arrhythmia disease through electrocardiogram signals using sampling vector random forest classifier*. 2022: p. 1-31.
30. Padmavathi, S. and E.J.P.C.S. Ramanujam, *Naïve Bayes classifier for ECG abnormalities using multivariate maximal time series motif*. 2015. **47**: p. 222-228.
31. Kaouter, K., et al. *Full training convolutional neural network for ECG signals classification*. in *AIP conference proceedings*. 2019. AIP Publishing.
32. Celin, S. and K.J.J.o.m.s. Vasanth, *ECG signal classification using various machine learning techniques*. 2018. **42**(12): p. 241.
33. Marzog, H.A. and H.J. Abd. *ECG-Signal classification using efficient machine learning approach*. in *2022 International Congress on Human-Computer Interaction, Optimization and Robotic Applications (HORA)*. 2022. IEEE.
34. Lantz, B., *Machine learning with R: expert techniques for predictive modeling*. 2019: Packt publishing ltd.
35. Lehr, D. and P.J.U.R. Ohm, *Playing with the data: what legal scholars should learn about machine learning*. 2017. **51**: p. 653.
36. Mahesh, B.J.I.J.o.S. and R. . *Machine learning algorithms-a review*. 2020. **9**(1): p. 381-386.
37. Alzubaidi, L., et al., *Review of deep learning: Concepts, CNN architectures, challenges, applications, future directions*. 2021. **8**: p. 1-74.
38. Sen, P.C., M. Hajra, and M. Ghosh. *Supervised classification algorithms in machine learning: A survey and review*. in *Emerging Technology in Modelling and Graphics: Proceedings of IEM Graph 2018*. 2020. Springer.
39. Srivastava, A., S. Saini, and D. Gupta. *Comparison of various machine learning techniques and its uses in different fields*. in *2019 3rd International conference on electronics, communication and aerospace technology (ICECA)*. 2019. IEEE.
40. Ji, Z., Z.C. Lipton, and C.J.a.p.a. Elkan, *Differential privacy and machine learning: a survey and review*. 2014.

41. Mahdavinejad, M.S., et al., *Machine learning for Internet of Things data analysis: A survey*. 2018. **4**(3): p. 161-175.
42. Kowsari, K., et al., *Text classification algorithms: A survey*. 2019. **10**(4): p. 150.
43. Corsaro, C., et al., *NMR in metabolomics: From conventional statistics to machine learning and neural network approaches*. 2022. **12**(6): p. 2824.
44. Puica, M.-A. and A.-M.J.I.J.o.A.R.i.A.I. Florea, *Emotional belief-desire-intention agent model: Previous work and proposed architecture*. 2013. **2**(2): p. 1-8.
45. Berkhin, P., *A survey of clustering data mining techniques*, in *Grouping multidimensional data: Recent advances in clustering*. 2006, Springer. p. 25-71.
46. Guha, S. and N. Mishra, *Clustering data streams*, in *Data stream management: processing high-speed data streams*. 2016, Springer. p. 169-187.
47. Zhou, Z.-H. and Z.-H.J.M.L. Zhou, *Semi-supervised learning*. 2021: p. 315-341.
48. Curchoe, C.L., C.L.J.J.o.a.r. Bormann, and genetics, *Artificial intelligence and machine learning for human reproduction and embryology presented at ASRM and ESHRE 2018*. 2019. **36**: p. 591-600.
49. Taylor, M.E. and P.J.J.o.M.L.R. Stone, *Transfer learning for reinforcement learning domains: A survey*. 2009. **10**(7).
50. Dastres, R., M.J.I.J.o.I. Soori, and Robotics, *Artificial neural network systems*. 2021. **21**(2): p. 13-25.
51. Chen, M., et al., *Artificial neural networks-based machine learning for wireless networks: A tutorial*. 2019. **21**(4): p. 3039-3071.
52. Huang, J., et al., *Research output of artificial intelligence in arrhythmia from 2004 to 2021: a bibliometric analysis*. 2022. **14**(5): p. 1411.
53. Van Gerven, M. and S.M. Bohte, *Artificial neural networks as models of neural information processing*. 2017.
54. Parisi, G.I., et al., *Continual lifelong learning with neural networks: A review*. 2019. **113**: p. 54-71.
55. Anderson, D. and G.J.K.S.C. McNeill, *Artificial neural networks technology*. 1992. **258**(6): p. 1-83.
56. Balakrishnan, H.N., et al., *ChaosNet: A chaos based artificial neural network architecture for classification*. 2019. **29**(11).
57. Singh, S., et al. *Nebula: a neuromorphic spin-based ultra-low power architecture for snns and anns*. in *2020 ACM/IEEE 47th Annual International Symposium on Computer Architecture (ISCA)*. 2020. IEEE.

58. Liu, Weiqiang, Rujun Chen, and Liangyong Yang. "Cole-Cole model parameter estimation from multi-frequency complex resistivity spectrum based on the artificial neural network." *Journal of Environmental and Engineering Geophysics* 26.1 (2021): 71-77.
59. Alcamí, P. and A.E.J.N.R.N. Pereda, *Beyond plasticity: the dynamic impact of electrical synapses on neural circuits*. 2019. **20**(5): p. 253-271.
60. Uhrig, R.E. *Introduction to artificial neural networks*. in *Proceedings of IECON'95-21st Annual Conference on IEEE Industrial Electronics*. 1995. IEEE.
61. Sharkawy, A.-N.J.J.o.A.i.A. and C. Mathematics, *Principle of neural network and its main types*. 2020. **7**: p. 8-19.
62. Owida, H.A., et al., *Classification of chest X-ray images using wavelet and MFCC features and Support Vector Machine classifier*. 2021. **11**(4): p. 7296-7301.
63. Amjad, M., et al., *Empirical performance analysis of decision tree and support vector machine based classifiers on biological databases*. 2019. **10**(9).
64. Nancy, P., et al. *Deep Learning and Machine Learning Based Efficient Framework for Image Based Plant Disease Classification and Detection*. in *2022 International Conference on Advanced Computing Technologies and Applications (ICACTA)*. 2022. IEEE.
65. Durgesh, K.S., B.J.J.o.t. Lekha, and a.i. technology, *Data classification using support vector machine*. 2010. **12**(1): p. 1-7.
66. Mitri, M. and V. Gaugé, *Forecasting Equity Realized Volatility using Machine Learning Methods*.
67. Awad, M., et al., *Support vector machines for classification*. 2015: p. 39-66.
68. Gamazo-Real, J.-C., V. Martínez-Martínez, and J.J.M. Gomez-Gil, *ANN-based position and speed sensorless estimation for BLDC motors*. 2022. **188**: p. 110602.
69. Montasser, O., S. Hanneke, and N. Srebro. *Vc classes are adversarially robustly learnable, but only improperly*. in *Conference on Learning Theory*. 2019. PMLR.
70. Pal, M. and P.M.J.I.j.o.r.s. Mather, *Support vector machines for classification in remote sensing*. 2005. **26**(5): p. 1007-1011.
71. Collobert, R. and S.J.J.o.m.l.r. Bengio, *SVMTorch: Support vector machines for large-scale regression problems*. 2001. **1**(Feb): p. 143-160.
72. Otchere, D.A., et al., *Application of supervised machine learning paradigms in the prediction of petroleum reservoir properties: Comparative analysis of ANN and SVM models*. 2021. **200**: p. 108182.

73. Hearst, M.A., et al., *Support vector machines*. 1998. **13**(4): p. 18-28.
74. Su, B., et al., *Discriminative dimensionality reduction for multi-dimensional sequences*. 2017. **40**(1): p. 77-91.
75. Wang, Y., et al., *A perception-driven approach to supervised dimensionality reduction for visualization*. 2017. **24**(5): p. 1828-1840.
76. Chen, J., et al., *Mixture factor analysis with distance metric constraint for dimensionality reduction*. 2022. **121**: p. 108156.
77. Awad, M. and R. Khanna, *Efficient learning machines: theories, concepts, and applications for engineers and system designers*. 2015: Springer nature.
78. Samui, P.J.E.G., *Slope stability analysis: a support vector machine approach*. 2008. **56**: p. 255-267.
79. Duan, L., et al., *Domain transfer multiple kernel learning*. 2012. **34**(3): p. 465-479.
80. Mantero, P., et al., *Partially supervised classification of remote sensing images through SVM-based probability density estimation.* 2005. **43**(3): p. 559-570.
81. Erfani, S.M., et al., *High-dimensional and large-scale anomaly detection using a linear one-class SVM with deep learning*. 2016. **58**: p. 121-134.
82. Vapnik, V.N.J.I.t.o.n.n., *An overview of statistical learning theory.* 1999. **10**(5): p. 988-999.
83. Campbell, C. and Y. Ying, *Learning with support vector machines*. 2022: Springer Nature.
84. Kumar, V., et al., *Proximal maximum margin matrix factorization for collaborative filtering*. 2017. **86**: p. 62-67.
85. Lauer, F. and G.J.N. Bloch, *Incorporating prior knowledge in support vector machines for classification: A review.* 2008. **71**(7-9): p. 1578-1594.
86. Deng, J., et al. *What does classifying more than 10,000 image categories tell us?* in *Computer Vision–ECCV 2010: 11th European Conference on Computer Vision, Heraklion, Crete, Greece, September 5-11, 2010, Proceedings, Part V 11*. 2010. Springer.
87. Lee, W.S. and B. Liu. *Learning with positive and unlabeled examples using weighted logistic regression*. in *ICML*. 2003.
88. Farquhar, J., et al., *Two view learning: SVM-2K, theory and practice*. 2005. **18**.
89. Jakkula, V.J.S.o.E., Washington State University, *Tutorial on support vector machine (svm).* 2006. **37**(2.5): p. 3.
90. Boswell, D.J.D.o.C.S. and E.U.o.C.S. Diego, *Introduction to support vector machines*. 2002. **11**.

91. Heo, J.-P., et al. *Spherical hashing*. in *2012 IEEE conference on computer vision and pattern recognition*. 2012. IEEE.
92. Liu, L., et al., *Fractional wavelet scattering network and applications*. 2018. **66**(2): p. 553-563.
93. Liu, Z., et al., *Wavelet scattering transform for ECG beat classification*. 2020. **2020**.
94. Nahak, S., A. Pathak, and G.J.E.S.w.A. Saha, *Fragment-level classification of ECG arrhythmia using wavelet scattering transform*. 2023. **224**: p. 120019.
95. Marzog, H.A. and H.J. Abd, *Research Article Machine Learning ECG Classification Using Wavelet Scattering of Feature Extraction*. 2022.
96. Zhang, D. and G.J.P.r. Lu, *Review of shape representation and description techniques*. 2004. **37**(1): p. 1-19.
97. Malinin, A., et al., *Shifts: A dataset of real distributional shift across multiple large-scale tasks*. 2021.
98. Yurish, S., *Advances in Signal Processing: Reviews, Book Series, Vol. 1*. 2018: Lulu. com.
99. Toumi, I., S. Caldarelli, and B.J.P.i.n.m.r.s. Torrésani, *A review of blind source separation in NMR spectroscopy*. 2014. **81**: p. 37-64.
100. Fahes, M., et al., *Unrolling PALM for sparse semi-blind source separation*. 2021.
101. Zmolikova, K., et al. *Speaker-aware neural network based beamformer for speaker extraction in speech mixtures*. in *Interspeech*. 2017.
102. Nakatani, T., *Speaker-aware neural network based beamformer for speaker extraction in speech mixtures*. 2017.
103. Sawada, H., et al., *A review of blind source separation methods: two converging routes to ILRMA originating from ICA and NMF*. 2019. **8**: p. e12.
104. Boya, C., et al., *Identification of multiple partial discharge sources using acoustic emission technique and blind source separation*. 2015. **22**(3): p. 1663-1673.
105. Jain, S.N., C.J.I.J.o.E.S. Rai, and Technology, *Blind source separation and ICA techniques: a review*. 2012. **4**(4): p. 1490-1503.
106. Talib, M., A.A. Al-bakri, and A.K. Abdullah. *Enhancement Separation of ECG Signals for Twin Fetuses Based on Modified Blind Source Separation*. in *2019 4th Scientific International Conference Najaf (SICN)*. 2019. IEEE.
107. Al-Dujaili, M.J. and M.T.J.W.P.C. Mezeel, *Novel approach for reinforcement the extraction of ECG signal for twin fetuses based on modified BSS*. 2021. **119**(3): p. 2431-2450.

108. Abdullah, A.K., et al., *Blind source separation techniques based eye blinks rejection in EEG signals*. 2014. **13**(3): p. 401.
109. Nechyba, M.J.U.o.F., February, *Introduction to the discrete wavelet transform (DWT).* 2004.
110. Kumar, R. and M.J.M. Singh, *Outer race defect width measurement in taper roller bearing using discrete wavelet transform of vibration signal*. 2013. **46**(1): p. 537-545.
111. Chowdhury, T.H., K.N. Poudel, and Y.J.I.A. Hu, *Time-frequency analysis, denoising, compression, segmentation, and classification of PCG signals*. 2020. **8**: p. 160882-160890.
112. Riera-Guasp, M., et al., *A general approach for the transient detection of slip-dependent fault components based on the discrete wavelet transform*. 2008. **55**(12): p. 4167-4180.
113. Zhou, Y. and M.J.T.E. Kot, *Discrete-time growth-dispersal models with shifting species ranges*. 2011. **4**: p. 13-25.
114. Rashid, A.K., Z.J.I.T.o.A. Shen, and Propagation, *A novel band-reject frequency selective surface with pseudo-elliptic response*. 2010. **58**(4): p. 1220-1226.
115. Salih, T.A.J.J.o.T. and A.I. Technology, *New approach to eliminate noise attendants ECG signal corrupted*. 2021. **99**(3).
116. Yukawa, M.J.I.T.o.S.P., *Multikernel adaptive filtering*. 2012. **60**(9): p. 4672-4682.
117. Luque, A., et al., *The impact of class imbalance in classification performance metrics based on the binary confusion matrix*. 2019. **91**: p. 216-231.
118. Ren, D., et al., *Squares: Supporting interactive performance analysis for multiclass classifiers*. 2016. **23**(1): p. 61-70.
119. Paunski, Y.K. and G.T.J.I.-P. Angelov, *Performance and power consumption analysis of low-cost single board computers in educational robotics*. 2019. **52**(25): p. 424-428.
120. Álvarez, J.L., J.D. Mozo, and E.J.S. Durán, *Analysis of single board architectures integrating sensors technologies*. 2021. **21**(18): p. 6303.
121. Khan, B.M., et al., *Performance Analysis of Raspberry Pi 3 IP PBX Based on Asterisk*. 2022. **11**(20): p. 3313.
122. Mohammed, S.J., M.S. Nasr, and A.J.J.I.J.o.C.A. Ramadhan, *Portable Monitoring/Diagnostic System based on the Combining of Real Time WSN with GSM and Internet*. 2014. **975**: p. 8887.
123. Yang, H. and E.K. Lee, *Healthcare analytics: from data to knowledge to healthcare improvement*. 2016: John Wiley & Sons.
124. Mandpe, P., et al., *Glucose oxidase-based biosensor for glucose detection from biological fluids*. 2020. **40**(4): p. 497-511.

125. Movassaghi, Samaneh, et al. "Wireless body area networks: A survey." *IEEE Communications surveys & tutorials* 16.3 (2014): 1658-1686.
126. Thajudeen, Anshif, Prakash Goud, and Akanksha Gupta. *Analysis of Emotional Health using ECG Data Acquisition System*. No. 3799. EasyChair, 2020.

Appendix A

The results of ECG diagnostic system

Practical results of patients' cases taken from hospitals

Cases of ARR							
ECG	T	ECG	T	ECG	T	ECG	T
0	0.1772	0	0.1194	0	0.125	0	-0.0246
0.001	0.2785	0.0078	0.1876	0.0078	0.005	0.002	-0.0363
0.002	0.2526	0.0156	0.1696	0.0156	0.025	0.0039	-0.036
0.0029	0.2586	0.0234	0.1786	0.0234	0.065	0.0059	-0.0302
0.0039	0.2585	0.0312	0.2118	0.0312	-0.085	0.0078	-0.0458
0.0049	0.2478	0.0391	0.1966	0.0391	0.005	0.0098	-0.0931
0.0059	0.246	0.0469	0.0729	0.0469	-0.065	0.0117	-0.0914
0.0068	0.2434	0.0547	0.1659	0.0547	-0.015	0.0137	-0.129
0.0078	0.2199	0.0625	0.0832	0.0625	-0.035	0.0156	-0.1125
0.0088	0.226	0.0703	0.1992	0.0703	-0.035	0.0176	-0.1273
0.0098	0.207	0.0781	0.179	0.0781	0.015	0.0195	-0.1056
0.0107	0.2131	0.0859	0.1116	0.0859	0.155	0.0215	-0.1243
0.0117	0.1886	0.0938	0.1202	0.0938	0.435	0.0234	-0.1194
0.0127	0.2005	0.1016	0.1142	0.1016	0.655	0.0254	-0.1212
0.0137	0.1808	0.1094	0.0234	0.1094	0.865	0.0273	-0.1135
0.0146	0.1948	0.1172	-0.0122	0.1172	0.125	0.0293	-0.1087
0.0156	0.1777	0.125	-0.0956	0.125	-0.925	0.0312	-0.1201
0.0166	0.1743	0.1328	-0.1189	0.1328	-0.935	0.0332	-0.1114
0.0176	0.18	0.1406	-0.1155	0.1406	-0.615	0.0352	-0.1103
0.0186	0.1901	0.1484	-0.1444	0.1484	-0.235	0.0371	-0.0917
0.0195	0.1756	0.1562	-0.1568	0.1562	0.005	0.0391	-0.1228
0.0205	0.1854	0.1641	-0.1818	0.1641	0.035	0.041	-0.108
0.0215	0.1654	0.1719	-0.1741	0.1719	0.035	0.043	-0.1343
0.0225	0.166	0.1797	-0.197	0.1797	0.015	0.0449	-0.1258
0.0234	0.1663	0.1875	-0.194	0.1875	0.005	0.0469	-0.1438
0.0244	0.1497	0.1953	-0.2045	0.1953	0.045	0.0488	-0.1318
0.0254	0.164	0.2031	-0.2055	0.2031	0.045	0.0508	-0.1452
0.0264	0.148	0.2109	-0.169	0.2109	0.045	0.0527	-0.1247
0.0273	0.1672	0.2188	-0.1892	0.2188	0.105	0.0547	-0.1392
0.0283	0.1429	0.2266	-0.1696	0.2266	0.105	0.0566	-0.1282
0.0293	0.157	0.2344	-0.1822	0.2344	0.095	0.0586	-0.1411
0.0303	0.136	0.2422	-0.1894	0.2422	0.125	0.0605	-0.1442
0.0312	0.1444	0.25	-0.1851	0.25	0.115	0.0625	-0.1447
0.0322	0.1375	0.2578	-0.2367	0.2578	0.105	0.0645	-0.156
0.0332	0.1513	0.2656	-0.1283	0.2656	0.165	0.0664	-0.1411
0.0342	0.1347	0.2734	0.1474	0.2734	0.155	0.0684	-0.1454
0.0352	0.1476	0.2812	0.2117	0.2812	0.235	0.0703	-0.1185
0.0361	0.1426	0.2891	0.4363	0.2891	0.185	0.0723	-0.118
0.0371	0.1376	0.2969	0.6266	0.2969	0.205	0.0742	-0.0792
0.0381	0.1403	0.3047	0.5581	0.3047	0.315	0.0762	-0.0853
0.0391	0.1462	0.3125	0.5081	0.3125	0.295	0.0781	-0.068

0.04	0.1575	0.3203	0.3691	0.3203	0.305	0.0801	-0.0994
0.041	0.1356	0.3281	0.2182	0.3281	0.325	0.082	-0.0842
0.042	0.1926	0.3359	-0.0059	0.3359	0.415	0.084	-0.1182
0.043	0.2147	0.3438	-0.3768	0.3438	0.425	0.0859	-0.1293
0.0439	0.2232	0.3516	-0.5629	0.3516	0.495	0.0879	-0.1518
0.0449	0.2142	0.3594	-0.6739	0.3594	0.475	0.0898	-0.1481
0.0459	0.1797	0.3672	-0.675	0.3672	0.525	0.0918	-0.1769
0.0469	0.1607	0.375	-0.6515	0.375	0.475	0.0938	-0.1944
0.0479	0.174	0.3828	-0.6011	0.3828	0.505	0.0957	-0.1951
0.0488	0.1398	0.3906	-0.5834	0.3906	0.415	0.0977	-0.2072
0.0498	0.1564	0.3984	-0.5383	0.3984	0.355	0.0996	-0.2024
0.0508	0.1353	0.4062	-0.4777	0.4062	0.265	0.1016	-0.2273
0.0518	0.1231	0.4141	-0.4721	0.4141	0.175	0.1035	-0.2204
0.0527	0.1098	0.4219	-0.4598	0.4219	0.105	0.1055	-0.2408
0.0537	0.1072	0.4297	-0.472	0.4297	0.085	0.1074	-0.221
0.0547	0.1106	0.4375	-0.4831	0.4375	-0.015	0.1094	-0.2477
0.0557	0.0938	0.4453	-0.5056	0.4453	-0.015	0.1113	-0.2273
0.0566	0.1089	0.4531	-0.4871	0.4531	-0.045	0.1133	-0.2409
0.0576	0.1075	0.4609	-0.5252	0.4609	-0.095	0.1152	-0.2215
0.0586	0.1178	0.4688	-0.5077	0.4688	-0.035	0.1172	-0.2347
0.0596	0.096	0.4766	-0.508	0.4766	-0.085	0.1191	-0.2265
0.0605	0.1106	0.4844	-0.5111	0.4844	-0.085	0.1211	-0.1928
0.0615	0.0709	0.4922	-0.5138	0.4922	-0.135	0.123	-0.1298
0.0625	0.0617	0.5	-0.4952	0.5	-0.065	0.125	0.0326
0.0635	0.0367	0.5078	-0.4865	0.5078	-0.085	0.127	0.2202
0.0645	-0.0523	0.5156	-0.4742	0.5156	-0.105	0.1289	0.116
0.0654	-0.2555	0.5234	-0.4476	0.5234	-0.075	0.1309	-0.0992
0.0664	-0.4234	0.5312	-0.4181	0.5312	-0.095	0.1328	0.1078
0.0674	-0.3468	0.5391	-0.3998	0.5391	-0.095	0.1348	0.491
0.0684	-0.2423	0.5469	-0.3626	0.5469	-0.065	0.1367	0.6706
0.0693	-0.1429	0.5547	-0.3667	0.5547	-0.085	0.1387	0.3793
0.0703	-0.0261	0.5625	-0.3246	0.5625	-0.075	0.1406	0.0815
0.0713	0.0545	0.5703	-0.2628	0.5703	-0.085	0.1426	-0.2317
0.0723	0.1041	0.5781	-0.2708	0.5781	-0.075	0.1445	-0.4555
0.0732	0.1471	0.5859	-0.2076	0.5859	-0.085	0.1465	-0.496
0.0742	0.1708	0.5938	-0.2376	0.5938	-0.075	0.1484	-0.3853
0.0752	0.1902	0.6016	-0.1932	0.6016	-0.045	0.1504	-0.3253
0.0762	0.1555	0.6094	-0.1885	0	0.125	0.1523	-0.3127
0.0771	0.1922	0.6172	-0.1651	0.0078	0.005	0.1543	-0.3125
0.0781	0.1785	0.625	-0.1813	0.0156	0.025	0.1562	-0.2974
0.0791	0.1875	0.6328	-0.1738	0.0234	0.065	0.1582	-0.2771
0.0801	0.1916	0.6406	-0.1778	0.0312	-0.085	0.1602	-0.2926
0.0811	0.2024	0.6484	-0.1333	0.0391	0.005	0.1621	-0.2798
0.082	0.2037	0.6562	-0.1475	0.0469	-0.065	0.1641	-0.2861
0.083	0.2115	0.6641	-0.1772	0.0547	-0.015	0	-0.0246
0.084	0.213	0.6719	-0.1595	0.0625	-0.035	0.002	-0.0363
0.085	0.2021	0.6797	-0.1909	0.0703	-0.035	0.0039	-0.036
0.0859	0.2202	0.6875	-0.2042	0.0781	0.015	0.0059	-0.0302
0.0869	0.2167	0.6953	-0.2202	0.0859	0.155	0.0078	-0.0458
0.0879	0.2239	0.7031	-0.1569	0.0938	0.435	0.0098	-0.0931
0.0889	0.2312	0.7109	-0.1963	0.1016	0.655	0.0117	-0.0914
0.0898	0.2471	0.7188	-0.1829	0.1094	0.865	0.0137	-0.129

0.0908	0.2259	0.7266	-0.2161	0.1172	0.125	0.0156	-0.1125
0.0918	0.2497	0.7344	-0.1873	0.125	-0.925	0.0176	-0.1273
0.0928	0.2374	0.7422	-0.2427	0.1328	-0.935	0.0195	-0.1056
0.0938	0.2628	0.75	-0.297	0.1406	-0.615	0.0215	-0.1243
0.0947	0.2567	0.7578	-0.3738	0.1484	-0.235	0.0234	-0.1194
0.0957	0.2603	0.7656	-0.4325	0.1562	0.005	0.0254	-0.1212
0.0967	0.2522	0.7734	-0.4458	0.1641	0.035	0.0273	-0.1135
0.0977	0.2735	0.7812	-0.4247	0.1719	0.035	0.0293	-0.1087
0.0986	0.253	0.7891	-0.443	0.1797	0.015	0.0312	-0.1201
0.0996	0.2395	0.7969	-0.4654	0.1875	0.005	0.0332	-0.1114
0.1006	0.2318	0.8047	-0.4689	0.1953	0.045	0.0352	-0.1103
0.1016	0.2126	0.8125	-0.4743	0.2031	0.045	0.0371	-0.0917
0.1025	0.2113	0.8203	-0.4571	0.2109	0.045	0.0391	-0.1228
0.1035	0.1965	0.8281	-0.4456	0.2188	0.105	0.041	-0.108
0.1045	0.1977	0.8359	-0.4566	0.2266	0.105	0.043	-0.1343
0.1055	0.174	0.8438	-0.4689	0.2344	0.095	0.0449	-0.1258
0.1064	0.1967	0.8516	-0.4543	0.2422	0.125	0.0469	-0.1438
0.1074	0.172	0.8594	-0.4956	0.25	0.115	0.0488	-0.1318
0.1084	0.1828	0.8672	-0.4279	0.2578	0.105	0.0508	-0.1452
0.1094	0.1751	0.875	-0.464	0.2656	0.165	0.0527	-0.1247
0.1104	0.1864	0.8828	-0.4508	0.2734	0.155	0.0547	-0.1392
0.1113	0.1781	0.8906	-0.4842	0.2812	0.235	0.0566	-0.1282
0.1123	0.1849	0.8984	-0.4931	0.2891	0.185	0.0586	-0.1411
0.1133	0.1659	0.9062	-0.4654	0.2969	0.205	0.0605	-0.1442
0.1143	0.1707	0.9141	-0.2018	0.3047	0.315	0.0625	-0.1447
0.1152	0.1785	0.9219	-0.0614	0.3125	0.295	0.0645	-0.156
0.1162	0.1659	0.9297	0.103	0.3203	0.305	0.0664	-0.1411
0.1172	0.157	0.9375	0.3551	0.3281	0.325	0.0684	-0.1454
0.1182	0.1554	0.9453	0.3967	0.3359	0.415	0.0703	-0.1185
0.1191	0.16	0.9531	0.369	0.3438	0.425	0.0723	-0.118
0.1201	0.1438	0.9609	0.2398	0.3516	0.495	0.0742	-0.0792
0.1211	0.1579	0.9687	0.117	0.3594	0.475	0.0762	-0.0853
0.1221	0.1296	0.9766	-0.1239	0.3672	0.525	0.0781	-0.068
0.123	0.1374	0.9844	-0.4741	0.375	0.475	0.0801	-0.0994
0.124	0.1426	0.9922	-0.7617	0.3828	0.505	0.082	-0.0842
0.125	0.1533	1	-0.8791	0.3906	0.415	0.084	-0.1182
0.126	0.1249	1.0078	-0.9209	0.3984	0.355	0.0859	-0.1293
0.127	0.1448	1.0156	-0.8868	0.4062	0.265	0.0879	-0.1518
0.1279	0.1314	1.0234	-0.8382	0.4141	0.175	0.0898	-0.1481
0.1289	0.1353	1.0312	-0.7994	0.4219	0.105	0.0918	-0.1769
0.1299	0.1397	1.0391	-0.7413	0.4297	0.085	0.0938	-0.1944
0.1309	0.1374	1.0469	-0.7029	0.4375	-0.015	0.0957	-0.1951
0.1318	0.1375	1.0547	-0.6883	0.4453	-0.015	0.0977	-0.2072
0.1328	0.1459	1.0625	-0.6962	0.4531	-0.045	0.0996	-0.2024
0.1338	0.1987	1.0703	-0.6993	0.4609	-0.095	0.1016	-0.2273
0.1348	0.2181	1.0781	-0.7123	0.4688	-0.035	0.1035	-0.2204
0.1357	0.2372	1.0859	-0.7194	0.4766	-0.085	0.1055	-0.2408
0.1367	0.2036	1.0938	-0.7301	0.4844	-0.085	0.1074	-0.221
0.1377	0.1985	1.1016	-0.7154	0.4922	-0.135	0.1094	-0.2477
0.1387	0.1742	1.1094	-0.7513	0.5	-0.065	0.1113	-0.2273
0.1396	0.1555	1.1172	-0.727	0.5078	-0.085	0.1133	-0.2409
0.1406	0.1353	1.125	-0.7399	0.5156	-0.105	0.1152	-0.2215

0.1416	0.1631	1.1328	-0.7123	0.5234	-0.075	0.1172	-0.2347
0.1426	0.1353	1.1406	-0.7159	0.5312	-0.095	0.1191	-0.2265
0.1436	0.1286	1.1484	-0.688	0.5391	-0.095	0.1211	-0.1928
0.1445	0.1312	1.1562	-0.661	0.5469	-0.065	0.123	-0.1298
0.1455	0.1256	1.1641	-0.6461	0.5547	-0.085	0.125	0.0326
0.1465	0.1176	1.1719	-0.6057	0.5625	-0.075	0.127	0.2202
0.1475	0.1278	1.1797	-0.5904	0.5703	-0.085	0.1289	0.116
0.1484	0.1266	1.1875	-0.5339	0.5781	-0.075	0.1309	-0.0992
0.1494	0.1168	1.1953	-0.5149	0.5859	-0.085	0.1328	0.1078
0.1504	0.1355	1.2031	-0.4605	0.5938	-0.075	0.1348	0.491
0.1514	0.1188	1.2109	-0.4443	0.6016	-0.045	0.1367	0.6706
0.1523	0.1224	1.2188	-0.3958	0	0.125	0.1387	0.3793

Cases of CHF							
ECG	T	ECG	T	ECG	T	ECG	T
0	-0.5217	0	-0.2792	0	0.1194	0	-0.2792
0.002	-0.91	0.002	-0.4156	0.0078	0.1876	0.002	-0.4156
0.0039	-0.8781	0.0039	-0.3913	0.0156	0.1696	0.0039	-0.3913
0.0059	-0.9321	0.0059	-0.4134	0.0234	0.1786	0.0059	-0.4134
0.0078	-0.942	0.0078	-0.4066	0.0312	0.2118	0.0078	-0.4066
0.0098	-0.9891	0.0098	-0.3989	0.0391	0.1966	0.0098	-0.3989
0.0117	-0.9971	0.0117	-0.3913	0.0469	0.0729	0.0117	-0.3913
0.0137	-0.9886	0.0137	-0.3459	0.0547	0.1659	0.0137	-0.3459
0.0156	-1.0167	0.0156	-0.3513	0.0625	0.0832	0.0156	-0.3513
0.0176	-1.016	0.0176	-0.3288	0.0703	0.1992	0.0176	-0.3288
0.0195	-1.0265	0.0195	-0.3188	0.0781	0.1790	0.0195	-0.3188
0.0215	-1.0305	0.0215	-0.3133	0.0859	0.1116	0.0215	-0.3133
0.0234	-1.0206	0.0234	-0.3133	0.0938	0.1202	0.0234	-0.3133
0.0254	-1.0106	0.0254	-0.3153	0.1016	0.1142	0.0254	-0.3153
0.0273	-1.0122	0.0273	-0.3074	0.1094	0.0234	0.0273	-0.3074
0.0293	-1.0701	0.0293	-0.3137	0.1172	-0.0122	0.0293	-0.3137
0.0312	-1.1416	0.0312	-0.3076	0.1250	-0.0956	0.0312	-0.3076
0.0332	-1.1582	0.0332	-0.3246	0.1328	-0.1189	0.0332	-0.3246
0.0352	-1.1372	0.0352	-0.3279	0.1406	-0.1155	0.0352	-0.3279
0.0371	-1.1802	0.0371	-0.3272	0.1484	-0.1444	0.0371	-0.3272
0.0391	-1.3468	0.0391	-0.3245	0.1562	-0.1568	0.0391	-0.3245
0.041	-1.47	0.041	-0.3408	0.1641	-0.1818	0.041	-0.3408
0.043	-1.3607	0.043	-0.3273	0.1719	-0.1741	0.043	-0.3273
0.0449	-1.0741	0.0449	-0.3096	0.1797	-0.1970	0.0449	-0.3096
0.0469	-0.7966	0.0469	-0.3234	0.1875	-0.1940	0.0469	-0.3234
0.0488	-0.6111	0.0488	-0.3226	0.1953	-0.2045	0.0488	-0.3226
0.0508	-0.7637	0.0508	-0.3186	0.2031	-0.2055	0.0508	-0.3186
0.0527	-0.9822	0.0527	-0.3231	0.2109	-0.1690	0.0527	-0.3231
0.0547	-1.0563	0.0547	-0.3248	0.2188	-0.1892	0.0547	-0.3248
0.0566	-1.017	0.0566	-0.3262	0.2266	-0.1696	0.0566	-0.3262
0.0586	-1.018	0.0586	-0.3412	0.2344	-0.1822	0.0586	-0.3412

0.0605	-1.0386	0.0605	-0.3239	0.2422	-0.1894	0.0605	-0.3239
0.0625	-1.0037	0.0625	-0.3294	0.2500	-0.1851	0.0625	-0.3294
0.0645	-0.9882	0.0645	-0.3354	0.2578	-0.2367	0.0645	-0.3354
0.0664	-0.9522	0.0664	-0.3197	0.2656	-0.1283	0.0664	-0.3197
0.0684	-0.9262	0.0684	-0.3098	0.2734	0.1474	0.0684	-0.3098
0.0703	-0.952	0.0703	-0.3203	0.2812	0.2117	0.0703	-0.3203
0.0723	-0.9362	0.0723	-0.3181	0.2891	0.4363	0.0723	-0.3181
0.0742	-0.9205	0.0742	-0.315	0.2969	0.6266	0.0742	-0.315
0.0762	-0.903	0.0762	-0.3151	0.3047	0.5581	0.0762	-0.3151
0.0781	-0.8943	0.0781	-0.3281	0.3125	0.5081	0.0781	-0.3281
0.0801	-0.9091	0.0801	-0.3458	0.3203	0.3691	0.0801	-0.3458
0.082	-0.892	0.082	-0.3499	0.3281	0.2182	0.082	-0.3499
0.084	-0.8722	0.084	-0.3346	0.3359	-0.0059	0.084	-0.3346
0.0859	-0.8565	0.0859	-0.3275	0.3438	-0.3768	0.0859	-0.3275
0.0879	-0.8682	0.0879	-0.3378	0.3516	-0.5629	0.0879	-0.3378
0.0898	-0.8793	0.0898	-0.3144	0.3594	-0.6739	0.0898	-0.3144
0.0918	-0.8781	0.0918	-0.3043	0.3672	-0.6750	0.0918	-0.3043
0.0938	-0.8492	0.0938	-0.257	0.3750	-0.6515	0.0938	-0.257
0.0957	-0.8539	0.0957	-0.2281	0.3828	-0.6011	0.0957	-0.2281
0.0977	-0.8711	0.0977	-0.2305	0.3906	-0.5834	0.0977	-0.2305
0.0996	-0.8778	0.0996	-0.2454	0.3984	-0.5383	0.0996	-0.2454
0.1016	-0.8671	0.1016	-0.2738	0.4062	-0.4777	0.1016	-0.2738
0.1035	-0.8351	0.1035	-0.311	0.4141	-0.4721	0.1035	-0.311
0.1055	-0.8446	0.1055	-0.315	0.4219	-0.4598	0.1055	-0.315
0.1074	-0.8412	0.1074	-0.3222	0.4297	-0.4720	0.1074	-0.3222
0.1094	-0.8404	0.1094	-0.3367	0.4375	-0.4831	0.1094	-0.3367
0.1113	-0.843	0.1113	-0.356	0.4453	-0.5056	0.1113	-0.356
0.1133	-0.8556	0.1133	-0.3608	0.4531	-0.4871	0.1133	-0.3608
0.1152	-0.9001	0.1152	-0.3636	0.4609	-0.5252	0.1152	-0.3636
0.1172	-0.9144	0.1172	-0.3524	0.4688	-0.5077	0.1172	-0.3524
0.1191	-0.9026	0.1191	-0.3753	0.4766	-0.5080	0.1191	-0.3753
0.1211	-0.9178	0.1211	-0.3629	0.4844	-0.5111	0.1211	-0.3629
0.123	-0.9619	0.123	-0.3731	0.4922	-0.5138	0.123	-0.3731
0.125	-0.9594	0.125	-0.37	0.5000	-0.4952	0.125	-0.37
0.127	-0.9364	0.127	-0.3598	0.5078	-0.4865	0.127	-0.3598
0.1289	-0.9291	0.1289	-0.3648	0.5156	-0.4742	0.1289	-0.3648
0.1309	-0.934	0.1309	-0.3595	0.5234	-0.4476	0.1309	-0.3595
0.1328	-0.9352	0.1328	-0.357	0.5312	-0.4181	0.1328	-0.357
0.1348	-0.9565	0.1348	-0.3495	0.5391	-0.3998	0.1348	-0.3495
0.1367	-0.9087	0.1367	-0.3368	0.5469	-0.3626	0.1367	-0.3368
0.1387	-0.8819	0.1387	-0.3124	0.5547	-0.3667	0.1387	-0.3124
0.1406	-0.9176	0.1406	-0.2908	0.5625	-0.3246	0.1406	-0.2908
0.1426	-0.9336	0.1426	-0.4487	0.5703	-0.2628	0.1426	-0.4487
0.1445	-0.9047	0.1445	-0.8426	0.5781	-0.2708	0.1445	-0.8426
0.1465	-0.8974	0.1465	-1.0497	0.5859	-0.2076	0.1465	-1.0497
0.1484	-0.8561	0.1484	-0.9571	0.5938	-0.2376	0.1484	-0.9571
0.1504	-0.8644	0.1504	-0.7221	0.6016	-0.1932	0.1504	-0.7221
0.1523	-0.8796	0.1523	-0.4383	0.6094	-0.1885	0.1523	-0.4383
0.1543	-0.9104	0	-0.2792	0.6172	-0.1651	0.1543	-0.166
0.1562	-0.9727	0.002	-0.4156	0.6250	-0.1813	0.1562	-0.0039

0.1582	-1.0364	0.0039	-0.3913	0.6328	-0.1738	0.1582	-0.0102
0.1602	-1.097	0.0059	-0.4134	0.6406	-0.1778	0.1602	-0.0394
0.1621	-1.1151	0.0078	-0.4066	0.6484	-0.1333	0.1621	-0.0651
0.1641	-1.0964	0.0098	-0.3989	0.6562	-0.1475	0.1641	-0.0931
0.166	-1.0727	0.0117	-0.3913	0.6641	-0.1772	0.166	-0.0989
0.168	-1.1007	0.0137	-0.3459	0.6719	-0.1595	0.168	-0.1009
0.1699	-1.0836	0.0156	-0.3513	0.6797	-0.1909	0.1699	-0.1459
0.1719	-1.0636	0.0176	-0.3288	0.6875	-0.2042	0.1719	-0.1941
0.1738	-1.0711	0.0195	-0.3188	0.6953	-0.2202	0.1738	-0.2583
0.1758	-1.1135	0.0215	-0.3133	0.7031	-0.1569	0.1758	-0.3528
0.1777	-1.1274	0.0234	-0.3133	0.7109	-0.1963	0.1777	-0.3864
0.1797	-1.1107	0.0254	-0.3153	0.7188	-0.1829	0.1797	-0.3431
0.1816	-1.066	0.0273	-0.3074	0.7266	-0.2161	0.1816	-0.3087
0.1836	-1.1398	0.0293	-0.3137	0.7344	-0.1873	0.1836	-0.3121
0.1855	-1.1614	0.0312	-0.3076	0.7422	-0.2427	0.1855	-0.3065
0.1875	-1.1566	0.0332	-0.3246	0.7500	-0.2970	0.1875	-0.3108
0.1895	-1.1947	0.0352	-0.3279	0.7578	-0.3738	0.1895	-0.2992
0.1914	-1.2724	0.0371	-0.3272	0.7656	-0.4325	0.1914	-0.2887
0.1934	-1.4461	0.0391	-0.3245	0.7734	-0.4458	0.1934	-0.2862
0.1953	-1.5802	0.041	-0.3408	0.7812	-0.4247	0.1953	-0.2924
0.1973	-1.4585	0.043	-0.3273	0.7891	-0.4430	0.1973	-0.2647
0.1992	-1.1785	0.0449	-0.3096	0.7969	-0.4654	0.1992	-0.2725
0.2012	-0.8996	0.0469	-0.3234	0.8047	-0.4689	0.2012	-0.2789
0.2031	-0.8205	0.0488	-0.3226	0.8125	-0.4743	0.2031	-0.2675
0.2051	-1.0106	0.0508	-0.3186	0.8203	-0.4571	0.2051	-0.2885
0.207	-1.1263	0.0527	-0.3231	0.8281	-0.4456	0.207	-0.2863
0.209	-1.0869	0.0547	-0.3248	0.8359	-0.4566	0.209	-0.3003
0.2109	-1.0936	0.0566	-0.3262	0.8438	-0.4689	0.2109	-0.3198
0.2129	-1.1517	0.0586	-0.3412	0.8516	-0.4543	0.2129	-0.3426
0.2148	-1.152	0.0605	-0.3239	0.8594	-0.4956	0.2148	-0.3589
0.2168	-1.1335	0.0625	-0.3294	0.8672	-0.4279	0.2168	-0.3783
0.2188	-1.1282	0.0645	-0.3354	0.8750	-0.4640	0.2188	-0.3971
0.2207	-1.1035	0.0664	-0.3197	0.8828	-0.4508	0.2207	-0.3875
0.2227	-1.0897	0.0684	-0.3098	0.8906	-0.4842	0.2227	-0.3889
0.2246	-1.1188	0.0703	-0.3203	0.8984	-0.4931	0.2246	-0.379
0.2266	-1.1363	0.0723	-0.3181	0.9062	-0.4654	0.2266	-0.3741
0.2285	-1.1221	0.0742	-0.315	0.9141	-0.2018	0.2285	-0.3411
0.2305	-1.0985	0.0762	-0.3151	0.9219	-0.0614	0.2305	-0.3289
0.2324	-1.0914	0.0781	-0.3281	0.9297	0.1030	0.2324	-0.3193
0.2344	-1.0546	0.0801	-0.3458	0.9375	0.3551	0.2344	-0.3074
0.2363	-1.0113	0.082	-0.3499	0.9453	0.3967	0.2363	-0.2985
0.2383	-1.0389	0.084	-0.3346	0.9531	0.3690	0.2383	-0.2726
0.2402	-1.0893	0.0859	-0.3275	0.9609	0.2398	0.2402	-0.302
0.2422	-1.0726	0.0879	-0.3378	0.9687	0.1170	0.2422	-0.308
0.2441	-1.1489	0.0898	-0.3144	0.9766	-0.1239	0.2441	-0.2954
0.2461	-1.1753	0.0918	-0.3043	0.9844	-0.4741	0.2461	-0.3042
0.248	-1.1406	0.0938	-0.257	0.9922	-0.7617	0.248	-0.2917
0.25	-1.114	0.0957	-0.2281	1.0000	-0.8791	0.25	-0.2905
0.252	-1.0779	0.0977	-0.2305	1.0078	-0.9209	0.252	-0.3001
0.2539	-1.0947	0.0996	-0.2454	1.0156	-0.8868	0.2539	-0.3056

0.2559	-1.0497	0.1016	-0.2738	1.0234	-0.8382	0.2559	-0.2994
0.2578	-1.0547	0.1035	-0.311	1.0312	-0.7994	0.2578	-0.295
0.2598	-1.0876	0.1055	-0.315	1.0391	-0.7413	0.2598	-0.3075
0.2617	-1.0533	0.1074	-0.3222	1.0469	-0.7029	0.2617	-0.3123
0.2637	-1.1128	0.1094	-0.3367	1.0547	-0.6883	0.2637	-0.2977
0.2656	-1.1371	0.1113	-0.356	1.0625	-0.6962	0.2656	-0.2911
0.2676	-1.123	0.1133	-0.3608	1.0703	-0.6993	0.2676	-0.2989
0.2695	-1.1225	0.1152	-0.3636	1.0781	-0.7123	0.2695	-0.3038
0.2715	-1.1063	0.1172	-0.3524	1.0859	-0.7194	0.2715	-0.306
0.2734	-1.1086	0.1191	-0.3753	1.0938	-0.7301	0.2734	-0.3035
0.2754	-1.105	0.1211	-0.3629	1.1016	-0.7154	0	-0.2792
0.2773	-1.1054	0.123	-0.3731	1.1094	-0.7513	0.002	-0.4156
0.2793	-1.1094	0.125	-0.37	1.1172	-0.7270	0.0039	-0.3913
0.2812	-1.1175	0.127	-0.3598	1.1250	-0.7399	0.0059	-0.4134
0.2832	-1.1199	0.1289	-0.3648	1.1328	-0.7123	0.0078	-0.4066
0.2852	-1.1471	0.1309	-0.3595	1.1406	-0.7159	0.0098	-0.3989
0.2871	-1.1222	0.1328	-0.357	1.1484	-0.6880	0.0117	-0.3913

Cases of NSR

ECG	T	ECG	T	ECG	T	ECG	T
0	-0.165	0	-0.275	0	0.125	0	-0.355
0.0078	-0.155	0.002	-0.245	0.0078	0.005	0.001	-0.355
0.0156	-0.195	0.0039	-0.285	0.0156	0.025	0.002	-0.345
0.0234	-0.205	0.0059	-0.265	0.0234	0.065	0.0029	-0.335
0.0312	-0.185	0.0078	-0.235	0.0312	-0.085	0.0039	-0.335
0.0391	-0.155	0.0098	-0.215	0.0391	0.005	0.0049	-0.345
0.0469	-0.135	0.0117	-0.165	0.0469	-0.065	0.0059	-0.345
0.0547	-0.095	0.0137	-0.165	0.0547	-0.015	0.0068	-0.375
0.0625	-0.075	0.0156	-0.145	0.0625	-0.035	0.0078	-0.365
0.0703	-0.065	0.0176	-0.095	0.0703	-0.035	0.0088	-0.355
0.0781	-0.065	0.0195	-0.085	0.0781	0.015	0.0098	-0.365
0.0859	-0.125	0.0215	-0.045	0.0859	0.155	0.0107	-0.355
0.0938	-0.125	0.0234	0.025	0.0938	0.435	0.0117	-0.385
0.1016	-0.125	0.0254	0.085	0.1016	0.655	0.0127	-0.385
0.1094	-0.115	0.0273	0.175	0.1094	0.865	0.0137	-0.375
0.1172	-0.125	0.0293	0.215	0.1172	0.125	0.0146	-0.415
0.125	-0.165	0.0312	0.255	0.125	-0.925	0.0156	-0.405
0.1328	-0.115	0.0332	0.305	0.1328	-0.935	0.0166	-0.415
0.1406	-0.145	0.0352	0.285	0.1406	-0.615	0.0176	-0.415
0.1484	-0.115	0.0371	0.285	0.1484	-0.235	0.0186	-0.385
0.1562	-0.135	0.0391	0.245	0.1562	0.005	0.0195	-0.395
0.1641	-0.135	0.041	0.175	0.1641	0.035	0.0205	-0.395
0.1719	-0.125	0.043	0.125	0.1719	0.035	0.0215	-0.405
0.1797	-0.175	0.0449	0.015	0.1797	0.015	0.0225	-0.395
0.1875	-0.145	0.0469	-0.075	0.1875	0.005	0.0234	-0.395
0.1953	-0.125	0.0488	-0.125	0.1953	0.045	0.0244	-0.385

0.2031	-0.145	0.0508	-0.175	0.2031	0.045	0.0254	-0.385
0.2109	-0.145	0.0527	-0.205	0.2109	0.045	0.0264	-0.355
0.2188	-0.135	0.0547	-0.195	0.2188	0.105	0.0273	-0.365
0.2266	-0.165	0.0566	-0.205	0.2266	0.105	0.0283	-0.375
0.2344	-0.155	0.0586	-0.165	0.2344	0.095	0.0293	-0.345
0.2422	-0.095	0.0605	-0.185	0.2422	0.125	0.0303	-0.325
0.25	-0.105	0.0625	-0.185	0.25	0.115	0.0312	-0.325
0.2578	-0.075	0.0645	-0.185	0.2578	0.105	0.0322	-0.285
0.2656	-0.085	0.0664	-0.195	0.2656	0.165	0.0332	-0.215
0.2734	0.025	0.0684	-0.195	0.2734	0.155	0.0342	-0.195
0.2812	0.025	0.0703	-0.185	0.2812	0.235	0.0352	-0.235
0.2891	-0.025	0.0723	-0.165	0.2891	0.185	0.0361	-0.285
0.2969	-0.085	0.0742	-0.145	0.2969	0.205	0.0371	-0.315
0.3047	-0.115	0.0762	-0.135	0.3047	0.315	0.0381	-0.395
0.3125	-0.145	0.0781	-0.145	0.3125	0.295	0.0391	-0.415
0.3203	-0.125	0.0801	-0.155	0.3203	0.305	0.04	-0.415
0.3281	-0.155	0.082	-0.185	0.3281	0.325	0.041	-0.385
0.3359	-0.205	0.084	-0.185	0.3359	0.415	0.042	-0.385
0.3438	-0.215	0.0859	-0.165	0.3438	0.425	0.043	-0.395
0.3516	-0.215	0.0879	-0.175	0.3516	0.495	0.0439	-0.405
0.3594	-0.165	0.0898	-0.145	0.3594	0.475	0.0449	-0.325
0.3672	-0.165	0.0918	-0.165	0.3672	0.525	0.0459	-0.505
0.375	-0.155	0.0938	-0.165	0.375	0.475	0.0469	-0.765
0.3828	-0.615	0.0957	-0.175	0.3828	0.505	0.0479	-0.695
0.3906	-0.855	0.0977	-0.185	0.3906	0.415	0.0488	0.095
0.3984	-0.185	0.0996	-0.195	0.3984	0.355	0.0498	1.265
0.4062	1.295	0.1016	-0.195	0.4062	0.265	0.0508	2.455
0.4141	2.575	0.1035	-0.175	0.4141	0.175	0.0518	3.025
0.4219	2.675	0.1055	-0.165	0.4219	0.105	0.0527	1.425
0.4297	2.445	0.1074	-0.165	0.4297	0.085	0.0537	-0.625
0.4375	0.735	0.1094	-0.175	0.4375	-0.015	0.0547	-1.085
0.4453	-0.415	0.1113	-0.175	0.4453	-0.015	0.0557	-0.935
0.4531	-0.295	0.1133	-0.185	0.4531	-0.045	0.0566	-0.765
0.4609	-0.285	0.1152	-0.205	0.4609	-0.095	0.0576	-0.485
0.4688	-0.345	0.1172	-0.195	0.4688	-0.035	0.0586	-0.375
0.4766	-0.365	0.1191	-0.185	0.4766	-0.085	0.0596	-0.375
0.4844	-0.345	0.1211	-0.165	0.4844	-0.085	0.0605	-0.325
0.4922	-0.305	0.123	-0.135	0.4922	-0.135	0.0615	-0.335
0.5	-0.315	0.125	-0.115	0.5	-0.065	0.0625	-0.305
0.5078	-0.305	0.127	-0.065	0.5078	-0.085	0.0635	-0.285
0.5156	-0.265	0.1289	-0.075	0.5156	-0.105	0.0645	-0.245
0.5234	-0.235	0.1309	-0.075	0.5234	-0.075	0.0654	-0.205
0.5312	-0.265	0.1328	0.035	0.5312	-0.095	0.0664	-0.175
0.5391	-0.245	0.1348	0.005	0.5391	-0.095	0.0674	-0.185
0.5469	-0.215	0.1367	-0.065	0.5469	-0.065	0.0684	-0.125
0.5547	-0.195	0.1387	-0.085	0.5547	-0.085	0.0693	-0.115
0.5625	-0.175	0.1406	-0.105	0.5625	-0.075	0.0703	-0.075
0.5703	-0.185	0.1426	-0.155	0.5703	-0.085	0.0713	-0.025
0.5781	-0.155	0.1445	-0.175	0.5781	-0.075	0.0723	0.045
0.5859	-0.125	0.1465	-0.195	0.5859	-0.085	0.0732	0.135
0.5938	-0.145	0.1484	-0.185	0.5938	-0.075	0.0742	0.185
0.6016	-0.125	0.1504	-0.175	0.6016	-0.045	0.0752	0.275
0.6094	-0.145	0.1523	-0.145	0.6094	-0.065	0.0762	0.365

0.6172	-0.155	0.1543	-0.155	0.6172	-0.055	0.0771	0.435
0.625	-0.185	0.1562	-0.165	0.625	-0.075	0.0781	0.495
0.6328	-0.175	0.1582	-0.175	0.6328	-0.075	0.0791	0.545
0.6406	-0.175	0.1602	-0.175	0.6406	-0.105	0.0801	0.555
0.6484	-0.165	0.1621	-0.155	0.6484	-0.055	0.0811	0.565
0.6562	-0.165	0.1641	-0.335	0.6562	-0.095	0.082	0.445
0.6641	-0.115	0.166	-0.675	0.6641	-0.085	0.083	0.295
0.6719	-0.065	0.168	-0.345	0.6719	-0.095	0.084	0.145
0.6797	-0.095	0.1699	1.275	0.6797	-0.055	0.085	-0.025
0.6875	-0.115	0.1719	2.465	0.6875	-0.095	0.0859	-0.145
0.6953	-0.075	0.1738	2.895	0.6953	-0.105	0.0869	-0.245
0.7031	-0.115	0.1758	1.805	0.7031	-0.085	0.0879	-0.285
0.7109	-0.155	0.1777	0.195	0.7109	-0.105	0.0889	-0.305
0.7188	-0.105	0.1797	-0.125	0.7188	-0.065	0.0898	-0.345
0.7266	-0.125	0.1816	-0.155	0.7266	-0.065	0.0908	-0.365
0.7344	-0.135	0.1836	-0.175	0.7344	-0.025	0.0918	-0.365
0.7422	-0.125	0.1855	-0.215	0.7422	-0.075	0.0928	-0.385
0.75	-0.115	0.1875	-0.235	0.75	-0.125	0.0938	-0.385
0.7578	-0.105	0.1895	-0.215	0.7578	-0.065	0.0947	-0.375
0.7656	-0.135	0.1914	-0.255	0.7656	-0.095	0.0957	-0.365
0.7734	-0.135	0.1934	-0.255	0.7734	-0.105	0.0967	-0.365
0.7812	-0.135	0.1953	-0.225	0.7812	-0.045	0.0977	-0.365
0.7891	-0.145	0.1973	-0.225	0.7891	-0.045	0.0986	-0.365
0.7969	-0.125	0.1992	-0.195	0.7969	0.015	0.0996	-0.355
0.8047	-0.115	0.2012	-0.195	0.8047	0.015	0.1006	-0.375
0.8125	-0.135	0.2031	-0.195	0.8125	0.075	0.1016	-0.355
0.8203	-0.135	0.2051	-0.165	0.8203	0.055	0.1025	-0.365
0.8281	-0.165	0.207	-0.195	0.8281	0.035	0.1035	-0.355
0.8359	-0.155	0.209	-0.165	0.8359	-0.045	0.1045	-0.335
0.8438	-0.115	0.2109	-0.125	0.8438	-0.045	0.1055	-0.335
0.8516	-0.085	0.2129	-0.105	0.8516	-0.015	0.1064	-0.345
0.8594	-0.055	0.2148	-0.035	0.8594	-0.075	0.1074	-0.355
0.8672	-0.055	0.2168	-0.015	0.8672	-0.135	0.1084	-0.365
0.875	-0.045	0.2188	0.025	0.875	-0.145	0.1094	-0.365
0.8828	0.065	0.2207	0.085	0.8828	-0.105	0.1104	-0.355
0.8906	0.005	0.2227	0.105	0.8906	-0.165	0.1113	-0.385
0.8984	-0.015	0.2246	0.175	0.8984	-0.145	0.1123	-0.375
0.9062	-0.055	0.2266	0.235	0.9062	-0.085	0.1133	-0.385
0.9141	-0.115	0.2285	0.275	0.9141	-0.085	0.1143	-0.385
0.9219	-0.135	0.2305	0.355	0.9219	0.005	0.1152	-0.385
0.9297	-0.135	0.2324	0.395	0.9297	0.295	0.1162	-0.395
0.9375	-0.175	0	-0.275	0.9375	0.585	0.1172	-0.395
0.9453	-0.205	0.002	-0.245	0.9453	0.885	0.1182	-0.385
0.9531	-0.225	0.0039	-0.285	0	0.125	0	-0.355
0.9609	-0.175	0.0059	-0.265	0.0078	0.005	0.001	-0.355
0.9687	-0.175	0.0078	-0.235	0.0156	0.025	0.002	-0.345
0.9766	-0.155	0.0098	-0.215	0.0234	0.065	0.0029	-0.335
0.9844	-0.255	0.0117	-0.165	0.0312	-0.085	0.0039	-0.335
0.9922	-0.875	0.0137	-0.165	0.0391	0.005	0.0049	-0.345
1	-0.645	0.0156	-0.145	0.0469	-0.065	0.0059	-0.345
1.0078	0.645	0.0176	-0.095	0.0547	-0.015	0.0068	-0.375
1.0156	2.315	0.0195	-0.085	0.0625	-0.035	0.0078	-0.365
1.0234	2.925	0.0215	-0.045	0.0703	-0.035	0.0088	-0.355

1.0312	2.725	0.0234	0.025	0.0781	0.015	0.0098	-0.365
1.0391	1.225	0.0254	0.085	0.0859	0.155	0.0107	-0.355
1.0469	-0.185	0.0273	0.175	0.0938	0.435	0.0117	-0.385
1.0547	-0.275	0.0293	0.215	0.1016	0.655	0.0127	-0.385
1.0625	-0.275	0.0312	0.255	0.1094	0.865	0.0137	-0.375
1.0703	-0.285	0.0332	0.305	0.1172	0.125	0.0146	-0.415
1.0781	-0.285	0.0352	0.285	0.125	-0.925	0.0156	-0.405
1.0859	-0.335	0.0371	0.285	0.1328	-0.935	0.0166	-0.415
1.0938	-0.305	0.0391	0.245	0.1406	-0.615	0.0176	-0.415
1.1016	-0.285	0.041	0.175	0.1484	-0.235	0.0186	-0.385
1.1094	-0.275	0.043	0.125	0.1562	0.005	0.0195	-0.395
1.1172	-0.275	0.0449	0.015	0.1641	0.035	0.0205	-0.395
1.125	-0.245	0.0469	-0.075	0.1719	0.035	0.0215	-0.405
1.1328	-0.245	0.0488	-0.125	0.1797	0.015	0.0225	-0.395
1.1406	-0.225	0.0508	-0.175	0.1875	0.005	0.0234	-0.395
1.1484	-0.195	0.0527	-0.205	0.1953	0.045	0.0244	-0.385
1.1562	-0.205	0.0547	-0.195	0.2031	0.045	0.0254	-0.385

الخلاصة

نبضات القلب هي مجموعة من الاشكال الموجية التي تنشأ من انسجة القلب وتقلص وانبساط عضلات القلب. الصعوبة في تصنيف اشارة القلب هوالتغيرات الموجودة في مخطط كهربائية القلب والتي تعتبر بالغة الاهمية والاساس في تشخيص حالة المريض وقد تم استخدام العديد من الخوارزميات الحديثة في تشخيص اشارة القلب وفقا لسجلات مخطط كهربائية القلب. بالاستعانة بالخوارزميات الحديثة تم تصميم جهاز يساعد الطبيب بالتشخيص المسبق.

تتعرض اشارة تخطيط القلب الى انواع متعددة من الضوضاء التي تؤثر على دقة تصنيف الاشارة والتشخيص الصحيح من هذا الانواع ضوضاء تداخل خط الطاقة (powerline)، والضوضاء الأساسية(baseline wander) ، وضوضاء حركة القطب الكهربائي(electrode motion artifact) ، وضوضاء تخطيط كهربية العضل (EMG) الضوضاء التي تم ذكرها الان هي الضوضاء الأكثر شيوعًا التي تؤثر بإشارات مخطط كهربية القلب(ECG).

يعد تقليل ضوضاء من إشارات مخطط كهربية القلب خطوة اساسية في الحصول على ميزات إشارة نقية للتشخيص الدقيق. تبحث الدراسة في أنواع متعددة من الضوضاء الشائعة في إشارات تخطيط القلب ، وكذلك طرق معالجة إشارات إزالة الضوضاء. لإزالة ضوضاء خط الأساس(baseline wander) من إشارة تخطيط القلب يمكن استخدام التحويل المويج المنفصل Discrete Wavelet (Transform). أما مرشح (Notch filter) قادر على إزالة ضوضاء خطوط الطاقة(power (line. يُعتقد أن التصفية التكيفية (Adaptive filter) طريقة فعالة لإزالة ضوضاء تخطيط كهربية العضل (EMG) ، وقد تم أستخدم المرشحات التكيفية ذات المتوسطات المربعة (LMS) والمرشحات المربعة الأقل تكرارية (RLS) لتقليل الضوضاء الناتجة عن حركة القطب الكهربي.

وكما ذكرنا سابقا، تصنيف إشارة تخطيط القلب يتم عادة بهدف تحديد حالة القلب وتشخيص الأمراض القلبية والتحقق من صحة القلب. يشمل التصنيف الأمراض مثل تسارع القلب، تباطؤ القلب، اضطرابات النظم الكهربائية، وغيرها من التغيرات الكهربائية المرتبطة بالقلب في هذا البحث تم استخدام الحالة الطبيعية (Normal)التي تمثلت ب Normal Sine Rhythmal(NSR)،والحالة غير الطبيعية والتي تتمثل(Arrhythmia (ARR و(CHF) congestive heart failure

عند تصنيف إشارة تخطيط القلب، يتم تحليل أمواج الإشارة الكهربائية واستخراج الميزات المميزة للحالة القلبية. يمكن استخدام مجموعة من التقنيات لهذا الغرض، بما في ذلك تحويل الإشارات إلى ترددات مختلفة باستخدام محول نثر الموجات (Wavelet scattering Transform) أو فصل الإشارات المختلطة باستخدام فصل المصادر الاعمى(Blind Source Separation) ، تم تصنيف الإشارات باستخدام تقنيات التعلم الآلي مثل الشبكات العصبية ،متجه الدعم الالي وتقسم البيانات بنسب مختلفة بشكل عشوائي ٧٠% للتدريب و٣٠% للاختبار وقد تم تطبيق خوارزمية فصل المصادر الاعمى مع الشبكة العصبية وسجلت دقة بنسبة ٩٩ .٤ في حين حصلت خوارزميات فصل المصادر الاعمى ودعم المتجه نسبة ٩٩. ٣٨.% استخدمت خوارزمية نثر المويجات لاستخراج الميزات مع الشبكة العصبية والتعلم للدعم المتجه وكانت نسب الدقة متفاوته حيث حصلت نثر المويجات مع الشبكة العصبية على نسبة ٩٩ .٧ % بينما نثر المويجات مع الدعم المتجه نسبة دقة ٩٩ .٩٢ % وبعد مقارنة النسب وجد ان تطبيق نثر المويجات مع دعم المتجه الاكثر دقة والتي تم تطبيقها عملية من خلال جهاز تم تصميمها بالاعتماد على جهاز صغير يدعى الباندا الذي يشابه كمبيوتر صغير ويعمل على وندوز ١٠ مع مستشعرات ومستشعر خاص باشارة مخطط كهربائية القلب يعمل كوحدة ECG تم استخدام GUI لعرض النتائج على شاشة تم ربطها مع الباندا عند فحص المريض التي تعطي نتائج تصنيف للاشارة القلب للحالات التي تم ذكرها مسبقا

جمهورية العراق

وزارة التعليم العالي والبحث العلمي

جامعة بابل – كلية الهندسة

قسم الهندسة الكهربائية

تصنيف أمراض القلب بالاعتماد على تخطيط القلب باستخدام وسائل التعلم الآلي

اطروحة

مقدمة إلى كلية الهندسة في جامعة بابل
وهي جزء من متطلبات الحصول على درجة الدكتوراه
فلسفة في هندسة الالكترونيك والاتصالات

قدمت من قبل

هيام عبيد مرزوك

بأشراف

الأستاذ الدكتور

حيدر جبار عبد

تشرين الأول ٢٠٢٣ ربيع الأول ١٤٤٥